RECLAMATION

Managing Water in the West

Technical Report No. SRH 2013-25

North Central Arizona Pipeline Scour Study – Part I

North Central Arizona Pipeline
Phoenix Area Office

U.S. Department of the Interior
Bureau of Reclamation

December 2013

Mission Statements

The U.S. Department of the Interior protects America's natural resources and heritage, honors our cultures and tribal communities, and supplies the energy to power our future.

The mission of the Bureau of Reclamation is to manage, develop, and protect water and related resources in an environmentally and economically sound manner in the interest of the American public.

Technical Report No. SRH 2013-25

North Central Arizona Pipeline Scour Study – Part I

North Central Arizona Pipeline
Phoenix Area Office

Prepared by:

Lisa Fotherby, Ph.D., P.E., Hydraulic Engineer
Sedimentation and River Hydraulics Group, 85-824000

Michael Sixta, M.S., P.E., Hydraulic Engineer
Sedimentation and River Hydraulics Group, 85-824000

Jeanne Godaire, M.S., Geomorphologist
Seismotectonics and Geophysics Group, 85-833000

Lee Mauney, Hydrologic Engineer
Flood Hydrology and Consequences Group, 85-825000

Joseph Wright, Hydraulic Engineer
Flood Hydrology and Consequences Group, 85-825000

Peer reviewed by:

Drew Baird, Ph.D., P.E., D.WRE
Sedimentation and River Hydraulics Group, 85-824000

U.S. Department of the Interior
Bureau of Reclamation
Technical Service Center
Sedimentation and River Hydraulics Group
Denver, Colorado

December 2013

Technical Report No. SRH 2013-25

North Central Arizona Pipeline Scour Study – Part I

North Central Arizona Pipeline
Phoenix Area Office

Peer Review Certification: This document has been prepared by the Bureau of Reclamation, Technical Service Center. It has been peer reviewed per guidelines established by the Technical Service Center and is believed to be in accordance with the service agreement and standards of the profession.

Report prepared by:

12/8/13

Lisa Fotherby, Ph.D., P.E.
Hydraulic Engineer, Sedimentation and River Hydraulics Group (85-824000)

12/10/13

Michael Sixta, M.S., P.E.
Hydraulic Engineer, Sedimentation and River Hydraulics Group (85-824000)

12/10/13

Jeanne Godaire, M.S.
Geomorphologist, Seismotectonics and Geophysics Group (85-833000)

12/10/13

Lee Mauney, M.S.
Hydrologic Engineer, Flood Hydrology and Consequences Group (85-825000)

(for Joseph Wright) 12/10/13

Joseph Wright, P.E.
Hydraulic Engineer, Flood Hydrology and Consequences Group (85-825000)

Peer reviewed by:

12/10/2013

Drew Baird, Ph.D., P.E., D.WRE
Hydraulic Engineer, Sedimentation and River Hydraulics Group (85-824000)

Abbreviations and Acronyms

%	percent
1D	one-dimensional
2D	two-dimensional
AEP	Annual Flow Exceedance Probability
AGS	Arizona Geological Survey
ArcGIS	ESRI's Geographic Information System model
ASCE	American Society of Civil Engineers
AZ	Arizona
CORS	Continuously Operating Reference Stations network
CSU	Colorado State University
DEM	Digital Elevation Model
E.G.	Energy Gradeline
Emfreq	Reclamation program to compute peak discharge frequency relationship
ESRI	Environmental Systems Research Institute
ft/ft	feet per foot
ft/s	feet per second
ft^2/s	square feet per second
ft^3/s	cubic feet per second
ft/s	feet per second
FHWA	Federal Highway Administration
GCNP	Grand Canyon National Park
GIS	Geographic Information Systems
GPS	Global Positioning System
HEC-18	Hydraulic Engineering Circular 18
HEC-23	Hydraulic Engineering Circular 23
HEC-GeoRAS	Custom interface model between HEC-RAS and ArcGIS
HEC-RAS	USACE's Hydraulic Engineering Center River Analysis System one-dimensional numerical model
HIRE	Abutment Scour Equation developed by FHWA for USACE spur dike data
IACWD	Interagency Committee on Water Data
IfSAR	Interferometric Synthetic Aperture Radar
LCR	Little Colorado River
LIDAR	Light Detecting and Ranging mapping
mi^2	square miles
NAD83	North American Datum of 1983
NCAP	North Central Arizona Pipeline
NCHRP	National Cooperative Highways Research Program
NGS	National Geodetic Survey
No.	number
NOAA	National Oceanic and Atmospheric Administration
NRCS	National Resources Conservation Service
NSRS	National Spatial Reference System

NSS	National Streamflow Statistics
OPUS	Online Position User Service
PBS&J	engineering firm; now Atkins Corporation
PFDS	Precipitation Frequency Data Server
PXAO	Phoenix Area Office
Reclamation	Bureau of Reclamation
RTK	Real Time Kinematic Survey
SMS	Surface-Water Modeling System software
SRH-2D	Reclamation's Sedimentation and River Hydraulics two-dimensional numerical model
STATSGO	State Soil Geographic Database
TIN	Triangulated Irregular Network
tp	test pit
TSC	Technical Service Center, Bureau of Reclamation
USACE	U.S. Army Corps of Engineers
USGS	U.S. Geological Survey
UTM	Universal Transverse Mercator
WSE	water surface elevation

Conversions

1 cubic foot per second = 0.646 million gallons per day
1 million gallons per day = 1.547 cubic feet per second
1 acre-foot = 325,851 gallons
1 million gallons per day = 1,120 acre-feet per year
1 cubic foot per second = 1.98 acre-feet per day
1 pound per square inch = 2.31 feet of water elevation head
1 cubic meter per second = 35.29 cubic feet per second

Executive Summary

As part of the Design Feasibility Report for the North Central Arizona Pipeline (NCAP) Project, the potential for scour is assessed at 132 study sites in the study area. This report represents Part I of the scour study, which includes the mainline from Page, Arizona (AZ), to Flagstaff, AZ, and includes the Bitter Springs Spur and the Tuba City Spur. A proposed pipeline alignment crosses streams at 124 locations and parallels streams closely at 8 locations. The NCAP study area is an arid region with high relief, pervasive rock, limited vegetation, largely undeveloped areas, and primarily ephemeral streams. These factors contribute to a large sediment supply, and there are many ephemeral, braided streams in the valley bottoms that transport large sediment loads. Ephemeral flows may consist of intense, large volume flash floods. There are also regional floods that last for weeks or months, as well as flash floods that occur suddenly and last only hours.

Data collection included 1 week of field investigation in April 2013. During this time, the proposed alignment in general and 22 main crossings were reviewed. The main crossings were targeted for detailed observations and data collection. An additional 29 stops were made at secondary crossings to verify information acquired from mapping and for photos and general observations.

A stream cross section and bed profile was surveyed at main crossings using a Real Time Kinematic Survey. Cross sections were surveyed upstream and downstream of the old Highway 89 bridge at the LCR (LCR) to check Light Detecting and Ranging (LIDAR) mapping at this location, and a water surface profile was collected for verification of the numerical models. Sediment samples were collected from the bed of the main channel near pipeline stream crossings and submitted for a sieve gradation analysis. Geomorphic mapping was prepared at each main crossing, and the site was inspected for an assessment of wetted surfaces and lateral and vertical stability. Sediment, terrain, road structures, and terrain features were reviewed at each crossing and noted for scour analysis computations. In addition to site visit surveys and data, aerial photos, U.S. Geological Survey (USGS) maps, Interferometric Synthetic Aperture Radar 5-foot contour maps for most of the study area, and LIDAR mapping at the LCR are used in this study to develop the hydrologic, hydraulic, geomorphic, and scour data base.

Hydrology

Frequency peak discharge estimates for both main and secondary stream crossings are computed from regression equations provided by USGS (2006). The LCR is the largest crossing (Site No. 96) in the project area and conveys approximately six times the 100-year peak flow of the second largest crossing near Flagstaff.

Frequency peak discharge estimates for Site No. 96 were determined from historic annual peak discharge data for the history of record.

Hydraulics

Hydraulic parameters for the main crossings, including bankfull flow, are based on an analysis at a surveyed channel section and surveyed slope. Hydraulics and flow patterns at the LCR are determined from two numerical models: (1) a U.S. Army Corps of Engineers Hydraulic Engineering Center River Analysis System one-dimensional numerical model (HEC-RAS) that provides accurate water surface elevations; and (2) a Bureau of Reclamation Sedimentation and River Hydraulics two-dimensional numerical model (SRH-2D) that provides detailed descriptions of 2D flow patterns. The cross sections and the mesh representation of terrain in the models are constructed from LIDAR data verified from a field survey of cross sections upstream and downstream of the old Highway 89 bridge at the LCR. The results show the opening of the old bridge is nearly filled at a 5-year flow event, flow through the bridge is pressurized at a 10-year event, and the bridge is submerged at a 25-year flow event.

Lateral and Vertical Stream Stability

Landforms and human features were mapped on aerial photography at 27 sites. Characteristics such as channel relief, bed material, bank materials, knickpoints (sudden changes in stream gradient), high water marks, geologic deposits, height and character of geomorphic surfaces, and a schematic cross section at the crossing were described. Historical channel changes using aerial photography were investigated. These observations and features were used as a basis for estimating the relative vertical and lateral stability of each crossing and determining the minimum width of burial for the pipeline crossing under the channel. The detailed main crossings were then used to evaluate the secondary sites that were not visited in the field.

Scour Depths

Scour depth was computed at 22 main pipeline crossing sites based on a modified American Society of Civil Engineers 2004 method (ASCE, 2005) for the sites distant from a bridge or structure (>50 feet), and computed based on Federal Highway Administration (FHWA) Hydraulic Engineering Circular 18 (HEC-18) methods (FHWA, 2012) for four sites adjacent to a bridge or structure (<50 feet). Using a regression equation developed from the results at main sites, and using the unit discharge at each site, scour depth was estimated at 110 secondary sites. Unit discharge at each site was also used to estimate the scour depth at 15 secondary sites adjacent to a bridge or structure. A HEC-RAS model and SRH-2D model at the LCR pipeline crossing provided more detailed information

on hydraulics and on flow patterns for the scour analysis. Results from the vertical stability rating were integrated as a degradation depth. Degradation depth was added to scour depth estimates for a value of total potential scour depth. Scour depth results were also compared with 2011 test pit results on depth to refusal to begin investigating locations where total scour depth may be limited by subsurface conditions.

Results of the geomorphic investigation on lateral stability of streams at pipeline crossings, a summary of total scour depth estimates at study sites, and notes to aid the pipeline designer are presented in the concluding chapter of this report.

Contents

Page

1. Introduction 1
2. Methods 11
   2.1 Standards for Estimating Scour at Bridges 11
   2.2 Standards for Estimating Scour in Natural Systems 12
   2.3 Assessment of Vertical and Lateral Stability 13
   2.4 Field Investigation 13
      2.4.1 Main Sites 13
      2.4.2 Secondary Sites 15
3. Hydrology: Stream Discharge Estimates 17
   3.1 Relevant Data 17
   3.2 Frequency Peak Discharge Estimates–Regression Equations 18
   3.3 Frequency Peak Discharge Estimates–Historic Discharge Data 23
4. Hydraulics: Stream Parameters and Water Surface Elevations 27
   4.1 Real-Time Kinematic Survey 27
   4.2 Hydraulic Parameters and Water Surface Elevation 29
   4.3 LCR Models 32
   4.4 Topography Development 33
   4.5 HEC-RAS Model 35
   4.6 SRH-2D Model 38
   4.7 HEC-RAS Model Results 41
   4.8 SRH-2D Model Results 45
5. Geomorphology: Vertical and Lateral Stability of Streams 51
   5.1 Methodology 51
   5.2 Site Descriptions 51
      5.2.1 Site No. 13 52
      5.2.2 Site No. 16 52
      5.2.3 Site No. 18 53
      5.2.4 Site No. 20 54
      5.2.5 Site No. 21 55
      5.2.6 Site No. 26 56
      5.2.7 Site No. 31 57
      5.2.8 Site No. 32 59
      5.2.9 Site No. 33 60
      5.2.10 Site No. 50 60
      5.2.11 Site No. 51 62
      5.2.12 Site No. 52 62
      5.2.13 Site No. 57 63
      5.2.14 Site No. 58 63
      5.2.15 Site No. 75 65
      5.2.16 Site No. 78 66
      5.2.17 Site No. 84 66
      5.2.18 Site No. 86 68

Contents (continued)

Page

5.2.19 Site No. 90 69
5.2.20 Site No. 92 71
5.2.21 Site No. 94 72
5.2.22 Site No. 96 73
5.2.23 Site No. 97 76
5.2.24 Site No. 98 77
5.2.25 Site No. 103 78
5.2.26 Site No. 104 79
5.2.27 Site No. 125 79
5.3 Vertical and Lateral Stability and Stream Crossing Widths 80
6. Potential Scour Depths 103
6.1 Flow Risk Assessment 103
6.2 Methods 103
6.2.1 Methods for Computing Scour at Main Sites 104
6.2.2 Methods for Estimating Scour at Secondary Sites 106
6.3 Results for Main and Secondary Sites Distant from Bridges 107
6.4 Methods for Computing Scour at Sites Adjacent to Bridges 111
6.4.1 Contraction Scour at Main Sites 112
6.4.2 Local Scour at Main Sites 113
6.4.2.1 Local Scour at Piers 115
6.4.2.2 Local Scour at Abutments 115
6.4.3 Contraction Scour and Local Scour at Secondary Crossings 117
6.5 Total Scour Depth 119
6.5.1 Factor of Safety 137
6.5.2 Scour Countermeasures 137
6.5.3 Sites with Contraction and Local Scour Effects 137
6.5.4 Subsurface Materials 138
6.6 Subsurface Materials 138
6.6.1 Findings 140
6.6.2 LCR 151
7. Summary of Findings 153
7.1 Hydrology 153
7.2 Hydraulic Modeling 153
7.3 Geomorphic and Scour Analysis 154
7.4 Design Notes 155
7.4.1 Buried Crossings Versus Mounting on a Bridge 155
7.4.2 Vertical Controls 169
7.4.3 Avoiding Local Scour Conditions 170
7.4.4 Parallel Road and Stream Drainages 170
7.4.5 Scour Countermeasures 170
References 171

Appendices

A Study Site Locations
B Hydrology
C Geomorphology
D Scour
E Sediment and Slope

Tables

Table *Page*

Table 1-1 NCAP Project – Stream Study Sites ("a" indicates start of stream reach parallel to pipeline, and "b" indicates end of stream reach parallel to pipeline).....5
Table 2-1. Sites Visited during the April 8-12, 2013 Field Review.....15
Table 3-1 Peak Discharge Estimates in Cubic Feet Per Second (ft^3/s) from the USGS Regression Technique.....19
Table 3-2 Peak Discharge Estimates for Peak Annual Streamflow Analysis (LCR near Cameron, AZ).....25
Table 4-1 Hydraulic Parameters Including Water Surface Elevations for Surveyed Cross Sections.....30
Table 4-2 Modeled Flows Based on Hydrologic Streamflow Analysis.....37
Table 4-3 Material Type Roughness values for the SRH-2D Model.....40
Table 4-4 HEC-RAS WSEs used for SRH-2D downstream boundary condition.....40
Table 4-5 Hydraulic Parameters for the Cross Sections Upstream and Downstream of the Bridge.....42
Table 5-1 Rating Definitions for Vertical and Lateral Stream Stability at Pipeline Crossings.....81
Table 5-2 Assessment of Vertical and Lateral Stability.....82
Table 5-3 Coordinates for Channel Centerpoint Locations.....98
Table 6-1 Scour Equations for Main Sites.....105
Table 6-2 Investigating Degradation.....109
Table 6-3 Bend Scour and Bedform Scour Depths at Main Sites.....109
Table 6-4 Comparison of Scour Depth Values and Methods.....109
Table 6-5 Types of Scour Assessed for Pipeline Design.....112
Table 6-6 Equations for Main Sites Adjacent to a Bridge (<50 ft).....112
Table 6-7 Local and Contraction Scour Depths Computed at Main Sites for a 100-Year Flow Event.....116
Table 6-8 Local Scour Depth at Secondary Sites Estimated from Computed Local Scour Depths at Main Sites.....118
Table 6-9 Scour Depth Estimates for a 100-Year Event.....120
Table 6-10 Shifting Pipeline Alignment Can Reduce Potential Scour Depth at Specified Sites.....137

Tables (continued)

Table *Page*

Table 6-11 Comparison of Test Pit Refusal Elevation and Scour Depth Elevations at Adjacent Stream Crossing Sites 141
Table 7-1 Summary of Findings for NCAP Stream Sites 156

Figures

Figure *Page*

Figure 1-1 NCAP proposed PXAO pipeline alignment. 2
Figure 1-2 NCAP proposed pipeline alignments for Part I and Part II (GCNP and Tusayan Spur) and Part III (the Hopi Spur) 3
Figure 3-1 LCR flow prior to the April 2013 site visit. 23
Figure 3-2 Peak annual streamflow analysis, LCR near Cameron, AZ.....24
Figure 4-1 Plan view of the proposed pipeline crossing (red line) at Site No. 51.....27
Figure 4-2 Surveyed slope and cross section at Site No. 51.....28
Figure 4-3 RTK survey/LIDAR data comparison along a cross section immediately upstream of the old Highway 89 bridge.....34
Figure 4-4 Digital topographic surface representation (flow is from right to left). 35
Figure 4-5 Cross sections making up the HEC-RAS model (flow is from right to left). 36
Figure 4-6 Representation of old Highway 89 bridge in HEC-RAS model.....36
Figure 4-7 Ground survey recording a cross section directly downstream at the old Highway 89 bridge. 37
Figure 4-8 2D mesh against surface topography near the old Highway 89 bridge.....39
Figure 4-9 Roughness zone delineations for the SRH-2D model.....39
Figure 4-10 WSE change over time at monitoring point near proposed crossing.....41
Figure 4-11 Looking upstream from the old Highway 89 bridge.....41
Figure 4-12 WSEs and velocities for the upstream cross section at the old Highway 89 bridge.....43
Figure 4-13 WSEs and velocities for the downstream cross section at the old Highway 89 bridge.....44
Figure 4-14 Velocity magnitudes/vectors for the 5-year (12,400-ft^3/s) event. 46

Figures (continued)

Figure *Page*

Figure 4-15 Velocity magnitudes/vectors for the 100-year (63,600-ft^3/s)event. 47
Figure 4-16 Depths for the 5-year (12,400-ft^3/s) event. 48
Figure 4-17 Depths for the 100-year (63,600-ft^3/s) event. 49
Figure 5-1 Site No. 13 looking upstream....52
Figure 5-2 Site No. 16 looking upstream....52
Figure 5-3 Geomorphic features at Site No. 16....53
Figure 5-4 Site No. 18 looking downstream from the old bridge....53
Figure 5-5 Site No. 20 with concrete in channel bed at old road 54
Figure 5-6 Geomorphic features at Site No. 20....55
Figure 5-7 Site No. 21 looking upstream....55
Figure 5-8 Geomorphic features at Site No. 21....56
Figure 5-9 Site No. 26. 56
Figure 5-10 Geomorphic features at Site No. 26....57
Figure 5-11 Site No. 31 looking upstream....57
Figure 5-12 Geomorphic features at Site No. 31....58
Figure 5-13 Site No. 32 59
Figure 5-14 Geomorphic features at alignment Site No. 32 and Site No. 33 59
Figure 5-15 Site No. 33 looking downstream....60
Figure 5-16 Site No. 50 looking upstream....60
Figure 5-17 Geomorphic features at Sites No. 50 and 51....61
Figure 5-18 Site No. 51 looking upstream....62
Figure 5-19 Site No. 52 looking downstream from bridge....62
Figure 5-20 Site No. 57 looking downstream....63
Figure 5-21 Looking downstream at bedrock downstream of Site No. 58 63
Figure 5-22 Geomorphic features at Site No. 58....64
Figure 5-24 Site No. 75 looking upstream....65
Figure 5-23 Site No. 75 65
Figure 5-26 Site No. 78 looking downstream....66
Figure 5-25 Upstream of Site No. 78....66
Figure 5-27 Site No. 84 66
Figure 5-28 Geomorphic features at Site No. 84....67
Figure 5-29 Site No. 86 at white bucket between old and new bridges 68
Figure 5-30 Geomorphic features at Site No. 86....68
Figure 5-31 Site No. 90. The shovel is at proposed pipeline crossing 69
Figure 5-32 Looking upstream at Site No. 90 where white bucket sits on the bank....69

Figures (continued)

Figure *Page*

Figure 5-33 Geomorphic features at alignment Site No. 90, Moenkopi Wash 70
Figure 5-34 The white bucket upstream of the old bridge marks the location of Site No. 92 71
Figure 5-36 Looking downstream towards the old bridge from Site No. 94 72
Figure 5-35 Looking upstream at Site No. 94 proposed pipeline crossing 72
Figure 5-37 Geomorphic features at alignment Site No. 94 73
Figure 5-38 Old Highway 89 bridge at Site No. 96, looking upstream and across at the left bank 73
Figure 5-39 Looking upstream at Highway 89 bridge and the old Highway 89 bridge in the background at Site No. 96, the LCR 74
Figure 5-40 Geomorphic features at Site No. 96, LCR 74
Figure 5-41 Comparison of vegetation along the LCR near Cameron, AZ, between 1953 and 2012 75
Figure 5-42 Site No. 97 looking downstream from the crossing 76
Figure 5-43 Geomorphic features at Site No. 97 76
Figure 5-45 Spring-fed channel in active channel area 77
Figure 5-44 Site No. 98 looking upstream 77
Figure 5-46 Geomorphic features at alignment Site No. 98 78
Figure 5-47 Site No. 103 looking downstream 78
Figure 5-48 Site No. 104 looking downstream 79
Figure 5-49 Photo looking upstream at Site No. 125, next to the old bridge 79
Figure 5-50 Geomorphic features at alignment Site No. 125 80
Figure 6-1 Relation of scour depth to unit discharge 111
Figure 6-2 Flow structure including macro-turbulence generated by flow around abutments in a narrow main channel, causing contraction scour 112
Figure 6-3 Photo of a horseshoe scour pattern in a laboratory flume at a circular pier 114
Figure 6-5 Local scour at Site 92 pier - a circular eroded area in the sand 114
Figure 6-4 Local scour in a laboratory 114
Figure 6-6 Debris caught on pile-piers of the old Highway 89 bridge from spring flows at the LCR, April, 2013 115
Figure 6-7 Relic piers that can cause local scour 117

Figures (continued)

Figure *Page*

Figure 6-8 The proposed pipeline crossing at Crossing 84 is near the sediment sampling sight and is outside the expected local scour radius of 10 feet.....119
Figure 6-9 Examples from HEC-18 of scour in sandstone rock.....139
Figure 6-10 A map of test pit locations shown as black triangles and stream crossing sites.....140
Figure 7-2 Drainage wide and filled with sediment, upstream of culvert at old road 169
Figure 7-1 Aggradation filling downstream culvert at old road.....169
Figure 7-4 Looking across the downstream culvert at erosion headcuts from water flowing across the top of the old road 169
Figure 7-3 Upstream culvert at old road also partially filled from drainage deposition.....169

1. Introduction

The North Central Arizona Pipeline (NCAP) Project consists of construction of a new pipeline from a Lake Powell intake at Page, Arizona (AZ), to the last delivery point in Flagstaff, AZ (figure 1-1). The proposed alignment includes three spurs: (1) the Bitter Springs Spur from Bodaway Gap to Bitter Springs, (2) the Tuba City Spur from the Tuba City airport to Tuba City, and (3) the Keams Canyon Spur from Moenkopi to Keams Canyon. The proposed alignment may also include a Grand Canyon National Park (GCNP) Spur from Cameron to the town of Tusayan and to the GCNP. Proposed alignments are shown in figure 1-2. Appurtenant features of the NCAP Project are a reservoir-side pumping plant, booster/relift plants, forebay tanks, water storage tanks, air chambers, regulating tanks, pressure reducing valves, valve vaults, and participant delivery vaults. The pipeline serves the Cities of Page and Flagstaff; the Navajo Nation Indian Reservation Chapters: LeChee, Coppermine, Bitter Springs, Bodaway Gap, Tuba City, and Cameron; and the Hopi Nation Villages of Upper Moenkopi, Bacavi, Kykotsmovi, Sipaulovi, Mishongnovi, Shungopavi, Oraibi, Hotevilla, Lower Moenkopi, and First Mesa Consolidated Villages (Walpi, Shitchumovi, and Tewa). The pipeline may also potentially serve GCNP and the town of Tusayan.

The Bureau of Reclamation's (Reclamation) Technical Service Center (TSC) completed Part I of this investigation for the Reclamation Phoenix Area Office (PXAO) with funding from the Rural Water Program during the summer of 2013. This scour study, Part I, includes the mainline stream crossings from Page, AZ, to Flagstaff, AZ, and stream crossings on the Bitter Springs Spur and the Tuba City Spur. Part II of the scour study is planned for the Keams Canyon Spur that will serve the Hopi Nation Reservation. Part III of the scour study is proposed for the GCNP/Tusayan Spur, although the project extents and participants may change as the project advances.

Scour occurs in multiple forms; however, in all cases it can be defined as the removal of sediment by the flow of water. Scour of a streambed can threaten the integrity of a pipeline buried below the stream. To protect the system, a new pipeline is constructed below the maximum depth of scour for the maximum width of the stream crossing. Scour countermeasures (for example, the placement of riprap on the bed of the channel) are required when the pipe is not buried sufficiently deep. Main tasks of this scour investigation are to:

- Estimate a maximum scour depth at each pipeline crossing
- Assess the vertical stability of the stream at each crossing (a factor contributing to scour depth)

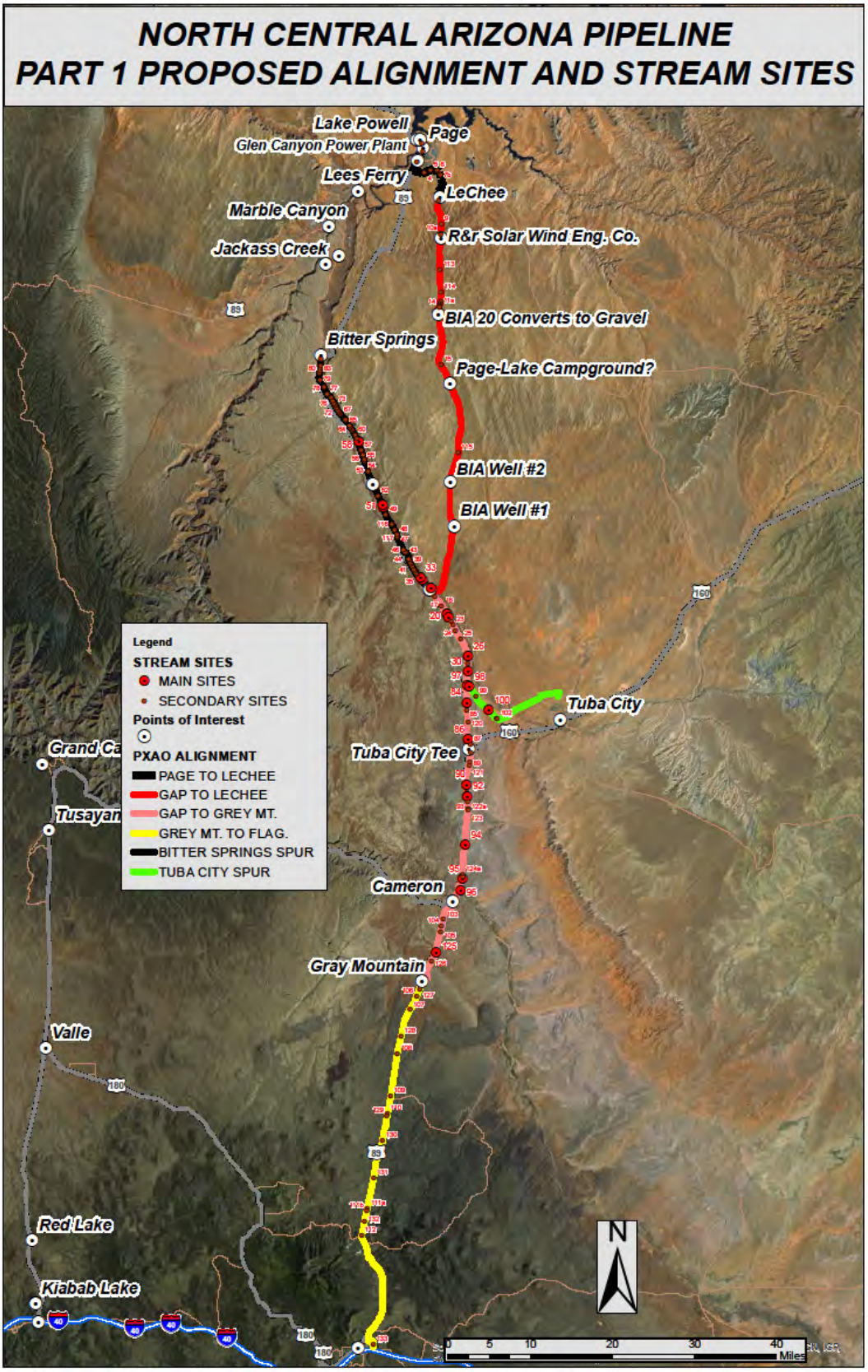

Figure 1-1. NCAP proposed PXAO pipeline alignment.

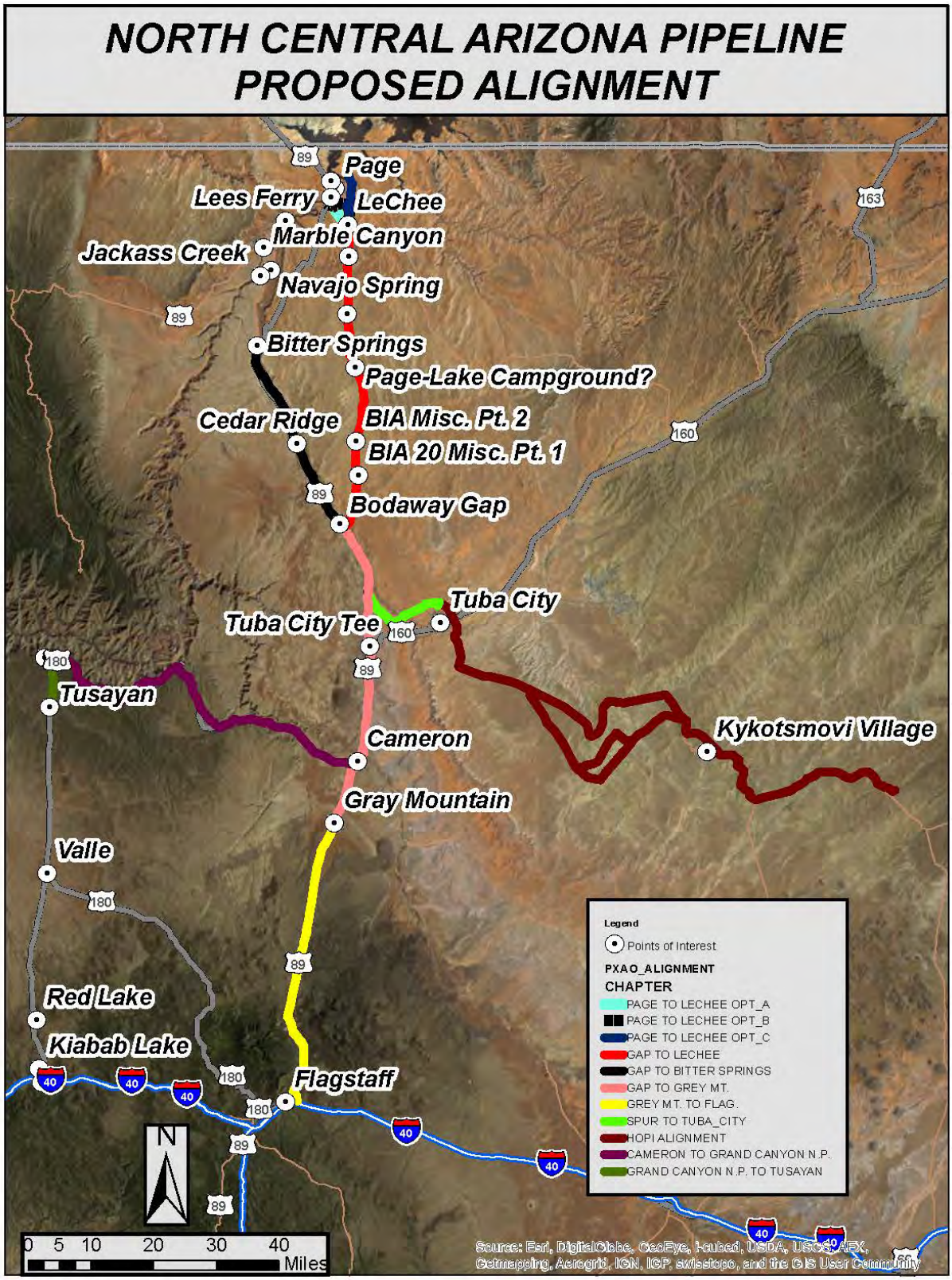

Figure 1-2. NCAP proposed pipeline alignments for Part I and Part II (GCNP and Tusayan Spur) and Part III (the Hopi Spur). The alignments shown are current as of August 2013 but are under development and subject to change.

- Assess the lateral stability of the stream crossed by the pipeline and provide this width
- Provide estimates of water surface elevations at crossings, when possible, to aid the design of appurtenant structures
- Consider stream stability at sites where streams parallel the proposed pipeline alignment

Under the first phase of this study (Part 1), scour or stream stability was considered at up to 132 sites on the mainline and at the Bitter Springs and Tuba City Spur (table 1-1). Stream sites were included in table 1-1 if the stream could be readily detected from Google aerial mapping (Google, 2013). There are two types of sites: (1) locations where the proposed pipeline alignment crosses the stream (crossings), and (2) locations where the stream parallels the proposed pipeline alignment. Stream segments that parallel the pipeline have an "a" or "b" designation indicating the start and end of the parallel segment. Crossings and parallel stream segments are evaluated the same way. Study sites, including crossings and parallel stream segments, are shown in figure 1-1. They are also shown in smaller scale on the 17 figures in appendix A.

Study sites were evaluated using terrain mapping, aerial photos, a photo log, data collected from a field investigation, and two constructed numerical hydraulics models. A U.S. Army Corps of Engineers Hydraulic Engineering Center River Analysis System one-dimensional numerical model (HEC-RAS) and a Bureau of Reclamation Sedimentation and River Hydraulics two-dimensional numerical model (SRH-2D) represent Site No. 96: the Little Colorado River (LCR) near Cameron, AZ (figure 1-1). The LCR crossing is the largest crossing in the study area.

Chapter 2 describes the general approach of this scour investigation. Chapter 3 presents a hydrologic investigation, which is the basis for all succeeding analyses. Chapter 4 discusses the hydraulics parameters for scour computations and a description of the development of the LCR hydraulic models. Vertical stream stability affects the final scour value, and horizontal stream stability determines the length of pipeline requiring deep burial. Chapter 5 presents a description by site of the geomorphic investigation of vertical and lateral stream stability. Chapter 6 contains a description of the methods and results from the scour investigation. This presentation concludes with a summary of findings in chapter 7, which blends geomorphic results from Chapter 5 and scour results from chapter 6. A summary of this report will be included in the NCAP Feasibility Design Report for the NCAP Project.

Table 1-1. NCAP Project – Stream Study Sites ("a" indicates start of stream reach parallel to pipeline, and "b" indicates end of stream reach parallel to pipeline)

Site No.	Northing	Easting	Esti-mated Width	Description	DMS Coordinates						
					°N	'	"		°W	'	"
Lake Powell to Tuba City Tee											
1	36.93356667	-111.4737306	10	Wash	36	56	0.84		111	28	25.43
2	36.92217222	-111.4723861	60	Wash; possibly culvert	36	55	19.82		111	28	20.59
3	36.90673611	-111.482775	30	Wash; possibly culvert	36	54	24.25		111	28	57.99
4	36.89170833	-111.46975	50	Wash	36	53	30.15		111	28	11.10
5	36.89583056	-111.4590056	35	Culvert	36	53	44.99		111	27	32.42
6	36.895025	-111.4472333	50	Culvert	36	53	42.09		111	26	50.04
7a	36.89061667	-111.442775	N/A	Wash stretch - 1,000 feet	36	53	26.22		111	26	33.99
7b	36.88818889	-111.441575			36	53	17.48		111	26	29.67
8	36.85272222	-111.4445639	40	Wash	36	51	9.80		111	26	40.43
9	36.81915	-111.4397306	12	Wash	36	49	8.94		111	26	23.03
10a	36.80600833	-111.4408389	N/A	Wash stretch - 250 feet	36	48	21.63		111	26	27.02
10b	36.80539722	-111.4409056			36	48	19.43		111	26	27.26
11a	36.70994722	-111.4418306	N/A	Wash stretch - 870 feet	36	42	35.81		111	26	30.59
11b	36.70751389	-111.442475			36	42	27.05		111	26	32.91
12	36.70615278	-111.4427639	10	Wash	36	42	22.15		111	26	33.95
13	36.70487222	-111.4430944	15	Wash	36	42	17.54		111	26	35.14
14	36.70198056	-111.4437806	36	Wash	36	42	7.13		111	26	37.61
15	36.62098056	-111.4407861	10	Wash	36	37	15.53		111	26	26.83
16	36.30482222	-111.4583667	100	Wash	36	18	17.36		111	27	30.12
17	36.29415556	-111.451475	12	Wash	36	17	38.96		111	27	5.31
18	36.28052778	-111.4390583	30	Wash	36	16	49.90		111	26	20.61
19	36.27217778	-111.4323389	15	Wash	36	16	19.84		111	25	56.42
20	36.26946111	-111.4308056	75	Wash	36	16	10.06		111	25	50.90
21	36.26394167	-111.4274889	85	Wash	36	15	50.19		111	25	38.96
22	36.25907222	-111.4227444	30	Wash	36	15	32.66		111	25	21.88
23	36.25403611	-111.4190444	200	Wash	36	15	14.53		111	25	8.56
24	36.24539722	-111.4146278	14	Wash; possibly culvert	36	14	43.43		111	24	52.66
25	36.23313889	-111.40505	18	Wash	36	13	59.30		111	24	18.18
26	36.20927778	-111.3937361	80	Wash	36	12	33.40		111	23	37.45

Table 1-1. NCAP Project – Stream Study Sites ("a" indicates start of stream reach parallel to pipeline, and "b" indicates end of stream reach parallel to pipeline)

Site No.	Northing	Easting	Esti-mated Width	Description	DMS Coordinates						
					°N	'	"		°W	'	"
27	36.1985	-111.3928639	35	Wash	36	11	54.60		111	23	34.31
28	36.18949722	-111.3934556	30	Wash	36	11	22.19		111	23	36.44
30	36.18782222	-111.3938056	20	Wash	36	11	16.16		111	23	37.70
31	36.16923333	-111.3958028	100	Wash	36	10	9.24		111	23	44.89
113	36.75553056	-111.4420667	13	Wash	36	45	19.91		111	26	31.44
114	36.72439444	-111.4407472	140	Wash	36	43	27.82		111	26	26.69
115	36.49761667	-111.4097417	20	Wash	36	29	51.42		111	24	35.07
Bitter Springs Spur: This reach runs adjacent to a riverbed.											
32	36.31730833	-111.4740806	85	Wash	36	19	2.31		111	28	26.69
33	36.32065	-111.4772778	60	Wash	36	19	14.34		111	28	38.20
34	36.32455833	-111.4826139	40	Wash; possibly culvert	36	19	28.41		111	28	57.41
35	36.32759167	-111.4848361	185	Wash	36	19	39.33		111	29	5.41
36	36.32991944	-111.4865917	60	Wash	36	19	47.71		111	29	11.73
37	36.33240833	-111.4884194	40	Wash	36	19	56.67		111	29	18.31
38	36.33628611	-111.4914444	80	Wash	36	20	10.63		111	29	29.20
39	36.34008889	-111.4938	10	Wash	36	20	24.32		111	29	37.68
40	36.34118056	-111.4944889	20	Wash	36	20	28.25		111	29	40.16
41	36.34377222	-111.4955667	20	Wash	36	20	37.58		111	29	44.04
42	36.347025	-111.4976917	55	Wash	36	20	49.29		111	29	51.69
43	36.35600278	-111.501775	40	Wash	36	21	21.61		111	30	6.39
44	36.35646944	-111.5029917	40	Wash	36	21	23.29		111	30	10.77
45	36.358775	-111.5060528	40	Wash	36	21	31.59		111	30	21.79
46	36.35988333	-111.5069028	20	Wash	36	21	35.58		111	30	24.85
47	36.37859167	-111.5169861	15	Wash	36	22	42.93		111	31	1.15
48	36.38113611	-111.5182722	15	Wash	36	22	52.09		111	31	5.78
49	36.40933611	-111.5372972	50	Wash	36	24	33.61		111	32	14.27
50	36.42044167	-111.5426639	22	Wash	36	25	13.59		111	32	33.59
51	36.42343611	-111.5440056	50	Wash	36	25	24.37		111	32	38.42
52	36.43684167	-111.5512944	25	Wash	36	26	12.63		111	33	4.66
53	36.47069167	-111.56965	35	Wash	36	28	14.49		111	34	10.74
54	36.48554167	-111.5753722	20	Wash	36	29	7.95		111	34	31.34
55	36.48804722	-111.5763583	80	Wash	36	29	16.97		111	34	34.89
56	36.49343056	-111.5783944	15	Wash	36	29	36.35		111	34	42.22

Table 1-1. NCAP Project – Stream Study Sites ("a" indicates start of stream reach parallel to pipeline, and "b" indicates end of stream reach parallel to pipeline)

Site No.	Northing	Easting	Esti-mated Width	Description	DMS Coordinates						
					°N	'	"		°W	'	"
57	36.50042778	-111.581	20	Wash	36	30	1.54		111	34	51.60
58	36.51221944	-111.5857722	130	Wash	36	30	43.99		111	35	8.78
59	36.51716111	-111.5887583	55	Wash	36	31	1.78		111	35	19.53
60	36.52239444	-111.5920611	15	Wash	36	31	20.62		111	35	31.42
61	36.52927222	-111.5965278	15	Wash	36	31	45.38		111	35	47.50
62	36.53088611	-111.5981194	15	Wash	36	31	51.19		111	35	53.23
63a	36.53304167	-111.6002722	N/A	Wash stretch - 100 feet	36	31	58.95		111	36	0.98
63b	36.53331111	-111.6004194			36	31	59.92		111	36	1.51
64	36.53505278	-111.6015056	30	Wash	36	32	6.19		111	36	5.42
65	36.54311944	-111.6080833	10	Wash	36	32	35.23		111	36	29.10
66a	36.54340556	-111.6083444	N/A	Wash stretch - 65 feet	36	32	36.26		111	36	30.04
66b	36.54352222	-111.6084944			36	32	36.68		111	36	30.58
67	36.55223056	-111.6174889	27	Wash	36	33	8.03		111	37	2.96
68	36.55355556	-111.618875	22	Wash	36	33	12.80		111	37	7.95
69	36.55510556	-111.6204583	12	Wash	36	33	18.38		111	37	13.65
70	36.55718056	-111.6222028	15	Wash	36	33	25.85		111	37	19.93
71	36.56030556	-111.6243056	15	Wash	36	33	37.10		111	37	27.50
72	36.56320833	-111.6262306	30	Wash	36	33	47.55		111	37	34.43
73	36.56520278	-111.62755	15	Wash	36	33	54.73		111	37	39.18
74	36.56711389	-111.6288667	20	Wash	36	34	1.61		111	37	43.92
75	36.57018056	-111.6308861	50	Wash	36	34	12.65		111	37	51.19
76	36.57518333	-111.6342306	14	Wash	36	34	30.66		111	38	3.23
77	36.57958333	-111.6407667	15	Wash	36	34	46.50		111	38	26.76
78	36.58981389	-111.6463972	35	Wash	36	35	23.33		111	38	47.03
79	36.59986944	-111.6536167	20	Wash	36	35	59.53		111	39	13.02
80	36.60941389	-111.6547861	10	Wash	36	36	33.89		111	39	17.23
81	36.61346389	-111.6541444	10	Wash	36	36	48.47		111	39	14.92
82	36.61572778	-111.6537028	20	Wash	36	36	56.62		111	39	13.33
83	36.6197	-111.6531278	15	Wash	36	37	10.92		111	39	11.26
116	36.39603889	-111.5267806	56	Wash	36	23	45.74		111	31	36.41
117	36.38866667	-111.5218694	25	Wash	36	23	19.20		111	31	18.73
118	36.62993333	-111.6514667	10	Wash	36	37	47.76		111	39	5.28
119	36.62875833	-111.65165	10	Wash	36	37	43.53		111	39	5.94

Table 1-1. NCAP Project – Stream Study Sites ("a" indicates start of stream reach parallel to pipeline, and "b" indicates end of stream reach parallel to pipeline)

Site No.	Northing	Easting	Esti-mated Width	Description	DMS Coordinates						
					°N	'	"		°W	'	"
Tuba City Spur Tee to Cameron											
84	36.14370556	-111.3948694	100	Wash	36	8	37.34		111	23	41.53
85	36.13268889	-111.3954083	42	Wash	36	7	57.68		111	23	43.47
86	36.09151389	-111.3933361	82	Wash	36	5	29.45		111	23	36.01
87	36.08314167	-111.3883333	80	Wash	36	4	59.31		111	23	18.00
88	36.07241389	-111.3870778	100	Wash	36	4	20.69		111	23	13.48
89	36.05906389	-111.3895972	150	Wash	36	3	32.63		111	23	22.55
90	36.02711667	-111.3959944	110	Wash	36	1	37.62		111	23	45.58
91	36.01481389	-111.3952806	40	Wash	36	0	53.33		111	23	43.01
92	36.01041944	-111.39455	50	Wash	36	0	37.51		111	23	40.38
93	36.00125833	-111.3930278	70	Wash	36	0	4.53		111	23	34.90
94	35.94111389	-111.3979083	150	Wash	35	56	28.01		111	23	52.47
95	35.89202222	-111.4029806	190	Wash	35	53	31.28		111	24	10.73
96	35.87613333	-111.4059139	300	Old riverbed	35	52	34.08		111	24	21.29
120	36.11609722	-111.3927778	10	Wash	36	6	57.95		111	23	34.00
121	36.05301111	-111.3907361	35	Wash	36	3	10.84		111	23	26.65
122a	35.992225	-111.3924083	N/A	Wash stretch - 280 feet	35	59	32.01		111	23	32.67
122b	35.9915	-111.3925861			35	59	29.40		111	23	33.31
123	35.99125833	-111.3926333	35	Wash	35	59	28.53		111	23	33.48
124a	35.89838889	-111.4022083	N/A	Wash stretch – 1,000 feet	35	53	54.20		111	24	7.95
124b	35.89540278	-111.4022972			35	53	43.45		111	24	8.27
Tuba City Spur											
97	36.1672	-111.3946	250	Wash	36	10	1.80		111	23	40.41
98	36.1662	-111.3913	15	Wash	36	9	58.41		111	23	28.63
99	36.1522	-111.3788	80	Wash	36	9	7.93		111	22	43.73
100	36.1333	-111.3568	140	Wash	36	7	59.88		111	21	24.34
101	36.1205	-111.3423	50	Wash	36	7	13.75		111	20	32.45
102	36.1198	-111.3410	100	Wash	36	7	11.31		111	20	27.44
Cameron to Flagstaff											
103	35.8348	-111.4366	20	Wash	35	50	5.23		111	26	11.60
104	35.8253	-111.3890	20	Wash	35	49	31.07		111	23	20.51
105	35.8173	-111.4411	95	Wash	35	49	2.23		111	26	28.07
106	35.7252	-111.4825	240	Wash	35	43	30.78		111	28	57.02
107	35.7059	-111.4949	40	Wash	35	42	21.27		111	29	41.62

Table 1-1. NCAP Project – Stream Study Sites ("a" indicates start of stream reach parallel to pipeline, and "b" indicates end of stream reach parallel to pipeline)

Site No.	Northing	Easting	Esti-mated Width	Description	DMS Coordinates						
					°N	'	"		°W	'	"
108	35.6436	-111.5171	65	Wash; possibly culvert	35	38	36.99		111	31	1.53
109	35.5831	-111.5290	60	Wash; possibly culvert	35	34	59.19		111	31	44.49
110	35.5579	-111.5345	95	Wash; possibly culvert	35	33	28.40		111	32	4.36
111a	35.4225	-111.5698	N/A	Wash stretch – 1,700 feet	35	25	20.93		111	34	11.13
111b	35.4184	-111.5708			35	25	6.36		111	34	14.91
112	35.3824	-111.5800	25	Wash	35	22	56.79		111	34	48.07
125	35.7884	-111.4497	65	Wash	35	47	18.21		111	26	58.77
126	35.7747	-111.4569	20	Wash	35	46	28.87		111	27	24.78
127	35.7347	-111.4781	10	Wash	35	44	4.78		111	28	41.16
128	35.6676	-111.5107	50	Wash	35	40	3.42		111	30	38.43
129	35.5540	-111.5355	13	Wash	35	33	14.35		111	32	7.77
130	35.5184	-111.5433	60	Wash	35	31	6.30		111	32	35.97
131	35.4658	-111.5586	15	Wash	35	27	56.93		111	33	30.85
132	35.4031	-111.6081	55	Wash	35	24	11.05		111	36	29.22
133	35.2257	-111.5596	50	Wash	35	13	32.43		111	33	34.68

Source: Locations and Measurements obtained from Google Earth (Google, 2013).

2. Methods

There are multiple forms of stream scour, and they are organized here as scour occurring near structures and scour occurring distant from bridges or structures. Scour depth is computed for each pertinent form, and the depths for each are summed as recommended in standards that are described in the next section. Most forms of scour are a result of secondary flow patterns, including helicoidal rollers of flow or flow turbulence. Secondary flow patterns are localized and move faster than the main current, creating more erosion on the bed and banks. Degradation is a form of stream erosion that acts for longer distances and at both bridge and nonbridge locations in the bed of the channel. The estimated depth of degradation is more difficult to quantify and is based on a geomorphic assessment of vertical stream stability. An estimate of bed degradation is summed with the individual scour values to get the total estimated depth of scour at a pipeline crossing. Values describing the hydrologic, hydraulic, sediment transport, and geomorphic stream conditions are developed in the early chapters and used in later chapters to estimate channel degradation and to compute the scour depth at each crossing.

2.1 Standards for Estimating Scour at Bridges

Types of scour occurring near bridges or other rigid structures include local scour and contraction scour. Local scour develops when the flow impacts a near-vertical surface in the flow path. A helicoidal pattern of secondary flow develops and spins off around the structure. Local scour often erodes deeper into the channel than contraction scour, and deeper than other forms of scour occurring distant from a bridge. Rock boulders or concrete blocks in the channel, hard banks, and even root wads can create the characteristic flow patterns of local scour. Bridge piers and abutments are the most common cause of local scour at pipeline crossings.

Contraction scour should also be considered at sites near bridges. Constricted flow lines accelerate, eroding sediment consistently across the bed of the channel. Rock walls or confining riparian vegetation can also generate contraction scour distant from bridges or road crossings and should be considered in specific cases.

In the previous two decades, the Federal Highway Administration (FHWA) funded and guided an extensive set of laboratory flume studies which investigated methods of predicting the potential scour at a bridge. This effort culminated with the fifth edition of Hydraulic Engineering Circular 18 (HEC-18). When pipeline crossing sites in this study are within 50 feet of a bridge or structure, contraction scour and local scour are calculated from the design guidelines presented in it (FHWA, 2012).

2.2 Standards for Estimating Scour in Natural Systems

Accepted methods of scour computation at locations distant from a bridge or structure have gone through several periods of transition since the 1970s. An approach presented by Williams in an American Society of Civil Engineers short course (ASCE, 2005) incorporates methods by Neil (1973) and the Reclamation standard: Pemberton and Lara (1984). The ASCE approach also includes results from bedform studies (Simons, Li, and Associates, 1985) and five bend scour studies (Zeller [Simons, Li & Associates, 1985]; USACE,[1] 1994a; Thorne et al., 1995; and Maynord, 1996). The ASCE methodology for predicting total bed scour distant from bridges is based on adding six scour components and a factor of safety:

- Long-term degradation
- General scour
- Local scour (when pertinent)
- Bend scour
- Bedform scour (in sand bed streams)
- Low flow channel incisement (when pertinent)
- Factor of safety (1 to 1.5)

During this investigation, general scour was found to be an earlier form of a bend scour computation based on a review of Neil (1973), Pemberton and Lara (1984), and the ASCE course book (ASCE, 2005). The ASCE method double-counts bend scour by including both a general scour component and a bend scour component. The TSC has removed the general scour component in this study but continues to consider all other components recommended in the ASCE (2005) methods. Similarly, the FHWA omitted general scour from bridge computations in the recent edition of HEC-18 (FHWA, 2012).

The modified ASCE (2005) methods are used at locations distant from bridges (> 50 feet), and the FHWA HEC-18 methods are applied at pipeline crossings within 50 feet of the bridge. Modified ASCE (2005) methods will also be added to a new Reclamation standards manual on bank stabilization design currently under development by the Sedimentation and River Hydraulics Group.

[1] USACE refers to the U.S. Army Corps of Engineers.

2.3 Assessment of Vertical and Lateral Stability

If a channel is vertically unstable and the channel is likely to degrade, an estimate of degradation depth is incorporated into the estimate of total scour depth. Changes in the vertical stability of a stream occur over time, do not always result from a single flow event, and can be difficult to predict. Field assessments of site-specific conditions are helpful in detecting the level of vertical instability. In the geomorphic assessments for this study, the physical character of geologic deposits along stream channels is investigated at each site. Historical channel changes are also reviewed using aerial photography from previous periods. These observations help verify and support the conclusions drawn from the hydrologic and hydraulic analyses. Since vertical stability is a qualitative assessment, all crossings have been assigned ratings to assist the pipeline designer with a system for relative comparison between study sites. The results from the channel stability investigation (chapter 5) and the scour investigation (chapter 6) are integrated in the summary of findings (chapter 7).

Estimating the width of deep burial of a pipeline at a stream crossing is dependent on the lateral stability of a channel. Channel alignments can shift naturally in the horizontal plane, causing scour at pipeline locations that were previously outside the limits of bed erosion during the original design. Lateral stability of a channel is also an assessed, not a computed, value. Field reviews and the use of historical aerial photos are necessary to develop a rating. Lateral stability is addressed in chapter 5 and summarized in chapter 7.

2.4 Field Investigation

Site-specific parameters and terrain observations are needed to develop hydrologic and hydraulic parameters, assess the vertical and lateral stability of streams, and compute scour at each of the 132 sites listed in table 1-1. Jeffrey Riley and Michael Miller, from PXAO, led the site visit of the pipeline stream crossings during the week of April 8-12, 2013. Due to administrative travel restrictions, not all crossings could be visited in the field. Although the proposed alignment was reviewed by TSC staff, only a limited number of stops could be made for field data collection. The list of 132 sites was divided into a main group and a secondary group. A complete set of data was collected onsite at the main sites. Secondary sites were either not visited, or they were visited for a short time to allow collection of a partial data set. Findings from the main sites helped define the range of scour values for the secondary sites in the study area.

2.4.1 Main Sites

PXAO visited most sites to assemble a photo log of the crossings prior to the scour site visit. They identified 17 main crossings to be visited in the field. These crossings were selected for large discharges, wide channels, large sediment

transport volume, large structures, and other concerns. This selection was based on previous field work and verified during development of the photo log.

TSC staff used field data collection, Interferometric Synthetic Aperture Radar (IfSAR) 5-foot contour terrain data, current and historical aerial photos, and the PXAO photo log to expand the list of main crossings from 17 to 22. Most of the crossings with large flows were included as main sites and visited in the field. Crossings with the largest adjacent bridges and box culverts were also identified as main crossings. Several smaller crossings with steeper slopes in the Bitter Springs Spur were added for a broader representation of sediment and hydraulic conditions in the field data collection effort.

During the site visit, a complete set of data was collected at main crossings including:

- Drainage areas and flow
- Measured channel bed slope, cross-section, and bank width
- Observed D_{50} and D_{90} grain sizes of the channel bed
- A bulk sediment sample from the bed of the channel
- Notes on channel alignment and features
- Notes on vegetation and sediment
- Noted structures, obstructions, or constrictions at each pipeline stream crossing and width of openings
- Scour observations and conditions of existing structures
- Assessment of vertical and lateral stability
- High water marks
- Site photos

A longer stop was made at main site, Crossing 96 at the LCR, to acquire data for development of two hydraulic models. LCR is the largest drainage in the study area and was anticipated to have the largest scour depths. Both a one-dimensional HEC-RAS flow model, and a two-dimensional SRH-2D flow model, are used to generate an accurate water surface for this pipeline crossing location and to determine the locations of potential scour. Chapter 4 describes the development of the numerical models for scour computations and water surface elevations.

2.4.2 Secondary Sites

There are 110 secondary sites, and 27 of them were visited in the field by different members of the team. As time allowed, checks were made on office computations of drainage area, stream slopes, bed materials, structures, terrain, and geology. Differing amounts of information were collected at 27 of the secondary sites, and field data was not collected at the remaining 83 secondary sites. Aerial photos, IfSAR contour mapping, and the photo log were the main sources of data for secondary sites not visited in the field. Including main and secondary sites, 49 of the original 132 identified stream sites were visited during the week of field work (table 2-1).

Table 2-1. Sites Visited during the April 8-12, 2013 Field Review

	Main Site No.	Secondary Site No.
	16	2
	20	3
	21	4
	26	7*
	31	13
	32	18
	33	19
	50	23
	51	24
	52	25
	57	27**
	58	34
	84	38
	86	39
	90	41
	92	42
	94	43
	95	44
	96	45
	97	46
	98	52
	125	75
		78
		95
		103
		104
		120
Total	22	27

* Site 7 is a stream segment that is parallel to the road between 7a and 7b.

** Tight alignment near this site.

3. Hydrology: Stream Discharge Estimates

Flows were analyzed at 132 identified river and wash intersections along the proposed pipeline alignment from Lake Powell to Flagstaff, AZ, including spurs to Bitter Springs and Tuba City. Hydrology results are applied in hydraulics (chapter 4), geomorphic (chapter 5), and scour (chapter 6) chapters that follow. Flood frequency estimates were determined using National Streamflow Statistics (NSS) regression equations provided by the United States Geological Survey (USGS). Frequency peak discharge estimates were made for the LCR using historic peak discharge data collected from USGS gages in combination with prehistoric flood estimates.

A site visit was conducted by Reclamation in April 2013 to verify basin attributes and to survey representative cross-sections and channel slope at the 22 main crossings. Survey data was used for slope conveyance calculations.

3.1 Relevant Data

Terrain data for the study area was assembled from 30-meter resolution Digital Elevation Model (DEM) tiles obtained from the USGS National Map (USGS, 2013a). The Environmental Systems Research Institute's Geographic Information System (ESRI AcrGIS) (ESRI, 2009) was used to mosaic the tiles to form a single DEM. The DEM was assigned a projected coordinate system (North American Datum of 1983 - Universal Transverse Mercator 12 [NAD_1983_UTM_12]). The UTM coordinate system was selected to best represent the study area in a plane projection.

Contributing drainage basins were delineated for each of the 140 points where streams and/or washes cross the proposed pipeline alignment. Drainage basins were delineated using ESRI ArcGIS ArcHydro Tools (ESRI, 2012). Basin characteristics including contributing drainage area, average basin slope, average basin elevation, basin length, and basin centroid were estimated for the entire contributing basins using the ArcGIS.

Soil data was obtained from the Natural Resources Conservation Service (NRCS) Soil Data Mart (NRCS, 2013). State Soil Geographic Database (STATSGO) soils data was downloaded for the State of Arizona and was processed through the ArcMap soil data viewer toolbar provided by NRCS. National Oceanic and Atmospheric Administration (NOAA) Atlas 14 precipitation frequency estimates were accessed from the NOAA Precipitation Frequency Data Server (PFDS) (NOAA, 2013b). Volume 1, semiarid southwest regional data rasters, were downloaded for recurrence intervals of interest.

Peak annual streamflow data was accessed through USGS National Water Information System Web Interface (USGS, 2013c). Peak streamflow was used for USGS gage 09402000 - LCR near Cameron, AZ. Although additional sites are located within the study area, no others gage sites have enough data to be included in the analysis.

3.2 Frequency Peak Discharge Estimates– Regression Equations

Estimates of the magnitude and frequency of peak discharges at ungaged stream sites in the Navajo Nation in Arizona, Utah, Colorado, and New Mexico are provided by USGS (2006) and are available on the NSS Web site (USGS, 2013b). Equations are provided for estimating the magnitude of peak discharges for recurrence intervals of 2, 5, 10, 25, 50, 100, and 500 years at ungaged sites, using data collected through 1999 at 146 gaging stations. Peak discharges for selected recurrence intervals were determined at gaging stations by fitting observed data to a log-Pearson Type III distribution. Within specified flood regions, peak discharges for selected recurrence intervals were related to basin and climatic characteristics using stepwise ordinary least-squares regression techniques in log-space. Input parameters are listed in appendix B, section B-1, and include drainage area, average basin slope, and average basin elevation.

The flood-frequency regression equations were applied to the 140 drainage basins where the proposed NCAP pipeline alignment crosses streams and/or washes. Peak discharge estimates for recurrence intervals of 2, 5, 10, 25, 50, 100, and 500 years at all sites are presented in table 3-1. Regression equations are listed in appendix B, section B-2. For consistency, all sites were assumed represented by the same flood region denoted in the 1996 USGS Report as Flood Region 11. As a reference, NOAA Atlas 14 Precipitation Frequency (24-hour duration) values for each watershed are noted in appendix B, section B-3 (NOAA, 2013b).

Table 3-1. Peak Discharge Estimates in Cubic Feet Per Second (ft^3/s) from the USGS Regression Technique

Site No.	Peak Discharge (ft^3/s) for specified return period						
	2-year	5-year	10-year	25-year	50-year	100-year	500-year
1	15	40	65	115	160	225	430
2	40	95	150	255	355	480	870
3	200	495	795	1,330	1,840	2,465	4,405
4	190	465	755	1,270	1,765	2,380	4,290
5	45	115	190	320	450	610	1,115
6	70	175	280	465	640	855	1,530
7a	5	15	25	40	55	75	145
7b	10	25	45	80	115	160	310
8	45	115	185	310	430	585	1,055
9	10	20	30	50	65	90	160
10a	5	10	20	30	40	60	105
10b	5	10	20	30	45	60	115
11a	5	10	15	30	40	60	110
11b	15	35	60	100	145	200	380
12	20	50	85	145	210	295	570
13	30	85	145	260	380	545	1,095
14	30	80	140	250	365	520	1,045
15	20	50	80	135	195	265	495
16	355	885	1,435	2,420	3,380	4,555	8,220
17	110	275	440	730	1,015	1,360	2,440
18	100	245	405	690	975	1,330	2,465
19	55	140	230	400	570	780	1,470
20	170	410	655	1,095	1,510	2,020	3,595
21	85	200	320	530	735	980	1,740
22	35	80	135	220	310	420	760
23	15	35	55	100	140	195	385
24	40	100	165	280	400	550	1,040
25	50	120	200	345	495	680	1,280
26	115	275	440	725	1,000	1,335	2,360
27	100	250	410	695	985	1,340	2,480
28	75	190	315	540	760	1,040	1,940
30	75	190	310	535	755	1,035	1,925
31	60	140	225	370	510	685	1,210
32	330	815	1,320	2,230	3,105	4,180	7,535
33	325	805	1,310	2,220	3,100	4,190	7,595
34	60	150	240	400	555	750	1,350

Table 3-1. Peak Discharge Estimates in Cubic Feet Per Second (ft^3/s) from the USGS Regression Technique

Site No.	Peak Discharge (ft^3/s) for specified return period						
	2-year	5-year	10-year	25-year	50-year	100-year	500-year
35	35	85	140	250	355	490	935
36	20	45	75	125	175	235	430
37	15	45	70	120	170	235	440
38	160	400	645	1,085	1,510	2,030	3,660
39	30	80	135	240	345	480	920
40	35	90	150	260	375	520	1,000
41	40	100	165	290	415	575	1,105
42	60	145	240	410	575	785	1,455
43	70	175	280	475	670	905	1,655
44	70	180	290	490	685	930	1,700
45	30	75	125	215	300	410	760
46	60	150	240	405	565	765	1,400
47	40	100	160	260	360	480	850
48	50	120	195	325	455	610	1,095
49	130	320	515	865	1,205	1,625	2,935
50	205	510	825	1,385	1,925	2,590	4,655
51	205	510	820	1,375	1,915	2,575	4,630
52	255	630	1,015	1,705	2,370	3,190	5,730
53	110	265	420	700	970	1,300	2,315
54	50	125	200	345	485	660	1,230
55	110	280	450	765	1,070	1,445	2,635
56	20	40	65	105	140	185	320
57	40	105	175	300	425	580	1,090
58	445	1,100	1,765	2,955	4,100	5,490	9,785
59	140	385	670	1,230	1,830	2,605	5,295
60	20	45	70	115	155	205	360
61	15	40	60	100	135	180	320
62	20	55	90	155	225	310	585
63a	150	405	710	1,315	1,960	2,800	5,730
63b	150	405	710	1,315	1,960	2,800	5,730
64	30	80	125	210	290	390	700
65	60	155	270	480	705	995	1,975
66a	65	180	310	560	825	1,170	2,350
66b	65	175	305	555	815	1,155	2,325
67	20	45	70	120	160	215	380
68	5	15	25	35	50	65	105

Table 3-1. Peak Discharge Estimates in Cubic Feet Per Second (ft^3/s) from the USGS Regression Technique

Site No.	Peak Discharge (ft^3/s) for specified return period						
	2-year	5-year	10-year	25-year	50-year	100-year	500-year
69	50	130	230	420	625	895	1,835
70	25	65	115	205	300	425	845
71	70	190	335	620	925	1,325	2,740
72	15	35	50	85	120	160	280
73	35	90	155	285	420	595	1,210
74	15	35	60	95	130	175	305
75	225	560	910	1,545	2,165	2,925	5,325
76	15	40	65	110	150	205	370
77	70	190	325	590	860	1,215	2,420
78	55	135	220	385	545	755	1,425
79	140	375	650	1,180	1,735	2,455	4,920
80	20	45	70	110	155	205	365
81	15	30	50	85	115	155	285
82	55	145	255	465	695	995	2,040
83	80	215	370	690	1,025	1,470	3,015
84	90	210	335	545	740	980	1,710
85	25	65	105	175	250	340	630
86	200	475	740	1,190	1,610	2,105	3,590
87	50	130	210	360	505	690	1,270
88	50	120	195	325	455	620	1,135
89	40	100	160	275	385	520	950
90	105	260	410	685	940	1,260	2,235
91	80	195	315	515	710	950	1,680
92	55	130	215	365	510	695	1,280
93	30	65	105	175	240	320	565
94	505	1,180	1,815	2,885	3,850	4,985	8,270
95	95	215	325	515	685	890	1,475
*96							
97	600	1,470	2,355	3,915	5,395	7,195	12,680
98	85	210	350	605	860	1,180	2,225
99	65	165	270	470	665	915	1,715
100	140	340	540	895	1,230	1,640	2,905
101	25	60	95	155	210	275	480
102	135	320	495	785	1,050	1,360	2,280
103	20	45	70	110	145	190	325
104	25	65	100	160	220	285	495

Table 3-1. Peak Discharge Estimates in Cubic Feet Per Second (ft^3/s) from the USGS Regression Technique

Site No.	Peak Discharge (ft^3/s) for specified return period						
	2-year	5-year	10-year	25-year	50-year	100-year	500-year
105	40	90	145	235	325	430	750
106	20	45	70	110	150	195	335
107	20	45	70	115	150	200	345
108	85	195	295	475	635	830	1,400
109	85	200	320	525	720	955	1,675
110	185	460	745	1,250	1,735	2,335	4,195
111a	255	645	1,065	1,830	2,585	3,530	6,535
111b	255	645	1,065	1,825	2,585	3,525	6,530
112	25	65	105	175	240	325	595
113	45	105	170	280	390	520	925
114	30	70	105	170	230	305	525
115	15	35	55	90	130	170	310
116	60	140	220	365	505	675	1,195
117	65	165	270	460	645	875	1,610
118	15	35	55	90	120	155	265
119	25	55	90	145	200	265	460
120	70	170	270	440	600	790	1,375
122a	10	20	30	45	55	70	115
122b	10	20	30	45	55	70	115
123	15	40	60	95	130	170	290
124a	15	25	35	55	65	80	120
124b	50	120	180	285	380	490	820
125	150	355	550	885	1,190	1,560	2,645
126	15	30	50	80	105	140	245
127	15	30	45	75	100	130	220
128	120	285	450	735	1,005	1,335	2,335
129	65	155	245	400	550	730	1,280
130	135	330	535	905	1,265	1,705	3,095
131	40	95	145	245	335	445	795
132	160	405	670	1,160	1,655	2,275	4,290
133	815	2,005	3,210	5,345	7,375	9,830	17,340

* Site No. 96 results were computed using gage data and are shown in figure 3-2.

3.3 Frequency Peak Discharge Estimates–Historic Discharge Data

Historic flood data is available near the proposed alignment crossing at the LCR (Site No. 96), which provides additional flood frequency information for this crossing. USGS gage 09402000: LCR near Cameron, AZ (figure 3-1) is located approximately 12 miles downstream of the proposed alignment. Peak annual streamflow data were available at the LCR gage for 1923, 1929, and 1947 to 2012.

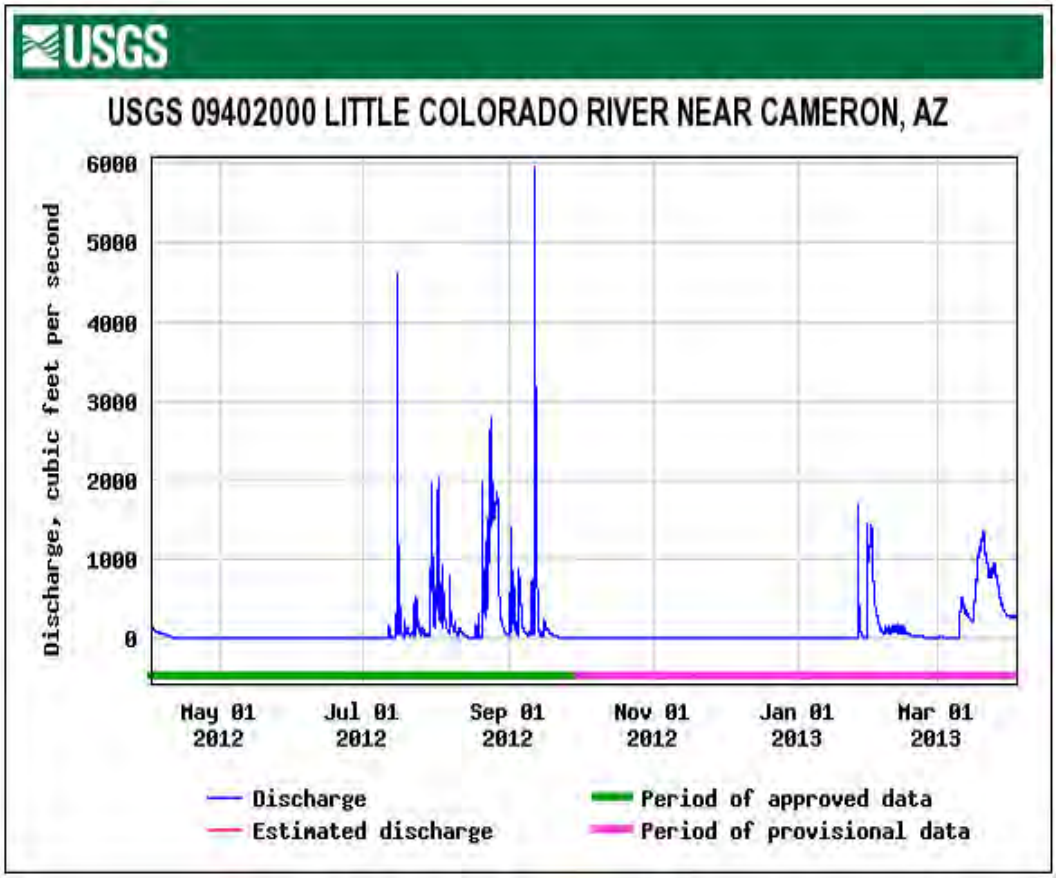

Figure 3-1. LCR flow prior to the April 2013 site visit.

A Log-Pearson Type III curve was fit to the 68 years of peak annual streamflow records. This process is consistent with the procedure described in the "Guidelines for Determining Flood Flow Frequency," Bulletin 17B (IACWD[2], 1982). The computer program "Emfreq," version 1.2 (England, 1999) was used for this analysis. This program requires a text input file of peak discharges in order to compute a peak discharge frequency relationship. Peak discharge for

[2] IACWD refers to the Interagency Committee on Water Data.

1923 and 1929 are historic estimates and were input into the model with a 5-percent (%) uncertainty range. All gage data from 1965 to the present are influenced to an unknown degree by diversions or dams.

The drainage area for the USGS gage station is 26,459 square miles (mi^2) (USGS, 2013c), while the drainage area at the proposed alignment crossing is approximately 23,090 mi^2. Peak discharge data for stream gages can be transferred to an ungaged point by multiplying the discharges by a ratio of the drainage areas. However, because the drainage areas are relatively similar, the gage is located only 12 miles downstream of the proposed crossing, and there is no major confluence between the points, the peak discharge values were assumed to remain unchanged.

Results of the peak annual streamflow analysis are plotted in figure 3-2 and presented in table 3-2. The weighted moments of the final input dataset have a mean of 3.845, standard deviation of 0.322, and a skew of 0.93. No regional skew was assumed for the model (IACWD, 1982); the calculations based on the station's skew alone were sufficient for this case. Gage records used for analysis are listed in appendix B, section B-4. Emfreq model input and output files are available in appendix B, section B-5.

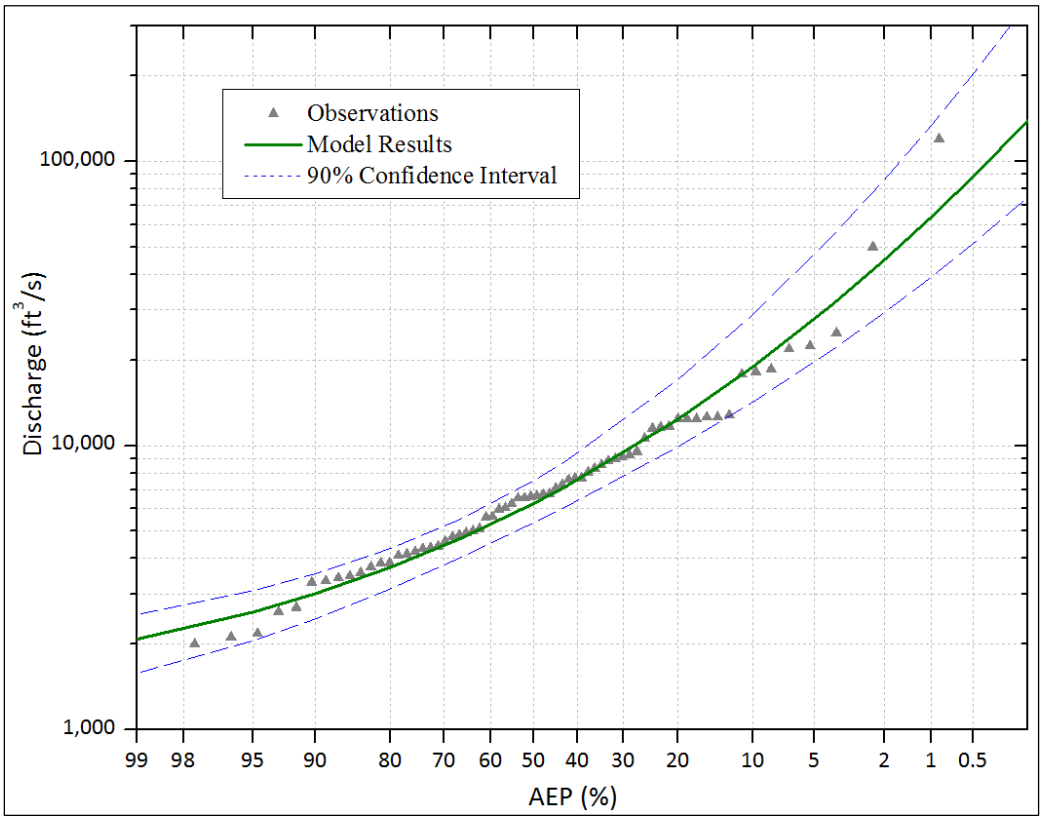

Figure 3-2. Peak annual streamflow analysis, LCR near Cameron, AZ.

Table 3-2. Peak Discharge Estimates for Peak Annual Streamflow Analysis (LCR near Cameron, AZ)

AEP	Return Period	Peak Discharge (ft^3/s)[1]		
		Best Estimate	5% Confidence Limit	95% Confidence Limit
0.5	2	6,300	5,400	7,500
0.2	5	12,400	9,900	17,000
0.1	10	18,900	14,200	28,900
0.04	25	31,400	21,800	54,700
0.02	50	45,000	29,400	86,200
0.01	100	63,600	39,100	133,500
0.005	200	88,700	51,600	203,800
0.002	500	136,100	73,500	350,900

Note: AEP = Annual Flow Exceedance Probability
[1] Peak discharge values are rounded to the nearest 100 ft^3/s.

Peak annual streamflow, including 1965 to the present only, was analyzed by the same methods discussed above for comparison purposes only. The LCR has been engineered, including dams and diversion, which has affected discharge to an unknown degree since 1965 (USGS, 2013c). This alternative analysis yields significantly lower flood frequency estimates. However, the more conservative method, which includes all peak annual streamflow gage data currently available, is recommended for use as peak discharge estimates at the LCR crossing. Alternative analysis results are available in appendix B, section B-6.

4. Hydraulics: Stream Parameters and Water Surface Elevations

Hydrologic information from the previous chapter is applied in this chapter to develop stream hydraulics. Hydraulic information is used to check basin flow and water surface elevations at the main crossings, as well as to determine stream parameters for scour depth computations. Surveyed cross sections are used in an at-a-section analysis to estimate hydraulic parameters at 21 main sites. The 22nd main crossing is the LCR. In table 3-1, the LCR has six times the discharge of Site No. 133, the second largest stream in the project area, and this site was modeled to provide a more detailed representation of the hydraulics at the LCR crossing. Two numerical models of the LCR crossing, HEC-RAS and SRH-2D, are described in the second half of this chapter.

4.1 Real-Time Kinematic Survey

A real-time kinematic (RTK) survey Global Positioning System (GPS) was used to obtain a cross section and a channel profile at each of the 22 main crossings (figures 4-1 and 4-2). In this arid study area, very few of the crossings had standing or flowing water. The Moenkoepi Wash and Willow Creek conveyed spring fed flows, and the LCR had approximately 100 ft^3/s on the day of the survey. Most other crossings were dry, and the bed of the channel was readily observed.

Figure 4-1. Plan view of the proposed pipeline crossing (red line) at Site No. 51. The blue line is the profile survey, and the black line marks the surveyed cross section.

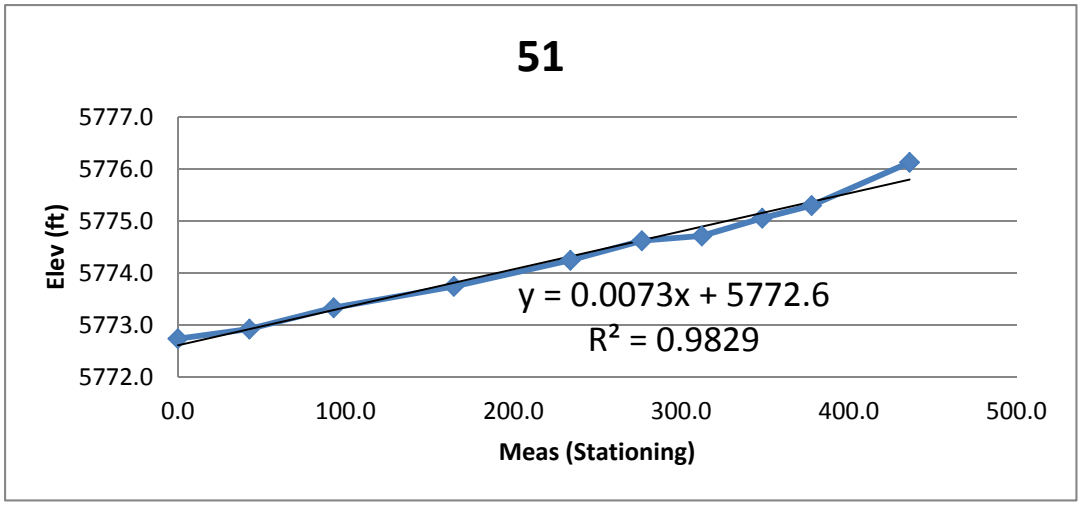

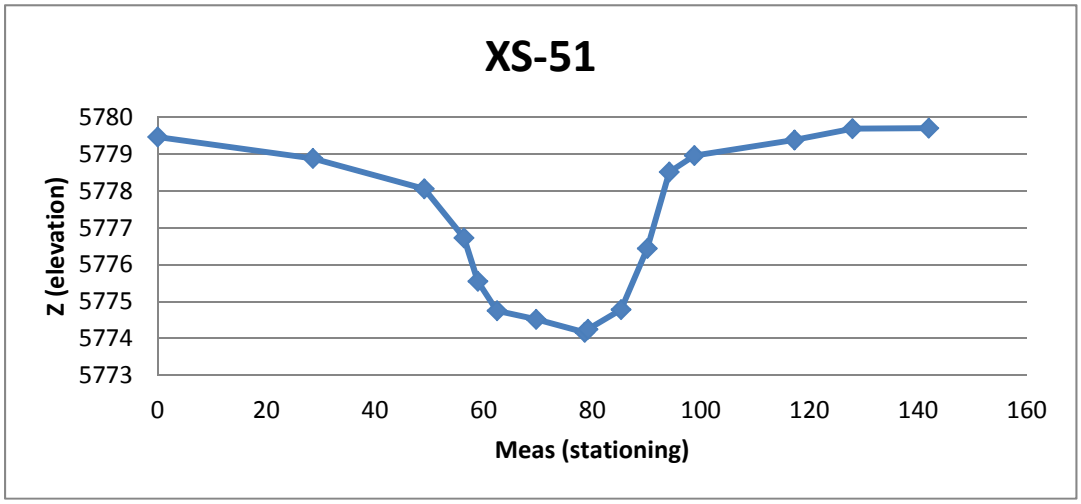

Figure 4-2. Surveyed slope and cross section at Site No. 51.

In addition to the cross section and thalweg slope surveys, cross sections were collected upstream and downstream of the old bridge at the LCR. Cross sections were used to verify LIDAR terrain data. The tops of bridge piles were located on the elevation of the bridge deck, and 2 miles of the water surface profile were recorded for checking model flows. During the cross section surveys at the old Highway 89 bridge, there were up to 6 inches of quicksand. The bottom of the survey rod was a point that easily sank 6 inches into the bed directly upstream and downstream of the bridge, but at greater distances from this location, it sank only 2 inches into the more stable sand bed.

The base station was set up within 5 miles of each site. All survey points were corrected using Online Position User Service (OPUS) (2013a), which provides access to high-accuracy National Spatial Reference System (NSRS) coordinates and uses software that computes coordinates for National Geodetic Survey's

(NGS) Continuously Operating Reference Stations (CORS) network. The resulting positions are accurate and consistent with other NSRS users.

Survey points were converted to cross sections and channel profiles (figure 4-2) for 22 of the 132 study sites. ArcGIS linear referencing was used to determine stationing and location of survey points within a search radius of user-defined cross sections and profiles. Cross sections and channel slope results were used for slope conveyance calculations and scour calculations, as well as flood frequency calculation inputs.

4.2 Hydraulic Parameters and Water Surface Elevation

Bentley Flowmaster V8i (SELECT series 1) software (Bentley Systems, Inc., 2009) was used for at-a-section estimates of flow conveyance at the 22 main pipeline stream crossings. Flowmaster uses the Manning formula with surveyed cross sections and channel slope data to develop peak discharge - normal depth relationships. A roughness coefficient of 0.03 was assumed within the streambed, and 0.05 was assumed to represent overbank flood plain roughness. At Site No. 96, the LCR crossing, slope, and other hydraulic parameters were calculated in the numeric models.

Bankfull, 50-year, and 100-year slope conveyance results for each cross section are shown in table 4-1. Additional flood frequency scenarios (i.e. 5-year, 10-year, etc.) can be modeled with the existing Flowmaster model.

Table 4-1. Hydraulic Parameters Including Water Surface Elevations for Surveyed Cross Sections

Cross section No.	Channel slope (ft/ft)	WSE (ft)	Discharge (ft^3/s)	Flow area (ft^2)	Wetted perim-eter (ft)	Hydraulic radius (ft)	Top width (ft)	Normal depth (ft)	Criti-cal depth (ft)	Velocity (ft/s)	Froude No.
XS-98 (bankfull)	0.020	4728.00	1,626	230	1.34	227	3.05	2.77	5.28	0.80	230
XS-98 (50-yr)	0.020	4727.31	860	157	1.14	154	2.36	2.13	4.82	0.79	157
XS-98 (100-yr)	0.020	4727.62	1180	185	1.25	181	2.67	2.44	5.10	0.80	185
XS-97 (bankfull)	0.009	4726.00	3,702	780	469	1.66	468	2.88	2.36	4.75	0.65
XS-97 (50-yr)	0.009	4726.48	5,395	1,015	504	2.01	503	3.36	2.80	5.31	0.66
XS-97 (100-yr)	0.009	4726.89	7,195	1,226	520	2.36	519	3.77	3.18	5.87	0.67
XS-95 (bankfull)	0.003	4165.00	215	98	88	1.11	88	2.14	1.39	2.20	0.37
XS-95 (50-yr)	0.003	4166.27	685	334	262	1.28	261	3.41	2.32	2.05	0.32
XS-95 (100-yr)	0.003	4166.51	890	400	275	1.45	273	3.66	2.70	2.23	0.32
XS-94 (bankfull)	0.005	4244.80	958	314	207	1.52	206	3.28	2.23	3.05	0.44
XS-94 (50-yr)	0.005	4246.76	3,850	1,018	449	2.27	446	5.24	4.04	3.78	0.44
XS-94 (100-yr)	0.005	4247.18	4,985	1,213	471	2.58	468	5.66	4.34	4.11	0.45
XS-92 (bankfull)	0.009	4329.10	217	70	102	0.69	101	1.62	1.37	3.12	0.66
XS-92 (50-yr)	0.009	4329.74	510	166	202	0.82	201	2.26	1.91	3.07	0.60
XS-92 (100-yr)	0.009	4329.96	695	215	230	0.94	229	2.48	2.11	3.24	0.59
XS-90 (bankfull)	0.001	4330.00	1,261	453	106	4.27	103	8.63	4.03	2.78	0.23
XS-90 (50-yr)	0.001	4328.76	940	338	83	4.04	80	7.39	3.53	2.78	0.24
XS-90 (100-yr)	0.001	4331.33	1,260	707	287	2.46	284	9.96	4.02	1.78	0.20
XS-86 (bankfull)	0.013	4492.30	136	51	157	0.32	157	1.08	1.03	2.67	0.83
XS-86 (50-yr)	0.013	4493.75	1,610	360	333	1.08	332	2.53	2.25	4.47	0.76
XS-86 (100-yr)	0.013	4493.95	2,105	430	343	1.26	342	2.73	2.52	4.89	0.77
XS-84 (bankfull)	0.020	4668.00	214	58	86	0.68	86	1.08	0.98	3.69	0.79
XS-84 (50-yr)	0.020	4668.82	740	132	101	1.30	101	1.90	1.76	5.59	0.86

Table 4-1. Hydraulic Parameters Including Water Surface Elevations for Surveyed Cross Sections

Cross section No.	Channel slope (ft/ft)	WSE (ft)	Discharge (ft^3/s)	Flow area (ft^2)	Wetted perim-eter (ft)	Hydraulic radius (ft)	Top width (ft)	Normal depth (ft)	Criti-cal depth (ft)	Velocity (ft/s)	Froude No.
XS-84 (100-yr)	0.020	4669.11	980	163	110	1.48	109	2.19	2.03	6.03	0.87
XS-58 (bankfull)	0.007	5477.00	875	222	148	1.50	148	2.76	2.17	3.93	0.57
XS-58 (50-yr)	0.007	5479.85	4,100	983	488	2.02	487	5.61	4.35	4.17	0.52
XS-58 (100-yr)	0.007	5480.29	5,490	1,208	524	2.30	524	6.05	5.00	4.54	0.53
XS-57 (bankfull)	0.010	5519.60	195	39	26	1.49	25	2.57	2.17	5.04	0.72
XS-57 (50-yr)	0.010	5520.60	425	116	93	1.25	91	3.56	3.16	3.66	0.57
XS-57 (100-yr)	0.010	5520.86	580	140	94	1.50	91	3.83	3.36	4.13	0.59
XS-52 (bankfull)	0.016	5728.40	1,069	107	39	2.72	37	3.55	3.66	10.02	1.05
XS-52 (50-yr)	0.016	5730.44	2,370	335	144	2.33	139	5.59	5.26	7.07	0.80
XS-52 (100-yr)	0.016	5730.92	3,190	402	145	2.77	139	6.07	5.72	7.94	0.82
XS-51 (bankfull)	0.007	5777.00	371	74	37	1.98	36	2.84	2.20	5.04	0.62
XS-51 (50-yr)	0.007	5780.67	1,915	383	145	2.63	142	6.50	5.59	5.00	0.54
XS-51 (100-yr)	0.007	5781.20	2,575	459	147	3.13	142	7.04	5.97	5.61	0.55
XS-50 (bankfull)	0.008	5787.90	381	75	41	1.80	41	2.75	2.23	5.11	0.67
XS-50 (50-yr)	0.008	5790.97	1,925	453	237	1.91	236	5.82	4.64	4.25	0.54
XS-50 (100-yr)	0.008	5791.38	2,590	554	251	2.21	249	6.24	5.32	4.67	0.55
XS-33 (bankfull)	0.008	5380.00	797	141	98	1.44	98	2.32	2.12	5.64	0.83
XS-33 (50-yr)	0.008	5382.27	3,100	592	263	2.25	262	4.59	3.90	5.24	0.62
XS-33 (100-yr)	0.008	5382.75	4,190	717	270	2.66	269	5.06	4.32	5.84	0.63
XS-32 (bankfull)	0.010	5365.00	4,522	537	205	2.62	205	3.67	3.51	8.43	0.92
XS-32 (50-yr)	0.010	5364.38	3,105	413	193	2.13	193	3.05	2.90	7.52	0.91
XS-32 (100-yr)	0.010	5364.86	4,180	508	202	2.51	202	3.53	3.37	8.23	0.92
XS-31 (bankfull)	0.015	4736.90	111	43	99	0.43	98	0.86	0.76	2.59	0.69

Table 4-1. Hydraulic Parameters Including Water Surface Elevations for Surveyed Cross Sections

Cross section No.	Channel slope (ft/ft)	WSE (ft)	Discharge (ft^3/s)	Flow area (ft^2)	Wetted perim-eter (ft)	Hydraulic radius (ft)	Top width (ft)	Normal depth (ft)	Criti-cal depth (ft)	Velocity (ft/s)	Froude No.
XS-31 (50-yr)	0.015	4737.59	510	118	119	1.00	118	1.55	1.37	4.31	0.76
XS-31 (100-yr)	0.015	4737.80	685	144	124	1.17	123	1.76	1.56	4.74	0.77
XS-26 (bankfull)	0.019	4892.60	110	35	71	0.48	71	1.04	0.98	3.20	0.81
XS-26 (50-yr)	0.019	4894.03	1,000	149	91	1.63	91	2.47	2.38	6.73	0.93
XS-26 (100-yr)	0.019	4894.42	1,335	185	100	1.85	99	2.86	2.75	7.22	0.93
XS-21 (bankfull)	0.026	5156.60	101	26	77	0.34	77	0.88	0.92	3.85	1.17
XS-21 (50-yr)	0.026	5157.35	735	97	99	0.98	99	1.64	1.86	7.57	1.35
XS-21 (100-yr)	0.026	5157.55	980	117	101	1.16	100	1.83	2.11	8.40	1.37
XS-20 (bankfull)	0.014	5148.50	287	56	69	0.81	69	1.21	1.21	5.10	1.00
XS-20 (50-yr)	0.014	5150.02	1,510	172	87	1.98	87	2.73	3.06	8.77	1.10
XS-20 (100-yr)	0.014	5151.25	2,020	367	229	1.60	228	3.96	3.54	5.50	0.77
XS-16 (bankfull)	0.009	5294.80	565	126	93	1.36	91	2.36	1.95	4.48	0.67
XS-16 (50-yr)	0.009	5297.29	3,380	598	241	2.48	237	4.85	4.18	5.65	0.63
XS-16 (100-yr)	0.009	5297.79	4,555	717	243	2.96	237	5.35	4.58	6.36	0.64
XS-125 (bankfull)	0.008	4479.50	264	71	90	0.79	89	1.58	1.43	3.73	0.74
XS-125 (50-yr)	0.008	4480.74	1,190	194	111	1.75	111	2.82	2.57	6.13	0.81
XS-125 (100-yr)	0.008	4481.09	1,560	235	117	2.00	117	3.18	2.91	6.65	0.83

Note: ft/ft = feet per foot, ft^2 = square feet, ft/s = feet per second.

4.3 LCR Models

Table 4-1 lists water surface elevations (WSE) calculated from a single section analysis at each main crossing. This information was requested to aid designers in locating pumping plants and other structures associated with the pipeline construction and operation. The LCR is the largest stream crossing in this study area and is the only location that is modeled to provide WSEs and other hydraulic parameters.

All numerical models require simplifying assumptions and, thus, have limitations. The choice of model is often governed by time and budget constraints, access to and knowledge of existing models, and the ability to develop the model. It is important to understand the formulation of the selected model, recognize the model limitations, and apply the model in a manner that takes advantage of the model's strengths. Numerical model predictions will always include some uncertainty because the physical processes being modeled are not completely represented in a numerical fashion.
The numerical models used for this study were HEC-RAS (v 4.1.0) and SRH-2D (v 3.0). HEC-RAS is a 1D backwater step hydraulic model developed by the USACE. This model was used to simulate cross section averaged river hydraulics for a series of steady, gradually varied flows. The basic computational procedure used in this model is based on the solution of the ID energy equation. Energy losses are represented through friction (Manning's equation) and contraction/ expansion (coefficient multiplied by the change in velocity head). HEC-RAS was used to set the downstream boundary condition for the SRH-2D model simulations, which consisted of a WSE.

SRH-2D is a 2D fixed-bed depth-averaged hydraulic model specifically focused on the flow hydraulics of river systems. SRH-2D adopts a zonal approach for coupled modeling of channels and flood plains; a river system is broken down into modeling zones (delineated based on natural features such as topography, vegetation, and bed roughness), each with unique parameters such as flow resistance. One of the major features of SRH-2D is the adoption of an unstructured hybrid mixed element mesh, which is based on the arbitrarily shaped element method of Lai (2000) for geometric representation. This meshing strategy is flexible enough to facilitate the implementation of the zonal modeling concept; it allows for greater modeling detail in areas of interest, and it ultimately leads to increased modeling efficiency through a compromise between solution accuracy and computing demand. SRH-2D does not currently have the ability to model bridges, while HEC-RAS does have this ability. Hence, the HEC-RAS model was used to evaluate bridge performance and scour under a series of hydrologic flow events. SRH-2D was mainly used to evaluate flow lines via velocity vectors and constriction scour.

4.4 Topography Development

One of the basic pieces of any numerical model is the representation of the surface topography. To represent the model terrain, a multi-resolution, three-dimensional surface was generated in a Geographic Information System (GIS) using a Triangulated Irregular Network (TIN) methodology. The model surface was created entirely from LIDAR data, which was collected in 2012. The bare earth form of the data was used, which filters out first-return data, resulting in data that represents native topography and eliminating such features as tree canopies, building rooftops, and bridge decks. The LIDAR data collection

methodology that was used cannot penetrate water. However, the LCR is ephemeral and was assumed dry at the time of the LIDAR collection, according to a USGS gage (09402000) located roughly 12 river miles downstream of the proposed pipeline crossing near the old Highway 89 bridge. To verify this, in-channel ground survey data was recently collected (April 9, 2013) using a ground-based RTK GPS system and compared to the LIDAR data. Figure 4-3 shows an example cross section of this comparison.

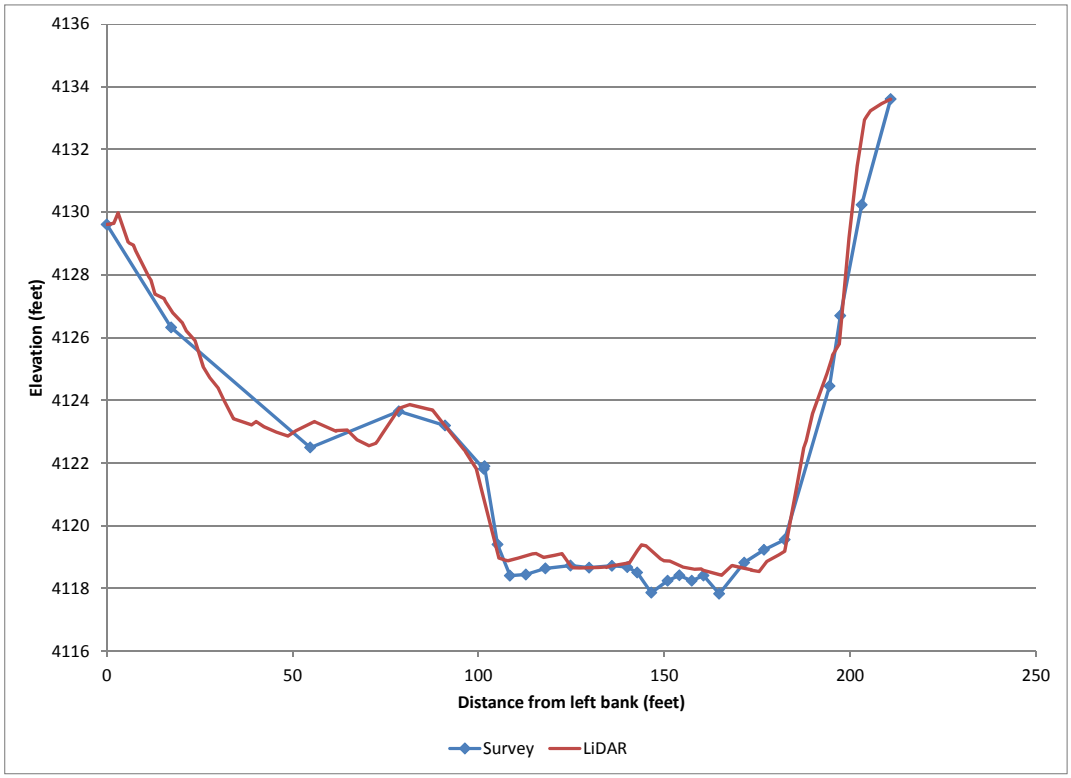

Figure 4-3. RTK survey/LIDAR data comparison along a cross section immediately upstream of the old Highway 89 bridge.

The bare earth LIDAR data was deemed dense enough to use directly in creating the model surface; interpolation schemes were not used. Approximately 1 million points made up the model surface. The upstream and downstream model boundaries were chosen based on the LIDAR extent, while the lateral boundaries were selected to fully contain the highest modeled flow event (500-year event). This resulted in a model domain representing approximately 440 acres that spanned 2.5 river miles; the old Highway 89 bridge is located roughly 0.9 river mile from the upstream boundary. Figure 4-4 shows an example area of the model surface near/around the highway bridges.

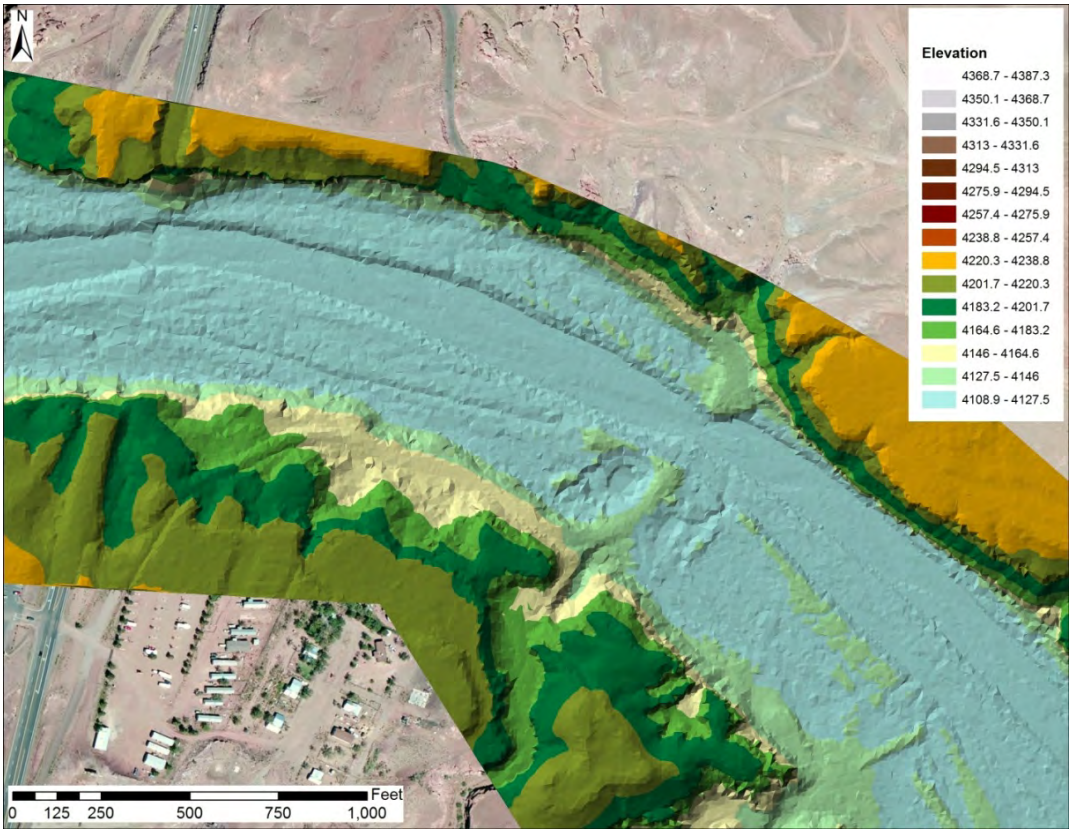

Figure 4-4. Digital topographic surface representation (flow is from right to left).

4.5 HEC-RAS Model

The HEC-RAS model was generated within ArcGIS using the developed topography and a custom interface model between HEC-RAS and ArcGIS (HEC-GeoRAS). Model input data, which include a centerline, bank lines, flow path lines, and cross sections, were developed within the GIS using HEC-GeoRAS. A total of 71 cross sections were used to represent the project area (figure 4-5). The old Highway 89 bridge was represented in the model using the ground survey data from April 2012 (figures 4-6 and 4-7). The bridge deck was assumed to act as a broad crested weir with a weir coefficient of 2.6 for all flows overtopping the bridge. As seen from the field photos, there was debris accumulation on two of the pier pilings that was accounted for in the model. The computational method selected for use in the bridge modeling was the standard step energy equation. The downstream boundary condition was set to a normal depth slope, which was determined by the average bed slope near the lower end of the model domain dictated by the LIDAR data. The upstream boundary condition consisted of various steady flow discharges related to flood recurrence interval events that were determined through a hydrologic streamflow analysis of the downstream USGS gage (table 4-2).

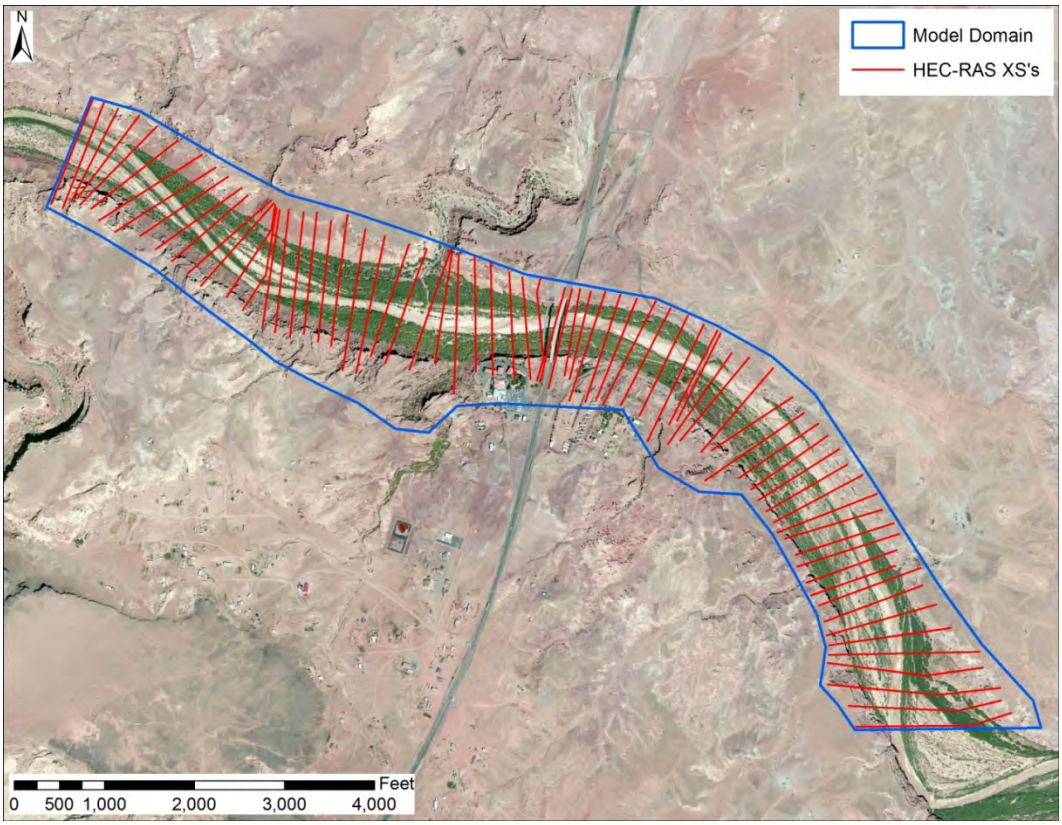

Figure 4-5. Cross sections making up the HEC-RAS model (flow is from right to left).

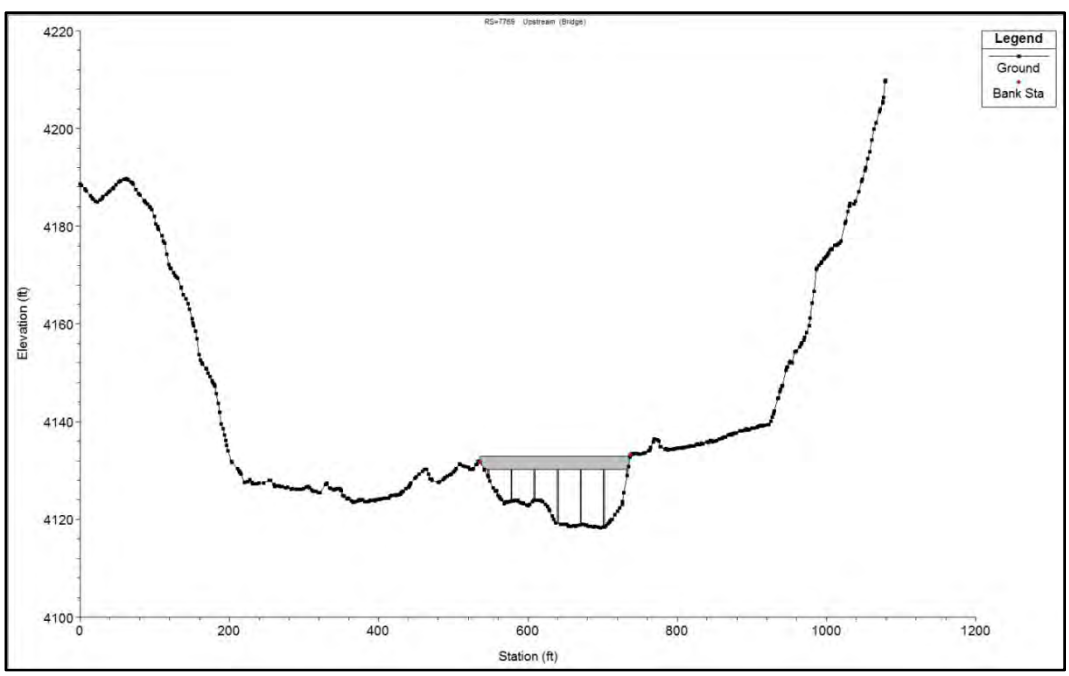

Figure 4-6. Representation of old Highway 89 bridge in HEC-RAS model.

Figure 4-7. Ground survey recording a cross section directly downstream at the old Highway 89 bridge.

Table 4-2. Modeled Flows Based on Hydrologic Streamflow Analysis

	Event							
Flow (ft^3/s)	Average annual[1]	2-year	5-year	10-year	25-year	50-year	100-year	500-year
	2,850	6,300	12,400	18,900	31,400	45,000	63,600	136,100

[1] Average annual peak from 2008-2012.

Model calibration was accomplished through varying Manning's n (roughness) values. A water surface profile for 2 miles of river was available from the ground survey in April 2012, when the flow in the river was estimated to be approximately 100 ft^3/s at the USGS LCR gage (09402000). Using this data, along with past experience, and identifying that the calibration data was collected at a seasonal low flow and likely not applicable to the higher range of flows being modeled, the resultant channel roughness value was set to 0.03. This value resulted in an average difference between the modeled and surveyed water surface elevations of 0.1 foot. Lacking calibration data for the overbanks, the roughness

value for these areas is based on previous modeling experience and the calibrated channel roughness. The resultant assigned overbank roughness value was 0.045.

4.6 SRH-2D Model

A 2D mesh is what drives the SRH-2D model. The mesh stores bed elevation information (the mesh was interpolated to the model surface) and consists of quadrilateral and triangle shaped elements. Surface-water Modeling System (SMS) software was used to generate the mesh and allows for areas with finer mesh cells near areas of interest, such as the main channel, and coarser mesh cells elsewhere. SMS was also used to delineate model roughness areas and assign model boundary conditions.

The fixed bed mesh for this study consisted primarily of quadrilateral elements within the channel and triangular elements in the flood plain/overbank areas. The size of the quadrilateral elements was, on average, 10 feet in the lateral (cross stream) direction and 15 feet in the longitudinal (downstream) direction. The shorter dimension in the lateral direction was used to capture the more rapidly changing topography transverse to the streamflow with respect to horizontal distance. The triangular elements in the flood plain areas increased in coarseness as the model approached the domain boundary to a maximum size of 40 feet. A total of roughly 41,750 elements was used to represent the entire model domain. Figure 4-8 shows an example area of the model mesh near the proposed pipeline crossing.

Hydraulic roughness is the resistance of the channel and overbank topography to the flow, and it is quantified in SRH-2D using the Manning's roughness coefficient. This is the only major calibration parameter for hydraulic modeling. Through SMS, the roughness coefficient may be distributed spatially across the model domain according to material type/land cover. The model domain was broken into four distinct roughness zones, which were delineated based on aerial photography. These four zones included "main channel," "dense flood plain," "sparse flood plain," and "rock/bare earth." Figure 4-9 shows the roughness zone delineations for the model domain.

The corresponding material type roughness values were largely based on the resultant calibration efforts for the HEC-RAS model. Recall that the main channel and overbank roughness in the HEC-RAS model were 0.03 and 0.045, respectively. Roughness values in a 2D model are often lower than those in a 1D model because the 2D model solves for eddy losses independently, as opposed to these losses being lumped into the roughness value or expansion/contraction loss coefficients. Table 4-3 shows the resultant roughness values for the SRH-2D model. The roughness coefficients were held constant for all discharges modeled.

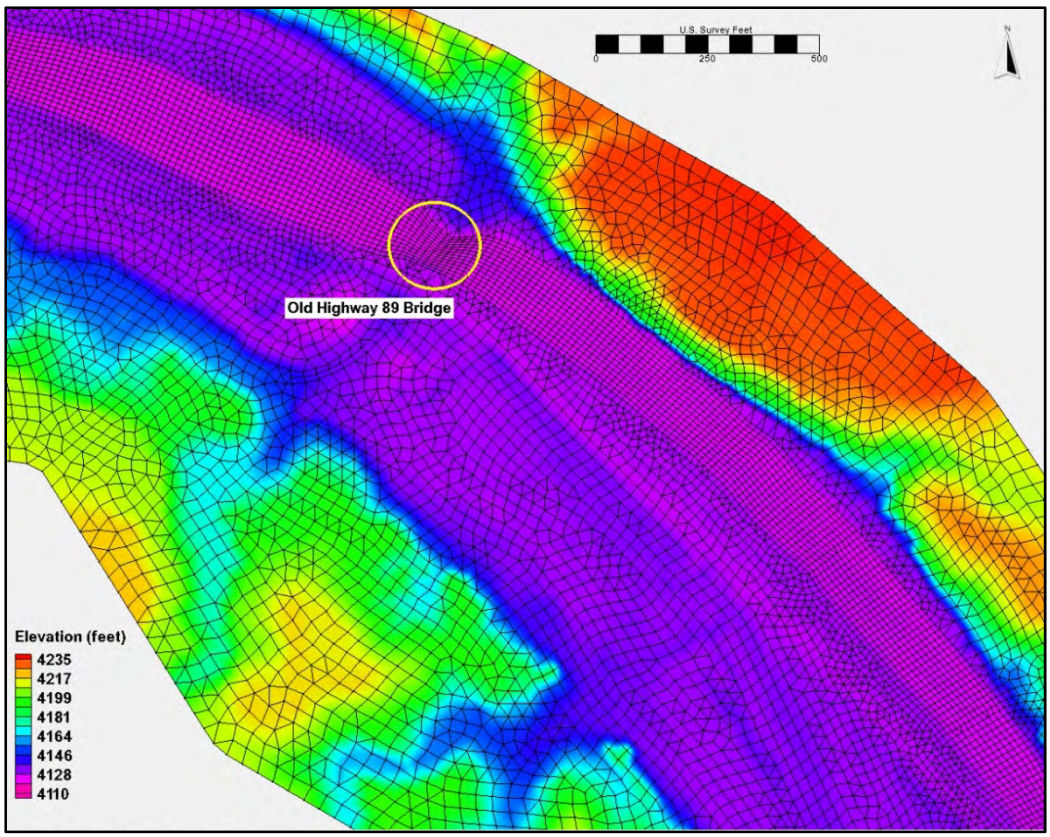

Figure 4-8. 2D mesh against surface topography near the old Highway 89 bridge.

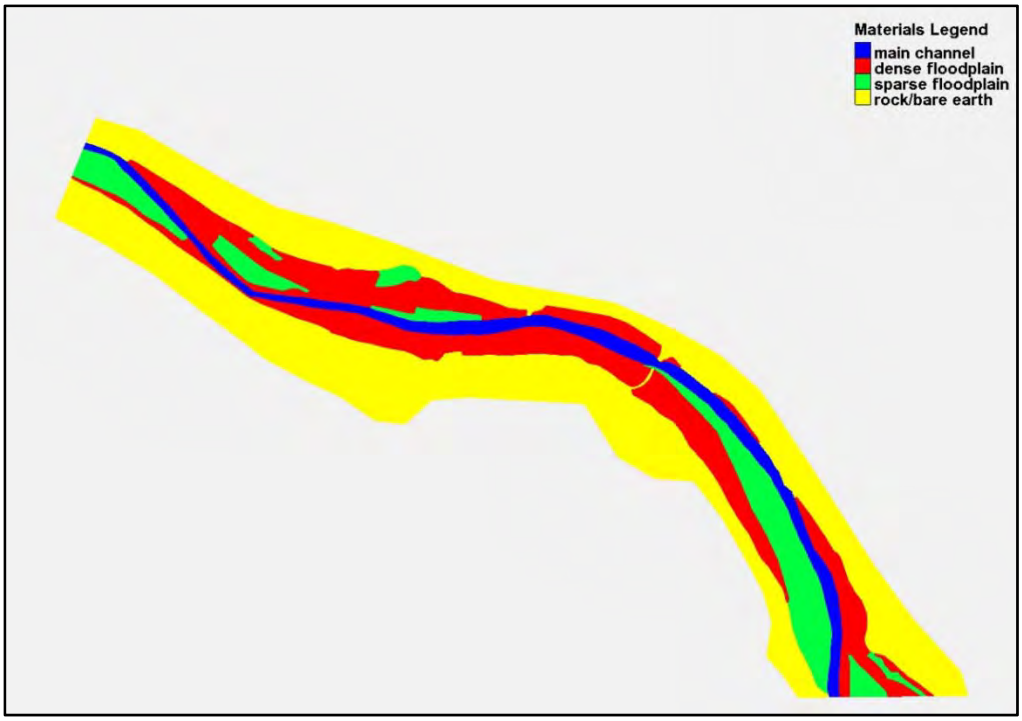

Figure 4-9. Roughness zone delineations for the SRH-2D model.

Table 4-3. Material Type Roughness values for the SRH-2D Model

Material	Roughness value
Main channel	0.025
Dense flood plain	0.045
Sparse flood plain	0.035
Rock/bare earth	0.02

Boundary conditions were specified at the upstream and downstream model extent. The upstream boundary condition was specified as a steady flow input rate (the same as for the HEC-RAS model) (see table 4-2). The downstream boundary was set to a corresponding WSE determined from the HEC-RAS model (see table 4-4). A monitoring line was placed near the model exit to ensure conservation of flow. A monitoring point was also placed at the proposed crossing location and used to evaluate the change in hydraulic parameters over time. This information was useful in evaluating model stability. A 3-second time step was initially used for all model runs. However, 3- to 5-foot oscillations in the water surface elevation were seen in the 100- and 500-year simulations, indicating model instability. To remedy this, the time step was decreased to 1 second for the 100-year simulation and even lower, to 0.05 seconds, for the 500-year simulation. Figure 4-10 shows the WSE changes with time at the monitoring point at a 1- and 3-second time step for the 100-year event. The model instability can be seen in the 3-second simulation, along with its elimination in the 1-second simulation.

Table 4-4. HEC-RAS WSEs used for SRH-2D downstream boundary condition

Event	Q total (ft^3/s)	WSE (ft)
Average annual	2,850	4117.5
2-year	6,300	4119.9
5-year	12,400	4122.5
10-year	18,900	4124.6
25-year	31,400	4127.7
50-year	45,000	4130.6
100-year	63,600	4134.0
500-year	136,100	4144.3

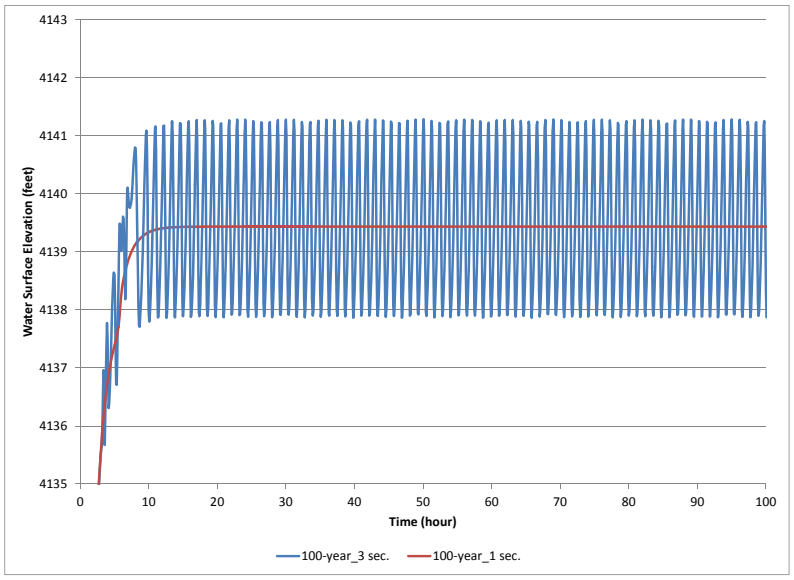

Figure 4-10. WSE change over time at monitoring point near proposed crossing.

4.7 HEC-RAS Model Results

Numerical modeling provides a detailed description of flow hydraulics that aid the analysis and design of the pipeline crossing. The pipeline may be suspended or mounted on the old Highway 89 bridge across the LCR, or it may be buried in the channel at a location upstream (figure 4-11) or downstream of the old Highway 89 bridge. WSEs are generated by the HEC-RAS model at increasing peak flow events at every cross section.

Figure 4-11. Looking upstream from the old Highway 89 bridge.

A cross section immediately upstream of the bridge is shown in figure 4-12 with the water surface elevations for peak flows. The cross section and water surface elevations at the cross section directly downstream of the old Highway 89 bridge can be seen in figure 4-13. At a 5-yr flow there is very little clearance between the water surface and the bottom chord of the bridge. A 10-yr flow creates constricted and pressurized flow through the bridge opening both upstream and downstream of the bridge, and a 25-yr flow overtops the deck.

Table 4-5. Hydraulic Parameters for the Cross Sections Upstream and Downstream of the Bridge

River station	Q total (ft^3/s)	Recur-rence	Minimum channel elevation (ft)	**WSE (ft)**	E.G. elevation (ft)	E.G. slope (ft/ft)	Velocity channel (ft/s)	Flow area (ft^2)	Top width (ft)	Froude No. channel
8126	12,400	5-yr	4118.75	**4130.27**	4130.5	0.000528	4.55	4,058.56	644.14	0.25
8126	18,900	10-yr	4118.75	**4132.26**	4132.54	0.000549	5.22	5,339.54	646.6	0.26
8126	31,400	25-yr	4118.75	**4135.19**	4135.58	0.000602	6.31	7,239.15	652.11	0.29
8126	63,600	100-yr	4118.75	**4141.23**	4141.86	0.000632	8.09	11,223.51	665.55	0.31
7965	12,400	5-yr	4118.48	**4130.17**	4130.41	0.000553	4.74	3,938.1	639.15	0.26
7965	18,900	10-yr	4118.48	**4132.14**	4132.45	0.000578	5.44	5,209.84	646.4	0.27
7965	31,400	25-yr	4118.48	**4135.06**	4135.48	0.000632	6.54	7,109.94	655.56	0.29
7965	63,600	100-yr	4118.48	**4141.1**	4141.76	0.000657	8.31	11,114.19	670.65	0.32
7795	12,400	5-yr	4118.24	**4129.68**	4130.24	0.001601	6.6	2,422.01	467.34	0.41
7795	18,900	10-yr	4118.24	**4131.58**	4132.27	0.001628	7.46	3,374.58	527.4	0.43
7795	31,400	25-yr	4118.24	**4134.46**	4135.3	0.001499	8.49	4,942.35	580.16	0.43
7795	63,600	100-yr	4118.24	**4140.56**	4141.59	0.001155	9.78	9,082.37	738.22	0.4
7769	Bridge									
7743	12,400	5-yr	4118.39	**4128.92**	4129.97	0.002831	8.31	1,625.28	462.48	0.55
7743	18,900	10-yr	4118.39	**4130.8**	4131.96	0.002554	9.09	2,657.17	580.93	0.54
7743	31,400	25-yr	4118.39	**4133.94**	4135.03	0.00187	9.39	4,666.87	667.43	0.48
7743	63,600	100-yr	4118.39	**4140.33**	4141.41	0.001188	9.97	9,011.82	704.01	0.41
7587	12,400	5-yr	4118.23	**4129.28**	4129.55	0.000646	4.72	3,591.08	605.4	0.27
7587	18,900	10-yr	4118.23	**4131.18**	4131.53	0.00069	5.52	4,766.57	624.37	0.29
7587	31,400	25-yr	4118.23	**4134.21**	4134.67	0.000703	6.53	6,672.42	634.92	0.31
7587	63,600	100-yr	4118.23	**4140.46**	4141.16	0.00068	8.19	10,704.95	656.89	0.32
7387	12,400	5-yr	4117.19	**4129.06**	4129.41	0.000709	5.14	3,300.93	628.47	0.29
7387	18,900	10-yr	4117.19	**4130.96**	4131.38	0.000738	5.9	4,502.43	637.25	0.3
7387	31,400	25-yr	4117.19	**4133.99**	4134.52	0.00074	6.89	6,449.59	648.11	0.32
7387	63,600	100-yr	4117.19	**4140.27**	4141.02	0.000691	8.43	10,591.84	667.37	0.32

Note: E.G. = Energy Gradeline

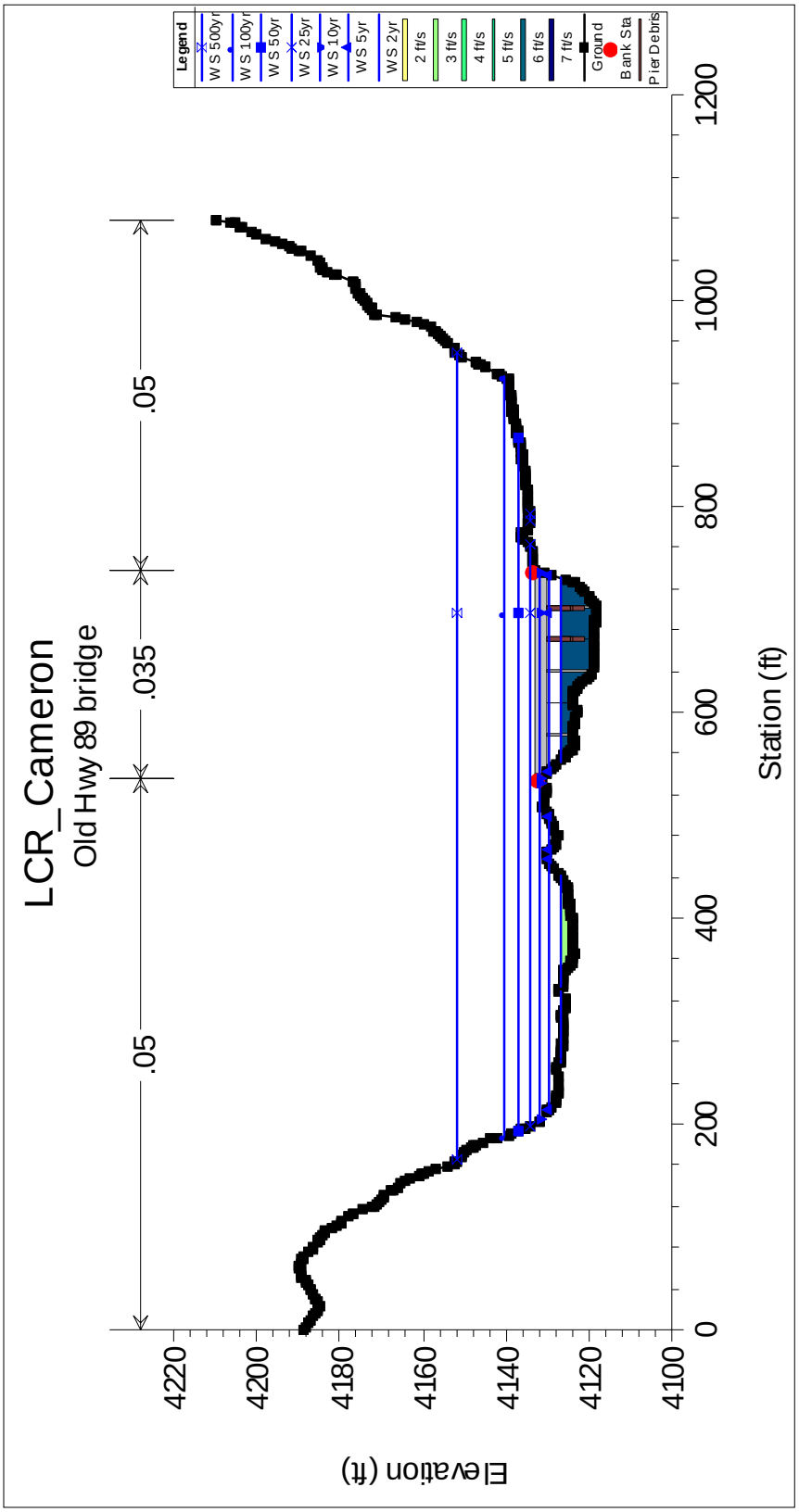

Figure 4-12. WSEs and velocities for the upstream cross section at the old Highway 89 bridge.

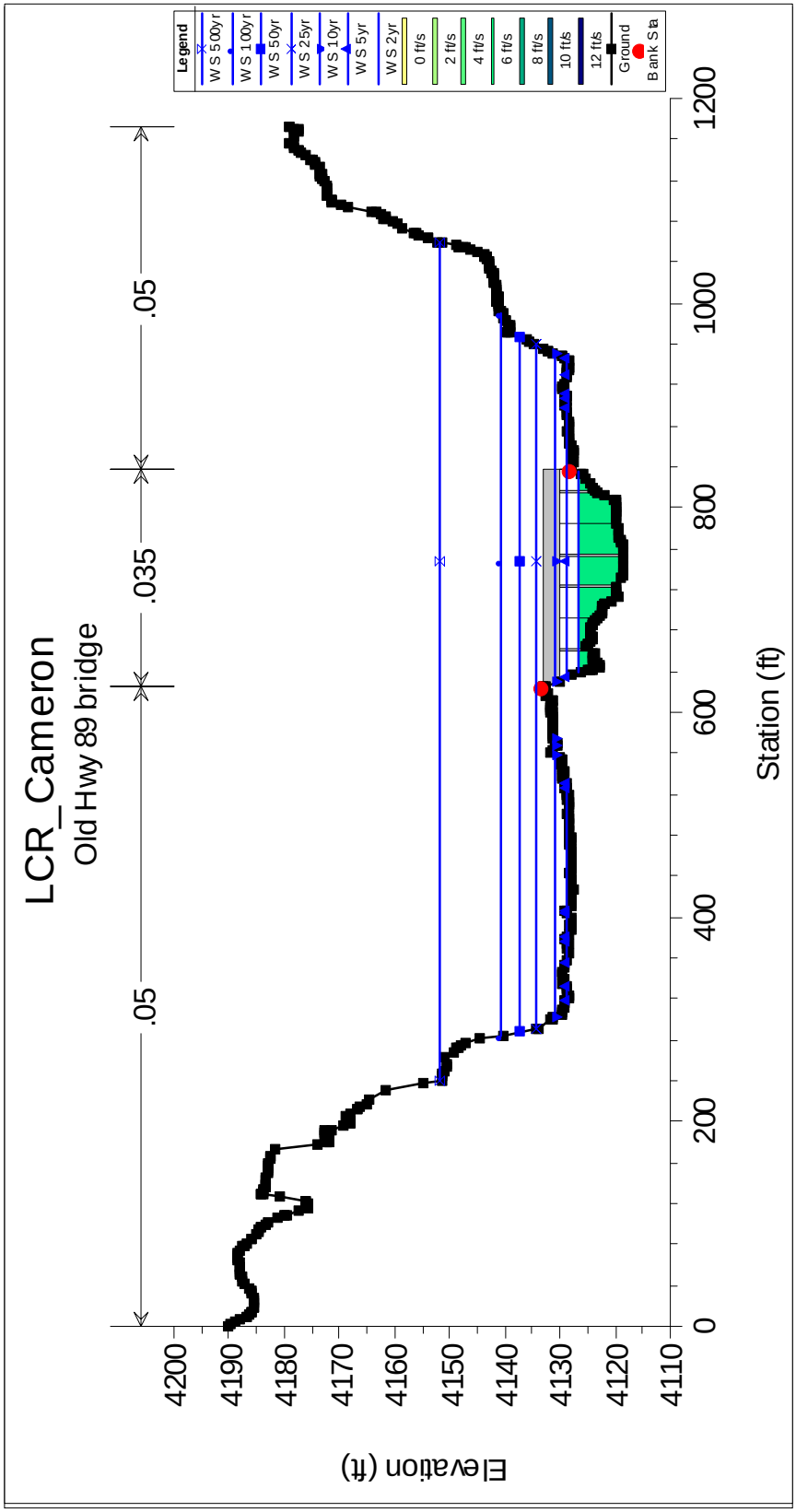

Figure 4-13. WSEs and velocities for the downstream cross section at the old Highway 89 bridge.

At a 50-year and 100-year peak discharge, more flow is conveyed over the bridge and in the flood plain outside the bridge limits than under the bridge. If a pipeline was mounted or suspended from the old Highway 89 bridge, it would be submerged and subjected to the flow velocities listed in table 4-5 on multiple occasions during a typical 50-year design life. Flow is exiting the bridge conveyance area during a 10-year flow event at 9 ft/s due to pressurized flow. In comparison, the average velocity for this cross section increases only 11% (10 ft/s) from a 10-year flow event to a 100-year flow event.

4.8 SRH-2D Model Results

The main objective of the hydraulic modeling was to evaluate the spatial distribution of various hydraulic parameters near the proposed pipeline crossing over a range of flow conditions. Spatial distributions provide a means for determining the location and magnitude (where and how they increase or decrease from one simulation to the next) of changes in the hydraulic parameters. This evaluation was performed using SMS software. The predicted hydraulic parameters from SRH-2D included flow depth, depth-averaged velocity and velocity vectors, shear stress, WSEs, etc. It is important to keep in mind that results only show the river hydraulics from the existing channel configuration and do not provide any prediction on potential future channel morphological changes.

The model results showed increased velocities in the main channel in the area near/around the old Highway 89 bridge due to an existing channel constriction. This indicates the likelihood of localized channel adjustments through contraction scour. The zone of increased velocity occurred near the proximity of the proposed crossing and had little propagating effects in the main channel. The flow velocity vectors in this area did not show any noticeable recirculating eddy patterns, confirming that contraction scour is the main factor driving the potential bed adjustment. The maximum velocities, roughly 10.5 ft/s) were seen at the 5-year (12,400-ft^3/s) event, above which the magnitudes started to decrease as more water dissipates over the adjacent flood plains, no longer confined to the main channel. This is true up until the 100-year event, where the velocities reached upwards of 12.5 ft/s in the proposed crossing area. This is likely because at this event, the water is once more confined, this time against the valley walls, having no more flood plain available to dissipate energy. Figures 4-14 through 4-17 show the resultant velocity magnitudes/vectors and depths for the 5- and 100-year events near/around the proposed crossing. The constriction area of influence, where the contraction scour will occur, shows well in the 5-year velocity plot.

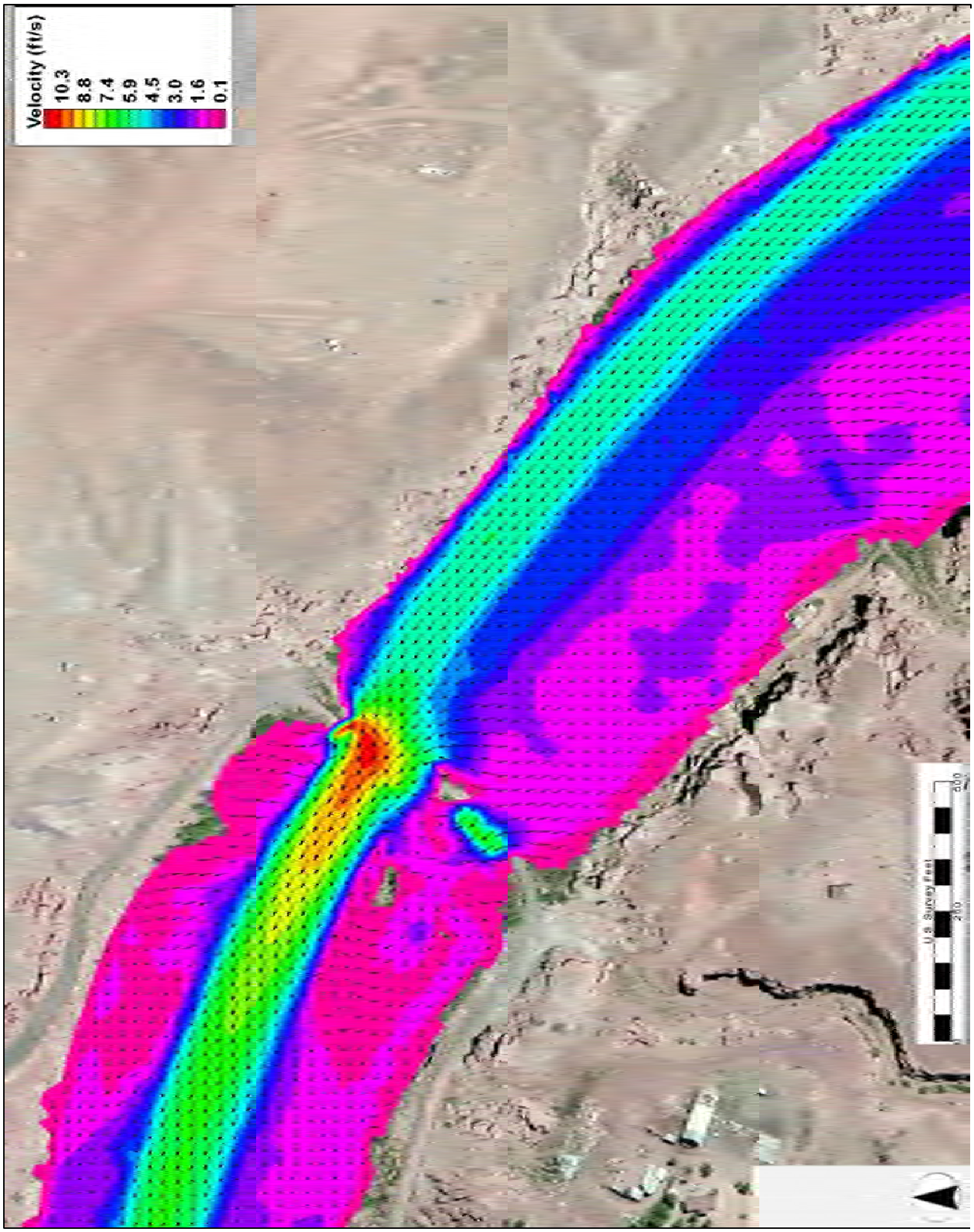

Figure 4-14. Velocity magnitudes/vectors for the 5-year (12,400-ft^3/s) event.

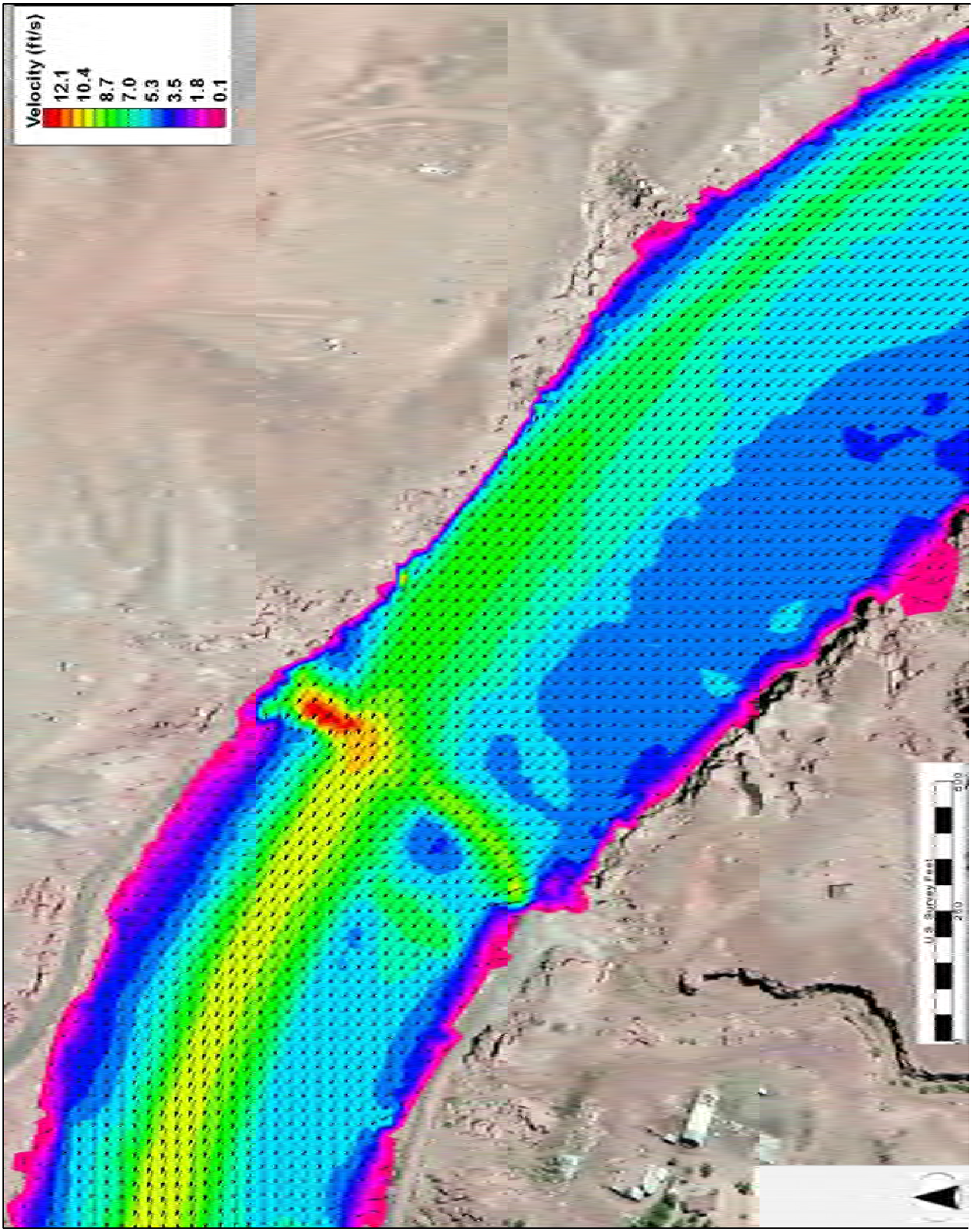

Figure 4-15. Velocity magnitudes/vectors for the 100-year (63,600-ft^3/s)event.

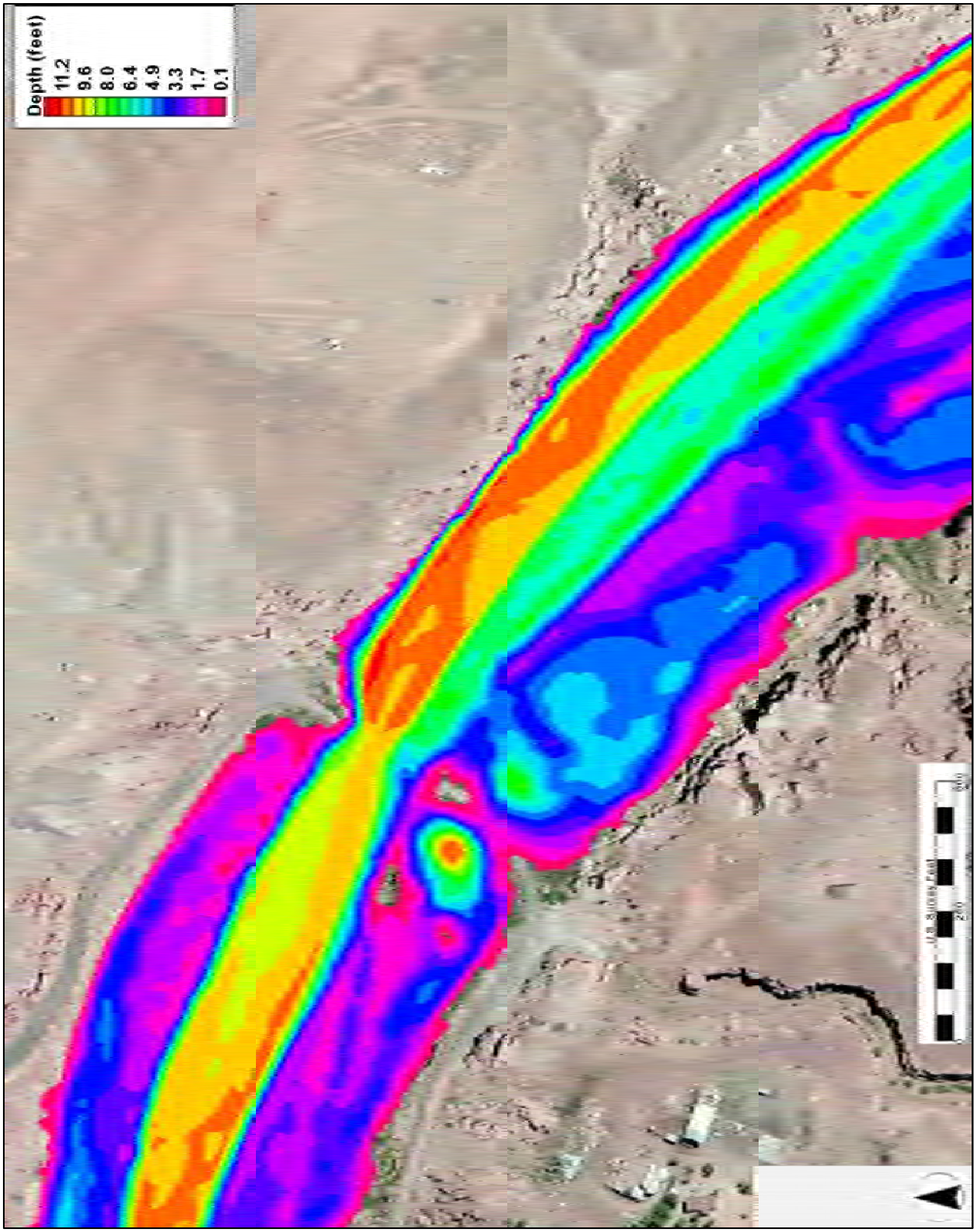

Figure 4-16. Depths for the 5-year (12,400-ft^3/s) event.

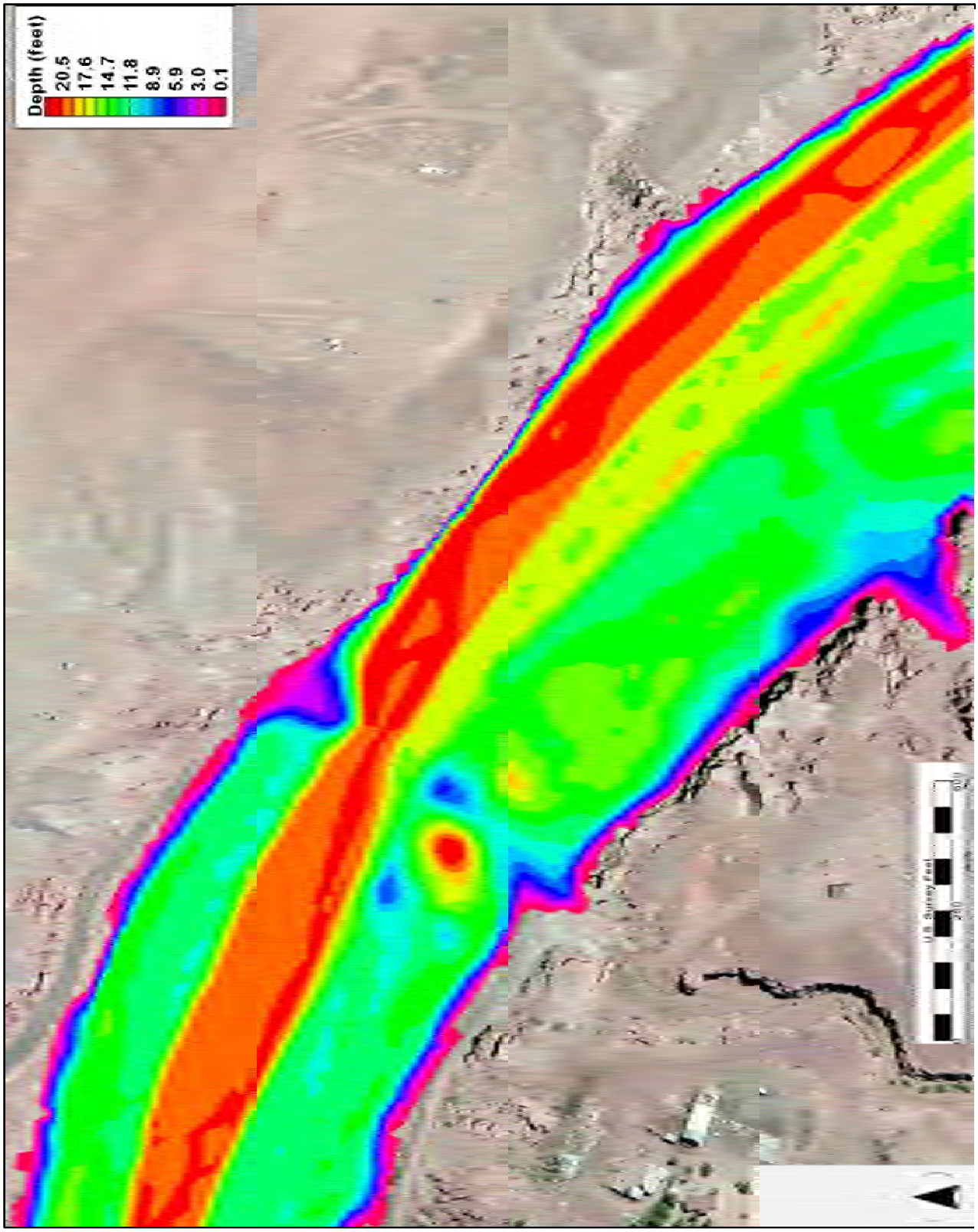

Figure 4-17. Depths for the 100-year (63,600-ft^3/s) event.

5. Geomorphology: Vertical and Lateral Stability of Streams

This chapter provides information about the geomorphic character of stream crossings along the proposed alignment in support of hydraulic and hydrologic computations that are being performed for this study. Geomorphic data provide information about the lateral and vertical stability of the river channel at the crossing locations through investigations of the physical character of geologic deposits along stream channels and historical channel changes using aerial photography. These observations help to verify and support the conclusions drawn from the hydrologic and hydraulic components of the scour analysis.

An assessment of high vertical instability at a stream crossing will indicate a need to increase the estimate of maximum depth of scour for that location. An assessment of lateral stability determines the distance or width of a stream and flood plain crossing, as well as the burial distance required for the pipeline. A prediction of lateral stability may also help determine adequate spacing between the road and river when the pipeline and road parallel the river.

5.1 Methodology

As part of the scour analysis, geomorphic characteristics were described at 27 main sites to provide a basis for conclusions about vertical and lateral stability of the channel at each site. This geomorphic grouping included all 22 main sites and 5 secondary sites that were added as time allowed. Detailed information from the 27 mapped sites was used to evaluate the remaining 105 secondary sites not visited in the field.

At the majority of the 27 sites, landforms were mapped on aerial photography for at least 100 feet upstream and downstream of the proposed crossing, or for a distance that was feasible for the amount of time available. Features that were mapped included bedrock in the channel bed or banks, stream terraces, flood plains, alluvial fan deposits, channel deposits and channel bars, and islands. Human features such as berms and embankments were also roughly mapped when they were adjacent to the channel. Characteristics such as channel relief, bed material, bank materials, knickpoints, high water marks, height and character of geomorphic surfaces, and a schematic cross section at the proposed alignment crossing were described on a field datasheet for each site.

5.2 Site Descriptions

A description of factors that contribute to the determination of lateral and vertical stability of a stream is presented below for 27 sites.

5.2.1 Site No. 13

Figure 5-1. Site No. 13 looking upstream. The bucket marks the pipeline crossing.

The channel at Site No. 13 is a single channel with high amplitude meanders. The channel is incised about 5 feet into sand dunes and slope deposits from nearby bedrock. Streambanks are weakly consolidated and are composed of reddish, sandy sediments. Channel bars are poorly formed, unvegetated, and less than 1 foot above the channel bed. A review of historical aerial photography shows negligible channel movement between 1992 and 2012. The width of potential lateral movement includes areas on both sides of the channel due to the unconsolidated nature of the sediments and the potential for lateral erosion. This width is equal to about 60 feet. There are no field indications for continued incision such as downstream headcuts.

5.2.2 Site No. 16

Figure 5-2. Site No. 16 looking upstream. The proposed alignment is adjacent to the sediment sampling site.

The channel at Site No. 16 is a single channel with broad, low-amplitude meanders (figures 5-2 and 5-3). The channel is braided at low flow and exhibits less than 5 feet of relief from the base of the thalweg to the top of unvegetated bars. Along the right bank near the crossing, a 5- to 10-foot-high terrace exists that has beds of pebbles and cobbles. On the left bank, a 1- to 2-foot-high flood plain surface is composed of unconsolidated sandy sediments. Flotsam can be observed on this surface and, along with the weak soil development, indicates that this surface is inundated frequently. A second terrace may be present above the flood plain surface on the left bank, but it is not well preserved. Bedrock outcrops were not observed at the channel crossing; however, bedrock may be present in the left bank downstream of the bridge. A review of historical aerial photography from 1953 to 2012 shows negligible change in the lateral channel position at the proposed crossing. It is possible, however, for the

channel to laterally migrate or avulse into the flood plain area because these sediments are unconsolidated, elevated only 2 feet above the channel bed, and show evidence of overtopping. The width of potential lateral movement along the proposed alignment, therefore, includes these areas and measures approximately 200 feet. There are no indicators that this section of channel is vertically unstable. Also, bedrock does not appear to be present in the channel bed, which could limit potential incision. It is likely, therefore, that incision would be limited to the amount computed by the bed scour equations.

Figure 5-3. Geomorphic features at Site No. 16. The red line shows the proposed alignment, and the blue line shows the width of potential lateral channel movement.

Figure 5-4. Site No. 18 looking downstream from the old bridge.

5.2.3 Site No. 18

The channel at Site No. 18 is braided with multiple channels that flow through vegetated bars (figure 5-4). Channel relief is 2 to 3 feet from the thalweg to the top of channel bars. Riprap and bedrock are located along the right bank at the proposed alignment crossing. Along the left bank, older alluvial fan materials associated with the

wash exist. Historical aerial photography between 1953 and 2012 reveals shifts in the dominant channel position within the braided channel along the reach near the proposed alignment. While lateral shifts in the channel are possible, it is likely that the width of the active channel at the crossing will remain similar (or about 120 feet). While bedrock was not observed in the channel bed, there are no indications that the channel would undergo significant incision in the future.

5.2.4 Site No. 20

Figure 5-5. Site No. 20 with concrete in channel bed at old road.

The channel at Site No. 20 is a straight, single channel that exits from a culvert under Highway 89 upstream of the proposed pipeline alignment (Figure 5-5). Downstream of the crossing, the channel expands into a braided, distributary planform with multiple channels that fan out from the main channel (figure 5-6). These channels feed into the main trunk stream approximately 1,200 to 1,500 feet downstream from the crossing. Along the left bank at the crossing, a berm associated with the old highway is armored with riprap and blocks distributary channels from exiting the main channel. A narrow flood plain surface exists adjacent to the channel on both sides and is about 2.5 feet above the channel bed. A higher terrace surface that is about 4.5 feet above the channel bed grades into upland landforms. Recent high water marks in the form of flotsam and flattened bushes are about 2.5 feet above the channel bed. Channel relief is less than 1foot at the crossing between the base of the thalweg and the top of unvegetated bars. Review of historical aerial photography from 1953 to 2012 reveals negligible change in lateral channel position. At the crossing, shifts in channel position are unlikely and should be limited to the channel and narrow overbank areas (or about 100 feet). Channel avulsions immediately downstream of the crossing are possible, especially on the left (north) bank. Should these avulsions occur along the left bank, they would shorten the channel length from the proposed alignment crossing to the main wash and could potentially trigger incision.

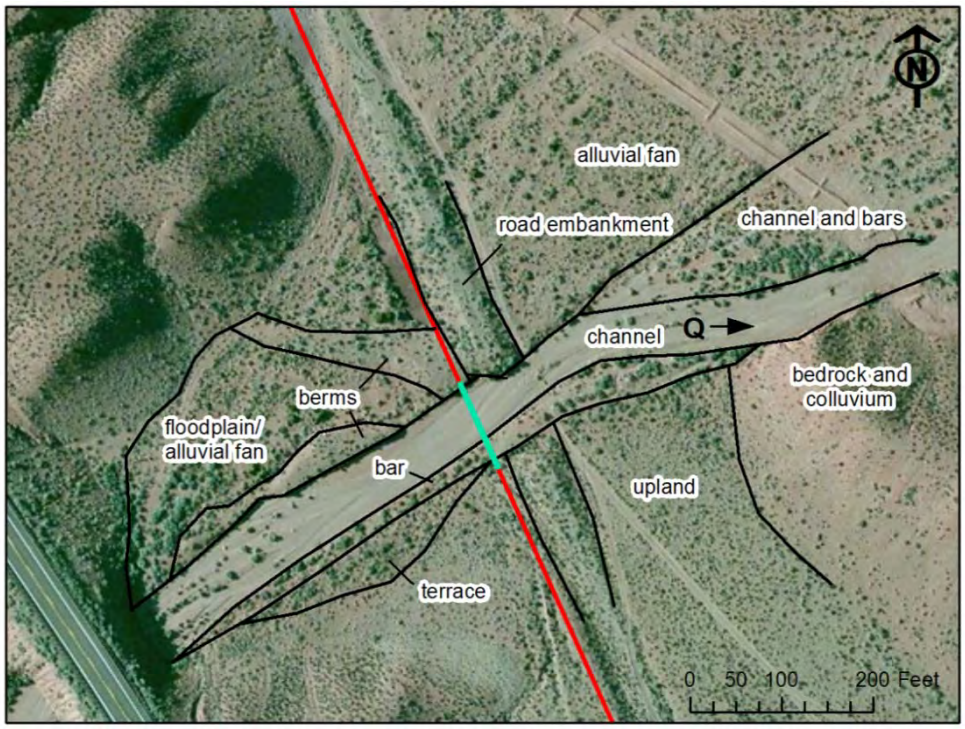

Figure 5-6. Geomorphic features at Site No. 20. The red line shows the proposed alignment, and the blue line shows the width of potential lateral channel movement.

5.2.5 Site No. 21

Figure 5-7. Site No. 21 looking upstream.

The channel at Site No. 21 is braided with multiple channels split around vegetated bars (figures 5-7 and 5-8). The channel bed exhibits less than 1 foot of relief between the top of the unvegetated bars and the channel thalweg. A narrow terrace is located along the left bank at the crossing, about 3 feet above the channel bed, and it is composed of bedded sand and gravel. Flotsam was observed wrapped around bushes on vegetated bars but not on the terrace surface. At the crossing, the channel is laterally confined by bedrock and colluvium along the left bank and high berms built to direct flow along the right bank. These berms were reconstructed after 1997 following breaches of previous berms between 1953 and 1997. Due to the lateral constraints on both sides of the wash at the proposed crossing, the potential for lateral migration is limited to the width of the existing channel and the narrow overbank area along the left bank,

which measures about 140 feet. Although bedrock was not observed in the channel bed at the crossing or downstream from the crossing, there are no potential mechanisms for incision that would suggest incision greater than the local scour of the channel bed as calculated in the scour analysis.

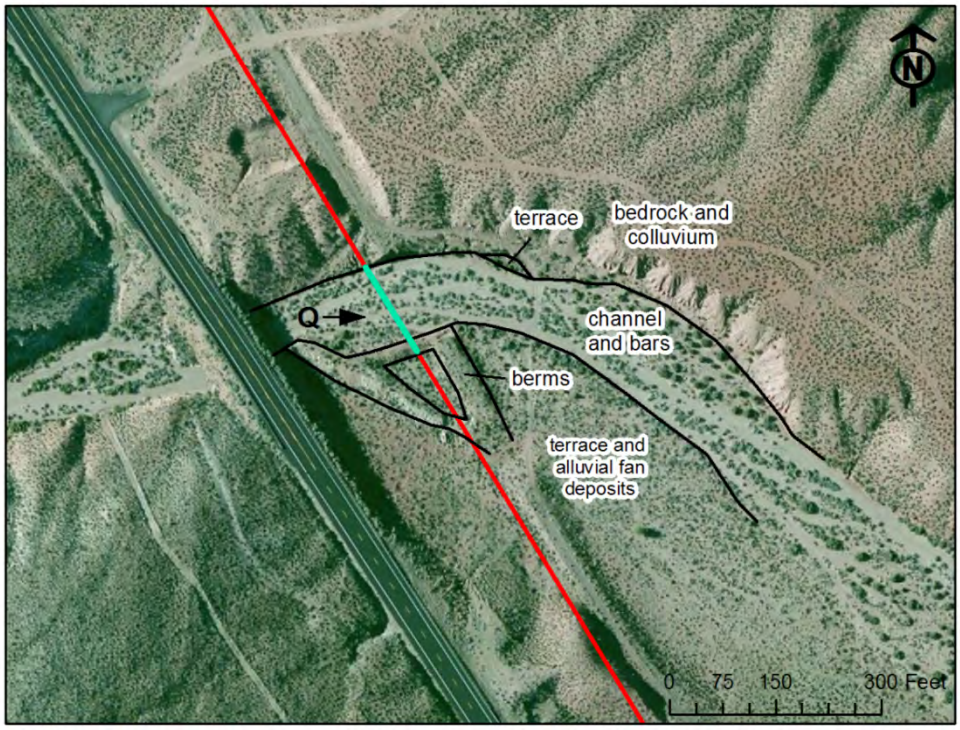

Figure 5-8. Geomorphic features at Site No. 21. The red line shows the proposed alignment, and the blue line shows the width of potential lateral channel movement.

Figure 5-9. Site No. 26.

5.2.6 Site No. 26

At Crossing 26, the channel is single thread and straight, joining a larger wash approximately 500 feet downstream from the alignment crossing (figures 5-9 and 5-10). Older alluvial fan surfaces are adjacent to the channel on both sides of the wash at the crossing and are about 3 feet above the channel bed. Soils on these surfaces are moderately indurated with clay stains and carbonate coatings on the undersides of the clasts; thus, these surfaces limit significant lateral movement of the channel at the proposed alignment crossing to the width of the channel (or about 70 to 75 feet). Downstream of the crossing, lower alluvial fan surfaces are

present that are formed by the present tributary drainage and that may also have some sediment derived from the mainstem wash as well. These surfaces are less than 1 foot above the channel bed and have weakly developed desert pavement in some areas. Minor vegetated bars are located within the channel and are less than 1 foot above the channel bed and have flotsam wrapped around bushes. Bedrock was not observed in the channel bed or banks. Channel avulsions would not cause a significant change in bed elevations at the crossing because the confluence with the main wash is only a short distance downstream. Therefore, the potential for incision that is greater than local scour is low at this crossing.

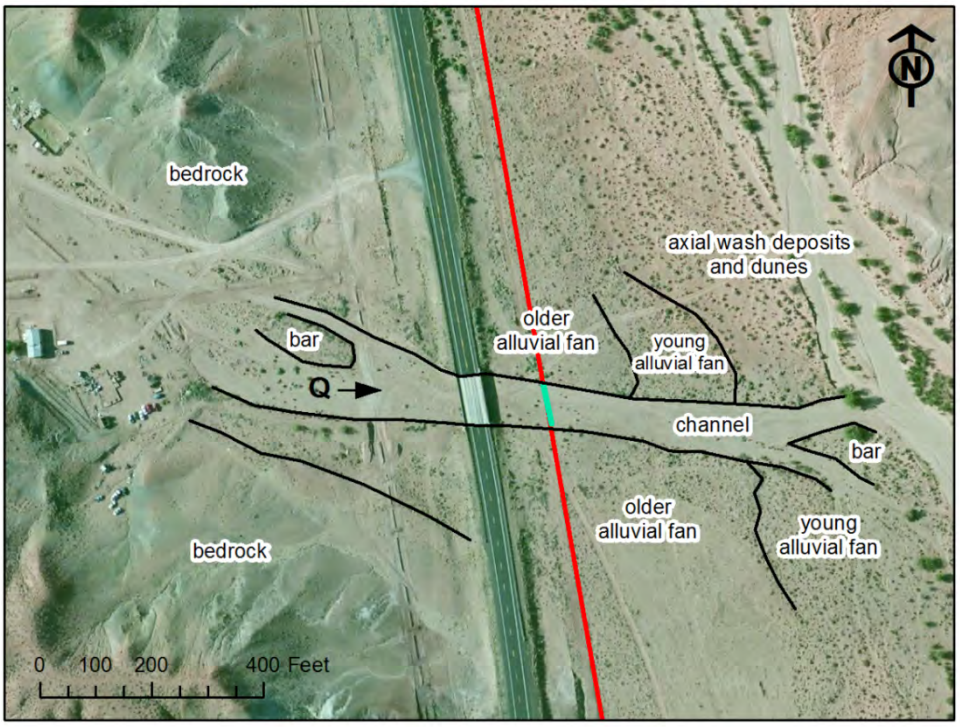

Figure 5-10. Geomorphic features at Site No. 26. The red line shows the proposed alignment, and the blue line shows the width of potential lateral channel movement.

5.2.7 Site No. 31

Figure 5-11. Site No. 31 looking upstream.

At Site No. 31(figure 5-11), the channel is characterized by split flow around a large island, with the majority of flow in the right (south) channel (figure 5-12). Downstream of the crossing, the two channels combine into a single, straight channel. Channel relief is less than 5 feet between the tops of unvegetated bars and the channel thalweg.

Low bars are less than 1 foot above the average channel bed elevation with some flotsam wrapped around the bases of trees in the channel. A distributary network of drainages enters upstream of the crossing along the right bank and is at, or just above, the grade of the wash. At the crossing, the right bank is bounded by bedrock, which is continuous along the bank to the confluence with the main wash. Bedrock is also noted upstream of the crossing along the left bank and in the channel bed. On the left bank, the terrace is about 3.5 feet above the channel bed and consists of about 1 to 2 feet of unconsolidated sand and gravel underlain by cemented sand and gravel. The left (north) branch of the channel has been eroding the berm of old Highway 89. If this continues, there is potential to breach the berm in this location and to erode into young alluvial fan sediments and flood plain deposits on the other side of the berm. Due to the presence of consolidated sediments and bedrock along the channel margins, the potential for shifts in the main channel is low. Including both channel branches, the length of potential lateral movement along the proposed alignment is about 330 feet. Due to the presence of bedrock in the channel bed and banks, channel incision greater than local scour is not expected.

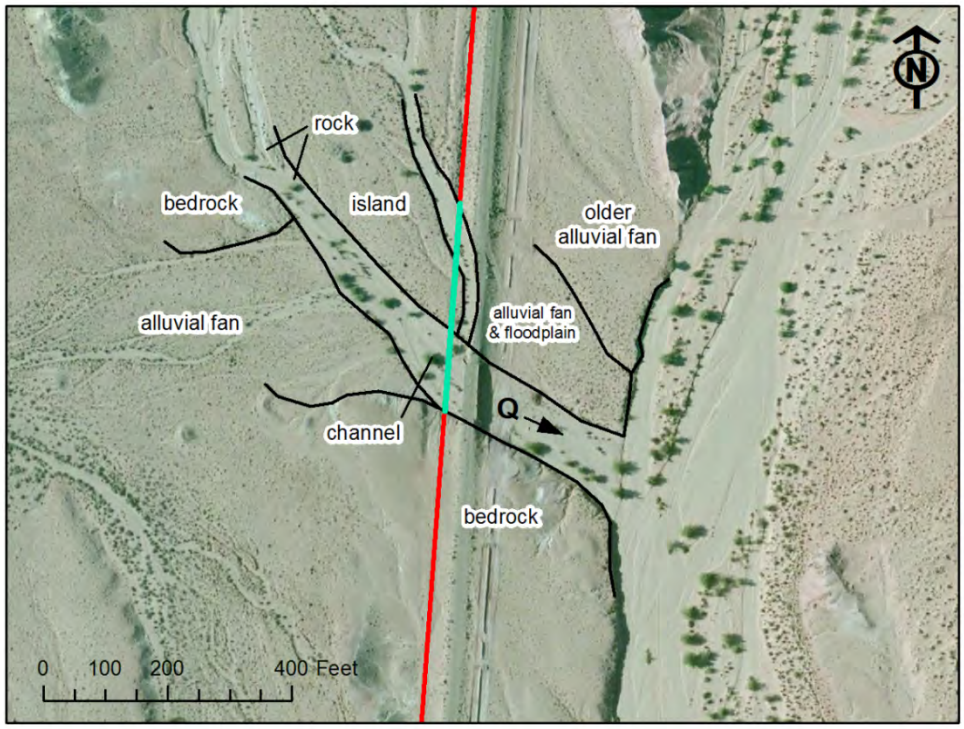

Figure 5-12. Geomorphic features at Site No. 31. The red line shows the proposed alignment, and the blue line shows the width of potential lateral channel movement.

5.2.8 Site No. 32

Figure 5-13. Site No. 32.

Near Crossing 32, the channel is single thread with low sinuosity (figures 5-13 and 5-14). Over a longer length, the channel has a moderate sinuosity, with broad meanders through the reach. At the crossing, the channel is braided at low flow, with multiple flow paths around longitudinal, vegetated, mid-channel bars that are less than 1 foot above the channel bed. Bedrock outcrops are discontinuous along the channel banks and are set back from the channel. A flood plain surface is about 1 to 2 feet above the channel bed and is vegetated with sparse brush. This surface appears to be frequently inundated. A slightly higher terrace surface is present near the crossing and appears to be inundated less frequently, as it is higher in elevation above the channel and exhibits weakly developed soils. A review of aerial photography between 1953 and 2012 shows minor changes, with greater channel widths apparent in 1953 when compared to 2012. Lateral channel change is limited to the current channel width and flood plain area along the left (north) bank, which is about 190 feet. Although bedrock was not observed in the channel bed, there are no indications that channel incision would occur along this reach; therefore, bed scour is likely to be localized and limited to values produced by the scour analysis.

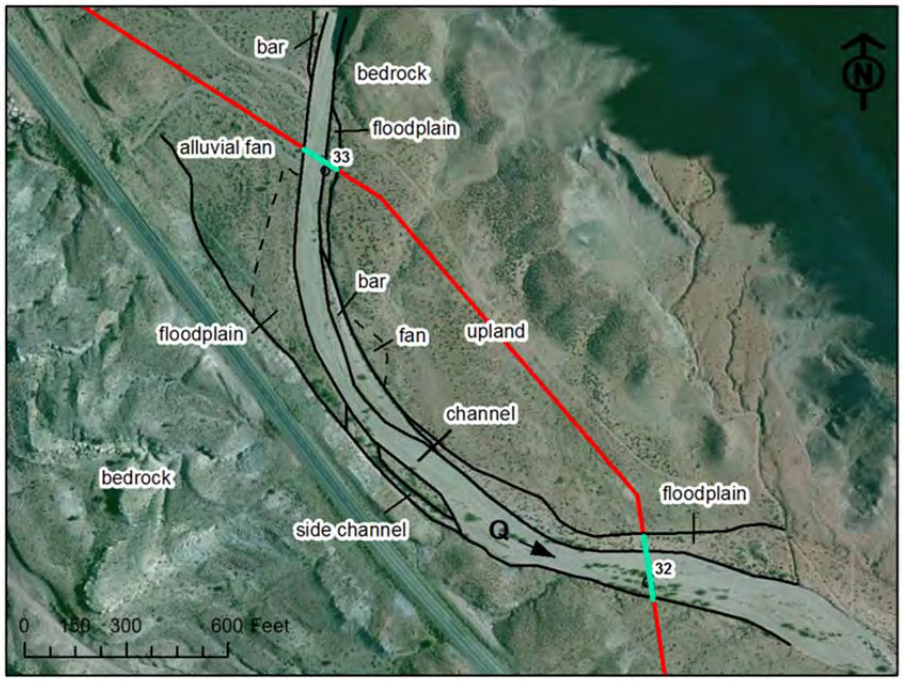

Figure 5-14. Geomorphic features at alignment Site No. 32 and Site No. 33. The red line shows the alignment, and the blue line shows the width of potential lateral channel movement.

5.2.9 Site No. 33

Figure 5-15. Site No. 33 looking downstream.

The channel at Site No. 33 is a single thread channel with low sinuosity (similar to Site No. 32), which is located about 1,700 feet downstream (figures 5-14 and 5-15). Bars are 1 to 2 feet above the channel bed and have flotsam wrapped around brushy vegetation. A low terrace along the left bank is about 2 feet above the channel bed and grades steeply upward into upland surfaces. Soils are weakly developed on the low terrace. Young alluvial fan deposits are located along the right bank and are graded to the level of the wash. These fan deposits appear to be contributing sediment to the wash on a regular basis. Bedrock exists intermittently along the left and right banks and is, observed in the bed of a small side channel downstream of the crossing. Lateral channel change between 1953 and 2012 is similar to changes noted at Site No. 32, where the 1953 channel appears wider than the 2012 channel. Lateral channel movement along the main wash, therefore, is likely limited to the width of the current channel and its flood plain, which equals approximately 114 feet. Potential for incision greater than local scour is low, due to the limited ability of the channel to migrate laterally in this reach, create accentuated meanders and meander cutoffs, and, in effect, lower local base levels in the wash. The proposed alignment also runs parallel to active channels on a young alluvial fan. This length is not included in the distance computed for lateral movement at this crossing. While lateral movement of channels on the fan is likely along the proposed alignment, the potential for scour beyond the depth of existing channels is low.

Figure 5-16. Site No. 50 looking upstream. Crossing at orange flagging.

5.2.10 Site No. 50

The channel at Site No. 50 is a single thread with a straight to slight curvature in planform (figures 5-16 and 5-17). Less than 1 foot of relief exists between the channel thalweg and the top of unvegetated bars. Narrow lateral bars exist in the reach and are vegetated with poplars; these surfaces are about 1 foot above the channel bed.

Terraces are composed of fine-grained sediments with eolian sand on their surfaces. They exist along both banks at the crossing and are about 2 feet above the channel. High water marks in the form of flotsam can be observed on the margins of the terrace surface. Bedrock was not observed in the channel bed or banks in the vicinity of the crossing.

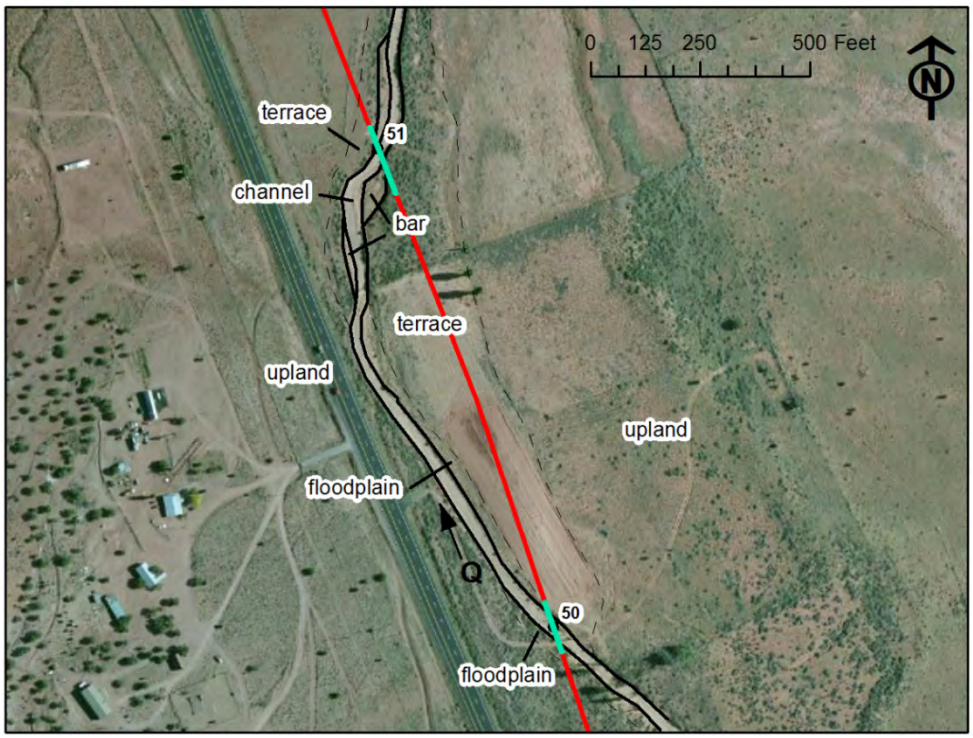

Figure 5-17. Geomorphic features at Sites No. 50 and 51. The red line shows the proposed alignment, and the blue line shows the width of potential lateral channel movement.

Historical aerial photography shows that the terrace surface along the right bank was inundated by a large flow prior to 1953. Light-colored sediment and channels on this surface suggest that the flood substantially inundated this surface. Although it could be possible for a new main channel to form across the terrace surface and abandon the current channel, it is more likely that this area will continue to be inundated during large flows and remain a landform with only small channels on its surface. The width of lateral movement is, therefore, defined for channel and bars and is about 120 feet long along the proposed alignment. Although bedrock is not observed in the channel bed or banks near this crossing, there are no indications such as knickpoints or likely base level changes downstream that would trigger vertical incision at this site greater than the depth calculated in the scour analysis.

5.2.11 Site No. 51

Figure 5-18. Site No. 51 looking upstream.

The channel at Site No. 51 is single thread with irregular width and low sinuosity meanders (figure 5-18). Approximately 2 feet of relief exists in the channel. Flood plain surfaces exist along both streambanks and are about 3 to 4 feet above the channel bed. Soils are weakly developed with eolian sands on the surface of the flood plain. The flood plain is narrow along the left bank and broad on the right bank upstream of the crossing. Near the crossing and downstream of this point, the flood plain on the left bank broadens; shallow reentrant channels are present on the surface and imply that overbank flow is conveyed back to the main channel during times of high flow. Bedrock was not observed in the channel bed or banks in the vicinity of the crossing. Observations from historical aerial photography are similar as described for Site No. 50 in that a large flow overtopped the flood plain and terrace surfaces, but it did not create a new main channel. The width of lateral movement is defined similarly to Site No. 50 and includes the channel and low bars. This width is measured at about 160 feet. In addition, there are no indications that substantial vertical incision greater than the depth calculated in the scour analysis will occur at this crossing.

5.2.12 Site No. 52

Figure 5-19. Site No. 52 looking downstream from bridge.

The channel at Site No. 52 is a straight, single thread channel that is part of a larger alluvial fan landform (figure 5-19). Flow from drainages on the alluvial fan were directed by berms into the main channel during the historical period, thus isolating most of the fan from further flooding. Channel relief is about 2 to 3 feet. Narrow lateral bars exist along the margins of the channel. Recent high water marks in the form of flotsam and trim lines along streambanks are located approximately 2 to 3 feet above the channel bed. Streambanks have weakly to moderately developed, fine-grained soils. While

some minor channel changes were observed in a review of historical aerial photography between 1953 and 2012, it is unlikely that the channel will migrate considerably from its current location along the proposed alignment. The width of potential lateral movement equals about 90 feet. Bedrock was observed in the channel bed downstream from the culvert and upstream from the crossing; thus, the potential for incision greater than local scour is low at this crossing.

5.2.13 Site No. 57

Figure 5-20. Site No. 57 looking downstream.

The channel at Site No. 57 is a narrow straight channel with a 1-foot-high narrow flood plain along the channel margin (figure 5-20). The channel is bounded by upland sediments, which appear to be composed of sand and gravel. Negligible lateral channel change was observed in historical aerial photography between 1992 and 2012. Based on the size of the channel and the lack of historical channel movement, the potential for lateral channel change is low and is restricted to the width of the channel and flood plain, a distance of about 30 feet. Bedrock is continuous across the channel bed downstream of the crossing and, therefore, limits channel incision at the crossing.

Figure 5-21. Looking downstream at bedrock downstream of Site No. 58. Rock diagonally crosses the full width of the channel.

5.2.14 Site No. 58

The channel near Site No. 58 is single thread with irregular width and meanders (figures 5-21 and 5-22). Channel bars are less than 5 ft above the channel bed along the insides of meander bends and are relatively unvegetated. Flotsam can be observed around brushy vegetation on the bars. Floodplain surfaces exist along the right and left banks and are composed of sand and gravel with weakly developed soils.

These surfaces may also have an eolian sand component on the surface. Upstream of the crossing, a higher terrace is about 5 to 7 ft above the channel bed and consists of horizontally stratified pebble and sand beds. Ridges of bedrock outcrop in the channel downstream of the crossing and are oriented nearly perpendicular to the flow direction (figure 5-21).

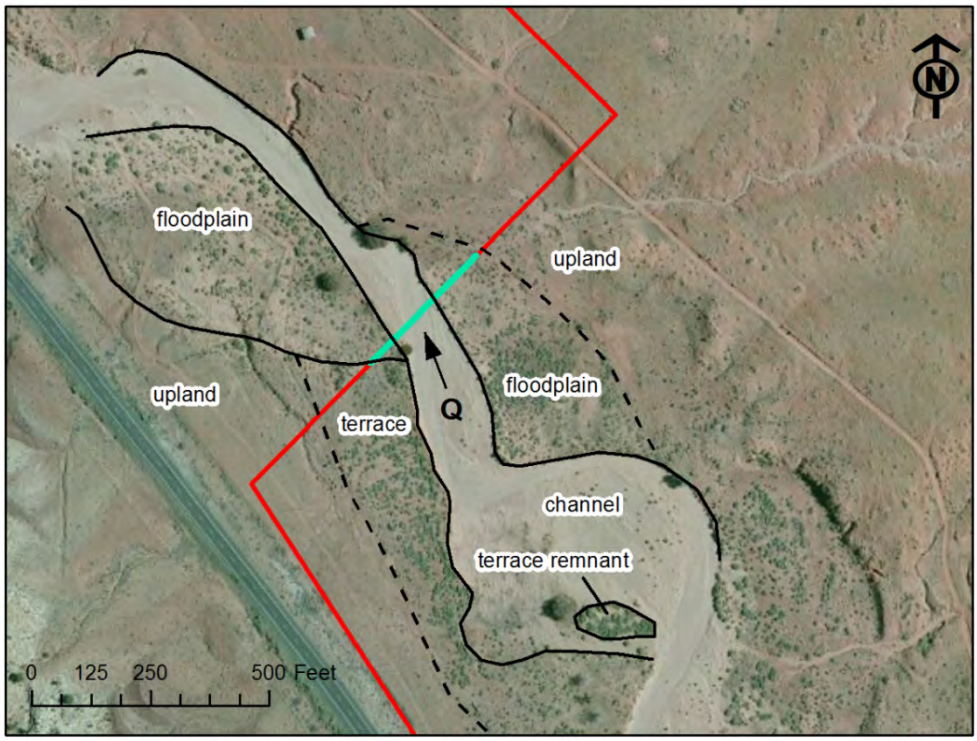

Figure 5-22. Geomorphic features at Site No. 58. The red line shows the proposed alignment, and the blue line shows the width of potential lateral channel movement.

Historical aerial photography from 1951 to 2012 shows that this reach has experienced lateral channel change in the form of lateral erosion and pronounced widening of the active channel upstream of the crossing. Therefore, this crossing is likely to undergo lateral channel change in the future. This width of potential lateral movement is defined across the channel and flood plain landforms and measures approximately 320 feet. The presence of bedrock downstream of the crossing indicates that the potential for incision is low.

5.2.15 Site No. 75

Figure 5-23. Site No. 75.

Figure 5-24. Site No. 75 looking upstream.

The channel at Site No. 75 is single thread with meanders of moderate sinuosity (figure 5-24). The channel is incised into older alluvial fan surfaces and sand dunes. Channel relief is less than 2 feet; bars within the channel are mostly unvegetated with eolian sediments draping the surfaces. Terrace surfaces are about 9 feet above the channel bed and are composed of weakly developed, fine-grained soils. At least some of the deposits are dunes. Overflow channels exist on the terrace surfaces with distinct connections to the main channel. These channels convey flow during large events and could be avulsion paths in the future. Large boulders were observed in the channel bed near the crossing—it is unlikely that these boulders are being transported from the mountain front by the current flood regime; it is more likely that they are being exhumed from a buried fan surface as the channel scours into the older material. A review of historical aerial photography from 1951 to 2012 reveals significant lateral channel change, with multiple channel avulsions along the channel corridor near the crossing. With the potential for an avulsion across the terrace surface, it is recommended that the channel and terrace are included in the area of lateral channel movement. This width equals approximately 300 feet. The potential for incision is moderate to high at the crossing due to likely channel avulsions and the unknown depth to which these new channels will incise and potentially capture the main channel.

Figure 5-25. Upstream of Site No. 78.

Figure 5-26. Site No. 78 looking downstream.

Figure 5-27. Site No. 84.

5.2.16 Site No. 78

The channel at Site No. 78 is a single thread channel with irregular meanders (figures 5-25 and 5-26). Bedrock, terraces, and dunes are located along the channel in the vicinity of the crossing. Bars are less than 2 feet above the channel bed and are composed of sand and gravel with sparse brushy vegetation. Two terrace levels are present at about 2 feet and 4 feet above the channel bed, and they are composed of fine grained and pebbly sediments with loose sand capping some exposures. Channel position is largely controlled by bedrock and other upland deposits and, therefore, is unlikely to migrate laterally. The width of potential lateral movement at the crossing includes the channel and low terraces, a distance of about 30 feet. The potential for incision is low to moderate because it is likely that bedrock is near the surface downstream from the crossing.

5.2.17 Site No. 84

The channel at Site No. 84 consists of two channels that split around a longitudinal vegetated bar (figures 5-27 and 5-28). Downstream of the crossing, the vegetated bar becomes more extensive, with multiple channels running through its interior. At the crossing, bedrock outcrops along the right bank. Upstream of the bedrock, a low terrace is formed along the right bank that

is about 2 to 3.5 feet above the channel bed. The left bank is composed of alluvial fan deposits that are derived from the surrounding piedmont and that are approximately 1 to 3.5 feet above the channel bed. Bedrock outcrops were limited to the right bank at the crossing; bedrock was not observed in the channel bed near the crossing or downstream from the crossing. Historical aerial photography between 1952 and 2012 shows negligible change in the lateral position of the channel. Alluvial fan deposits and bedrock constrain the position of the channel at the crossing and, therefore, limit the lateral channel movement of the main channel. However, lateral changes in channel position on the alluvial fan are possible. The width of potential lateral movement includes the width of the channel, which is about 90 feet. The potential for incision of the main channel is probably low, even though there is no bedrock in the channel bed because flow spreads into multiple channels downstream of the crossing, dissipating stream energy and the likelihood for incision. On the alluvial fan at the crossing, the case is similar, in which new channels could form but are unlikely to incise beyond the depth of existing channels.

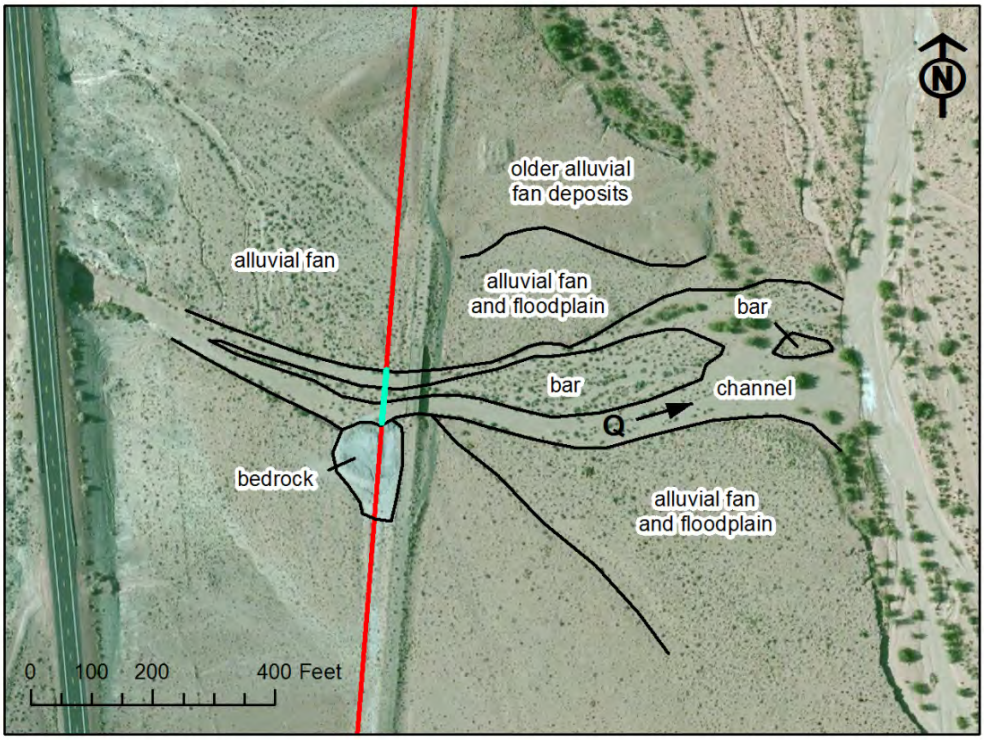

Figure 5-28. Geomorphic features at Site No. 84. The red line shows the proposed alignment, and the blue line shows the width of potential lateral channel movement.

5.2.18 Site No. 86

Figure 5-29. Site No. 86 at white bucket between old and new bridges.

The channel at Site No. 86 is single thread with small, longitudinal channel bars (figures 5-29 and 5-30). Upstream and downstream of the crossing, the channel has a braided morphology with multiple channels that flow through vegetated bars. Channel relief is about 1 foot. On the left bank, the proposed alignment crosses a broad swale between the old and new highway berms. On the right bank, the proposed alignment crosses a low bar and slopes upward into bedrock. Bedrock was not observed in the channel bed; however, the close proximity of bedrock outcrops to the channel suggests that bedrock is close to the surface.

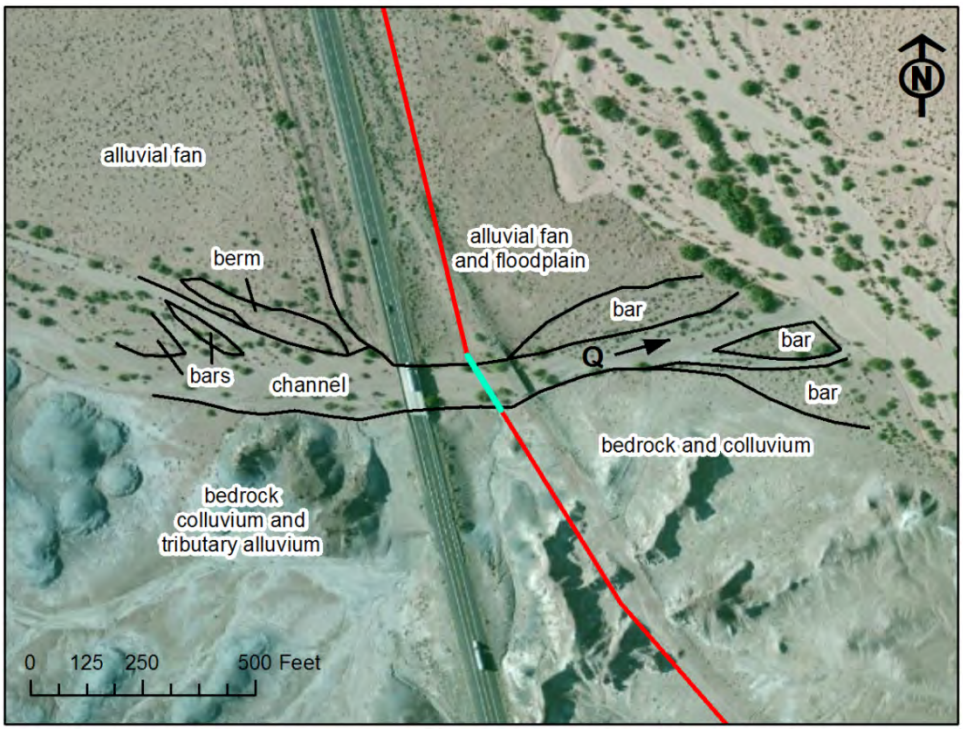

Figure 5-30. Geomorphic features at Site No. 86. The red line shows the proposed alignment, and the blue line shows the width of potential lateral channel movement.

Based on the above description, limited lateral channel movement is possible at this crossing; therefore, the length of potential lateral movement includes only the channel and bars, a distance of about 140 feet. Potential for incision at the crossing is likely low because it is upstream of the grade control for the old Highway 89 bridge, and there are no nearby headcuts or avulsion paths downstream that would significantly change the base level of the wash.

5.2.19 Site No. 90

Figure 5-31. Site No. 90. The shovel is at proposed pipeline crossing. Photo is looking upstream at incised channel and the right abutment of the old bridge. Note the salt cedar on the banks.

Figure 5-32. Looking upstream at Site No. 90 where white bucket sits on the bank

The channel near Site No. 90 at Moenkopi Wash is single thread with irregular meanders and high sinuosity (figures 5-31, 5-32, and 5-33). Relief in the channel is between 5 and 10 feet from the base of the thalweg to the top of channel bars. Bars occur mostly as point bars along the insides of meander bends. Thick salt cedar line the streambanks and typically have dunes formed around them. Rock is exposed along the right bank just downstream from the crossing; however, bedrock was not observed in any other locations in the bed or in the banks. The irregular channel morphology is likely caused by bedrock in the channel bed or older alluvium that is resistant to erosion—this alluvium is located along the outside of the meander bends in the vicinity of the crossing and likely at many of the irregular meander bends along Moenkopi Wash.

Flood plain terrace surfaces exist along both sides of the river at about 8 to 9 feet above the channel bed. A recent flood over these surfaces demonstrates that flows access this surface during larger events on Moenkopi Wash. High water marks were observed in the form of flotsam around vegetation, trim lines, and mud drapes on flood plain surfaces. The high water marks at this site were

abundant, relatively undisturbed, and deposited against young vegetation, which suggests that this flood occurred recently (likely within the past year). Based on gaging stations on Moenkopi Wash upstream of the crossing, these high water marks are likely associated with the flood that occurred on September 12, 2012, at USGS gage No. 09401260 (Moenkopi Wash at Moenkopi, AZ). This gage is located upstream of the crossing and is the only gage still in operation on Moenkopi Wash.

Figure 5-33. Geomorphic features at alignment Site No. 90, Moenkopi Wash. The red line shows the alignment, and the blue line shows the width of potential lateral channel movement.

While the channel has accentuated meanders that could suggest a high potential for avulsion, the fact that the channel is entrenched into older alluvium would suggest that avulsions across surfaces outside flood plain areas are not common

and can be restricted to the active channel and some of the flood plain areas. A review of historical aerial photography between 1953 and 2012 shows significant lateral channel change in the active channel area within the reach and a marked increase in vegetation along the channel. Most of the new vegetation growth is the salt cedar that line the banks and old channels in the reach. At the crossing, the width of potential lateral movement equals 285 feet. Channel incision beyond that of local scour is possible if the base level changes downstream. In the vicinity of the alignment crossing, headcuts or knickpoints in the channel were not observed.

Figure 5-34. The white bucket upstream of the old bridge marks the location of Site No. 92.

5.2.20 Site No. 92

The channel at Site No. 92 is a single, straight channel located just downstream of the confluence of two smaller tributaries. Channel relief is less than 1 foot with low unvegetated bars and a flood plain surface that is about 1 to 2 feet above the channel bed (figure 5-34). Piedmont alluvium, or alluvium associated with the surrounding upland, is present on gently sloping surfaces near the channels. While no bedrock is found in the banks or channel bed near the crossing, bedrock knobs are found in the vicinity and suggest that bedrock is probably only shallowly buried. Prior to human disturbance, these channels were broad distributary networks that covered a larger area. During construction of major roads through the area, berms were built to redirect distributary flow under the culvert or bridge openings. One of these berms is located along the alignment and captures flow from the drainages to the south of the crossing. Due to the construction of these features, significant channel change is observed in historical aerial photography between 1953 and 2012. However, the potential for lateral change is low because the channel is restricted by berms. The width of potential lateral channel movement at the crossing is about 160 feet and includes the channel and narrow flood plain areas. The potential for channel incision greater than local scour at the crossing is low to moderate because of the likelihood of bedrock close to the surface.

5.2.21 Site No. 94

Figure 5-35. Looking upstream at Site No. 94 proposed pipeline crossing

Figure 5-36. Looking downstream towards the old bridge from Site No. 94. The bridge deck on the old bridge has collapsed.

The channel at Site No. 94 is single thread with braided sections downstream of the crossing (figures 5-35 through 5-37). Several tributary channels enter just upstream of the crossing. An abandoned tributary channel is located at the crossing and has been mostly filled in with sediment so that it appears as a shallow swale on the surface of the flood plain. Flood plain surfaces are about 2 feet above the channel bed and show evidence of recent inundation in the form of flotsam, small channels, and clay drapes on surfaces. Higher islands on flood plain surfaces have eolian features with some established vegetation. Bedrock was not observed in the channel bed or streambanks near the crossing. Riprap is located along the right bank just downstream of the crossing near the old Highway 89 bridge. Recent lateral movement of the channel has been toward the left bank, where the channel continues to erode the berm along old Highway 89 downstream of the crossing. Along the right bank, older piedmont alluvium restricts lateral movement to the north. Historical aerial photography shows significant channel narrowing between 1953 and 2012. The width of potential lateral movement should include areas that were previously part of the active channel and adjacent flood plain areas. This width totals about 400 feet along the length of the alignment. Due to the presence of grade control at the Highway 89 bridge, the potential for incision greater than the depth of local scour is low.

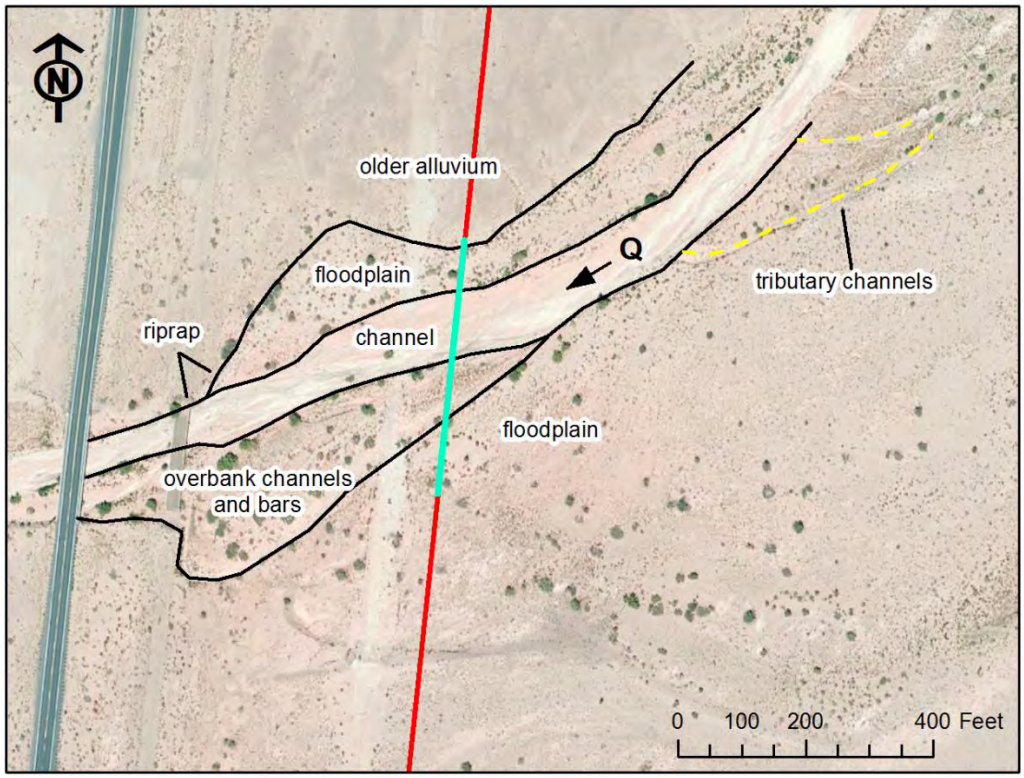

Figure 5-37. Geomorphic features at alignment Site No. 94. The red line shows the alignment, and the blue line shows the width of potential lateral channel movement.

Figure 5-38. Old Highway 89 bridge at Site No. 96, looking upstream and across at the left bank. The bridge has pile groupings of four.

5.2.22 Site No. 96

In the study reach, the LCR is incised in a bedrock canyon and is a single channel with broad meanders that are controlled by the bedrock walls of the canyon (figures 5-38 through 5-40). At low flows, the channel has a braided character; while at high flows, the channel is single thread. The inner channel is approximately 2.5 to 3 feet below a narrow bar surface vegetated with willows at the crossing. A higher flood plain surface exists along the left and right banks in the study reach that is about 8 feet above the water surface and about 4.5 to 5 feet above the lower bar surface. Salt cedar vegetation has grown densely across this surface. Hereford (1984) describes the surface as the flood plain surface, between about

6 and 12 feet above the channel. A higher surface that Hereford terms the cottonwood terrace also exists in some reaches along the LCR and can range from about 6 to 15 feet above the channel. In some cases, sediment that predates these surfaces can be found underlying deposits of the flood plain and cottonwood surfaces. Sediments in these landforms are fine-grained and composed of sand and silt.

Figure 5-39. Looking upstream at Highway 89 bridge and the old Highway 89 bridge in the background at Site No. 96, the LCR. This photo also shows river constriction at the old bridge.

Figure 5-40. Geomorphic features at Site No. 96, LCR. The red line shows the proposed alignment, and the blue line shows the width of potential lateral channel movement.

Historical changes in channel morphology have been significant along the LCR. Aerial photographs from 1953 show a wide, sandy channel with no vegetation along it, except for the alluvial fan at the confluence with Moenkopi Wash and a few narrow strips in the channel (figure 5-41). Hereford (1984) documents the changes in historical channel morphology and links these changes predominantly to subtle changes in climate during the 20th century. From 1900 to 1940, floods were frequent and mobilized sediment across the channel on a regular basis such that the channel remained free of vegetation. Beginning in the 1940s, average annual precipitation and discharge declined, resulting in fewer floods that were able to mobilize sediment across the entire channel. Riparian vegetation, mainly the invasive plant salt cedar, was able to establish itself on surfaces that remained dry for portions of the year. From 1952 to 1978, precipitation and discharge increased, resulting in widespread aggradation of flood plain surfaces through overbank deposition. At the time of his research in 1980, Hereford indicated that aggradation had ceased on the flood plain surfaces. Whether this still remains true in the current year within the study reach would be a matter of further investigation. However, it is apparent that channel morphology currently is similar to the conditions in 1980, based on Hereford's (1984) description of the channel.

Figure 5-41. Comparison of vegetation along the LCR near Cameron, AZ, between 1953 and 2012. Flow is from right to left.

5.2.23 Site No. 97

Figure 5-42. Site No. 97 looking downstream from the crossing.

The channel at Site No. 97 is braided with multiple channels that flow around vegetated, longitudinal mid-channel bars (figures 5-42 and 5-43). Relief in the channel is less than 2 feet, with bars about 1 foot above the channel bed. Flood plain surfaces are about 2 feet above the channel bed and show evidence of recent inundation, including flotsam and overflow channels on the surface. Flood plain surfaces are located along the left and right banks at the proposed alignment crossing. A narrow terrace (about 7 feet above the channel bed) is inset against bedrock along the right bank upstream of the crossing. The terrace is composed of fine-grained sediments and pebbly beds with moderate soil development. Bedrock is located in the right bank near the alignment crossing and is set back slightly from the active channel along the left bank. Eolian features are common in this reach and consist of approximately 3-foot-high dunes that are sparsely vegetated. A review of historical aerial photography between 1953 and 2012 reveals that shifts in the dominant channel position within the active channel are common. The potential for avulsions onto flood plain surfaces is high based on existing overflow channels and scour on the surfaces from recent flows. The potential for lateral movement, therefore, includes the flood plain surfaces, along with the active channel, and equals a width of about 625 feet along the length of the alignment. The potential for incision beyond that of local scour appears to be low based on the broad and braided character of the channel.

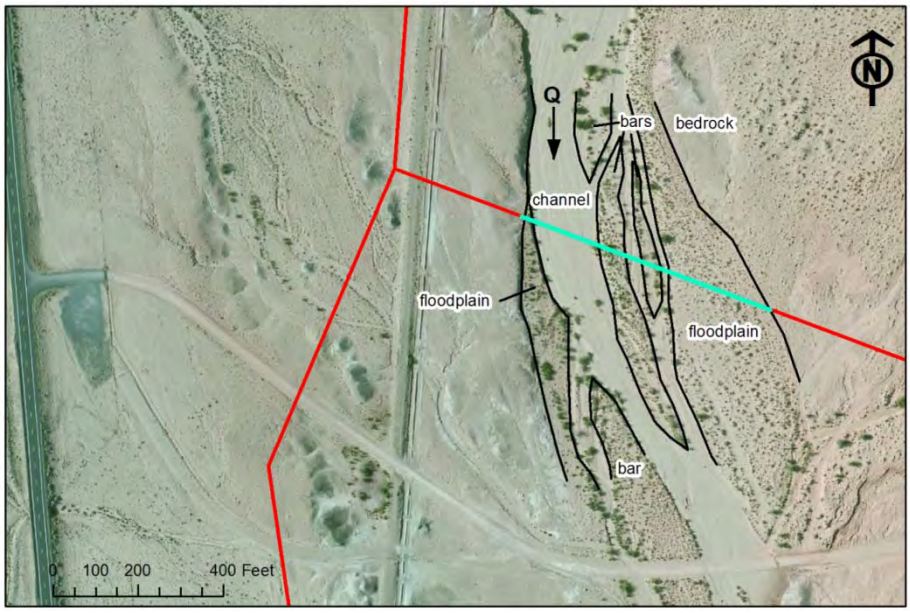

Figure 5-43. Geomorphic features at Site No. 97. The red line shows proposed alignment, and the blue line shows the width of potential lateral channel movement.

Figure 5-44. Site No. 98 looking upstream.

Figure 5-45. Spring-fed channel in active channel area. The channel formed from a recent avulsion between 2010 and 2012.

5.2.24 Site No. 98

The channel at Site No. 98 is braided with multiple channels through vegetated and unvegetated islands and bars that are about 2 to 3 feet above the channel bed (figures 5-44 through 5-46). The reach is essentially a network of distributary channels that feed into the main stem wash about 450 feet downstream. Flood plain surfaces and terraces are not well defined in this reach. Bank materials are composed of unconsolidated, laminated sand and silt. Eolian deposits are also common and have sparse brushy vegetation. Recent high water marks are evident in this reach and include flotsam around bushes and salt cedar, secondary channels and channel splays, and scoured deposits of fine-grained alluvium. Avulsions appear to be common in this reach. Based on a review of aerial photographs, a significant channel avulsion occurred just upstream of the alignment crossing between 2010 and 2012. It is likely that high flows on the northern, unvegetated tributary largely contributed to the avulsion. This avulsion scoured a channel to a 2-foot depth in the vicinity of the crossing. The new channel directs flow over the road downstream from the crossing. Based on historical channel change, the potential for continued lateral channel change in this reach and at the crossing is high. The width of potential lateral movement at the alignment crossing is equal to about 300 feet. Based on observations of the recent channel avulsion, it is unlikely that new channels would scour to a depth greater than the depth of existing channels.

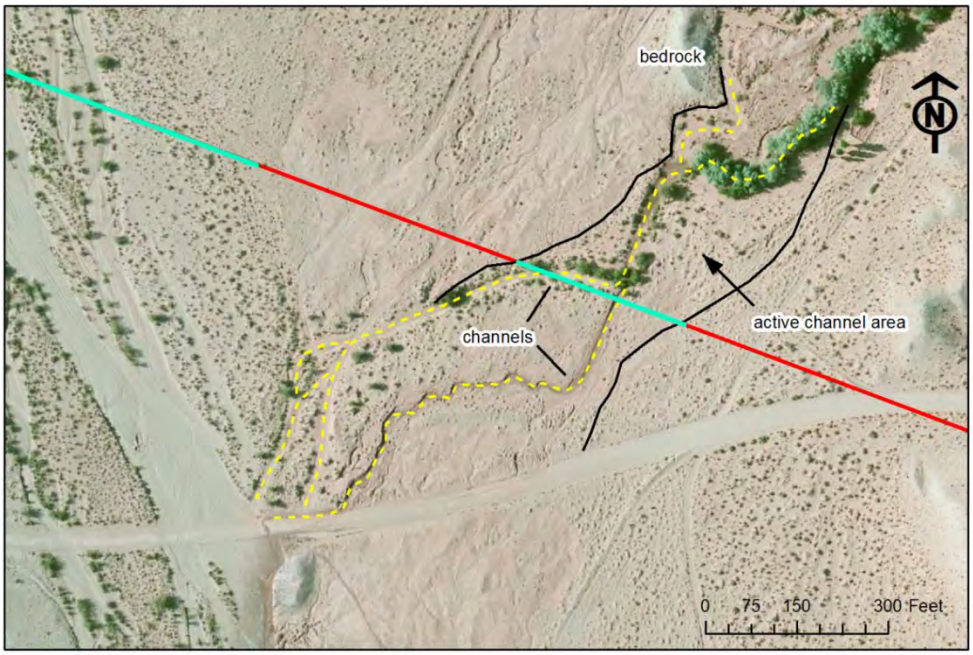

Figure 5-46. Geomorphic features at alignment Site No. 98. The red line shows the proposed alignment, and the blue line shows the width of potential lateral channel movement.

5.2.25 Site No. 103

Figure 5-47. Site No. 103 looking downstream.

The channel at Site No. 103 is a single, narrow channel that flows through upland sediments at the proposed alignment crossing (figure 5-47). A weak, narrow terrace is formed along the right bank that is about 1 to 2 feet above the channel bed. The channel bed has low relief with low bars. Bedrock can be observed in aerial photography just upstream of the crossing along Highway 89. Based on the small size of this channel and the presence of bedrock, the potential for lateral and vertical changes at the crossing is low. The width of potential lateral movement is about 20 feet.

5.2.26 Site No. 104

Figure 5-48. Site No. 104 looking downstream.

The channel at Site No. 104 is a single, narrow channel with low amplitude meanders (figure 5-48). At the proposed alignment crossing, a low bar has developed in the channel, along with two terrace levels at about 2 and 4 feet above the channel bed. The 4-foot terrace has moderate soil development and is located along the left bank. Upland sediments are located along the right bank adjacent to a channel bar and 2-foot terrace. Lateral movement of the channel is unlikely at this location; thus, the width of potential lateral movement is limited to the channel and its related landforms, a distance of about 40 feet. Due to the small size of the channel and the likelihood that bedrock is close to the surface, the potential for incision greater than local scour is also low.

5.2.27 Site No. 125

Figure 5-49. Photo looking upstream at Site No. 125, next to the old bridge. The new road alignment crosses the three-barrel culverts seen upstream.

The channel at Site No. 125 is a single thread, straight channel (figure 5-49). Downstream of the crossing, the channel bends to the south and has a braided character with multiple channels that flow through vegetated bars about 1.5 feet above the lowest channel (figure 5-50). Flood plain surfaces show evidence of inundation in the form of trim or scour lines. Deposits that comprise the flood plain surfaces are sandy and gravelly and have a cemented base with thin clay stains on clasts. Bedrock is located along the left and right banks and, possibly, in the bed of the channel downstream of the alignment crossing. The alignment is located at the old Highway 89 bridge crossing, and it crosses where the channel flows between the road embankments. Lateral channel change is limited to the channel and low bars between the embankments, a distance of about 70 feet. The lack of knickpoints downstream and potential bedrock in the channel bed downstream of the crossing would suggest that the potential for incision greater than local scour is low.

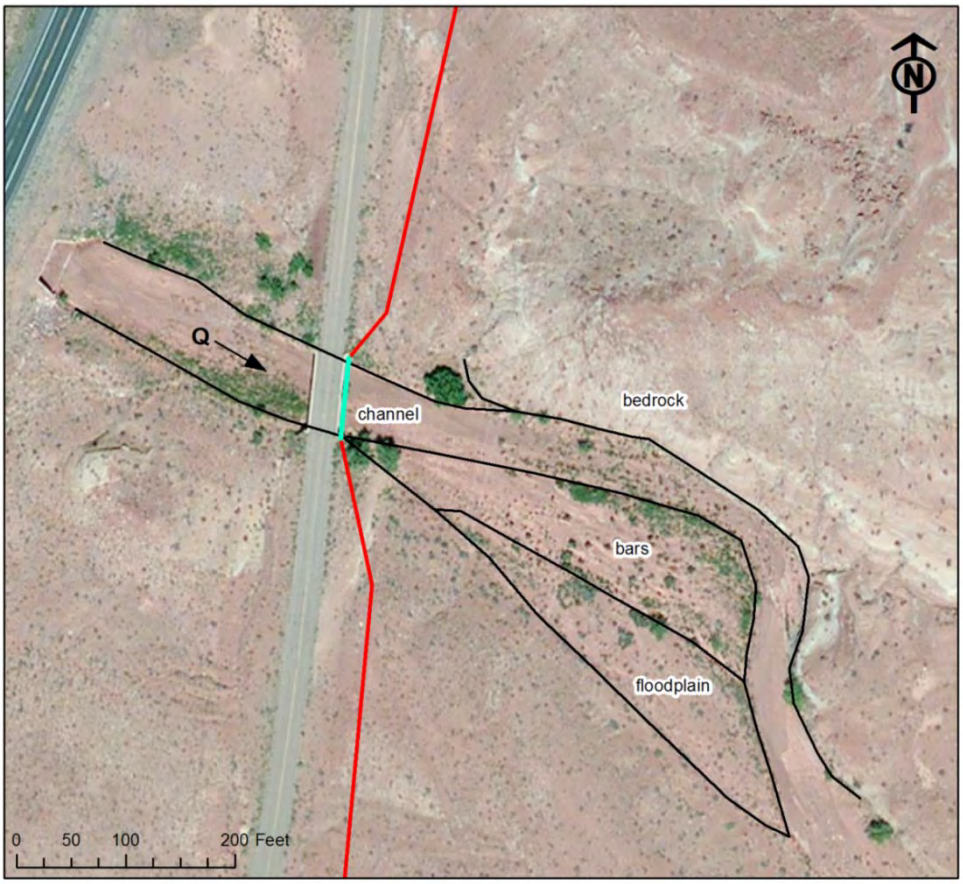

Figure 5-50. Geomorphic features at alignment Site No. 125. The red line shows the alignment, and the blue line shows the width of potential lateral channel movement.

5.3 Vertical and Lateral Stability and Stream Crossing Widths

Vertical and lateral stability at stream crossings are rated in this summary using categories of low, low to moderate, moderate, and high potential for instability. Table 5-1 defines the basis for the categories.

A rating of the vertical (incision) and lateral stability of a crossing, and a minimum width of potential lateral movement, are assembled in table 5-2, with supporting notes on bedrock, historical channel change, and types of surfaces. Notes on historical channel change are based on reviews of aerial photography. Aerial photos used in the review are documented in table C-1 of appendix C.

Detailed information on the main sites is presented in the previous section and summarized in table 5-2. Information on secondary stream sites is also included. Assessments of vertical and lateral stability, and suggested crossing widths, are specific to the location of the proposed pipeline stream crossing. Other sections

of the channel located upstream or downstream of the alignment crossing may have a different potential for lateral or vertical movement.

Table 5-1. Rating Definitions for Vertical and Lateral Stream Stability at Pipeline Crossings

Potential for incision greater than local scour	
Low	Bedrock is visible in bed at or downstream of crossing. Channel is very small, and surrounding bedrock suggests that potential is low. Other type of grade control is present, such as detention structure, concrete, etc., that would prevent a change in base level.
Low to Moderate	Bedrock was not observed and/or crossing was not visited. Sand bed; depth to rock is unknown. Channel is small.
Moderate	Sand bed; no bedrock is visible in the bed. Potential for avulsions to new locations, which could create change in base level and incision at crossing.
High	Headcuts are present and likely to migrate upstream.
Potential for lateral movement	
Low	Physical constraints prevent lateral movement. Berms, levees, upstream culvert. Bedrock, older alluvium, colluvial slope, indurated sediments in streambanks. Channel is very small and incised into upland landforms.
Low to Moderate	Minor lateral changes in historical channel position. Flood plain areas are narrow but have the potential for lateral erosion or avulsion.
Moderate	Unconsolidated sediments in streambanks. Flood plain surfaces have the potential for lateral erosion or avulsion. Instability may be detected in historical aerial photography. Channel movement along a nearby mainstem wash may impact lateral movement at crossing. No bedrock or human structural control.
High	Historical channel change is significant. Field evidence for potential avulsion paths.

Table 5-2. Assessment of Vertical and Lateral Stability

Site No.	Bedrock in banks or bed	Potential for degradation >local scour	Historical channel change near crossing	Potential for lateral channel change at/near crossing	Burial width from channel centerpoint along alignment					Notes
					Width (ft)	Direction	Width (ft)	Direction	Total width (ft)	
1	None	Low to moderate	Not reviewed	Low	10	N	10	S	19	Shallow swale in sandy, unconsolidated sediments
2	In bed	Low	Not reviewed	Low	22	N	22	S	44	
3	In bed	Low	Not reviewed	Low	27	N	27	S	53	
4	None	Low to moderate	Not reviewed	Low	22	E	22	W	43	Broad, sandy single channel
5	None	Low to moderate	Not reviewed	Low	11	E	11	W	22	
6	In bed and banks	Low	Not reviewed	Low	28	E	28	W	56	Trapezoidal channel cut in rock
7	In bed	Low	Not reviewed	Low to moderate	109	N	1,573	S	1,682	Rectangular shaped channel with sandy, laminated sediments in banks; channel runs along road
8	In bed	Low	Negligible (1992-2012)	Low to moderate	146	N	31	S	176	Unable to tell what surfaces are along wash
9	Unknown	Low	Not reviewed	Low	28	N	15	S	42	Channel inset into older surfaces
10	In bed	Low	Not reviewed	Low	9	N	9	S		Channel inset into older surfaces
					10	N	10	S	147	Measurement near point 10b
					11	N	97	S		Measurement between points 10a and 10b
11	Unknown	Low to moderate	Not reviewed	Moderate (unconsolidated banks)	923	N			923	Measurement near point 10a
12	Unknown	Low to moderate	Not reviewed	Moderate (unconsolidated banks)	11	N	10	S	21	

Table 5-2. Assessment of Vertical and Lateral Stability

Site No.	Bedrock in banks or bed	Potential for degradation >local scour	Historical channel change near crossing	Potential for lateral channel change at/near crossing	Burial width from channel centerpoint along alignment					Notes
					Width (ft)	Direction	Width (ft)	Direction	Total width (ft)	
13	None	Low to moderate	Negligible (post-1992)	Moderate (unconsolidated banks)	36	N	21	S	57	Channel is incised, building inner flood plain
14	Unknown	Low to moderate	Not reviewed	Moderate (unconsolidated banks)	40	N	30	S	70	
15	Unknown	Low	Not reviewed	Low	12	N	14	S	26	Small channel on bedrock surface, bedrock outcrop close by
16	Left bank downstream of bridge	Low to moderate	Negligible (post-1953)	Low	135	E	66	W	201	
17	Set back from channel	Moderate	negligible (1997-2012)	Low	24	N	58	S	82	Potential for avulsion and associated incision
18	Along right bank	Moderate	Shift in channel dominance (1953-2012)	Moderate	117	N	8	S	124	Unconfined alluvial fan, some lateral bedrock controls; potential for shifts upstream of crossing
19	Along right bank	Low to moderate	Negligible (1997-2012)	Low	8	N	8	S	17	
20	None	Moderate	Negligible (post-1953); alternate paths on alluvial fan blocked by berms by 1953	Low; shifts downstream of crossing are possible	37	N	62	S	99	Semi-confined alluvial fan, altered by berms

Table 5-2. Assessment of Vertical and Lateral Stability

Site No.	Bedrock in banks or bed	Potential for degradation >local scour	Historical channel change near crossing	Potential for lateral channel change at/near crossing	Burial width from channel centerpoint along alignment					Notes
					Width (ft)	Direction	Width (ft)	Direction	Total width (ft)	
21	Colluvium in left bank	Low to moderate	Berms directed channel in 1953; breached between 1953 and 1997; new berm built to contain flow in new position	Low	60	N	78	S	139	Braided channel
22	Along left bank, possibly right bank	Low to Moderate	Minor (1997-2012)	Low to moderate	108	N	31	S	139	Potential shifts in main channel position within braided channel
23	Along both banks	High -- potential for headcuts to migrate u/s of road to crossing	Minor (1953-2012)	Low	75	N	85	S	160	Headcuts not present in 1953; braided channel/fan - historical aggradation filled culverts; flow goes over road, creating headcuts
24	Along both banks	Low	Negligible (1997-2012)	Low	11	N	11	S	22	Single channel confined between bedrock hills
25	Unknown	Moderate	Minor (1997-2012)	Moderate	105	N	6	S	111	Potential for knickpoint to migrate upstream; braided channel could take different paths
26	None; located upstream of crossing near banks	Low	Negligible (post-1953);	Low	37	N	37	S	73	Berm along right bank upstream of crossing - hard to tell when berm was built
27	Along right bank	Low	Not reviewed	Low	33	N	26	S	59	Potential minor lateral erosion of banks
28	Unknown	Low	Negligible (1997-2012)	Low	13	N	13	S	26	Incised into older alluvium

Table 5-2. Assessment of Vertical and Lateral Stability

Site No.	Bedrock in banks or bed	Potential for degradation >local scour	Historical channel change near crossing	Potential for lateral channel change at/near crossing	Burial width from channel centerpoint along alignment					Notes
					Width (ft)	Direction	Width (ft)	Direction	Total width (ft)	
30	In bed near culvert(?)	Low	Negligible (1997-2012)	Low	14	N	14	S	27	Incised into older alluvium; berm along left bank(?)
31	In bed upstream of crossing; along left bank upstream of crossing and in right bank	Low - bedrock likely close to surface	Left channel upstream of crossing, developing since 1953	Moderate	261	N	73	S	334	Channel has been progressively eroding old highway abutment
32	Along right bank	Low	Minor change (1953-2012)	Low to moderate	111	N	76	S	188	1953 active channel area appears wider in photos than in 2012
33	In bed of small side channel and along left bank	Low	Minor change (1953-2012)	Low to moderate	73	E	41	W	114	1953 active channel area appears wider in photos than in 2012
34	Along banks	Low to moderate	Negligible (1997-2012)	Low	35	N	71	S	106	
35	Along banks	Low	Photos are too blurry	Low	85	N	37	S	122	Potential for channel to shift within bedrock constraints
36	Along banks	Low to moderate	Negligible (1997-2012)	Low	23	N	28	S	51	Single channel locked between bedrock hills
37	Along left bank	Low to moderate	Negligible (1997-2012)	Low	31	N	64	S	95	Single channel, just downstream of confluence of several tributaries
38	Along left bank	Low to moderate	Negligible (1997-2012)	Moderate	33	N	227	S	260	Potential for channel to shift or avulse on right bank

Table 5-2. Assessment of Vertical and Lateral Stability

Site No.	Bedrock in banks or bed	Potential for degradation >local scour	Historical channel change near crossing	Potential for lateral channel change at/near crossing	Burial width from channel centerpoint along alignment					Notes
					Width (ft)	Direction	Width (ft)	Direction	Total width (ft)	
39	Along banks	Low	Negligible (1997-2012)	Low to moderate	28	N	14	S	43	Single channel, confined setting - potential for avulsion toward right bank (south), but limited due to bedrock constraints
40	Along banks	Low	Negligible (1997-2012)	Low	16	N	17	S	34	Single channel, confined setting
41	Along banks and in bed(?)	Low	Negligible (1997-2012)	Low to moderate (within bedrock confines)	96	N	38	S	134	Braided to single channel, confined in bedrock - main channel could shift within bedrock confines
42	Along left bank downstream of crossing and right bank upstream of crossing, in bed(?)	Low	Negligible (1997-2012)	Low	21	N	10	S	31	Single channel, berms along both sides of channel upstream of crossing
43	Along banks and in bed downstream of crossing	Low	Negligible (1997-2012)	Low	41	E	36	W	78	Single channel at meander bend, braided at low flow, incised into bedrock canyon
44	Along banks and in bed downstream of crossing	Low	Negligible (1997-2012)	Low	22	E	24	W	46	Single channel at meander bend, braided at low flow, incised into bedrock canyon
45	Along banks and in bed	Low	Negligible (1997-2012)	Low to moderate	16	N	16	S	33	Steep drainage on hillside; weak drainage development

Table 5-2. Assessment of Vertical and Lateral Stability

Site No.	Bedrock in banks or bed	Potential for degradation >local scour	Historical channel change near crossing	Potential for lateral channel change at/near crossing	Burial width from channel centerpoint along alignment					Notes
					Width (ft)	Direction	Width (ft)	Direction	Total width (ft)	
46	Along banks and in bed	Low	Negligible (1997-2012)	Low to moderate	18	N	18	S	36	Steep drainage on hillside; weak drainage development
47	Along banks and in bed	Low	Negligible (1997-2012)	Low	10	N	10	S	19	Single channel incised
48	Along banks and in bed downstream	Low	Negligible (1997-2012)	Low	15	N	15	S	29	Single channel incised
49	Unknown	Low to moderate	Negligible (1997-2012)	Moderate	58	N	32	S	90	Alluvial fan; potential for avulsion downstream from crossing could cause channel to incise further
50	None	Low	Moderate (1953-2012)	Moderate	66	N	52	S	117	Big flow from tributary upstream prior to 1953 – flood plain surfaces are overtopped, channels in surface
51	None	Low to Moderate	Moderate (1953-2012)	Moderate	58	N	102	S	160	Big flow from tributary upstream prior to 1953 – flood plain surfaces are overtopped, channels in surface
52	In bed	Low	Minor change (1953-2012)	Low to moderate (berms direct flow; channel is bounded mostly by alluvial fan deposits)	48	N	42	S	90	Channel appears less defined in 1953; also, large berms placed on main channel to block and direct flow into tributary channel post-1953; channel is part of large alluvial fan landform

Table 5-2. Assessment of Vertical and Lateral Stability

Site No.	Bedrock in banks or bed	Potential for degradation >local scour	Historical channel change near crossing	Potential for lateral channel change at/near crossing	Burial width from channel centerpoint along alignment					Notes
					Width (ft)	Direction	Width (ft)	Direction	Total width (ft)	
53	Unknown	Moderate	Minor change (1997-2012)	Moderate	79	N	42	S	121	Alluvial fan; potential for avulsions along left or right bank near crossing; recent channel splays on north (left) bank
54	Unknown	Low to moderate	Negligible (1997-2012)	Low	24	N	24	S	48	Single channel, funnels into incised channel just downstream from culvert
55	Unknown	Low to moderate	Negligible (1951-2012)	Low to moderate	60	N	39	S	99	Potential for channel splays and avulsions to the north from current channel along left bank
56	Unknown	Moderate	Negligible (1992-2012)	Moderate	8	N	8	S	16	Potential for avulsion along left bank downstream of culvert
57	In bed	Low	Negligible (1992-2012)	Low	13	N	15	S	28	1951 photo too small scale and blurry to use
58	In bed	Low	Significant (1951-2012)	High	192	E	125	W	318	Irregular channel width and meanders during historical map and photo record
59	Unknown	Low to moderate	Moderate (1951-2012) - in reach near crossing	Low to moderate	82	N	23	S	106	Potential for lateral erosion of dune on left bank
60	Along banks(?)	Low	Negligible (1992-2012)	Low	24	N	12	S	36	Single channel
61	Along banks and in bed	Low	Negligible (1951-2012)	Low	5	N	31	S	36	Incised single channel
62	Unknown	Low	Negligible (1992-2012)	Low	4	N	4	S	8	Incised single channel
63	In bed(?)	Low	Minor (1992-2012)	Low to moderate	61	N	27	S	89	Some potential for movement

Table 5-2. Assessment of Vertical and Lateral Stability

Site No.	Bedrock in banks or bed	Potential for degradation >local scour	Historical channel change near crossing	Potential for lateral channel change at/near crossing	Burial width from channel centerpoint along alignment					Notes
					Width (ft)	Direction	Width (ft)	Direction	Total width (ft)	
64	In bed(?)	Low	Negligible (1992-2012)	Moderate	48	N	157	S	205	Potential for movement to the south and southeast but within confined valley
65	In bed	Low	Negligible (1992-2012)	Low to moderate	20	N	17	S	38	Single channel, flows over bedrock cliff downstream of crossing
66	In bed	Low	Negligible (1992-2012)	Low to moderate	28	N	111	S	138	Single channel, flows over bedrock cliff downstream of crossing
67	In bed	Low	Negligible (1992-2012)	Low	17	N	10	S	27	Single channel, appears to be incised; bedrock ridge runs parallel to alignment and outcrops in channel downstream of crossing
68	Unknown	Low	Moderate (1992-2012)	Low to moderate	33	N	34	S	67	Some channel movement evident, avulsions within confined valley
69	Unknown	Low	Negligible (1992-2012)	Low	12	N	11	S	23	Single channel, appears to be incised; bedrock ridge runs parallel to alignment downstream of crossing
70	Unknown	Low	Negligible (1992-2012)	Low	14	N	11	S	25	Single channel, appears to be incised; bedrock ridge runs parallel to alignment downstream of crossing

Table 5-2. Assessment of Vertical and Lateral Stability

Site No.	Bedrock in banks or bed	Potential for degradation >local scour	Historical channel change near crossing	Potential for lateral channel change at/near crossing	Burial width from channel centerpoint along alignment					Notes
					Width (ft)	Direction	Width (ft)	Direction	Total width (ft)	
71	Unknown	Low	Negligible (1992-2012)	Low	13	N	13	S	25	Single channel, appears to be incised; bedrock ridge runs parallel to alignment downstream of crossing
72	Unknown	Low	Negligible (1992-2012)	Low	8	N	6	S	14	Single channel, appears to be incised; bedrock ridge runs parallel to alignment downstream of crossing
73	Unknown	Low	Negligible (1992-2012)	Low	7	N	6	S	13	Single channel, appears to be incised; bedrock ridge runs parallel to alignment downstream of crossing
74	Unknown	Low	Negligible (1992-2012)	Low	7	N	8	S	15	Single channel, appears to be incised; bedrock ridge runs parallel to alignment downstream of crossing; bedrock outcrops along channel margin downstream of crossing
75	None	Moderate to high	Significant (1951-2012)	Moderate	69	N	237	S	305	Semi-confined channel (high alluvial fan surfaces border channel and flood plain)
76	Unknown	Low	Negligible (1992-2012)	Low	10	N	6	S	16	Single channel, appears to be incised; bedrock ridge outcrops downstream, unknown if directly visible in channel

Table 5-2. Assessment of Vertical and Lateral Stability

Site No.	Bedrock in banks or bed	Potential for degradation >local scour	Historical channel change near crossing	Potential for lateral channel change at/near crossing	Burial width from channel centerpoint along alignment					Notes
					Width (ft)	Direction	Width (ft)	Direction	Total width (ft)	
77	Unknown	Low to moderate	Moderate (1992-2012)	Moderate	11	N	38	S	49	Single channel, shallow swale; 1992 photos show multiple channels near crossing in low surface
78	Along left bank	Low to moderate	Negligible (1992-2012)	Low	16	N	16	S	32	Single channel, some evidence for lateral movement (i.e., secondary or abandoned channels) but not at crossing
79	Unknown	Low to moderate	Negligible (1992-2012)	Low	16	N	15	S	30	Single channel, no significant lateral movement since 1992
80	Unknown	Moderate	Negligible (1992-2012)	Low	5	N	11	S	16	Single channel, no significant lateral movement since 1992
81	Unknown	Moderate	Negligible (1992-2012)	Low	4	N	4	S	7	Single channel, no significant lateral movement since 1992
82	Unknown	Moderate	Negligible (1992-2012)	Low	10	N	6	S	17	Single channel, no significant lateral movement since 1992
83	Unknown	Moderate	Negligible (1992-2012)	Low	9	N	7	S	16	Single channel, no significant lateral movement since 1992
84	Along right bank	Low	Negligible (1953-2012)	Low	44	N	44	S	87	Channel exits from confined setting, bounded by fans and bedrock at crossing

Table 5-2. Assessment of Vertical and Lateral Stability

Site No.	Bedrock in banks or bed	Potential for degradation >local scour	Historical channel change near crossing	Potential for lateral channel change at/near crossing	Burial width from channel centerpoint along alignment					Notes
					Width (ft)	Direction	Width (ft)	Direction	Total width (ft)	
85	Along left bank and in bed(?)	Low	Not reviewed	Low	19	N	25	S	44	Single channel; berm built along right bank, bedrock on left bank; canyon downstream of crossing
86	Along right bank	Low	Berm breach visible on left bank in 1953; minimal change between 1953 and 2012	Low	74	N	69	S	143	Berms upstream of bridge prevent significant lateral movement; however, if berm could be breached, channel could avulse upstream of crossing; alluvial fan materials and bedrock likely limit movement at crossing; potential for lateral change downstream of crossing
87	Unknown	Low to moderate	Minor (1997-2012)	Moderate	94	N	109	S	204	Heavily manipulated channel - berms direct flow, channel is straightened both upstream and downstream of culvert
88	Unknown	Low	Minor (1997-2012)	Moderate	63	N	87	S	150	Braided channel - potential to shift lateral position
89	Along right bank	Moderate (if incision could progress upstream of bridge)	Negligible (1997-2012)	Low	112	N	115	S	227	Berms built along left bank at crossing; potential lateral erosion of right bank

Table 5-2. Assessment of Vertical and Lateral Stability

Site No.	Bedrock in banks or bed	Potential for degradation >local scour	Historical channel change near crossing	Potential for lateral channel change at/near crossing	Burial width from channel centerpoint along alignment					Notes
					Width (ft)	Direction	Width (ft)	Direction	Total width (ft)	
90	Along right bank	Moderate	Significant (1953-2012)	High within channel and flood plain; otherwise, moderate; channel appears to be constrained by older alluvium in many places	212	E	73	W	285	Increase in vegetation density along river between 1953 and 2012; channel is incised 8 to 9 ft below flood plain surface (not sure if this was true in 1953)
91	Along both banks	Low	Not reviewed	Low	22	N	16	S	38	Alignment crosses at berms
92	Bedrock mounds observed near crossing	Low to moderate	Significant (1953-2012)	Low due to berms	39	N	123	S	162	Broad, distributary channel network; major channel manipulation post 1953 - berms placed to direct flow
93	Along right bank	Low to moderate	Moderate (1997-2012) upstream of crossing	Low	76	N	28	S	104	Shallow channel; potential incision if knickpoints were to migrate upstream (located >1/2 mile downstream from crossing)
94	None	Low to moderate	Significant (1953-2012)	High - channel could move toward left bank	180	N	217	S	397	Active channel narrowing from 1953 to 2012; potential for active channel to be much wider

Table 5-2. Assessment of Vertical and Lateral Stability

Site No.	Bedrock in banks or bed	Potential for degradation >local scour	Historical channel change near crossing	Potential for lateral channel change at/near crossing	Burial width from channel centerpoint along alignment					Notes
					Width (ft)	Direction	Width (ft)	Direction	Total width (ft)	
95	In bed	Low	Negligible (1953-2012)	Moderate	107	S	278	S	384	Stopped at this crossing but did not fill out form; braided channel form; main channel could shift positions but will stay within constraints of migration area (1953-2012); centerpoint in northern branch
96	Along both banks	Low to moderate	Moderate (1953-2012); significant increase in vegetation	Low	177	N	489	S	666	Channel may have incised since 1953 due to tamarisk vegetating banks
97	Along both banks	Low to moderate	Shifts in dominant channel position (1953-2012)	Moderate to high	511	E	113	W	624	
98	None	High - for new channels forming	Avulsions could be common - evidence for many incipient channels between 1953 and 2012; major avulsion between 2010 and 2012	High	240	E	52	W	292	Unconfined alluvial fan; new channel formed between 2010 and 2012
99	Along right bank and in bed(?)	Low	Moderate (1997-2012)	High	54	N	198	S	253	Potential for channel avulsion upstream of crossing; potentially bedrock in bed downstream; big flow went through this drainage recently

Table 5-2. Assessment of Vertical and Lateral Stability

Site No.	Bedrock in banks or bed	Potential for degradation >local scour	Historical channel change near crossing	Potential for lateral channel change at/near crossing	Burial width from channel centerpoint along alignment					Notes
					Width (ft)	Direction	Width (ft)	Direction	Total width (ft)	
100	Likely in bed	Low	Minor (1997-2012)	High	185	E	113	W	298	Broad braided high flow area; potential for main channel avulsion
101	Along banks and in bed	Low	Not reviewed	Low	11	E	20	W	32	Single channel, confined
102	Along banks and in bed	Low	Not reviewed	Low	101	E	54	W	155	Single confined channel, braided at low flow
103	Near banks	Low	Not reviewed	Low	6	N	16	S	21	High potential for bedrock to be located close to surface
104	None	Low	Not reviewed	Low	13	N	25	S	37	Crossing is immediately downstream of culvert - low potential for movement
105	Along both bank and in bed(?)	Low	Negligible (1997-2012)	Low to moderate	29	N	17	S	46	Split channel, migration constrained by bedrock on both sides
106	Along banks	Low	Not reviewed	Low	60	N	119	S	179	Broad and shallow wash
107	Unknown	Low	Not reviewed	Low	6	N	36	S	42	Small drainage
108	Along banks	Low	Not reviewed	Low	23	N	23	S	45	Confined wash
109	Along banks	Low	Not reviewed	Low	31	N	31	S	62	Shallow, confined wash
110	Along banks	Low	Not reviewed	Low	46	N	46	S	93	Shallow wash
111	Unknown	Low	Not reviewed	Low to moderate	620	N	2034	S	2654	Measurement from point 111a
112	Unknown	Low to moderate	Moderate (1997-2012) upstream of crossing	Moderate	18	N	43	S	61	Single channel at crossing, incised into alluvium(?)
113	Unknown	Low to moderate	Not reviewed	Low	7	N	8	S	15	Is this an old road?
114	Unknown	Low	Not reviewed	Low						Shallow wash
115	In bed	Low	Not reviewed	Low	13	N	14	S	27	Single channel, swale

Table 5-2. Assessment of Vertical and Lateral Stability

Site No.	Bedrock in banks or bed	Potential for degradation >local scour	Historical channel change near crossing	Potential for lateral channel change at/near crossing	Burial width from channel centerpoint along alignment					Notes
					Width (ft)	Direction	Width (ft)	Direction	Total width (ft)	
116	Unknown	Low	Negligible (1997-2012)	Low	29	N	29	S	58	Channel flows into stock pond downstream of crossing
117	In bed and along banks	Low	Negligible (1997-2012)	Low	37	N	24	S	61	Incised single channel, lined with juniper(?)
118	Unknown	Low	Negligible (1992-2012)	Low	14	N	8	S	22	Single channel, appears to be incised
119	Unknown	Low	Negligible (1992-2012)	Low	37	N	67	S	104	Single channel, appears to be incised
120	Unknown	Low	Not reviewed	Low	337	N	6	S	343	Near confluence of two small washes
121	Along right bank	Low to moderate	Not reviewed	Low	25	N	25	S	51	Channelized; several berms built
122	Along banks	Low to moderate	Negligible (1997-2012)	Low	143	N	177	S	320	Single channel, braided at low flow; bedrock laterally constrains channel in some locations
123	Along banks	Low to moderate	Negligible (1997-2012)	Low	24	N	18	S	42	Single channel, braided at low flow; bedrock laterally constrains channel in some locations
124	In bed	Low	Not reviewed	Moderate	1,096	N			1,096	Channel could avulse at multiple locations into alignment between points 124a and 124b
125	Along left bank and in bed(?)	Low	Negligible (1953-2012)	Low	37	N	37	S	74	
126	In bed and along left bank	Low	Not reviewed	Low	21	N	101	S	122	Bedrock channel

Table 5-2. Assessment of Vertical and Lateral Stability

Site No.	Bedrock in banks or bed	Potential for degradation >local scour	Historical channel change near crossing	Potential for lateral channel change at/near crossing	Burial width from channel centerpoint along alignment					Notes
					Width (ft)	Direction	Width (ft)	Direction	Total width (ft)	
127	Unknown	Low	Not reviewed	Low	18	N	18	S	73	Poorly defined drainages
	Along left bank	Low	Not reviewed	Low	18	N	18	S		Looks channelized, potentially rock in channel bed downstream from crossing and culvert; possible avulsions upstream of crossing, but these channels should merge back to current channel location
128					19	N	21	S	40	
129	Unknown	Low	Negligible (1997-2012)	Moderate	14	N	14	S	29	Hard to tell if channel could shift or not
130	In both banks and likely in bed	Low	Not reviewed	Low	15	N	15	S	30	Channel confined in bedrock
131	Unknown	Low	Not reviewed	Low	12	N	12	S	25	Shallow wash
132	Unknown	Low	Minor (1997-2012)	Moderate	67	N	365	S	432	Shallow wash, potential for multiple paths through juniper
133	Unknown	Low to moderate	Negligible (1997-2012)	Low	89	N	89	S	177	Single channel bound by older surfaces

Legend: certainty of data evaluation

High	Visited crossing in field with detailed site description
Moderate	Visited crossing in field with no detailed site description
Low	Did not visit crossing in field

Table 5-3. Coordinates for Channel Centerpoint Locations

Site No.	Latitude						Longitude			
		Degrees	Minutes	Seconds	Decimal degrees		Degrees	Minutes	Seconds	Decimal degrees
1	N	36	56	1.2	36.934	W	111	28	26.4	-111.474
2	N	36	55	19.8	36.922	W	111	28	19.2	-111.472
3	N	36	54	24.6	36.907	W	111	28	58.8	-111.483
4	N	36	53	30.0	36.892	W	111	28	12.0	-111.470
5	N	36	53	45.0	36.896	W	111	27	32.4	-111.459
6	N	36	53	42.0	36.895	W	111	26	49.2	-111.447
7	N	36	53	26.4	36.891	W	111	26	34.8	-111.443
8	N	36	51	10.2	36.853	W	111	26	42.0	-111.445
9	N	36	49	9.0	36.819	W	111	26	24.0	-111.440
10	N	36	48	19.2	36.805	W	111	26	27.6	-111.441
10	N	36	48	20.4	36.806	W	111	26	27.6	-111.441
10	N	36	48	21.6	36.806	W	111	26	27.6	-111.441
11	N	36	42	27.0	36.708	W	111	26	31.2	-111.442
12	N	36	42	22.2	36.706	W	111	26	34.8	-111.443
13	N	36	42	17.4	36.705	W	111	26	34.8	-111.443
14	N	36	42	7.2	36.702	W	111	26	38.4	-111.444
15	N	36	37	15.6	36.621	W	111	26	27.6	-111.441
16	N	36	18	17.4	36.305	W	111	27	32.4	-111.459
17	N	36	17	39.0	36.294	W	111	27	3.6	-111.451
18	N	36	16	49.8	36.281	W	111	26	20.4	-111.439
19	N	36	16	19.8	36.272	W	111	25	55.2	-111.432
20	N	36	16	10.2	36.270	W	111	25	51.6	-111.431
21	N	36	15	50.4	36.264	W	111	25	37.2	-111.427
22	N	36	15	33.0	36.259	W	111	25	22.8	-111.423
23	N	36	15	15.0	36.254	W	111	25	8.4	-111.419
24	N	36	14	43.2	36.245	W	111	24	54.0	-111.415
25	N	36	13	59.4	36.233	W	111	24	18.0	-111.405
26	N	36	12	33.6	36.209	W	111	23	38.4	-111.394
27	N	36	11	54.6	36.199	W	111	23	34.8	-111.393
28	N	36	11	22.2	36.190	W	111	23	34.8	-111.393
30	N	36	11	16.2	36.188	W	111	23	38.4	-111.394
31	N	36	10	9.0	36.169	W	111	23	45.6	-111.396
32	N	36	19	2.4	36.317	W	111	28	26.4	-111.474
33	N	36	19	15.0	36.321	W	111	28	37.2	-111.477
34	N	36	19	28.8	36.325	W	111	28	58.8	-111.483
35	N	36	19	39.6	36.328	W	111	29	6.0	-111.485

Table 5-3. Coordinates for Channel Centerpoint Locations

Site No.	Latitude						Longitude			
		Degrees	Minutes	Seconds	Decimal degrees		Degrees	Minutes	Seconds	Decimal degrees
36	N	36	19	47.4	36.330	W	111	29	13.2	-111.487
37	N	36	19	56.4	36.332	W	111	29	16.8	-111.488
38	N	36	20	10.8	36.336	W	111	29	27.6	-111.491
39	N	36	20	24.6	36.340	W	111	29	38.4	-111.494
40	N	36	20	28.2	36.341	W	111	29	38.4	-111.494
41	N	36	20	37.8	36.344	W	111	29	45.6	-111.496
42	N	36	20	49.2	36.347	W	111	29	52.8	-111.498
43	N	36	21	21.6	36.356	W	111	30	7.2	-111.502
44	N	36	21	23.4	36.357	W	111	30	10.8	-111.503
45	N	36	21	31.8	36.359	W	111	30	21.6	-111.506
46	N	36	21	35.4	36.360	W	111	30	25.2	-111.507
47	N	36	22	43.2	36.379	W	111	31	1.2	-111.517
48	N	36	22	52.2	36.381	W	111	31	4.8	-111.518
49	N	36	24	33.6	36.409	W	111	32	13.2	-111.537
50	N	36	25	13.2	36.420	W	111	32	34.8	-111.543
51	N	36	25	24.0	36.423	W	111	32	38.4	-111.544
52	N	36	26	12.6	36.437	W	111	33	3.6	-111.551
53	N	36	28	14.4	36.471	W	111	34	12.0	-111.570
54	N	36	29	7.8	36.486	W	111	34	30.0	-111.575
55	N	36	29	17.4	36.488	W	111	34	33.6	-111.576
56	N	36	29	36.0	36.493	W	111	34	40.8	-111.578
57	N	36	30	1.2	36.500	W	111	34	51.6	-111.581
58	N	36	30	43.8	36.512	W	111	35	9.6	-111.586
59	N	36	31	1.8	36.517	W	111	35	20.4	-111.589
60	N	36	31	20.4	36.522	W	111	35	31.2	-111.592
61	N	36	31	45.6	36.529	W	111	35	49.2	-111.597
62	N	36	31	51.0	36.531	W	111	35	52.8	-111.598
63	N	36	31	59.4	36.533	W	111	35	60.0	-111.600
64	N	36	32	6.6	36.535	W	111	36	7.2	-111.602
65	N	36	32	35.4	36.543	W	111	36	28.8	-111.608
66	N	36	32	36.6	36.544	W	111	36	28.8	-111.608
67	N	36	33	7.8	36.552	W	111	37	1.2	-111.617
68	N	36	33	13.2	36.554	W	111	37	8.4	-111.619
69	N	36	33	18.6	36.555	W	111	37	12.0	-111.620
70	N	36	33	25.8	36.557	W	111	37	19.2	-111.622
71	N	36	33	37.2	36.560	W	111	37	26.4	-111.624

Table 5-3. Coordinates for Channel Centerpoint Locations

Site No.	Latitude						Longitude			
		Degrees	Minutes	Seconds	Decimal degrees		Degrees	Minutes	Seconds	Decimal degrees
72	N	36	33	47.4	36.563	W	111	37	33.6	-111.626
73	N	36	33	54.6	36.565	W	111	37	40.8	-111.628
74	N	36	34	1.8	36.567	W	111	37	44.4	-111.629
75	N	36	34	12.6	36.570	W	111	37	51.6	-111.631
76	N	36	34	30.6	36.575	W	111	38	2.4	-111.634
77	N	36	34	46.8	36.580	W	111	38	27.6	-111.641
78	N	36	35	23.4	36.590	W	111	38	45.6	-111.646
79	N	36	35	59.4	36.600	W	111	39	14.4	-111.654
80	N	36	36	33.6	36.609	W	111	39	18.0	-111.655
81	N	36	36	48.6	36.614	W	111	39	14.4	-111.654
82	N	36	36	56.4	36.616	W	111	39	14.4	-111.654
83	N	36	37	10.8	36.620	W	111	39	10.8	-111.653
84	N	36	8	37.2	36.144	W	111	23	42.0	-111.395
85	N	36	7	57.6	36.133	W	111	23	42.0	-111.395
86	N	36	5	30.0	36.092	W	111	23	34.8	-111.393
87	N	36	4	59.4	36.083	W	111	23	16.8	-111.388
88	N	36	4	21.0	36.073	W	111	23	13.2	-111.387
89	N	36	3	33.0	36.059	W	111	23	24.0	-111.390
90	N	36	1	38.4	36.027	W	111	23	45.6	-111.396
91	N	36	0	53.4	36.015	W	111	23	42.0	-111.395
92	N	36	0	37.8	36.011	W	111	23	42.0	-111.395
93	N	36	0	4.8	36.001	W	111	23	34.8	-111.393
94	N	35	56	28.2	35.941	W	111	23	52.8	-111.398
95	N	35	53	31.2	35.892	W	111	24	10.8	-111.403
96	N	35	52	34.2	35.876	W	111	24	21.6	-111.406
97	N	36	10	1.8	36.167	W	111	23	42.0	-111.395
98	N	36	9	58.2	36.166	W	111	23	27.6	-111.391
99	N	36	9	8.4	36.152	W	111	22	44.4	-111.379
100	N	36	7	59.4	36.133	W	111	21	25.2	-111.357
101	N	36	7	13.8	36.121	W	111	20	31.2	-111.342
102	N	36	7	11.4	36.120	W	111	20	27.6	-111.341
103	N	35	50	5.4	35.835	W	111	26	13.2	-111.437
104	N	35	49	31.2	35.825	W	111	26	20.4	-111.439
105	N	35	49	2.4	35.817	W	111	26	27.6	-111.441
106	N	35	43	30.6	35.725	W	111	28	58.8	-111.483
107	N	35	42	21.6	35.706	W	111	29	42.0	-111.495

Table 5-3. Coordinates for Channel Centerpoint Locations

Site No.	Latitude						Longitude			
		Degrees	Minutes	Seconds	Decimal degrees		Degrees	Minutes	Seconds	Decimal degrees
108	N	35	38	37.2	35.644	W	111	31	1.2	-111.517
109	N	35	34	55.8	35.582	W	111	31	44.4	-111.529
110	N	35	33	28.2	35.558	W	111	32	6.0	-111.535
111	N	35	25	21.0	35.423	W	111	34	12.0	-111.570
112	N	35	22	57.0	35.383	W	111	34	48.0	-111.580
113	N	36	45	19.2	36.755	W	111	26	31.2	-111.442
115	N	36	29	51.6	36.498	W	111	24	36.0	-111.410
116	N	36	23	46.2	36.396	W	111	31	37.2	-111.527
117	N	36	23	19.2	36.389	W	111	31	19.2	-111.522
118	N	36	37	47.4	36.630	W	111	39	3.6	-111.651
119	N	36	37	43.8	36.629	W	111	39	7.2	-111.652
120	N	36	6	58.2	36.116	W	111	23	34.8	-111.393
121	N	36	3	10.8	36.053	W	111	23	27.6	-111.391
122	N	35	59	30.6	35.992	W	111	23	31.2	-111.392
123	N	35	59	28.2	35.991	W	111	23	34.8	-111.393
124	N	35	53	43.2	35.895	W	111	24	7.2	-111.402
125	N	35	47	18.0	35.788	W	111	27	0.0	-111.450
126	N	35	46	28.8	35.775	W	111	27	25.2	-111.457
127	N	35	44	4.2	35.735	W	111	28	40.8	-111.478
127	N	35	44	6.0	35.735	W	111	28	40.8	-111.478
128	N	35	40	4.2	35.668	W	111	30	39.6	-111.511
129	N	35	33	14.4	35.554	W	111	32	6.0	-111.535
130	N	35	31	6.0	35.518	W	111	32	34.8	-111.543
131	N	35	27	57.0	35.466	W	111	33	32.4	-111.559
132	N	35	24	13.2	35.404	W	111	34	30.0	-111.575
133	N	35	13	32.4	35.226	W	111	33	36.0	-111.560
133	N	35	13	33.0	35.226	W	111	33	32.4	-111.559

6. Potential Scour Depths

The NCAP study area is an arid region with high relief, frequent rock outcrops, limited vegetation, and mostly ephemeral streams. Ephemeral flows may consist of intense, large volume flash floods. There are regional floods that last for weeks or months, as well as flash floods that occur suddenly and last only hours (AGS,[3] 2012). Much of the land is part of the Hopi or Navajo Reservations with small pockets of development. These factors combine to produce a large sediment supply to many streams, and there are many ephemeral braided streams in the valley bottoms that transport large sediment loads. An unlimited sediment supply to the streams is assumed for these computations of scour depth, and live-bed scour equations are used. Bedrock was noted in the bed of different channels, but the possible presence of erosion resistant materials in the channel bed or subsurface is ignored during the initial computation of scour depth. In the last section of this chapter, erosion resistant materials are considered by comparing computed scour depth to the depth-to-refusal information from a 2012 test pit investigation (Miller, 2012). This is a first step to assess in determining locations where geology may limit the scour depth (i.e., actual scour may not be as deep as estimated due to rock in the stream bed.

6.1 Flow Risk Assessment

A risk-based assessment is recommended (FHWA, 2012) for selecting the flow return interval for scour assessments. The hydraulic event selected for a scour evaluation is often larger than the design flow for the structure. A 50-year design life was assumed for the pipeline, and a 100-year flow recurrence interval was selected for the analysis of scour depth. A 50-year flow event would have a 63.4% chance of exceedance during the design life of the pipeline, but there is only a 39.5% chance that a high flow will exceed a 100-year storm event during the 50-year period following construction of the pipeline (FHWA, 2012). Chapter 3 describes the computation of flow rates.

6.2 Methods

There are 132 study sites: 8 sites are stream segments that parallel the proposed pipeline alignment, and 124 sites are pipeline crossings. Scour was computed the same way for stream segments and pipeline crossings. Sites were also organized into two groups based on the proximity of the proposed pipeline to a bridge or similar structure. At locations distant from bridges, the main forms of scour are bend scour and bedform scour. At pipeline sites adjacent to structures, the main forms of scour are local scour and contraction scour. Measurements from

[3] AGS refers to the Arizona Geological Survey.

laboratory flume studies indicate that the radius of a scour hole that develops at a structure (local scour) can be twice the depth of the scour hole in a sandy bed (FHWA, 2012). With the exception of the LCR bridge, local scour was initially assumed (and later confirmed) to be less than 25 feet deep. At twice the scour depth, the maximum extent of a local scour hole is less than 50 feet in radius. If the pipeline crossing is more than 50 feet distant from a structure, local and contraction scour are not considered.

Section 6.3 of this report describes the bend and bedform scour analysis and results for assessing scour at all locations. In section 6.4, results from the constriction and local scour assessment at sites adjacent to bridges and other structures are presented. The largest scour depth from the two methods is selected for the sites adjacent to bridges and presented as total scour values in section 6.5.

Complete hydraulic information is available at 22 pipeline crossings described as main sites. Hydraulic parameters were determined at a cross section using the selected flow return interval, as described in chapter 4. Slope helps determine the flow depth, and a cross section can define the flow area. The D_{50} and D_{90} grain sizes for sediment in the bed of the channel are also required for scour computations. Cross sections, slope measurements, and soil samples have been collected at the 22 main sites.

At main sites distant from bridges (>50 feet), scour is computed following modified ASCE (2005) methods. At main sites adjacent to bridges (<50 feet), scour is computed following HEC-18 (FHWA, 2012) standards. At the remaining 110 secondary sites, there is not sufficient hydraulic data and field observations to compute scour. Instead, a shifted regression equation (envelop curve) is developed and applied to all sites, to relate scour depth values (modified ASCE, 2005 method) from main sites to secondary sites. The function is based on the unit discharge at each site. At secondary sites adjacent to a bridge, unit discharge is also used to relate the bridge scour (HEC-18 methods) from main sites to secondary sites, and the larger scour estimate (ASCE, 2005, or FHWA, 2012) is selected for the site adjacent to a bridge.

6.2.1 Methods for Computing Scour at Main Sites

Total scour computed from the modified ASCE (2005) approach at locations distant from bridges (> 50 feet) is the summation of the components listed below:

- Degradation
- Bend scour
- Bedform scour (in sand bed streams)
- Low flow channel incisement (when not defined by survey)
- Factor of safety (1 to 1.5)

ASCE (2005) methods were modified by removing the component "general scour" from this list. General scour was determined to be a duplication of the bend scour component. Degradation depth is added to total scour depth as determined by a geomorphic assessment of vertical instability. Determination of the degradation depth is arbitrary, but the selection of a depth is partially improved by a "depth to armor" assessment and a "slope stability" assessment (Pemberton and Lara, 1984).

Bend scour was computed in this study as an average of values from four bend scour methods: Zeller, Maynord, Thorne, and USACE (see table 6-1 for reference source information). A severe bend is assumed for all the bend scour computations, although many of the streams are braided and relatively straight. Bend scour may not be present in a straight section of braided stream, but the assumption is made that a bend could migrate to the crossing location during the life of the project. This value also serves as a surrogate value for confluence scour, which is another scour form that occurs in braided rivers at the confluence of two braid paths.

Bedform scour is computed from methods described by Simons, Li and Associates, and the value is compared to results from a dune scour equation described by Maricopa County (see table 6-1 for reference source information). The larger value for bedform scour is used. A low flow channel is detectible in the stream surveys, so the estimate of low flow channel incisement (a fourth component of ASCE, 2005 methods) is not used. Table 6-1 lists scour equations for main sites.

Table 6-1. Scour Equations for Main Sites

General equation type	Specific equation	Reference source
Bend Scour Equations	Zeller Bend Scour	Simons Li & Associates (1985); pp. 5, 105 106
	Maynord Bend Scour	Maynord (1996); as referenced in ASCE (2005)
	Thorne Bend Scour	Thorne et al. (1995); as referenced in ASCE (2005)
	USACE Bend Scour Design Curves – sand	EM 1110-2-1601, Plate B41, in USACE (1994a)
Bedform Equations	Simons Li & Associates (1985)	
	Dune Scour Equation	Flood Control District of Maricopa County (2003), as presented in the PBS&J Scour Spreadsheet (PBS&J, 2008)
Comparison Equation	Reclamation Envelope Curve	Pemberton & Lara (1984); as referenced in ASCE (2005)

A scour estimate method presented in Pemberton and Lara (1984) was developed from field measurements at several USGS gage sites during high flow events, and they verified the curve with data from five additional New Mexico streams. Stream form was described as wide, sand bed, and ephemeral. Pemberton and Lara's method is referenced as the "Reclamation Envelop Curve" (ASCE, 2005)

and the curve is applied here as a comparison for the modified ASCE (2005) computed bend and bedform scour values.

6.2.2 Methods for Estimating Scour at Secondary Sites

No cross section data is available at the remaining 110 secondary sites to compute scour depth. Instead, a function is developed for a 100-year event, to estimate bend scour and bedform scour based on 22 calculated scour depths at main sites. Contraction scour depth computations are often related to the unit discharge of a stream. An assumption is made here that bend scour and bedform scour is similarly related to unit discharge.

$$q = Q / w \qquad \text{eq. 6-1}$$

Where:

q = unit discharge, ft^2/s
Q = flow at the site, ft^3/s
W = width of the channel, ft

The procedure for computing total scour at both main sites and secondary sites, when the sites are distant from bridges (>50 feet), is described in nine steps:

1. Complete an armor analysis and a slope stability analysis to help determine a reasonable degradation depth for all sites.

2. Compute bend scour as the average of four methods and bedform scour as the larger of two methods. Add average bend scour to maximum bedform scour.

3. Compute the unit discharge of the main sites based on bankfull values (scour depth is based on a 100-year flow event) and plot the values for combined bend scour and bedform scour value at each site.

4. Define a trend line or linear best fit for the 22 plotted site values.

5. Add a standard degradation depth as an offset to the scour trend line and ensure that it envelops most of the 22 main site points.

6. Compare the offset trend line to the bend scour plus bedform scour points, multiplied by a safety factor.

7. Compare the bend scour plus bedform scour value to values from the Reclamation Envelop Curve and the scour values from the offset trend line.

8. Compute the unit discharge for each secondary site at bankfull conditions, and use the unit discharge and the offset trend line function to estimate the scour depth for all main and secondary sites.

9. Add an additional degradation value to sites with medium and high vertical instability.

6.3 Results for Main and Secondary Sites Distant from Bridges

A scour spreadsheet, version 1.2 (May 28, 2008), developed by the firm PBS&J (2008), automates computational methods from Neil, Pemberton and Lara (1984), Simons Li & Associates (1985), and the more recent bedform and bend scour equations (table 6-1). The PBS&J spreadsheet was used for scour computations at all main sites.

Step 1: Results from an armoring analysis and a stable slope analysis are shown in table 6-2. These values indicate that a stable slope is much flatter than existing slopes. If the sediment supply were cut off, there would be high potential for degradation. Results from the armoring analysis indicated only one-third of the channels would be able to armor to prevent excessive degradation; however, this result may be affected by the size of the sediment bulk sample.

Step 2: Results from the bend scour and bedform scour computations are listed in table 6-3. Required parameters for these computations are listed in appendix D-4.

Step 3: Bend scour and bedform scour depths for the main sites are plotted in figure 6-1 against the unit discharge for each site. At the 22 main crossings, bankfull discharge (the discharge when a stream is filled to the top of its lowest bank; see table 4-2) was computed in chapter 4 from a surveyed cross section and slope. Unit discharge is computed by dividing the bankfull discharge by the top width at bankfull.

Step 4: A best-fit trend line is matched to the 22 main site points. The function is shown in figure 6-1.

Step 5: The trend line is offset 3 feet to account for degradation and envelops all 22 bend scour plus bedform scour points.

$$\text{Scour depth} = 0.1812\ q + 3.3167 \qquad \text{eq. 6-2}$$

Where:

q = unit discharge, ft^2/s

Step 6: In figure 6-1, the offset trend line is also compared to the scour points at main sites multiplied by a safety factor of 1.2.

Step 7: Total bend scour and bedform scour values are compared to values from the Reclamation Envelop Curve in table 6-4.

Step 8: Total bend scour and bedform scour can be estimated, specific to this project area, using the offset trend line function if the bankfull discharge and channel width of the stream are known. Bankfull discharge varies by location but commonly occurs between a 1-year and 5-year return interval. A surveyed cross section and slope are not available at secondary crossings. Instead, bankfull discharge is estimated for secondary sites using a function developed from the main crossing bankfull discharge values. Bankfull discharge at the main crossings (table 3-1) was determined to be a factor of 1.28 times the average of the 2-yr and 5-yr discharge values.

$$1.28 * (Q2+Q5)/2 \qquad \text{eq. 6-3}$$

Where:

Q_{2+}
$_{++}$ = discharge (ft^3/s) at the 2-year recurrence interval and
Q_5 = discharge (ft^3/s) at the 5-year recurrence interval.

Channel top widths at secondary crossings were measured adjacent to the stream crossing and perpendicular to the flow using GIS mapping. Bankfull top width values and unit discharge values for secondary sites are listed in table 6-9 at the end of this section.

Step 9: As a function of unit discharge, scour depth is computed from the offset regression equation for all main and secondary sites. An additional degradation depth of 2 feet to 4 feet is added to the scour depth estimate if the geomorphic rating of vertical instability is medium (2 feet), medium to high (3 feet), or high (4 feet). Table 6-9 provides a summary of results.

Table 6-2. Investigating Degradation

Degradation Controlled by Armoring

Gradation based on bulk sample from channel bed. Negative values indicate armoring, "sand" indicates no coarser particles in channel bed bulk sample. May not be indicative of coarse materials available.

Crossing Sites	16	20	21	26	31	32	33	50	51	52	57	58	84	86	90	92	94	95	96	97	98	125
$D_{critical}$, feet, final	0.28	0.23	0.32	0.37	0.19	0.27	0.22	0.19	0.23	0.47	0.16	0.17	0.31	0.17	0.04	0.09	0.09	0.04	0.21	0.25	0.26	0.17
$D_{critical}$, millimeters, final	87	71	96	113	57	81	69	57	71	143	49	51	96	51	12	28	28	13	65	78	80	53
Percent gradation larger than $D_{critical}$	0	0.005	0.03	0	0	0	0.03	0.06	0			29	0		16	0	0	2	0	0	0	0
Depth of degradation to $3xD_{50}$ armor develops (feet)	Sand	**139.3**	**30.7**	Sand	Sand	Sand	**21.8**	**8.8**	Sand			**-0.5**	Sand		**-0.1**	Sand	Sand	**-0.1**	Sand	Sand	Sand	Sand

Conclusion: Bulk sample at 12 sites does not contain coarse materials to armor, 4 sites would degrade to large depth before armoring, 3 sites are already armored.

Degradation Controlled by Stable (Equilibrium Slope)

Crossing Sites	16	20	21	26	31	32	33	50	51	52	57	58	84	86	90	92	94	95	96	97	98	125
Schoklitsh Method	0.00085	0.00273	0.00202	0.00018	0.00227	0.00115	0.00069	0.00017	0.00017	0.00007	0.00045	0.00026	0.00141	0.00097	0.00011	0.00046	0.00046	0.00066	0.00005	0.00021	0.00012	0.00077
Meyer-Peter, Muller Method	0.00050	0.00186	0.00107	0.00017	0.00089	0.00050	0.00042	0.00009	0.00011	0.00003	0.00025	0.00014	0.00098	0.00024	0.00002	0.00014	0.00014	0.00025	0.00003	0.00014	0.00010	0.00070
Lane's Tractive Force Method	0.00046	0.00156	0.00092	0.00019	0.00100	0.00055	0.00046	0.00017	0.00016	0.00013	0.00028	0.00028	0.00076	0.00042	0.00008	0.00024	0.00024	0.00027	na	0.00019	0.00026	0.00077
Shield's Diagram	0.00024	0.00089	0.00037	0.00004	0.00025	0.00017	0.00024	0.00003	0.00003	0.00002	0.00010	0.00005	0.00027	0.00007	0.00001	0.00004	0.00004	0.00005	na	0.00004	0.00003	0.00023
Average stable slope	0.00051	0.00176	0.00110	0.00015	0.00110	0.00059	0.00045	0.00011	0.00012	0.00006	0.00027	0.00018	0.00086	0.00043	0.00005	0.00022	0.00022	0.00031	0.00004	0.00014	0.00013	0.00062
Energy slope	0.0091	0.0138	0.0258	0.0189	0.0150	0.0100	0.0080	0.0080	0.0070	0.0160	0.0102	0.0069	0.0201	0.0126	0.0010	0.0091	0.0091	0.0028	0.0011	0.0092	0.0198	0.0082
Ratio of energy slope/average equilibrium (stable) slope	17.7	7.8	23.5	130.3	13.6	16.8	17.6	69.9	59.7	253.3	37.8	37.8	23.5	29.6	18.5	41.7	41.7	9.0	27.5	64.1	156.5	13.3

Conclusion: Most streams in this project area are much steeper than a stable slope due to the large sediment supply in the system. Degradation is possible, but large degradation would require a reduction in the sediment supply, no natural development of channel armor, and no downstream bedrock control.

The sediment supply could be reduced by construction of an upstream dam or the establishment of more vegetation in the overbank area and riparian vegetation such as salt cedar.

Table 6-3. Bend Scour and Bedform Scour Depths at Main Sites

Crossing Sites	16	20	21	26	31	32	33	50	51	52	57	58	84	86	90	92	94	95	96	97	98	125
Bend Scour (ft)																						
Zeller Bend Scour (Simons Li & Associates, 1985; p 5.105, 106)	0.6	0.5	0.3	0.5	0.4	0.6	0.7	0.7	0.8	0.8	0.4	0.7	0.3	0	0.7	0.3	0.7	0.4	2.9	0.5	0.33	0.5
Maynord Bend Scour (Maynord, 1996; as referenced in ASCE, 2005)	4.5	0.4	1.5	1.9	1.1	2.4	1.2	0	0	0.2	0.1	0	1.5	0.4	2.9	1.6	1.8	0.5	1.3	4.3	1.15	1.7
Thorne Bend Scour (Thorne et al., 1995; as referenced in ASCE, 2005)	4.5	1.6	1.2	1.9	1.2	2.5	2.6	2.2	3.2	2.9	1.5	2.3	1.5	1.3	3.9	0.9	2.5	1.5	19.5	2.6	1.26	2
USACE Bend Scour Design Curves-sand (COE 1110-2-1601, Plate B41)	5.3	0	0.9	1.7	1.3	2.4	1.2	0	0.5	0.8	0	0	1.4	0.8	3.9	0	0.4	0	22.2	2.3	0.35	1.6
Average bend scour	**3.7**	**0.6**	**1**	**1.5**	**1**	**2**	**1.4**	**0.7**	**1.1**	**1.2**	**0.5**	**0.8**	**1.2**	**0.6**	**2.9**	**0.7**	**1.3**	**0.6**	**11.5**	**2.4**	**0.8**	**1.4**
Bedform Scour																						
Bedform Scour (Simons Li & Associates, 1985)	**0.9**	**0.7**	**0.3**	**0.5**	**0.3**	**0.6**	**0.8**	**1.0**	**1.2**	**1.0**	**0.6**	**1.0**	**0.4**	**0.5**	**0.9**	**0.4**	**0.4**	**0.6**	**4.0**	**0.6**	**0.4**	**0.5**
Maricopa County bedform dune scour method (Flood Control District of Maricopa County, 2003)	0.1	0.1	0.0	0.1	0.0	0.1	0.1	0.1	0.1	0.1	0.1	0.1	0.1	0.0	0.2	0.0	0.0	0.1	1.2	0.1	0.0	0.1
Maximum bedform scour	**0.9**	**0.7**	**0.3**	**0.5**	**0.3**	**0.6**	**0.8**	**1.0**	**1.2**	**1.0**	**0.6**	**1.0**	**0.4**	**0.5**	**0.9**	**0.4**	**0.4**	**0.6**	**4.0**	**0.6**	**0.4**	**0.5**
Bend Scour + Bedform Scour																						
Average bend scour + maximum bedform scour	4.6	1.3	1.3	2.0	1.3	2.6	2.2	1.7	2.3	2.2	1.1	1.8	1.6	1.1	3.8	1.1	1.7	1.2	15.5	3.1	1.2	1.9

Table 6-4. Comparison of Scour Depth Values and Methods

Crossing Sites	16	20	21	26	31	32	33	50	51	52	57	58	84	86	90	92	94	95	96	97	98	125
unit discharge, q	6.9	6.2	2.1	2.7	2.3	5.7	9.8	18.3	13.1	18.9	4.6	23.5	3.0	3.3	6.7	3.3	12.0	3.1	71.8	5.5	9.0	7.2
USBR Envelope Curve-Ephemeral Streams in SW	5	4.1	4.2	4.6	3.7	5.1	4.7	4.3	4.9	5.2	3.8	4.3	4.2	3.8	4.4	3.2	4.3	3.3	8	4.9	3.8	4.6
BEND SCOUR + BEDFORM SCOUR	4.6	1.3	1.3	2.0	1.3	2.6	2.2	1.7	2.3	2.2	1.1	1.8	1.6	1.1	3.8	1.1	1.7	1.2	15.5	3.1	1.2	1.9
SECONDARY SITE'S CURVE (trend line + 3' offset)	4.9	4.7	4.0	4.1	4.0	4.7	5.4	6.9	6.0	7.0	4.5	7.9	4.1	4.2	4.8	4.2	5.8	4.2	16.6	4.6	5.2	4.9
BEND + BEDFORM + 2 ft DEG + FS (1.3)	8.6	4.2	4.3	5.2	4.3	6.0	5.5	4.9	5.6	5.5	4.1	5.0	4.6	4.0	7.6	4.0	4.8	4.2	22.8	6.6	4.2	5.1
TOTAL SCOUR, ASCE METHOD (2005)	14.5	6.2	6.4	8.0	6.1	11.2	9.3	8.2	10.4	10.7	6.2	8.2	6.9	5.9	12.6	5.5	8.3	5.8	47.6	12.3	7.7	8.7

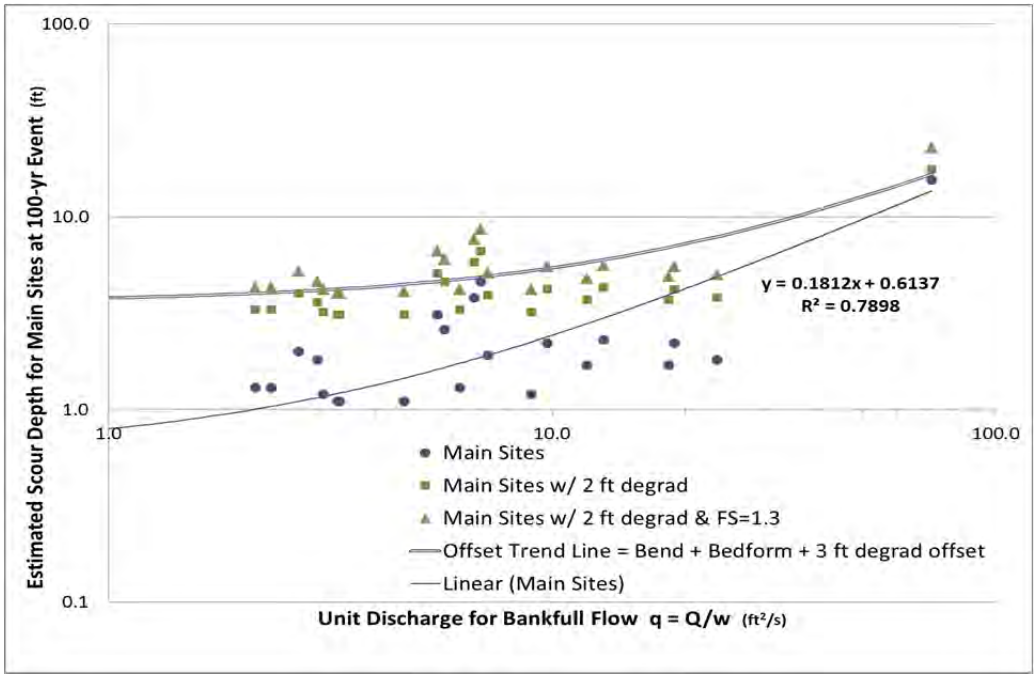

Figure 6-1. Relation of scour depth to unit discharge. Main site points are plotted to develop an offset regression line, which can be used to estimate scour depth at secondary locations distant from bridges or other structures.

6.4 Methods for Computing Scour at Sites Adjacent to Bridges

Table 6-5 lists the types of scour considered for sites distant or adjacent to a bridge. Table 6-6 shows the equations used for estimating scour at sites adjacent to bridges. Contraction scour and local scour are also considered if a pipeline crossing is located adjacent to a relatively fixed structure in the bed of the channel that could cause erosive flow. The FHWA HEC-18 (FHWA, 2012) method is used to compute scour at pipeline crossings less than 50 feet from a bridge or other structure. Similar to sites distant from bridges, contraction scour and local scour can be computed at main sites and estimated at secondary sites. Contraction scour and local scour components are summed with an estimate of degradation. This value becomes the maximum scour depth if it is larger than the previously computed bend and bedform scour for sites distant from a bridge:

- Degradation
- Contraction scour
- Local scour (pier or abutment scour equations)

Table 6-5. Types of Scour Assessed for Pipeline Design

Distant from a bridge (>50 ft) modified ASCE (2005) methods	Adjacent to a bridge (<50 ft) FHWA HEC-18 (FHWA, 2012) Methods
Bend scour	Contraction scour
Bedform scour	Local scour - pier or abutment
Degradation[1]	Degradation[1]

[1]Dependent on stream vertical stability assessment.

Table 6-6. Equations for Main Sites Adjacent to a Bridge (<50 ft)

Contraction scour equations	Laursen Live Bed Equation (Laursen, 1960)
Equations for local scour at piers	CSU Equation (Richardson, 1990)
Equations for abutment scour	Froehlich Equation (Froehlich, 1989) – in HEC-RAS
	HIRE Equation (Richardson, 1990) – in HEC-RAS
	NCHRP 24-20 Equation (HEC-18, FHWA, 2012)

6.4.1 Contraction Scour at Main Sites

Bridges or other road crossing structures are the most common cause of contraction scour and local scour. Rock walls and other natural features can also produce scour. Contraction scour is caused by flow that is confined and accelerated between erosion-resistant walls. If the bed is not erosion resistant; for example, at a bridge or a bottomless culvert, constriction scour erodes material across the full width of the channel bed. Contraction scour can also cause bed erosion for a short distance downstream of the structure (figure 6-2).

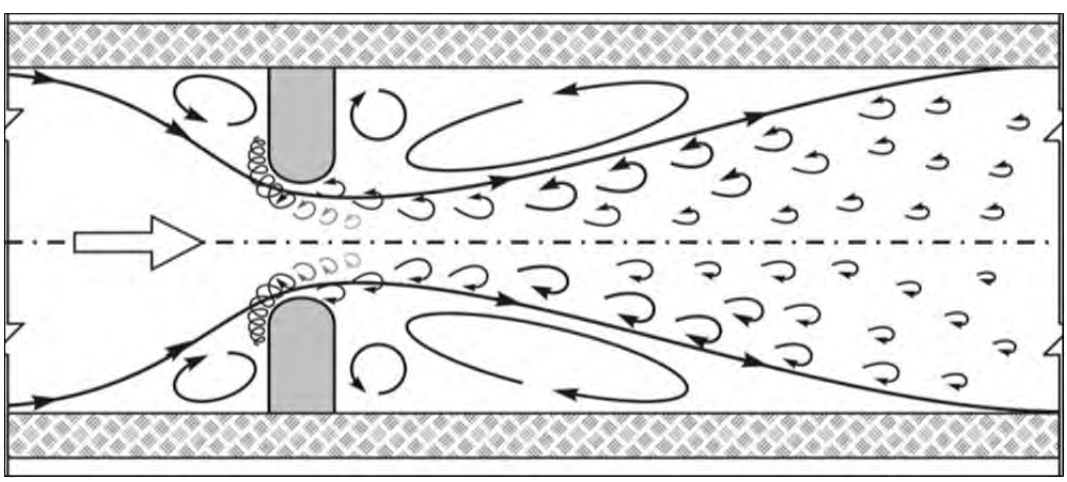

Figure 6-2. Flow structure including macro-turbulence generated by flow around abutments in a narrow main channel (NCHRP, 2011), causing contraction scour.

Contraction scour is present at lower flows at Crossing 96, the LCR crossing. The 1D HEC-RAS model shows flow overtopping the old Highway 89 bridge at flows greater than a 10-year event (figures 4-8 and 4-9). Velocity maps from the SRH-2D model show flow is constricted as it moves between the bridge abutments of the old bridge. The colored shading on the velocity maps indicate that contraction scour extends both upstream and downstream of the bridge.

Contraction flow lines do not extend as far upstream at higher flows as seen in the velocity map from the 5-year flow event (figure 4-10). At a 100-year flow event, when most of the flow passes over the top of the bridge or is conveyed in the flood plain, there is less detectible contraction scour. The main impact is to the right abutment as flow passes over the top of the abutment. Bridge piers and bridge decks cannot be included in the 2D flow model at this time, so the model results do not represent all flow detail. Riprap on the right approach bank was observed in the field. Despite the lack of a bridge deck, the SRH-2D results at the 100-year flow event demonstrate that contraction scour will decrease and local scour concerns will increase at higher flows (figure 4-11).

6.4.2 Local Scour at Main Sites

Local scour occurs when approach flow is impeded by a hard, vertical surface. Flow is diverted into a roller that spins towards the bed and removes material through accelerated flow (figure 6-3). At a vertical obstruction like a pier, the roller spins off to both the left and right, creating the signature scour pattern in the bed of the channel (figures 6-4 and 6-5). At abutments, the flow can spin inwards and downstream after striking the structure protruding into the flow path. Bed surface area where erosion occurs can be defined by a radius extending horizontally for a distance 2x the scour depth from the obstruction (FHWA, 2012).

The deepest local scour occurs at the upstream face of the obstruction. Wake scour is caused downstream by flow vortices shedding off the structure. Wake vortices also cause erosion; however, this depth is shallow compared to the scour hole upstream of the structure (figure 6-4). Good locations to bury the pipeline are upstream, out of range of the scour hole radius (>2x scour depth); or downstream if there is no contraction scour effect (wake scour is less of a concern). Contraction and local scour are computed if the proposed pipeline crosses within 50 feet of a bridge or structure. A local scour hole or contraction scour could expose the pipeline at this location.

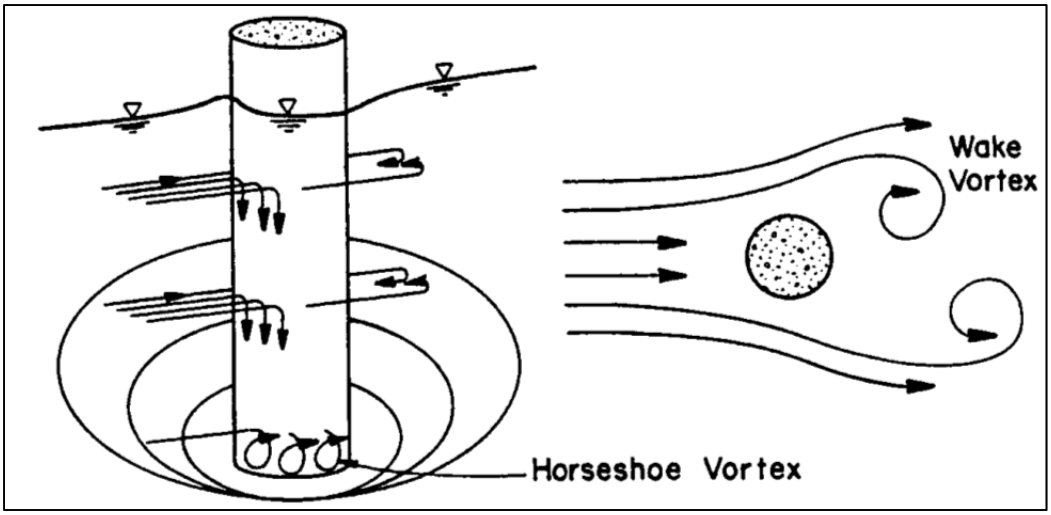

Figure 6-3. Photo of a horseshoe scour pattern in a laboratory flume at a circular pier (FHWA, 2012).

Figure 6-4. Local scour in a laboratory. Looking upstream, past the shallow wake scour, at the deeper scour around the pier (FHWA, 2012).

Figure 6-5. Local scour at Site 92 pier - a circular eroded area in the sand. Photo is looking downstream at the nose of the pier (Reclamation, 2013).

6.4.2.1 Local Scour at Piers

Table 6-7 lists contraction and local scour depths computed at 4 of the 22 main sites when a pipeline crossing is near a bridge. The Laursen (1960) live-bed equation was used to compute contraction scour, and the Colorado State University (CSU) equation (Richardson, et al, 1990) was used to compute pier scour for all locations. The LCR is the largest stream crossing in the study area and is modeled with both a HEC-RAS and an SRH-2D numerical model. The HEC-RAS model was also used to compute scour at the LCR. Woody debris had accumulated on two of the upstream piles of the old Highway 89 bridge at the LCR at the time of the site visit (figure 6-6). Pier scour depth is dependent on pier width, and debris increases the apparent pier width. The pier width was increased in the HEC-RAS model to account for the debris. Contraction scour and pier scour are added for total depth.

Figure 6-6. Debris caught on pile-piers of the old Highway 89 bridge from spring flows at the LCR, April, 2013.

6.4.2.2 Local Scour at Abutments

HEC-RAS computes abutment scour using either the Froehlich (1989) or the HIRE[4] (Richardson, 1990) equation. At the LCR, the Froehlich equation was selected by HEC-RAS for the right abutment, and the HIRE equation was selected for the left abutment based on a ratio of abutment length to approach flow depth. In 2012, the National Cooperative Highways Research Program (NCHRP) 24-20 equation was added to the HEC-18 manual as a third method of computing abutment scour. The NCHRP 24-20 method is the least conservative method and appears to be favored by FHWA. Contraction scour patterns are the basis of the NCHRP 24-20 abutment equation and are included in the estimate, so contraction scour is not calculated separately. The NCHRP 24-20 abutment scour/ constriction scour equation was used for all four main crossings and values are listed in table 6-7.

[4] HIRE refers to the Abutment Scour Equation developed by FHWA for USACE spur dike data.

Table 6-7. Local and Contraction Scour Depths Computed at Main Sites for a 100-Year Flow Event

Site	Structures that create local scour			Local scour evaluation							
	Distance from pipeline crossing to structure (ft)	Structure		Contraction Laursen	Pier CSU (HEC-18)	Left abutment HEC-RAS	Right abutment HEC-RAS	Abutment plus contraction NCHRP 24-20 (live bed)	Maximum Scour Depth (ft)	Local Scour Radius*	Site affected by local scour?**
31	38	u/s	Four pier bridge, old road	0.5	4.7			2.3	5.2	10.4	No
84	42	u/s	Four pier bridge, old road	0	5.1			0.5	5.1	10.2	No
96	4	u/s	Bridge	6.1	12.4	48	37.4	25.7	25.7***	51.4	Yes
125	1	d/s	Two pier bridge	0.8	7.8			4	8.6	17.2	Yes

Note: u/s = upstream; d/s = downstream
*Local scour radius = the maximum scour depth multiplied by 2.
**Site affected by local scour if radius is greater than the crossing distance.
***HEC-RAS abutment scour estimates are larger, but the NCHRP 24-20 method is recommended by FHWA (2012).

Local scour is considered at the LCR where the pipeline crossing is 4 feet upstream of the old Highway 89 bridge. The NCHRP 24-20 value for abutment scour is used instead of the HEC-RAS computations of abutment scour. NCHRP 24-20 abutment/contraction scour (25.7 feet) is deeper than pier scour and contraction scour added together (18.5 feet).

Figure 6-7. Relic piers that can cause local scour.

6.4.3 Contraction Scour and Local Scour at Secondary Crossings

Including 4 main sites, there are 19 sites where a bridge or structure is within 50 feet of the pipeline crossing. Contraction and local scour at four main sites have been computed in the previous section. Contraction scour and local scour are estimated at the 15 remaining secondary sites using unit discharge values and the computed values from main sites. Table 6-8 lists secondary and main crossings by increasing unit discharge. Main site scour depths that bracket secondary sites are used to estimate scour at secondary sites. A straight-line relation is assumed between the main site scour depths and unit discharge values. Secondary sites that are not bracketed by main sites (unit discharge <3) are assumed to have a maximum scour depth of 5 feet, the upper limit set by Site 84 (see table 6-8). Local scour at piers is also dependent on pier width, so an inherent assumption for this estimate is that most of the piers in the study area have a blunt nose that is 18 inches wide. This was a common size at the main sites.

The estimated scour depth assigned to secondary crossings is multiplied by 2 to get the radius of the erosion affected area (table 6-8). The scour radius is compared to the actual distance the pipeline crossing is located from a structure. When the pipeline crossing is located within the area affected by local scour, the larger scour depth is used. When the pipeline crossing is outside the scour radius, bend and bedform scour from the offset regression equation define the maximum scour depth (figure 6-8).

Table 6-8. Local Scour Depth at Secondary Sites Estimated from Computed Local Scour Depths at Main Sites. (Main crossings are shaded yellow. Radius of local scour area, local scour depth multiplied by 2, is calculated from the estimated scour depth)

Site No.	Unit discharge, q (ft^2/s)	Local scour depth (ft)	Radius of scour hole = local scour depth multiplied by 2 (ft)
37	1.2	5 max	10 max
23	1.3	5 max	10 max
104	1.4	5 max	10 max
36	1.7	5 max	10 max
105	2	5 max	10 max
22	2.1	5 max	10 max
35	2.6	5 max	10 max
2	2.9	5 max	10 max
84	3	5.1	10.2
31	3	5.2	10.4
41	5	6.8	13.6
120	6.1	7.7	14.4
43	6.3	7.9	15.8
44	6.4	8	16
125	7.2	8.6	17.2
28	8.5	9.3	18.6
91	9	9.6	19.2
3	17.8	11.4	22.9
96	72	25.7	52

Note: Computed scour depths from main sites are shaded yellow.
All piers are assumed to be blunt and 18 inches wide.

In table 6-8, scour radius values range from 10 feet to 23 feet, and then they jump to 52 feet for Site 96 (the LCR). If the pipeline is buried upstream, and within 52 feet of the old Highway 89 bridge at the LCR, the design scour depth is the larger value of local scour (26 feet) or bend and bedform scour.

Figure 6-8. The proposed pipeline crossing at Crossing 84 is near the sediment sampling sight and is outside the expected local scour radius of 10 feet. Local scour is not considered at this site.

6.5 Total Scour Depth

Table 6-9 shows the compiled scour depth results for all sites. Assembled in the table are calculated scour from the main sites, estimated scour depths at secondary sites, unit discharge values, the distance to nearby structures, scour radius, maximum scour depth, and additional assignments of degradation depth. Total scour depth at sites with a moderate rating of vertical instability is increased 2 feet for degradation, a site with a moderate to high rating is assigned 3 feet for degradation, and sites with a high rating of vertical instability are increased 4 feet for degradation. The minimum total scour depth at a 100-year flow event is estimated at 3.6 feet at Site 7, and the maximum scour depth is estimated at 25.7 feet at the LCR, Site 96.

Table 6-9. Scour Depth Estimates for a 100-Year Event

Unit discharge (bankfull) and slope					Bend and bedform scour		Structures causing contraction or local scour			Contraction or local scour			Maxi-mum scour	Degradation		Total scour depth	
Site No.	Bed slope S_o (ft/ft)	Bank-full flow Q_{bf} (ft^3/s)	Top width w (ft)	Unit discharge q (ft^2/s)	Compu-ted at main site (ft)	Trend line +3 ft (ft)	Xing is: (ft)		Type of structure	Com-puted at main site (ft)	Estima-ted at secon-dary site (ft)	Scour radius (ft)	(ft)	Vertical instability rating	Assigned depth (ft)	Total scour depth (ft)	With F.S.= 1.3 (ft)
1	0.0472	35	15	2.3		4.0	264	u/s	Road crossing				4.0	Low to moderate		4.0	5.2
2	0.0425	86	30	2.9		4.1	32	u/s	Road crossing – culvert		5 max	10 max	4.1	Low		4.1	5.4
3	0.0184	445	25	17.8		6.8	20	u/s	Road crossing – culvert		11.4	22.9	11.4	Low		11.4	14.8
4	0.0121	419	55	7.6		5.0	790	u/s	Road crossing – culvert				5.0	Low to moderate		5.0	6.5
5	0.0333	102	35	2.9		4.1			NONE				4.1	Low to moderate		4.1	5.4
6		157	50	3.1		4.2	75	d/s	Culvert				4.2	Low		4.2	5.4
7	0.0391	35				3.6			NONE - parallels road				3.6	Low		3.6	4.7
8	0.0159	102	35	2.9		4.1	320	u/s	Road crossing				4.1	Low		4.1	5.4

Table 6-9. Scour Depth Estimates for a 100-Year Event

Unit discharge (bankfull) and slope					Bend and bedform scour		Structures causing contraction or local scour			Contraction or local scour			Maxi-mum scour	Degradation		Total scour depth	
Site No.	Bed slope S_o (ft/ft)	Bank-full flow Q_{bf} (ft^3/s)	Top width w (ft)	Unit discharge q (ft^2/s)	Compu-ted at main site (ft)	Trend line +3 ft (ft)	Xing is: (ft)		Type of structure	Com-puted at main site (ft)	Estima-ted at secon-dary site (ft)	Scour radius (ft)	(ft)	Vertical instability rating	Assigned depth (ft)	Total scour depth (ft)	With F.S.= 1.3 (ft)
9	0.0243	19	20	1		3.8	115-240	d/s	road crossing				3.8	Low		3.8	4.9
10	0.0441	19	15	1.3		3.8	135	d/s and u/s	Road crossing - channel on top for 230 ft				3.8	Low		3.8	5.0
11	0.0506	42	25	1.7		3.9	110		Parallels road				3.9	Low to moderate		3.9	5.1
12	0.046	45	10	4.5		4.4	125	u/s	Box culvert				4.4	Low to moderate		4.4	5.8
13	0.0472	74	15	4.9		4.5	140-190	u/s	Road crossing				4.5	Low to moderate		4.5	5.9
14	0.0178	70	20	3.5		4.2	171	u/s	Road crossing				4.2	Low to moderate		4.2	5.5
15	0.0601	45	10	4.5		4.4	200	u/s	Side road - culvert				4.4	Low		4.4	5.8
16	0.0091	794	115	6.9	4.6	4.9	150	u/s	Bridge				4.9	Low to moderate		4.9	6.3

Table 6-9. Scour Depth Estimates for a 100-Year Event

Unit discharge (bankfull) and slope					Bend and bedform scour		Structures causing contraction or local scour			Contraction or local scour			Maxi-mum scour	Degradation		Total scour depth	
Site No.	Bed slope S_o (ft/ft)	Bank-full flow Q_{bf} (ft^3/s)	Top width w (ft)	Unit discharge q (ft^2/s)	Compu-ted at main site (ft)	Trend line +3 ft (ft)	Xing is: (ft)		Type of structure	Com-puted at main site (ft)	Estima-ted at secon-dary site (ft)	Scour radius (ft)	(ft)	Vertical instability rating	Assigned depth (ft)	Total scour depth (ft)	With F.S.= 1.3 (ft)
17	0.0173	246	35	7		4.9	95	d/s	Bridge/box culverts				4.9	Moderate	2	6.9	8.9
18	0.0247	221	40	5.5		4.6	53	d/s	Box culverts				4.6	Moderate	2	6.6	8.6
19	0.0307	125	25	5		4.5	55	u/s	Box culverts, old road				4.5	Low to moderate		4.5	5.9
20	0.0138	371	60	6.2	1.3	4.7	422	d/s	Six box culverts				4.7	Moderate	2	6.7	8.8
21	0.0258	182	85	2.1	1.3	4.0	200	d/s	Three box culverts				4.0	Low to moderate		4.0	5.2
22	0.0355	74	35	2.1		4.0	44	u/s	Old road		5 max.	10 max.	4.0	Low to moderate		4.0	5.2
23	0.0957	32	25	1.3		3.8	25	u/s	Old road - culvert		5 max.	10 max.	3.8	High - potential for headcuts to migrate u/s of road to crossing	4	7.8	10.2

Table 6-9. Scour Depth Estimates for a 100-Year Event

Unit discharge (bankfull) and slope					Bend and bedform scour		Structures causing contraction or local scour			Contraction or local scour			Maxi-mum scour	Degradation		Total scour depth	
Site No.	Bed slope S_o (ft/ft)	Bank-full flow Q_{bf} (ft^3/s)	Top width w (ft)	Unit discharge q (ft^2/s)	Compu-ted at main site (ft)	Trend line +3 ft (ft)	Xing is: (ft)		Type of structure	Com-puted at main site (ft)	Estima-ted at secon-dary site (ft)	Scour radius (ft)	(ft)	Vertical instability rating	Assigned depth (ft)	Total scour depth (ft)	With F.S.= 1.3 (ft)
24	0.0771	90	15	6		4.7		u/s	NONE - silted in to old road				4.7	Low		4.7	6.1
25	0.0225	109	15	7.3		4.9	160	d/s	Round culvert, old road				4.9	Moderate	2	6.9	9.0
26	0.0189	250	93	2.7	2.0	4.1	105	d/s	Three pier bridge				4.1	Low		4.1	5.3
27	0	224	40	5.6		4.6	105	d/s	bridge, main wash d/s				4.6	Low		4.6	6.0
28	0	170	20	8.5		5.2	40	d/s	bridge, main wash d/s		9.3	18.6	5.2	Low		5.2	6.7
30	0	170	29	5.8		4.7	110	d/s	bridge, main wash d/s				4.7	Low		4.7	6.1

Table 6-9. Scour Depth Estimates for a 100-Year Event

Unit discharge (bankfull) and slope					Bend and bedform scour		Structures causing contraction or local scour			Contraction or local scour			Maxi-mum scour	Degradation		Total scour depth	
Site No.	Bed slope S_o (ft/ft)	Bank-full flow Q_{bf} (ft^3/s)	Top width w (ft)	Unit discharge q (ft^2/s)	Compu-ted at main site (ft)	Trend line +3 ft (ft)	Xing is: (ft)		Type of structure	Com-puted at main site (ft)	Estima-ted at secon-dary site (ft)	Scour radius (ft)	(ft)	Vertical instability rating	Assigned depth (ft)	Total scour depth (ft)	With F.S.= 1.3 (ft)
31	0.015	128	55	2.3	1.3	4.0	38	u/s	Four pier bridge, old road	5.2		10.4	4.0	Low - bedrock likely close to surface		4.0	5.2
32	0.01	733	128	5.7	2.6	4.6			NONE				4.6	Low		4.6	6.0
33	0.008	723	74	9.8	2.2	5.4			NONE				5.4	Low		5.4	7.0
34	0.0274	134	55	2.4		4.0	95	u/s	Old road - culvert				4.0	Low to moderate		4.0	5.3
35	0.0641	77	30	2.6		4.1	30	u/s	Old road - culvert		5 max.	10 max.	4.1	Low		4.1	5.3
36	0.0551	42	25	1.7		3.9	30	u/s	Old road - culvert		5 max.	10 max.	3.9	Low to moderate		3.9	5.1
37	0.0442	38	33	1.2		3.8	30	u/s	Old road - culvert		5 max.	10 max.	3.8	Low to moderate		3.8	5.0
38	0.0185	358	30	11.9		5.8	100	u/s	Old road – two piers from old bridge				5.8	Low to moderate		5.8	7.5

Table 6-9. Scour Depth Estimates for a 100-Year Event

Unit discharge (bankfull) and slope					Bend and bedform scour		Structures causing contraction or local scour			Contraction or local scour			Maxi-mum scour	Degradation		Total scour depth	
Site No.	Bed slope S_o (ft/ft)	Bank-full flow Q_{bf} (ft^3/s)	Top width w (ft)	Unit discharge q (ft^2/s)	Compu-ted at main site (ft)	Trend line +3 ft (ft)	Xing is: (ft)		Type of structure	Com-puted at main site (ft)	Estima-ted at secon-dary site (ft)	Scour radius (ft)	(ft)	Vertical instability rating	Assigned depth (ft)	Total scour depth (ft)	With F.S.= 1.3 (ft)
39	0.0751	70	20	3.5		4.2	124	u/s	Old road - culvert				4.2	Low		4.2	5.5
40	0.0764	80	20	4		4.3	156	u/s	Old road – culvert				4.3	Low		4.3	5.6
41	0.0365	90	18	5		4.5	50	u/s	Old road – culvert		6.8	13.6	4.5	Low		4.5	5.9
42	0.0206	131	52	2.5		4.1	150	u/s	Old road - box culvert/ bridge				4.1	Low		4.1	5.3
43	0.0328	157	25	6.3		4.8	0	rd bed	Two box culverts, old road		7.9	15.8	7.9	Low		7.9	10.3
44	0.0266	160	25	6.4		4.8	0	rd bed	Two box culverts, old road		8	16	8.0	Low		8.0	10.4
45	0.1368	67	15	4.5		4.4	60	d/s	NONE - old road				4.4	Low		4.4	5.8
46		134	15	9		5.2	125	d/s	Old road				5.2	Low		5.2	6.8

Table 6-9. Scour Depth Estimates for a 100-Year Event

Unit discharge (bankfull) and slope					Bend and bedform scour		Structures causing contraction or local scour			Contraction or local scour			Maxi-mum scour	Degradation		Total scour depth	
Site No.	Bed slope S_o (ft/ft)	Bank-full flow Q_{bf} (ft^3/s)	Top width w (ft)	Unit discharge q (ft^2/s)	Compu-ted at main site (ft)	Trend line +3 ft (ft)	Xing is: (ft)		Type of structure	Com-puted at main site (ft)	Estima-ted at secon-dary site (ft)	Scour radius (ft)	(ft)	Vertical instability rating	Assigned depth (ft)	Total scour depth (ft)	With F.S.= 1.3 (ft)
47	0.0247	90	15	6		4.7	290	d/s	NONE - old road				4.7	Low		4.7	6.1
48	0.0268	109	12	9.1		5.3	272	d/s	New road, 100 ft from dry crossing				5.3	Low		5.3	6.8
49	0.0175	288	24	12		5.8	90	d/s	New road - bridge or box culvert				5.8	Low to moderate		5.8	7.5
50	0.008	458	25	18.3	1.7	6.9			NONE - parallels road				6.9	Low		6.9	9.0
51	0.007	458	35	13.1	2.3	6.0			NONE - parallels road				6.0	Low to moderate		6.0	7.8
52	0.016	566	30	18.9	2.2	7.0	180	d/s	Five box culverts				7.0	Low		7.0	9.1

Table 6-9. Scour Depth Estimates for a 100-Year Event

Unit discharge (bankfull) and slope					Bend and bedform scour		Structures causing contraction or local scour			Contraction or local scour			Maxi-mum scour	Degradation		Total scour depth	
Site No.	Bed slope S_o (ft/ft)	Bank-full flow Q_{bf} (ft^3/s)	Top width w (ft)	Unit discharge q (ft^2/s)	Compu-ted at main site (ft)	Trend line +3 ft (ft)	Xing is: (ft)		Type of structure	Com-puted at main site (ft)	Estima-ted at secon-dary site (ft)	Scour radius (ft)	(ft)	Vertical instability rating	Assigned depth (ft)	Total scour depth (ft)	With F.S.= 1.3 (ft)
53	0.0169	240	50	4.8		4.5	87	d/s	Box culverts/ bridge				4.5	Moderate	2	6.5	8.4
54	0.0235	112	15	7.5		5.0	80	d/s	Road crossing - box culvert				5.0	Low to moderate		5.0	6.5
55	0.0187	250	50	5		4.5	85	d/s	Box culverts/ bridge				4.5	Low to moderate		4.5	5.9
56	0.0228	38	20	1.9		4.0	95	d/s	Road crossing - box culvert				4.0	Moderate	2	6.0	7.7
57	0.0102	93	20	4.6	1.1	4.4	79	d/s	Two box culverts				4.4	Low		4.4	5.8
58	0.0069	989	42	23.5	1.8	7.9	250	d/s	NONE - old road				7.9	Low		7.9	10.2

Table 6-9. Scour Depth Estimates for a 100-Year Event

Unit discharge (bankfull) and slope					Bend and bedform scour		Structures causing contraction or local scour			Contraction or local scour			Maxi-mum scour	Degradation		Total scour depth	
Site No.	Bed slope S_o (ft/ft)	Bank-full flow Q_{bf} (ft^3/s)	Top width w (ft)	Unit discharge q (ft^2/s)	Compu-ted at main site (ft)	Trend line +3 ft (ft)	Xing is: (ft)		Type of structure	Com-puted at main site (ft)	Estima-ted at secon-dary site (ft)	Scour radius (ft)	(ft)	Vertical instability rating	Assigned depth (ft)	Total scour depth (ft)	With F.S.= 1.3 (ft)
59	0.0247	336	20	16.8		6.7	225		NONE - from dirt road				6.7	Low to moderate		6.7	8.7
60	0.0306	42	25	1.7		3.9		u/s	NONE - dirt road				3.9	Low		3.9	5.1
61	0.0384	35	20	1.8		3.9	390	d/s	NONE - dry crossing				3.9	Low		3.9	5.1
62	0.0492	48	15	3.2		4.2			NONE				4.2	Low		4.2	5.5
63	0.0198	710	25	28.4		8.8			NONE				8.8	Low		8.8	11.4
64	0.0195	70	20	3.5		4.2			NONE				4.2	Low		4.2	5.5
65	0.0285	138	15	9.2		5.3	35	u/s	NONE - dry crossing				5.3	Low		5.3	6.9
66	0.0197	310	12	25.9		8.3	30	d/s	NONE- dirt road				8.3	Low		8.3	10.8
67	0.0206	42	25	1.7		3.9			NONE				3.9	Low		3.9	5.1
68	0.0253	13	15	0.9		3.8			NONE				3.8	Low		3.8	4.9

Table 6-9. Scour Depth Estimates for a 100-Year Event

Unit discharge (bankfull) and slope					Bend and bedform scour		Structures causing contraction or local scour			Contraction or local scour			Maxi-mum scour	Degradation		Total scour depth	
Site No.	Bed slope S_o (ft/ft)	Bank-full flow Q_{bf} (ft^3/s)	Top width w (ft)	Unit discharge q (ft^2/s)	Compu-ted at main site (ft)	Trend line +3 ft (ft)	Xing is: (ft)		Type of structure	Com-puted at main site (ft)	Estima-ted at secon-dary site (ft)	Scour radius (ft)	(ft)	Vertical instability rating	Assigned depth (ft)	Total scour depth (ft)	With F.S.= 1.3 (ft)
69	0.023	115	12	9.6		5.4			NONE				5.4	Low		5.4	7.0
70	0.0358	58	15	3.8		4.3			NONE				4.3	Low		4.3	5.6
71	0.0314	166	15	11.1		5.6			NONE				5.6	Low		5.6	7.3
72	0.0409	32	30	1.1		3.8			NONE				3.8	Low		3.8	5.0
73	0.0313	80	30	2.7		4.1			NONE				4.1	Low		4.1	5.3
74	0.0206	32	20	1.6		3.9			NONE				3.9	Low		3.9	5.1
75	0.0192	502	60	8.4		5.1			NONE - edge of alluvial wash				5.1	Moderate to high	3	8.1	10.6
76	0.0307	35	25	1.4		3.9			NONE				3.9	Low		3.9	5.0
77	0.0173	166	20	8.3		5.1	95	d/s	NONE - dry crossing				5.1	Low to moderate		5.1	6.7
78	0.0138	122	20	6.1		4.7			NONE				4.7	Low to moderate		4.7	6.1
79	0.013	330	15	22		7.6			NONE				7.6	Low to moderate		7.6	9.9

Table 6-9. Scour Depth Estimates for a 100-Year Event

Unit discharge (bankfull) and slope					Bend and bedform scour		Structures causing contraction or local scour			Contraction or local scour			Maxi-mum scour	Degradation		Total scour depth	
Site No.	Bed slope S_o (ft/ft)	Bank-full flow Q_{bf} (ft^3/s)	Top width w (ft)	Unit discharge q (ft^2/s)	Compu-ted at main site (ft)	Trend line +3 ft (ft)	Xing is: (ft)		Type of structure	Com-puted at main site (ft)	Estima-ted at secon-dary site (ft)	Scour radius (ft)	(ft)	Vertical instability rating	Assigned depth (ft)	Total scour depth (ft)	With F.S.= 1.3 (ft)
80	0.0239	42	15	2.8		4.1	140	d/s	Road - box culvert				4.1	Moderate	2	6.1	8.0
81	0.0201	29	20	1.4		3.9	180	u/s	Road - box culvert				3.9	Moderate	2	5.9	7.6
82	0.0355	128	15-Jan	8.5		5.2	245	u/s	Road - culvert				5.2	Moderate	2	7.2	9.3
83	0.0326	189	15	12.6		5.9	410	u/s	Road - culvert				5.9	Moderate	2	7.9	10.3
84	0.0254	192	65	3	1.6	4.2	42	u/s	Four pier bridge, old road	5.1		10.2	4.2	Low		4.2	5.4
85	0.0144	58	15	3.8		4.3	54	d/s	Road				4.3	Low		4.3	5.6
86	0.0126	432	130	3.3	1.1	4.2	61	u/s	Four pier bridge, old road				4.2	Low		4.2	5.5
87	0.0109	115	65	1.8		3.9	204	u/s	Old road				3.9	Low to moderate		3.9	5.1
88	0.0091	109	25	4.4		4.4	144	u/s	Old road				4.4	Low		4.4	5.7

Table 6-9. Scour Depth Estimates for a 100-Year Event

Unit discharge (bankfull) and slope					Bend and bedform scour		Structures causing contraction or local scour			Contraction or local scour			Maxi-mum scour	Degradation		Total scour depth	
Site No.	Bed slope S_o (ft/ft)	Bank-full flow Q_{bf} (ft^3/s)	Top width w (ft)	Unit discharge q (ft^2/s)	Compu-ted at main site (ft)	Trend line +3 ft (ft)	Xing is: (ft)		Type of structure	Com-puted at main site (ft)	Estima-ted at secon-dary site (ft)	Scour radius (ft)	(ft)	Vertical instability rating	Assigned depth (ft)	Total scour depth (ft)	With F.S.= 1.3 (ft)
89	0.0102	90	125	0.7		3.7	300	u/s	Old road				3.7	Moderate (if incision could progress u/s of bridge)	2	5.7	7.5
90	0.001	234	35	6.7	3.8	4.8	74	d/s	Remnant vertical abutment				4.8	Moderate	2	6.8	8.9
91	0.0069	176	20	8.8		5.2	15	d/s	Old road, u/s new road bridge with piers		9.6	19.2	9.6	Low		9.6	12.5
92	0.0091	118	36	3.3	1.1	4.2	105	u/s	Three pier bridge, new road				4.2	Low to moderate		4.2	5.5
93	0.0943	61	25	2.4		4.0	100	u/s	Culvert				4.0	Low to moderate		4.0	5.3
94	0.0046	1078	90	12	1.7	5.8	490	u/s	Bridge, old road				5.8	Low to moderate		5.8	7.5

Table 6-9. Scour Depth Estimates for a 100-Year Event

Unit discharge (bankfull) and slope					Bend and bedform scour		Structures causing contraction or local scour			Contraction or local scour			Maxi-mum scour	Degradation		Total scour depth	
Site No.	Bed slope S_o (ft/ft)	Bank-full flow Q_{bf} (ft^3/s)	Top width w (ft)	Unit discharge q (ft^2/s)	Compu-ted at main site (ft)	Trend line +3 ft (ft)	Xing is: (ft)		Type of structure	Com-puted at main site (ft)	Estima-ted at secon-dary site (ft)	Scour radius (ft)	(ft)	Vertical instability rating	Assigned depth (ft)	Total scour depth (ft)	With F.S.= 1.3 (ft)
95	0.0028	198	65	3.1	1.2	4.2	66	u/s	Five pier bridge, old road				4.2	Low		4.2	5.4
96	0.0011	15430	215	71.8	15.5	16.6	4	u/s	Old bridge	25.7		51.4	25.7	Low to moderate		25.7	33.4
97	0.0092	1325	240	5.5	3.1	4.6			NONE - wash crossing, sandstone				4.6	Low to moderate		4.6	6.0
98	0.0198	189	21	9	1.2	5.2			NONE (incised, sand)				5.2	High - for new channels forming	4	9.2	12.0
99	0.0085	147	25	5.9		4.7			NONE (sandstone)				4.7	Low		4.7	6.1
100	0.01	307	206	1.5		3.9	260	u/s	NONE- dry crossing at wash				3.9	Low		3.9	5.1
101	0.0065	54	25	2.2		4.0	90	u/s	NONE- dry crossing				4.0	Low		4.0	5.2

Table 6-9. Scour Depth Estimates for a 100-Year Event

Unit discharge (bankfull) and slope					Bend and bedform scour		Structures causing contraction or local scour			Contraction or local scour			Maxi-mum scour	Degradation		Total scour depth	
Site No.	Bed slope S_o (ft/ft)	Bank-full flow Q_{bf} (ft^3/s)	Top width w (ft)	Unit discharge q (ft^2/s)	Compu-ted at main site (ft)	Trend line +3 ft (ft)	Xing is: (ft)		Type of structure	Com-puted at main site (ft)	Estima-ted at secon-dary site (ft)	Scour radius (ft)	(ft)	Vertical instability rating	Assigned depth (ft)	Total scour depth (ft)	With F.S.= 1.3 (ft)
102	0.01	291	30	9.7		5.4	70	u/s	NONE - dry crossing				5.4	Low		5.4	7.0
103	0.0174	42	20	2.1		4.0	44	d/s	Box culvert, old road		8	16	4.0	Low		4.0	5.2
104	0.0158	58	40	1.4		3.9	20	d/s	Box culvert, old road		5 max.	10 max.	3.9	Low		3.9	5.0
105	0.0152	83	35	2.4		4.0	23	d/s	Old road		5 max.	10 max.	4.0	Low		4.0	5.3
106	0.0062	42	30	1.4		3.9	100	u/s	Road				3.9	Low		3.9	5.0
107	0.0577	42	80	0.5		3.7	300	u/s	Road				3.7	Low		3.7	4.8
108	0.0107	179	25	7.2		4.9	174	u/s	Road				4.9	Low		4.9	6.4
109	0	182	25	7.3		4.9	87	d/s	Box culvert				4.9	Low		4.9	6.4
110	0.0157	413	20	20.6		7.3	65	d/s	Box culvert				7.3	Low		7.3	9.6
111	0.0352	1152	20	57.6		14.1	209	d/s	Closest road culvert				14.1	Low		14.1	18.3

Table 6-9. Scour Depth Estimates for a 100-Year Event

Unit discharge (bankfull) and slope					Bend and bedform scour		Structures causing contraction or local scour			Contraction or local scour			Maxi-mum scour	Degradation		Total scour depth	
Site No.	Bed slope S_o (ft/ft)	Bank-full flow Q_{bf} (ft^3/s)	Top width w (ft)	Unit discharge q (ft^2/s)	Compu-ted at main site (ft)	Trend line +3 ft (ft)	Xing is: (ft)		Type of structure	Com-puted at main site (ft)	Estima-ted at secon-dary site (ft)	Scour radius (ft)	(ft)	Vertical instability rating	Assigned depth (ft)	Total scour depth (ft)	With F.S.= 1.3 (ft)
112	0.0568	58	12	4.8		4.5	255	d/s	Road crossing				4.5	Low to moderate		4.5	5.8
113	0.0122	96	15	6.4		4.8	150	d/s	Road crossing				4.8	Low to moderate		4.8	6.2
114	0.0092	64	60	1.1		3.8	157	d/s	Box culvert/ bridge				3.8	Low		3.8	5.0
115	0.0514	32	15	2.1		4.0	140	d/s	Road crossing - culvert				4.0	Low		4.0	5.2
116	0.0156	128	35	3.7		4.3	60	d/s	New road crossing				4.3	Low		4.3	5.6
117	0.0154	147	25	5.9		4.7	278	d/s	New road, 85 from dry crossing				4.7	Low		4.7	6.1
118	0.0235	32	20	1.6		3.9	480	u/s	Road				3.9	Low		3.9	5.1
119	0.0238	51	25	2		4.0	540	u/s	Road				4.0	Low		4.0	5.2

Table 6-9. Scour Depth Estimates for a 100-Year Event

Unit discharge (bankfull) and slope					Bend and bedform scour		Structures causing contraction or local scour			Contraction or local scour			Maxi-mum scour	Degradation		Total scour depth	
Site No.	Bed slope S_o (ft/ft)	Bank-full flow Q_{bf} (ft^3/s)	Top width w (ft)	Unit discharge q (ft^2/s)	Compu-ted at main site (ft)	Trend line +3 ft (ft)	Xing is: (ft)		Type of structure	Com-puted at main site (ft)	Estima-ted at secon-dary site (ft)	Scour radius (ft)	(ft)	Vertical instability rating	Assigned depth (ft)	Total scour depth (ft)	With F.S.= 1.3 (ft)
120	0.0198	154	25	6.1		4.7	25	u/s	Culvert, old road		7.7	14.4	4.7	Low		4.7	6.1
121	0.0114	141	37	3.8		4.3	181	u/s	Old road				4.3	Low to moderate		4.3	5.6
122	0.0103	38	25	1.5		3.9	119	u/s	New road				3.9	Low to moderate		3.9	5.1
123	0.0193	35	20	1.8		3.9	95	u/s	New road				3.9	Low to moderate		3.9	5.1
124	0.0056	134	35	3.8		4.3	116	d/s	Old road				4.3	Low		4.3	5.6
125	0.0082	323	45	7.2	4.2	4.9	1	d/s	Two pier bridge	8.6		17.2	8.6	Low		8.6	11.2
126	0.0368	29	50	0.6		3.7	168	u/s	Old road				3.7	Low		3.7	4.8
127	0.0033	29	10	2.9		4.1	67	u/s	Road				4.1	Low		4.1	5.4
128	0	259	50	5.2		4.6	57	d/s	Culvert				4.6	Low		4.6	5.9
129	0.0269	141	13	10.8		5.6			NONE - parallels road fill				5.6	Low		5.6	7.2

Table 6-9. Scour Depth Estimates for a 100-Year Event

Unit discharge (bankfull) and slope					Bend and bedform scour		Structures causing contraction or local scour			Contraction or local scour			Maxi-mum scour	Degradation		Total scour depth	
Site No.	Bed slope S_o (ft/ft)	Bank-full flow Q_{bf} (ft^3/s)	Top width w (ft)	Unit discharge q (ft^2/s)	Compu-ted at main site (ft)	Trend line +3 ft (ft)	Xing is: (ft)		Type of structure	Com-puted at main site (ft)	Estima-ted at secon-dary site (ft)	Scour radius (ft)	(ft)	Vertical instability rating	Assigned depth (ft)	Total scour depth (ft)	With F.S.= 1.3 (ft)
130	0.082	298	30	9.9		5.4	173	d/s	At closest road crossing				5.4	Low		5.4	7.0
131	0.0093	86	15	5.8		4.7	191	d/s	Culvert				4.7	Low		4.7	6.1
132	0.0505	362	25	14.5		6.2	300	d/s	Road culvert				6.2	Low		6.2	8.1
133	0.0023	1805	50	36.1		10.2	770	d/s	Road crossing				10.2	Low to moderate		10.2	13.2

Note: u/s = upstream, d/s = downstream, F.S. = ?

KEY		
		= Sites impacted by contraction scour and local scour
		= Degradation depth is added to scour depth based on instability rating
		= Total scour depth (ft)

6.5.1 Factor of Safety

At the majority of sites (126 out of 132), total scour depth is defined by a bend/bedform/degradation scour value. Although the values should be somewhat conservative from the development of the envelop curve, there is no factor of safety directly applied to results. A factor between 1.1 and 1.5 is recommended in the ASCE (2005) method for uncertainties in the analysis. A column with scour depth multiplied by a factor of 1.3 has been included in table 6-9 for the designer's consideration.

6.5.2 Scour Countermeasures

At locations where it does not seem feasible to bury the pipeline below the depth of scour, scour countermeasures can be installed. Maintenance costs for scour countermeasures should be evaluated and compared against construction costs at each site to ensure that countermeasures are the most feasible option. Guidance on scour countermeasures can be found in the Hydraulic Engineering Circular 23 (HEC-23) manual (FHWA, 2009).

6.5.3 Sites with Contraction and Local Scour Effects

Although there are 19 crossings adjacent to a bridge (<50 feet distant), there are only 6 sites affected by local scour: Site 3, Site 43, Site 44, Site 91, Site 96, and Site 125. The remaining 126 sites are influenced by the lessor scour depth value for bend scour, bedform scour, and degradation effects. A shift in the proposed pipeline alignment at six sites influenced by bridges or structures can reduce estimated scour depths. Moving the alignment away from a structure and outside the radius of local scour reduces scour processes to bend scour, bedform scour, and degradation depth. Table 6-10 summarizes required distances and the reduction in estimated scour depth that could result. Similarly, the proposed pipeline alignment should not be shifted during design to within a radius of 50 feet of structures to avoid increasing potential scour at these sites.

Table 6-10. Shifting Pipeline Alignment Can Reduce Potential Scour Depth at Specified Sites

Site No.	Contraction and local scour (ft)	Shift alignment minimum (ft)	Reduces to bend and bedform scour (ft)
3	11.4	3	6.8
43	7.9	16	4.8
44	8	16	4.8
91	9.6	5	5.2
96	25.7	48	16.6
125	8.6	17	4.9

6.5.4 Subsurface Materials

Up to this point, there is an assumption that there are no erosion-resistant materials under the surface at the pipeline crossings. The total scour depth estimate is a maximum depth, and scour could be restricted to a more shallow depth if subsurface rock is present. Scour depth and the presence of subsurface materials that restrict erosion are explored in the next section, with a comparison of scour depths and available test pit information.

6.6 Subsurface Materials

Maximum scour depths were calculated in the previous sections assuming that the surface material is representative of materials to the full potential depth of scour. No consideration was given to subsurface, erosion resistant materials. Segments of the study area include bedrock and erosion resistant materials, including the Bitter Springs Spur; the sand stone area to the north that ends at Page, AZ; and the southern end of the proposed pipeline from Gray Mountain to the mountains around Flagstaff, AZ. Small, steep channels drain from the valley sides in the Bitter Springs Spur and have cobble and boulder armored beds. At the north end of the proposed pipeline, near Page, drainages convey a large amount of red sand, and the bed of the channel is sand. Although the streams drop steeply off the mesa to the reservoir, the slope of the sand bed streams is controlled by multiple sandstone controls. South of Gray Mountain, volcanic influences can be noted, and few drainages exist as the road climbs to Flagstaff. Information on subsurface materials is available at some locations from a 2012 test pit study (Miller, 2012).

> Reclamation excavated sixty-four test pits along portions of the proposed North Central Arizona Pipeline in order to determine the depth to bedrock and to obtain soil samples for materials testing. The excavations were conducted in June 2012. Test pits TP-1 through TP-48 were excavated along US Highway 89 or along the old Highway 89, which runs parallel to Highway 89. Test pits TP-49 through TP-63 were excavated along Tribal Route 20 (Copper Mine Road) from The Gap to about 6 miles north of Coppermine Chapter. The test pits were approximately 20 feet long by 6 feet wide and 13 to 15 feet deep unless the backhoe met refusal.

Figure 6-9 is a photo from the HEC-18 manual that illustrates the erosion of fractured and jointed rock over time at a high energy location (photo is of an unknown location). However, the assumption for most of the crossings in this study area is that the refusal point for the backhoe will be reasonably resistant to erosion. In this section, the values of maximum scour depth are compared against test pit information on depth to refusal to identify locations where it may not be necessary or possible to bury the pipeline below the maximum scour depth.

Figure 6-9. Examples from HEC-18 of scour in sandstone rock (FHWA, 2012). The location of the photo is unknown.

Stream crossings and numbered test pits (TP) are shown in figure 6-10 for the pipeline between TP41 and TP46. Crossings and test pits are listed as they occur from north to south along the main pipeline in table 6-11. Refusal depths from the test pits are compared against the scour depths at adjacent stream crossing sites. The spurs are listed in separate sections below the mainline, and the crossings and test pits along the Bitter Springs Spur are also ordered from north to south.

Relatively close test pits and stream crossings are shaded yellow. In figure 6-10, there are no crossings adjacent to TP45 or TP44, secondary Crossing 93 is adjacent to TP43, main Crossing 92 and secondary Crossing 91 are adjacent to TP42, and main Crossing 90 is adjacent to TP41. Adjacent crossings are shaded in table 6-11. If stream crossing numbers are not shaded, there is no test pit information available on the subsurface materials for these sites.

When the elevation of maximum scour depth is at or below the elevation of refusal in the test pit, the maximum scour depth for that location is highlighted in dark green. Scour at main Crossing 90 may be limited by an erosion resistant bed of sandstone (Chinle Formation). When the cell is highlighted a light green, maximum scour depth is within 1-3 feet of the test pit refusal elevation.

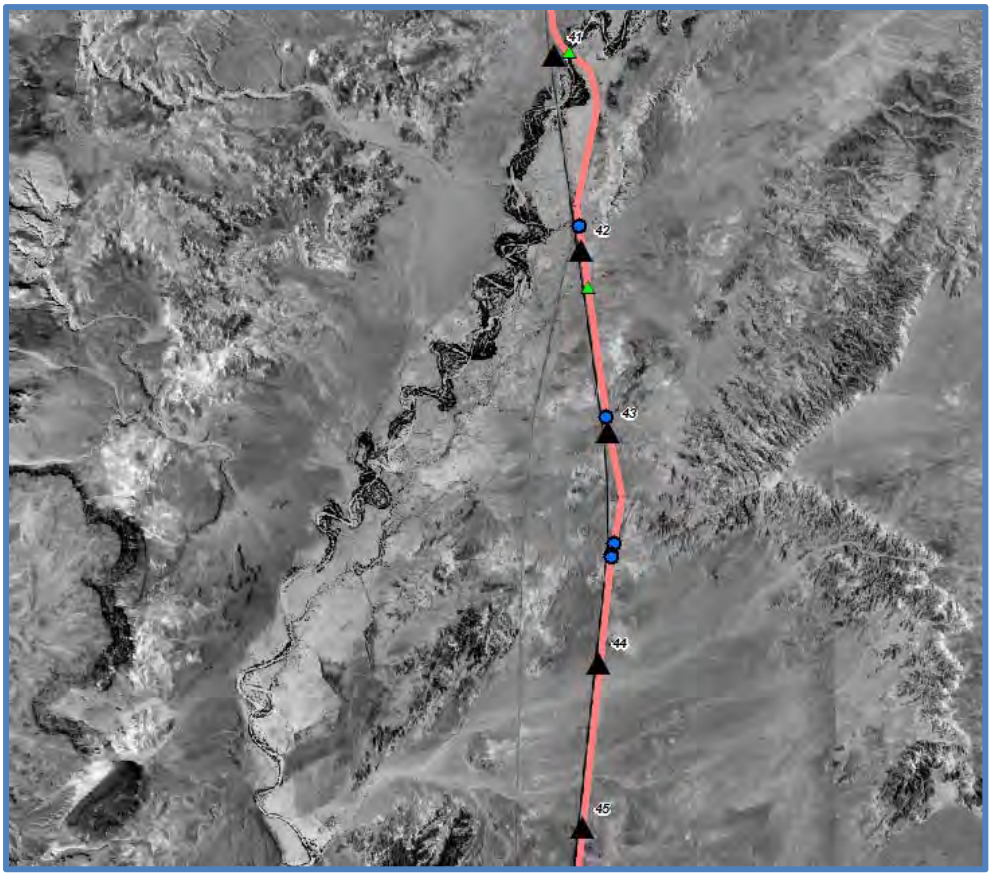

Figure 6-10. A map of test pit locations shown as black triangles and stream crossing sites. Main stream crossing sites are green triangles, and secondary sites are blue circles. From north to south, the points are: main site 90, TP41, site 91, TP42, main site 92, site 93, TP43, site 122a and 122b, TP44, and TP46.

6.6.1 Findings

This is a crude estimate at best because most of the test pits are a distance from the stream crossing sites and because the resistant bed materials may not extend equally in all directions. However, table 6-11 provides insight on locations where maximum scour depths may not occur due to scour resistant materials, and the pipeline will not be buried as deep at these locations. Shallow bedrock can also act as a vertical control for the steam and prevent degradation. Sites where nearby test pits indicate erosion resistant materials could prevent full development of the scour depth include 12, 115, 31, 84, 88, 90, 51, 117, and 40. Sites where the full development of scour depth is estimated to be within 0.1 to 3 feet above an erosion resistant surface are: 57, 55, 54, and 41.

Table 6-11. Comparison of Test Pit Refusal Elevation and Scour Depth Elevations at Adjacent Stream Crossing Sites

Green cells in the maximum scour depth column mark sites with scour depths at or below test pit refusal depths. All values are in feet. Minimum elevation is the elevation of the estimated scour depth or erosion resistant layer.

LEGEND

Pit refusal elevation
TP and site are close
TP and site are close
Scour is 0-3 ft above refusal
Scour is at or below refusal

	Ground elevation (ft)	Max-mum scour depth (ft)	Pit refusal depth (ft)	Refusal or scour depth elevation (ft)	Notes or geologic formation
MAINLINE					
Lake Powell Intake					
1	3912	4.0		3908.0	
Page					
2	4031	4.1		4026.9	
3	4088	11.4		4076.6	
4	4240	5.0		4235.0	
5	4240	4.1		4235.9	
6	4286	4.2		4281.8	
7a	4335	3.6		4331.4	
8	4763	4.1		4758.9	
LeChee					
9	5228	3.8		5224.2	
10a	5335	3.8		5331.2	
113	5655	4.8		5650.2	
114	5790	3.8		5786.2	
TP63	5836		**10**	**5826.0**	Sandstone - Navajo sandstone
11a	5870	3.9		5866.1	
12	5820	4.4		5815.6	
13	5812	4.5		5807.5	
14	5810	4.2		5805.8	
TP62	5802		**6.5**	**5795.5**	Sandstone - Navajo sandstone
TP61	5822		**7**	**5815.0**	Sandstone - Navajo sandstone
TP60	5867		**6.5**	**5860.5**	Sandstone - Navajo sandstone

Table 6-11. Comparison of Test Pit Refusal Elevation and Scour Depth Elevations at Adjacent Stream Crossing Sites

Green cells in the maximum scour depth column mark sites with scour depths at or below test pit refusal depths. All values are in feet. Minimum elevation is the elevation of the estimated scour depth or erosion resistant layer.

LEGEND

Pit refusal elevation
TP and site are close
TP and site are close
Scour is 0-3 ft above refusal
Scour is at or below refusal

	Ground elevation (ft)	Max-mum scour depth (ft)	Pit refusal depth (ft)	Refusal or scour depth elevation (ft)	Notes or geologic formation
TP59	5893		**5.5**	**5887.5**	Sandstone - Navajo sandstone
TP58	5994		>13	5981.0	Windblown sand
15	5987	4.4		5982.6	
TP57	5955		**10**	**5945.0**	Sandstone - Navajo sandstone
TP67 on 115	5670		**9**	**5661.0**	Sandstone - Navajo sandstone
115	5665	4		5661.0	
TP56	5605		>15	5590.0	Windblown sand
TP55	5557		>14.5	5542.5	Windblown sand
TP68	5480		**5.5**	**5474.5**	Sandstone - Navajo sandstone
TP54	5465		**6.5**	**5458.5**	Sandstone - Navajo sandstone
TP53	5456		**8**	**5448.0**	Sandstone - Navajo sandstone
TP52	5450		**7**	**5443.0**	Sandstone - Navajo sandstone
TP51	5450		**13**	**5437.0**	Sandstone - Navajo sandstone
TP50	5450		**5**	**5445.0**	Sandstone - Navajo sandstone
TP49	5440		**7**	**5433.0**	Sandstone - Navajo sandstone
BITTER SPRINGS SPUR					
16	5290	4.9		5285.1	
Bodeaway Gap					
TP21	5251		>14	5237.0	Breakable claystone - Chinle

Table 6-11. Comparison of Test Pit Refusal Elevation and Scour Depth Elevations at Adjacent Stream Crossing Sites

Green cells in the maximum scour depth column mark sites with scour depths at or below test pit refusal depths. All values are in feet. Minimum elevation is the elevation of the estimated scour depth or erosion resistant layer.

LEGEND

Pit refusal elevation
TP and site are close
TP and site are close
Scour is 0-3 ft above refusal
Scour is at or below refusal

	Ground elevation (ft)	Max-mum scour depth (ft)	Pit refusal depth (ft)	Refusal or scour depth elevation (ft)	Notes or geologic formation
17	5265	6.9		5258.1	
TP22	5203		>14	5189.0	Clayey sand with gravels, cobbles, boulders - Quaternary alluvium
18	5190	6.6		5183.4	
TP23	5175		>14	5161.0	Clayey silty gravel with sand, cobbles, boulders - Quaternary alluvium
19	5155	4.5		5150.5	
20	5145	6.7		5138.3	
TP24	5121		>15	5106.0	Silty gravel with sand, cobbles - Quaternary alluvium
21	5155	4		5151.0	
22	5125	4		5121.0	
23	5080	7.8		5072.2	
TP25	5053		>12	5041.0	Sand with clay - Quaternary alluvium
24	5044	4.7		5039.3	Looks too far away to be this close - same bench?
TP26	5004		**10.5**	**4993.5**	Chinle, petrified forest member
25	4990	6.9		4983.1	
TP27	4950		>6	4944.0	Silty sand - Quaternary alluvium
TP28	4892		>13.5	4878.5	Silty sand with grey cobbles, boulders - Quaternary alluvium
26	4895	4.1		4890.9	

Table 6-11. Comparison of Test Pit Refusal Elevation and Scour Depth Elevations at Adjacent Stream Crossing Sites

Green cells in the maximum scour depth column mark sites with scour depths at or below test pit refusal depths. All values are in feet. Minimum elevation is the elevation of the estimated scour depth or erosion resistant layer.

LEGEND

Pit refusal elevation
TP and site are close
TP and site are close
Scour is 0-3 ft above refusal
Scour is at or below refusal

	Ground elevation (ft)	Max-mum scour depth (ft)	Pit refusal depth (ft)	Refusal or scour depth elevation (ft)	Notes or geologic formation
27	4850	4.6		4845.4	
TP29	4840		**10**	**4830.0**	Claystone - Chinle
28	4812	5.2		4806.8	
30	4803	4.7		4798.3	
TP30	4793		>14	4779.0	Claystone - Chinle
31	4735	4.0		4731.0	
TP31	4742		**5**	**4737.0**	Sandstone - Chinle
Tuba City Spur					
TP32	4708		>14	4694.0	Silty sand with gravels - Quaternary alluvium
84	4665	4.2		4660.8	
TP33	4672		5.5	4666.5	Sandstone - Chinle
Tuba City Spur Rd					
85	4647	4.3		4642.7	
TP34	4620		>13	4607.0	Claystone – Chinle
120	4563	4.7		4558.3	
TP35	4553		**9.5**	**4543.5**	Claystone – Chinle
TP36	4510		>13.5	4496.5	Sand with clay - Quaternary alluvium
86	4496	4.2		4491.8	
TP37 on 87	4468		**10.5**	**4457.5**	Sandstone - Chinle
87	4468	3.9		4464.1	
RD160 Tuba City Tee					
88	4425	4.4		4420.6	
TP38	4428		**4**	**4424.0**	Sandstone - Chinle
89	4399	5.7		4393.3	

Table 6-11. Comparison of Test Pit Refusal Elevation and Scour Depth Elevations at Adjacent Stream Crossing Sites

Green cells in the maximum scour depth column mark sites with scour depths at or below test pit refusal depths. All values are in feet. Minimum elevation is the elevation of the estimated scour depth or erosion resistant layer.

LEGEND

Pit refusal elevation
TP and site are close
TP and site are close
Scour is 0-3 ft above refusal
Scour is at or below refusal

	Ground elevation (ft)	Max-mum scour depth (ft)	Pit refusal depth (ft)	Refusal or scour depth elevation (ft)	Notes or geologic formation
121	4395	4.3		4390.7	
TP39 close to 121	4395		**7.5**	**4387.5**	Sandstone - Chinle
TP40	4378		>13	4365.0	Claystone - Chinle
90	4330	6.8		4323.2	
TP41	4340		**12**	**4328.0**	Sandstone - Chinle
91	4330	9.6		4320.4	
TP42	4330		>14.5	4315.5	Clayey-sand - Quaternary alluvium
92	4327	4.2		4322.8	
93	4345	4.0		4341.0	
TP43	4350		**13**	**4337.0**	Claystone - Chinle
122a	4355	3.9		4351.1	
122b	4350			4350.0	
123	4350	3.9		4346.1	
TP44	4333		**8.5**	**4324.5**	Claystone with interbedded sandstone - Chinle
TP45	4310		>13.4	4296.6	Claystone - Chinle
TP46	4295		**8**	**4287.0**	Claystone with interbedded sandstone - Chinle
TP47	4254		>13.5	4240.5	Claystone - Chinle
94	4244	5.8		4238.2	
TP48	4224		**7.5**	**4216.5**	Claystone with interbedded sandstone - Chinle
124a	4182	4.3		4177.7	
124b	4176			4176.0	
95	4165	4.2		4160.8	

Table 6-11. Comparison of Test Pit Refusal Elevation and Scour Depth Elevations at Adjacent Stream Crossing Sites

Green cells in the maximum scour depth column mark sites with scour depths at or below test pit refusal depths. All values are in feet. Minimum elevation is the elevation of the estimated scour depth or erosion resistant layer.

LEGEND

Pit refusal elevation
TP and site are close
TP and site are close
Scour is 0-3 ft above refusal
Scour is at or below refusal

	Ground elevation (ft)	Max-mum scour depth (ft)	Pit refusal depth (ft)	Refusal or scour depth elevation (ft)	Notes or geologic formation
96	4114	28.7		4085.3	Three-foot degradation added to abutment scour depth
Camaron					
103	4490	4.0		4486.0	
104	4485	3.9		4481.1	
105	4512	4		4508.0	
125	4478	8.6		4469.4	
126	4580	3.7		4576.3	
Gray Mountain (Black Mesa pump station)					
127	5046	4.1		5041.9	
106	5050	3.9		5046.1	
107	5092	3.7		5088.3	
128	5240	4.6		5235.4	
108	5359	4.9		5354.1	
109	5549	4.9		5544.1	
110	5590	7.3		5582.7	
129	5604	5.6		5598.4	
130	5913	5.4		5907.6	
131	6280	4.7		6275.3	
111a	6586	14.1		6571.9	
132	6867	6.2		6860.8	
112	7243	4.5		7238.5	
133	6735	10.2		6724.8	
Flagstaff					

Table 6-11. Comparison of Test Pit Refusal Elevation and Scour Depth Elevations at Adjacent Stream Crossing Sites

Green cells in the maximum scour depth column mark sites with scour depths at or below test pit refusal depths. All values are in feet. Minimum elevation is the elevation of the estimated scour depth or erosion resistant layer.

LEGEND

Pit refusal elevation
TP and site are close
TP and site are close
Scour is 0-3 ft above refusal
Scour is at or below refusal

	Ground elevation (ft)	Max-mum scour depth (ft)	Pit refusal depth (ft)	Refusal or scour depth elevation (ft)	Notes or geologic formation
BITTER SPRINGS SPUR (all test pits, except TP1, at road across wash from pipeline)					
118	5125	3.9		5121.1	
119	5127	4.0		5123.0	
TP1	5160		>12	5148.0	Sand with silt cobbles, boulders - Quaternary alluvium
83	5180	7.9		5172.1	
82	5195	7.2		5187.8	
81	5195	5.9		5189.1	
80	5191	6.1		5184.9	
79	5169	7.6		5161.4	
TP2	5170		>13	5157.0	Silty sand with gravel - Quaternary alluvium
78	5204	4.7		5199.3	
TP3	5220		>13	5207.0	Silty sand with gravels, cobbles, boulders - Quaternary alluvium
77	5248	5.1		5242.9	
76	5305	3.9		5301.1	
75	5330	8.1		5321.9	
74	5325	3.9		5321.1	
TP4	5295		>13	5282.0	Sand with silt, gravels, cobbles, boulders - Quaternary alluvium
73	5337	4.1		5332.9	
72	5350	3.8		5346.2	
71	5355	5.6		5349.4	
70	5376	4.3		5371.7	

Table 6-11. Comparison of Test Pit Refusal Elevation and Scour Depth Elevations at Adjacent Stream Crossing Sites

Green cells in the maximum scour depth column mark sites with scour depths at or below test pit refusal depths. All values are in feet. Minimum elevation is the elevation of the estimated scour depth or erosion resistant layer.

LEGEND

Pit refusal elevation
TP and site are close
TP and site are close
Scour is 0-3 ft above refusal
Scour is at or below refusal

	Ground elevation (ft)	Max-mum scour depth (ft)	Pit refusal depth (ft)	Refusal or scour depth elevation (ft)	Notes or geologic formation
69	5371	5.4		5365.6	
68	5373	3.8		5369.2	
67	5368	3.9		5364.1	
TP5	5346		>12	5334.0	Lean clay with sand - Quaternary alluvium
66a	5454	8.3		5445.7	
65	5456	5.3		5450.7	
TP6	5390		>13.5	5376.5	Limestone – Kaibab
64	5478	4.2		5473.8	
63a	5460	8.8		5451.2	
62	5470	4.2		5465.8	
61	5475	3.9		5471.1	
TP7	5448		>14	5434.0	Clayey sand with trace of cobbles - Quaternary alluvium
60	5468	3.9		5464.1	
59	5470	6.7		5463.3	
58	5475	7.9		5467.1	
57	5523	4.4		5518.6	
TP8	5526		**7.5**	**5518.5**	Claystone - Chinle
56	5549	6.0		5543.0	
55	5580	4.5		5575.5	
TP9	5585		**12**	**5573.0**	Sandstone - Chinle
54	5580	5		5575.0	
TP10	5633		**13**	**5620.0**	(Breakable) claystone - Chinle
53	5632	6.5		5625.5	

Table 6-11. Comparison of Test Pit Refusal Elevation and Scour Depth Elevations at Adjacent Stream Crossing Sites

Green cells in the maximum scour depth column mark sites with scour depths at or below test pit refusal depths. All values are in feet. Minimum elevation is the elevation of the estimated scour depth or erosion resistant layer.

LEGEND

Pit refusal elevation

	Ground elevation (ft)	Max-mum scour depth (ft)	Pit refusal depth (ft)	Refusal or scour depth elevation (ft)	Notes or geologic formation
TP11	5667		**11.5**	**5655.5**	Sandstone - Chinle, Moenkopi outcrop formation 1,000 feet west across road
Cedar Ridge					
TP12	5716		>11.5	5704.5	Clayey sand - Quaternary alluvium
52	5728	7		5721.0	
TP13	5752		**11**	**5741.0**	Claystone - Chinle
51	5779	6		5773.0	
TP14	5785		**11**	**5774.0**	Sandstone - Chinle
50	5788	6.9		5781.1	
49	5839	5.8		5833.2	
TP15	5865		**7**	**5858.0**	Sandstone - Chinle
116	5909	4.3		5904.7	
TP16	5925		**6**	**5919.0**	Sandstone - Chinle
117	5914	4.7		5909.3	
48	5896	5.3		5890.7	
47	5894	4.7		5889.3	
46	5726	5.2		5720.8	
45	5704	4.4		5699.6	
44	5645	8		5637.0	
43	5625	7.9		5617.1	
42	5535	4.1		5530.9	
41	5506	4.5		5501.5	
TP18	5508		**9.5**	**5498.5**	Claystone - Chinle
40	5500	4.3		5495.7	
39	5495	4.2		5490.8	

Table 6-11. Comparison of Test Pit Refusal Elevation and Scour Depth Elevations at Adjacent Stream Crossing Sites

Green cells in the maximum scour depth column mark sites with scour depths at or below test pit refusal depths. All values are in feet. Minimum elevation is the elevation of the estimated scour depth or erosion resistant layer.

LEGEND

Pit refusal elevation
TP and site are close
TP and site are close
Scour is 0-3 ft above refusal
Scour is at or below refusal

	Ground elevation (ft)	Max-mum scour depth (ft)	Pit refusal depth (ft)	Refusal or scour depth elevation (ft)	Notes or geologic formation
38	5465	5.8		5459.2	
37	5465	3.8		5461.2	
36	5450	3.9		5446.1	
35	5434	4.1		5429.9	
34	5423	4.0		5419.0	
33	5380	5.4		5374.6	
32	5361	4.6		5356.4	
TP19	5364		>14	5350.0	Claystone - Chinle
TP20	5320		>12	5308.0	Claystone - Chinle
Bodaway Gap					
TUBA CITY SPUR (no test pits)					
97	4720	4.6		4715.4	
98	4725	9.2		4715.8	
99	4710	4.7		4705.3	
100		3.9			
101	4600	4.0		4596.0	
102	4595	5.4		4589.6	

There are no test pits near Page, AZ, but the streams on the hillsides are steep. The steep slope implies frequent rock outcrops or rock armoring. There is limited armoring in the bed (mainly sandy bedload) but the frequent rock bed controls were confirmed during the field visit. Steep slopes with large rock armoring were noted in some side drainages on the Bitter Springs Spur (figure 1-1). These locations are also anticipated to have shallower scour depths than predicted.

6.6.2 LCR

At Site No. 96, the LCR crossing, a rock wall on the upstream right bank guides flow towards the bridge. Estimated scour depth for this location is 26 feet if there are no erosion resistant materials in the bed of the channel. A geologic investigation at Site No. 96 would help determine if scour would be limited by natural rock in the bed. Mounting the pipeline on the bridge and pipeline burial at bedrock are two alternatives for this site.

7. Summary of Findings

The following information has been calculated or assessed to aid in the development of the NCAP pipeline design:

- An estimate of scour depth and vertical stream instability at all locations where the pipeline crosses streams or closely parallel streams
- An assessment of lateral stream instability and the minimum width of pipeline burial at the stream crossings
- Water surface elevations at main stream crossings to aid the design of support structures

7.1 Hydrology

Most stream crossings in the study area are ephemeral and were dry in April 2013. The Moenkopi Wash and the LCR (Site No. 96) were two exceptions, with the LCR flowing approximately 100 ft^3/s during the week of the field review. Peak annual streamflow data were available at a gage on the LCR (USGS 09402000) for 1923, 1929, and 1947 to 2012. The USGS noted the LCR has been engineered with dams and diversions that have affected discharge to an unknown degree since 1965 (USGS, 2013c). Most of the major flows have occurred prior to 1965. For this reason, peak annual streamflow was also analyzed for 1965 to the present. Flow analysis of 1965 to the present yields significantly lower flood frequency estimates; however, the analysis using all streamflow data was conservatively selected for the pipeline crossing analysis at the LCR.

7.2 Hydraulic Modeling

The 1D HEC-RAS flow model of the LCR shows the flow filling most of the old Highway 89 bridge opening at a 5-year event. Pressurized flow occurs at the 10-year event when the water surface strikes midway on the bridge deck, and flow overtops the bridge at a 25-year event. If the pipeline is mounted on the old Highway 89 bridge, it will have to withstand frequent submergence and high flow forces. One of the highest velocities in the river, 10 feet per second (ft/s), occurs at the 5-year event. During a 100-year event, flow velocity peaks at only 11 ft/s due to large conveyance in the flood plain and flows overtopping the bridge.

Bridge structures cannot be added to the 2D model at this time, although the abutments are reflected in the ground surface. Even without the piers and bridge deck, flow lines and velocity vectors from SRH-2D indicate the presence of

contraction scour in the main channel at the 5-year flow event (figure 4-10). There is no significant local scour at the 5-year event. Flow is confined to the channel at the bridge up to a 10-year event, then begins to spill over the bank. At the 100-year event (figure 4-11), evidence of contraction scour is nearly gone, and scour may occur where flow overtops the bridge abutment. Given the armoring placed on the right approach bank at the abutment, one can speculate that a bridge deck added to the 2D model might cause local scour to shift further towards the right overbank.

During the field survey, the surveyors wading in the channel commented on the loose or "quick" sand that was present immediately upstream of the bridge and also downstream (areas corresponding to contraction scour locations in the 2D model). The survey rod easily sank 6 inches in the sand at these locations.

If the pipeline is buried instead of mounted on the bridge, the alignment could be located a distance downstream to avoid contraction scour impacts, or it could be located a shorter distance upstream of the bridge to avoid the local scour effects. There is a rock wall on the right approach bank. A geologic investigation of subsurface materials below the channel or on the immediately adjacent flood plain at the old Highway 89 bridge would help to detect rock in the bed that could limit scour. This could aid in the selection of the crossing options (buried or mounted on the bridge) at this location.

7.3 Geomorphic and Scour Analysis

Chapter 5 includes the geomorphic mapping for each main site. These descriptions provide site-specific detail on vertical and lateral channel stability, and they include mapping that shows the recommended length of deep burial for the pipeline located on an aerial photograph. Table 7-1 combines results from the geomorphic assessment with the results of the scour computations. Additional information on the sites is available from the tables in both the geomorphic (chapter 5) and scour (chapter 6) chapters. In table 7-1, maximum scour depth is increased by 2 feet of degradation at sites rated as having moderate instability, increased by 3 feet of degradation at sites rated as having moderate to high instability, and increased by 4 feet of degradation at sites rated as having high vertical instability (potential for incision > local). Geologic notes have been added where bedrock near the surface or large rock that naturally armors the bed could limit scouring. Scour depths vary with each site, based on the unit discharge (ft^2/s), and range from 3.6 feet at Site No. 7 (stream parallels the road and a segment of pipeline) to 25.7 feet at Site No. 96, the LCR. The sections following table 7-1 contain design notes on the study area.

Designers are also directed to resources within the body of this report:

- WSEs for main crossings at a bankfull and 50-year return interval are available in chapter 4, table 4-1. Table 4-5 contains WSEs at multiple cross sections and return intervals for the LCR.

- Numerical modeling sections in chapter 4 contain detailed hydraulic information and 2D figures that provide flow visualization to aid design of the pipeline crossing at the LCR.

- Descriptions of main crossings in chapter 5, and table 5-2 notes, provide an in-depth review of vertical and lateral stability, the terrain, landforms, etc. These sections include an evaluation of design concerns at each crossing and identify the location for pipe burial on site maps.

- Subsurface information in chapter 6, table 6-11, compare estimated scour depths at pipeline crossings to test pit results on depth to refusal.

7.4 Design Notes

Discussion paragraphs touch on aspects of pipeline stream crossings.

7.4.1 Buried Crossings Versus Mounting on a Bridge

At two locations, the pipeline could be buried or mounted on a bridge. At the first site (the old Highway 89 bridge at the LCR), the bridge constricts flow and is pressurized or overtopped at relatively frequent flows. Overtopping must be considered in the design if a pipeline is mounted on the bridge. Alternatively, if the pipeline is buried at this crossing, a large scour depth must be considered. The bridge piers are small (18-inch beams) and do not cause deep scour individually; however, groups of piers catch debris, which increases the potential depth of scour. If the pipeline is buried, an alignment that crosses upstream of the radius of local scour, and crosses upstream or downstream of the limits of constriction scour, should be considered. Subsurface information at Site No. 96 (the LCR) would help in selecting the approach. Scour depth is estimated at 26 feet, but this value may be limited by subsurface rock because the outer bank of the channel is a vertical rock wall.

At Site 125, the proposed alignment is also close to the old Highway 89 bridge and may be mounted on the bridge or buried. This crossing has less flow than the LCR and was not modeled; however, chapter 4 lists estimates of WSEs. If the pipeline is buried, shifting the pipeline downstream of the bridge, outside the limits of constriction scour or wake scour would reduce the required burial depth.

Table 7-1. Summary of Findings for NCAP Stream Sites

Site No.	South bed slope	Q_{100} 100-yr dis-charge (ft^3/s)	Q_{bf} bankfull dis-charge (ft^3/s)	Top width (ft)	q unit dis-charge* (ft^2/s)	100-yr WSE* (ft)	Potential for incision* > local scour	Max-imum scour depth* (ft)	With factor of safety = 1.3	Potential for lateral instability*	Width of burial* (ft)	Structures and geologic formation	Bedrock in banks or bed
Lake Powell Intake													
1	0.0472	225	35	15	2.3		L to M	**4.0**	5.2		**19**		None
Page													
2	0.0425	480	86	30	2.9		L	**4.1**	5.3		**44**		Bed
3	0.0184	2,465	445	25	17.8		L	**6.8**	8.8		**53**		Bed
4	0.0121	2,380	419	55	7.6		L to M	**5.0**	6.5		**43**		None
5	0.0333	610	102	35	2.9		L to M	**4.1**	5.3		**22**		None
6		855	157	50	3.1		L	**4.2**	5.5		**56**		Bed, banks
7a	0.0391	235	35				L	**3.6**	4.7		**1682**		Channel, discontinuous
8	0.0159	585	102	35	2.9		L	**4.1**	5.3	L to M	**176**		Bed
LeChee													
9	0.0243	90	19	20	1.0		L	**3.8**	4.9	L	**42**		Unknown
10a	0.0441	120	19	15	1.3		L	**3.8**	4.9	L	**18**		Bed
113	0.0122	520	96	15	6.4		L to M	**4.8**	6.2	L	**15**		Unknown
114	0.0092	305	64	60	1.1		L	**3.8**	4.9	L	**narrow**		Unknown
11a	0.0506	260	42	25	1.7		L to M	**3.9**	5.1	M	**923**	Sandstone - Navajo sandstone	Unknown
12	0.0460	295	45	10	4.5		L to M	**4.4**	5.7	M	**21**	Sandstone - Navajo sandstone	Unknown
13	0.0472	545	74	15	4.9		L to M	**4.5**	5.9	M	**57**	Sandstone - Navajo sandstone	None
14	0.0178	520	70	20	3.5		L to M	**4.2**	5.5	M	**70**	Sandstone - Navajo sandstone	Unknown

Table 7-1. Summary of Findings for NCAP Stream Sites

Site No.	South bed slope	Q_{100} 100-yr dis-charge (ft^3/s)	Q_{bf} bankfull dis-charge (ft^3/s)	Top width (ft)	q unit dis-charge* (ft^2/s)	100-yr WSE* (ft)	Potential for incision* > local scour	Max-imum scour depth* (ft)	With factor of safety = 1.3	Potential for lateral instability*	Width of burial* (ft)	Structures and geologic formation	Bedrock in banks or bed
15	0.0601	265	45	10	4.5		L	**4.4**	5.7	L	**26**	Windblown sand	Unknown
115	0.0514	170	32	15	2.1		L	**4.0**	5.2	L	**27**	Sandstone - Navajo sandstone	Bed
Bitter Springs Spur									0				
16	0.0091	4,555	794	115	6.9	**5297.8**	L to M	**4.9**	6.4	L	**201**		Left bank downstream of bridge
Bodaway Gap									0				
17	0.0173	1,360	246	35	7.0		M	**4.9**	6.4	L	**82**	Breakable claystone - Chinle	Set back from channel
18	0.0247	1,330	221	40	5.5		M	**4.6**	6.0	M	**124**	Clayey silty gravel with sand cobble boulders - Quaternary alluvium	Discontinuous along right bank
19	0.0307	780	125	25	5.0		L to M	**4.5**	5.9	L	**17**		Along right bank
20	0.0138	2,020	371	60	6.2	**5151.3**	M	**4.7**	6.1	L	**99**		None
21	0.0258	980	182	85	2.1	**5157.6**	L to M	**4.0**	5.2	L	**139**	Silty gravel with sand cobbles - Quaternary alluvium	Colluvium in left bank
22	0.0355	420	74	35	2.1		L to M	**4.0**	5.2	L to M	**139**		In left bank, possibly right bank
23	0.0957	195	32	25	1.3		H[1]	**3.8**	4.9	L	**160**		Along banks

Table 7-1. Summary of Findings for NCAP Stream Sites

Site No.	South bed slope	Q_{100} 100-yr dis-charge (ft^3/s)	Q_{bf} bankfull dis-charge (ft^3/s)	Top width (ft)	q unit dis-charge* (ft^2/s)	100-yr WSE* (ft)	Potential for incision* > local scour	Max-imum scour depth* (ft)	With factor of safety = 1.3	Potential for lateral instability*	Width of burial* (ft)	Structures and geologic formation	Bedrock in banks or bed
24	0.0771	550	90	15	6.0		L	**4.7**	6.1	L	**22**	Sand with clay - Quaternary alluvium	Along channel/flood plain banks
25	0.0225	680	109	15	7.3		M	**4.9**	6.4	M	**111**	Sandstone - Chinle	Unknown
26	0.0189	1,335	250	93	2.7	**4894.4**	L	**4.1**	5.3	L	**73**	Silty sand with gravel cobble boulders - Quaternary alluvium	None; located upstream of crossing near channel banks but not directly in banks
27	0.0000	1,340	224	40	5.6		L	**4.6**	6.0	L	**58**	Claystone - Chinle	In right bank
28	0.0000	1,040	170	20	8.5		L	**5.2**	6.8	L	**26**		Unknown
30	0.0000	1,035	170	29	5.8		L	**4.7**	6.1	L	**27**	Claystone - Chinle	In bed near culvert(?)
31	0.0150	685	128	55	2.3	**4737.8**	L[1]	**4.0**	5.2	M	**334**		Bedrock in bed upstream of crossing; bedrock in left bank upstream of crossing and in right bank
Tuba City Spur									0				
84	0.0254	980	192	65	3.0	**4669.1**	L to M	**4.2**	5.5	L	**331**		Right bank at crossing; banks where wash exits from confined setting

Table 7-1. Summary of Findings for NCAP Stream Sites

Site No.	South bed slope	Q_{100} 100-yr dis-charge (ft^3/s)	Q_{bf} bankfull dis-charge (ft^3/s)	Top width (ft)	q unit dis-charge* (ft^2/s)	100-yr WSE* (ft)	Potential for incision* > local scour	Max-imum scour depth* (ft)	With factor of safety = 1.3	Potential for lateral instability*	Width of burial* (ft)	Structures and geologic formation	Bedrock in banks or bed
Tuba City Spur Rd													
85	0.0144	340	58	15	3.8		L	**4.3**	5.6	L	**44**	Claystone - Chinle	Along left bank; potentially in bed downstream
120	0.0198	790	154	25	6.1		L[2]	**4.7**	6.1	L	**343**		Unknown
86	0.0126	2,105	432	130	3.3	**4494.0**	L	**4.2**	5.5	L	**143**	Sand with clay - Quaternary alluvium	Right bank upstream of bridge
87	0.0109	690	115	65	1.8		L to M	**3.9**	5.1	M	**204**	Sandstone – Chinle	Unknown
RD160 Tuba City Tee													
88	0.0091	620	109	25	4.4		L to M	**4.4**	5.7	M	**150**	Sandstone - Chinle	Unknown
89	0.0102	520	90	125	0.7		M[1]	**5.7**	7.4	L	**227**		Along right bank downstream of crossing
121	0.0114	725	141	37	3.8		L to M	**4.3**	5.6	L	**51**	Sandstone - Chinle	On right bank downstream of crossing
90	0.0010	1,260	234	35	6.7	**4331.3**	M	**6.8**	8.8	H	**315**		Downstream of crossing in right bank
91	0.0069	950	176	20	8.8		L	**9.6**	12.5	L	**38**		Along channel banks
92	0.0091	695	118	36	3.3	**4330.0**	L to M	**4.2**	5.5	L	**162**	Clayey sand - Quaternary alluvium	Bedrock mounds near crossing
93	0.0943	320	61	25	2.4		L to M	**4.0**	5.2	L	**104**	Claystone - Chinle	Along right bank

Table 7-1. Summary of Findings for NCAP Stream Sites

Site No.	South bed slope	Q_{100} 100-yr dis-charge (ft^3/s)	Q_{bf} bankfull dis-charge (ft^3/s)	Top width (ft)	q unit dis-charge* (ft^2/s)	100-yr WSE* (ft)	Potential for incision* > local scour	Max-imum scour depth* (ft)	With factor of safety = 1.3	Potential for lateral instability*	Width of burial* (ft)	Structures and geologic formation	Bedrock in banks or bed
122a	0.0103	140	38	25	1.5		L to M	**3.9**	5.1	L	**320**		Banks near crossing
123	0.0193	170	35	20	1.8		L to M	**3.9**	5.1	L	**42**	Claystone with interbedded sandstone - Chinle	Banks near crossing
94	0.0046	4,985	1078	90	12.0	**4247.2**	L to M	**5.8**	7.5	H	**397**	Claystone - Chinle	None
124a	0.0056	570	134	35	3.8		L	**4.3**	5.6	M	**1096**		Bed
95	0.0028	890	198	65	3.1	**4166.5**	L	**4.2**	5.5	M	**384**		Bedrock across bed downstream of crossing
96	0.0011	68,935	15430	215	71.8		L to M	**28.7**	37.3	L	**666**		None in bed; bedrock walls confine channel and flood plain on both sides
Camaron													
103	0.0174	190	42	20	2.1		L	**4.0**	5.2	L	**21**		Near banks upstream of crossing
104	0.0158	285	58	40	1.4		L	**3.9**	5.1	L	**37**		None
105	0.0152	430	83	35	2.4		L	**4**	5.2	L to M	**46**		Along left bank and right bank; in bed downstream of crossing(?)

Table 7-1. Summary of Findings for NCAP Stream Sites

Site No.	South bed slope	Q_{100} 100-yr dis-charge (ft^3/s)	Q_{bf} bankfull dis-charge (ft^3/s)	Top width (ft)	q unit dis-charge* (ft^2/s)	100-yr WSE* (ft)	Potential for incision* > local scour	Max-imum scour depth* (ft)	With factor of safety = 1.3	Potential for lateral instability*	Width of burial* (ft)	Structures and geologic formation	Bedrock in banks or bed
125	0.0082	1,560	323	45	7.2	**4481.1**	L	**8.6**	11.2	L	**74**		Left bank downstream of crossing; large sandstone in bed; not sure if in place
126	0.0368	140	29	50	0.6		L	**3.7**	4.8	L	**122**		In bed, left bank
Gray Mountain (Black Mesa pump station)													
127	0.0033	130	29	10	2.9		L	**4.1**	5.3	L	**36**		Unknown
106	0.0062	195	42	30	1.4		L	**3.9**	5.1	L	**179**		Bedrock on both sides of braided channel
107	0.0577	200	42	80	0.5		L	**3.7**	4.8	L	**42**		Unknown
128	0.0000	1,335	259	50	5.2		L	**4.6**	6.0	L	**40**		Along left bank
108	0.0107	830	179	25	7.2		L	**4.9**	6.4	L	**45**		Bedrock on both sides of channel
109	0.0000	955	182	25	7.3		L	**4.9**	6.4	L	**62**		Bedrock on both sides of channel
110	0.0157	2,335	413	20	20.6		L	**7.3**	9.5	L	**93**		Bedrock on both sides of channel
129	0.0269	730	141	13	10.8		L	**5.6**	7.3	M	**29**		Unknown
130	0.0820	1,705	298	30	9.9		L	**5.4**	7.0	L	**30**		In both banks and likely in bed
131	0.0093	445	86	15	5.8		L	**4.7**	6.1	L	**25**		Unknown
111a	0.0352	4,055	1152	20	57.6			**14.1**	18.3		**2654**		
132	0.0505	2,275	362	25	14.5		L	**6.2**	8.1	M	**432**		Unknown
112	0.0568	325	58	12	4.8		L to M	**4.5**	5.9	M	**61**		Unknown
133	0.0023	9,830	1805	50	36.1		L to M	**10.2**	13.3	L	**177**		Unknown

Table 7-1. Summary of Findings for NCAP Stream Sites

Site No.	South bed slope	Q_{100} 100-yr dis-charge (ft^3/s)	Q_{bf} bankfull dis-charge (ft^3/s)	Top width (ft)	q unit dis-charge* (ft^2/s)	100-yr WSE* (ft)	Potential for incision* > local scour	Max-imum scour depth* (ft)	With factor of safety = 1.3	Potential for lateral instability*	Width of burial* (ft)	Structures and geologic formation	Bedrock in banks or bed
Flagstaff													
Bitter Springs Spur- test pits from site 79 to site 60 were at road across wash from pipeline													
118	0.0235	155	32	20	1.6		L	**3.9**	5.1	L	**22**		Unknown
119	0.0238	265	51	25	2.0		L	**4.0**	5.2	L	**104**		Unknown
83	0.0326	1,470	189	15	12.6		M	**7.9**	10.3	L	**16**	Sand with silt cobble boulders - Quaternary alluvium	Unknown
82	0.0355	995	128	15	8.5		M	**7.2**	9.4	L	**17**		Unknown
81	0.0201	155	29	20	1.4		M	**5.9**	7.7	L	**7**		Unknown
80	0.0239	205	42	15	2.8		M	**6.1**	7.9	L	**16**		Unknown
79	0.0130	2,455	330	15	22.0		M	**7.6**	9.9	L	**30**	Silty sand with gravel - Quaternary alluvium	Unknown
78	0.0138	755	122	20	6.1		L to M	**4.7**	6.1	L	**32**	Silty sand with gravel cobble boulders - Quaternary alluvium	Bedrock in left bank upstream from crossing
77	0.0173	1,215	166	20	8.3		L to M	**5.1**	6.6	M	**49**	Silty sand with gravel cobble boulders - Quaternary alluvium	Unknown
76	0.0307	205	35	25	1.4		L	**3.9**	5.1	L	**16**		Unknown

Table 7-1. Summary of Findings for NCAP Stream Sites

Site No.	South bed slope	Q_{100} 100-yr dis-charge (ft^3/s)	Q_{bf} bankfull dis-charge (ft^3/s)	Top width (ft)	q unit dis-charge* (ft^2/s)	100-yr WSE* (ft)	Potential for incision* > local scour	Max-imum scour depth* (ft)	With factor of safety = 1.3	Potential for lateral instability*	Width of burial* (ft)	Structures and geologic formation	Bedrock in banks or bed
75	0.0192	2,925	502	60	8.4		M to H	**8.1**	10.5	M	**305**		None
74	0.0206	175	32	20	1.6		L	**3.9**	5.1	L	**15**	Sand with silt gravel cobble boulders - Quaternary alluvium	Unknown
73	0.0313	595	80	30	2.7		L	**4.1**	5.3	L	**13**	Sand with silt, gravel cobble boulders - Quaternary alluvium	Unknown
72	0.0409	160	32	30	1.1		L	**3.8**	4.9	L	**14**		Unknown
71	0.0314	1,325	166	15	11.1		L	**5.6**	7.3	L	**25**		Unknown
70	0.0358	425	58	15	3.8		L	**4.3**	5.6	L	**25**		Unknown
69	0.0230	895	115	12	9.6		L	**5.4**	7.0	L	**23**		Unknown
68	0.0253	65	13	15	0.9		L	**3.8**	4.9	L to M	**67**		Unknown
67	0.0206	215	42	25	1.7		L	**3.9**	5.1	L	**27**	Lean clay with sand - Quaternary alluvium	In bed downstream of crossing
66a	0.0197	2,325	310	12	25.9		L	**8.3**	10.8	L to M	**138**		In bed downstream of crossing
65	0.0285	995	138	15	9.2		L	**5.3**	6.9	L to M	**38**		In bed downstream of crossing
64	0.0195	390	70	20	3.5		L	**4.2**	5.5	M	**205**	Limestone - Kaibab	Possible rock in channel downstream of crossing

Table 7-1. Summary of Findings for NCAP Stream Sites

Site No.	South bed slope	Q_{100} 100-yr dis-charge (ft^3/s)	Q_{bf} bankfull dis-charge (ft^3/s)	Top width (ft)	q unit dis-charge* (ft^2/s)	100-yr WSE* (ft)	Potential for incision* > local scour	Max-imum scour depth* (ft)	With factor of safety = 1.3	Potential for lateral instability*	Width of burial* (ft)	Structures and geologic formation	Bedrock in banks or bed
63a	0.0198	5,600	710	25	28.4		L	**8.8**	11.4	L to M	**89**		Possible rock in channel downstream of crossing
62	0.0492	310	48	15	3.2		L	**4.2**	5.5	L	**8**		Unknown
61	0.0384	180	35	20	1.8		L	**3.9**	5.1	L	**36**		In banks/bed downstream of crossing
60	0.0306	205	42	25	1.7		L	**3.9**	5.1	L	**36**	Clayey sand with trace of cobbles - Quaternary alluvium	In channel banks near crossing(?)
59	0.0247	2,605	336	20	16.8		L to M	**6.7**	8.7	L to M	**106**		Unknown
58	0.0069	5,490	989	42	23.5	**5480.3**	L	**7.9**	10.3	H	**318**		In bed, downstream from crossing
57	0.0102	580	93	20	4.6	**5520.9**	L	**4.4**	5.7	L	**28**	Claystone - Chinle	Continuous across channel bed
56	0.0228	185	38	20	1.9		M	**6.0**	7.8	M	**16**		Unknown
55	0.0187	1,445	250	50	5.0		M	**4.5**	5.9	L to M	**99**	Sandstone - Chinle	Unknown
54	0.0235	660	112	15	7.5		L to M	**5**	6.5	L	**48**	Sandstone - Chinle	Unknown
53	0.0169	1,300	240	50	4.8		M	**6.5**	8.5	M	**121**	(Breakable) claystone - Chinle	Unknown

Table 7-1. Summary of Findings for NCAP Stream Sites

Site No.	South bed slope	Q_{100} 100-yr dis-charge (ft^3/s)	Q_{bf} bankfull dis-charge (ft^3/s)	Top width (ft)	q unit dis-charge* (ft^2/s)	100-yr WSE* (ft)	Potential for incision* > local scour	Max-imum scour depth* (ft)	With factor of safety = 1.3	Potential for lateral instability*	Width of burial* (ft)	Structures and geologic formation	Bedrock in banks or bed
Cedar Ridge													
52	0.0160	3,190	566	30	18.9	**5730.9**	L	**7**	9.1	L to Me (berms direct flow, channel is bounded mostly by alluvial fan deposits)	**90**	Clayey sand, Quaternary alluvium or Claystone - Chinle	In bed, discontinuous downstream from culvert and upstream from crossing
51	0.0070	2,575	458	35	13.1	**5781.2**	L to M	**6**	7.8	M	**160**	Sandstone - Chinle	None
50	0.0080	2,590	458	25	18.3	**5791.4**	L to M	**6.9**	9.0	M	**117**	Sandstone - Chinle	None
49	0.0175	1,625	288	24	12.0		L to M	**5.8**	7.5	M	**90**	Sandstone - Chinle	Unknown
116	0.0156	675	128	35	3.7		L	**4.3**	5.6	L	**58**	Sandstone - Chinle	Unknown
117	0.0154	875	147	25	5.9		L	**4.7**	6.1	L	**61**	Sandstone - Chinle	In bed, 30 feet upstream of crossing and in banks and bed downstream of crossing
48	0.0268	610	109	12	9.1		L	**5.3**	6.9	L	**29**		In banks and in bed some distance downstream
47	0.0247	480	90	15	6.0		L	**4.7**	6.1	L	**19**		In banks and in bed
46		765	134	15	9.0		L	**5.2**	6.8	L to M	**36**		In banks and in bed

Table 7-1. Summary of Findings for NCAP Stream Sites

Site No.	South bed slope	Q_{100} 100-yr dis-charge (ft^3/s)	Q_{bf} bankfull dis-charge (ft^3/s)	Top width (ft)	q unit dis-charge* (ft^2/s)	100-yr WSE* (ft)	Potential for incision* > local scour	Max-imum scour depth* (ft)	With factor of safety = 1.3	Potential for lateral instability*	Width of burial* (ft)	Structures and geologic formation	Bedrock in banks or bed
45	0.1368	410	67	15	4.5		L	**4.4**	5.7	L to M	**33**		In banks and in bed
44	0.0266	930	160	25	6.4		L	**8**	10.4	L	**46**		In banks and in bed downstream of crossing
43	0.0328	905	157	25	6.3		L	**7.9**	10.3	L	**78**		In banks and in bed downstream of crossing
42	0.0206	785	131	52	2.5		L	**4.1**	5.3	L	**31**		In left bank downstream of crossing and right bank upstream of crossing, in bed(?)
41	0.0365	575	90	18	5.0		L	**4.5**	5.9	L to M[†]	**134**	Claystone - Chinle	In channel banks near crossing and in bed(?)
40	0.0764	520	80	20	4.0		L	**4.3**	5.6	L	**34**	Claystone - Chinle	In channel banks
39	0.0751	480	70	20	3.5		L	**4.2**	5.5	L to M	**43**		In channel banks
38	0.0185	2,030	358	30	11.9		L to M	**5.8**	7.5	M	**260**		In left bank at crossing
37	0.0442	235	38	33	1.2		L to M	**3.8**	4.9	L	**95**		In left bank at crossing
36	0.0551	235	42	25	1.7		L to M	**3.9**	5.1	L	**51**		Along banks at crossing

Table 7-1. Summary of Findings for NCAP Stream Sites

Site No.	South bed slope	Q_{100} 100-yr dis-charge (ft^3/s)	Q_{bf} bankfull dis-charge (ft^3/s)	Top width (ft)	q unit dis-charge* (ft^2/s)	100-yr WSE* (ft)	Potential for incision* > local scour	Max-imum scour depth* (ft)	With factor of safety = 1.3	Potential for lateral instability*	Width of burial* (ft)	Structures and geologic formation	Bedrock in banks or bed
35	0.0641	490	77	30	2.6		L	**4.1**	5.3	L	**122**		Along banks at crossing
34	0.0274	750	134	55	2.4		L to M	**4.0**	5.2	L	**106**		Along banks at crossing
33	0.008	4,190	723	74	9.8	**5382.8**	L	**5.4**	7.0	L to M	**478**		Bedrock in bed of small side channel and discontinuous along left bank
32	0.010	4,180	733	128	5.7	**5364.9**	L	**4.6**	6.0	L to M	**188**	Claystone - Chinle	Bedrock in right bank
Bodaway Gap													
Tuba City Spur (no test pits)													
97	0.0092	7,195	1325	240	5.5	**4726.9**	L to M	**4.6**	6.0	M to H	**652**		Against channel on right bank, on left bank removed from main channel and along left bank downstream of bridge
98	0.0198	1,180	189	21	9.0		H^2 for new channels forming	**9.2**	12.0	H	**292**		None
99	0.0085	915	147	25	5.9		L	**4.7**	6.1	H	**253**		In right bank at crossing; sandstone in bed?

Table 7-1. Summary of Findings for NCAP Stream Sites

Site No.	South bed slope	Q_{100} 100-yr dis-charge (ft^3/s)	Q_{bf} bankfull dis-charge (ft^3/s)	Top width (ft)	q unit dis-charge* (ft^2/s)	100-yr WSE* (ft)	Potential for incision* > local scour	Max-imum scour depth* (ft)	With factor of safety = 1.3	Potential for lateral instability*	Width of burial* (ft)	Structures and geologic formation	Bedrock in banks or bed
100	0.0100	1,640	307	206	1.5		L	**3.9**	5.1	H	**298**		Likely in bed downstream and upstream of crossing
101	0.0065	275	54	25	2.2		L	**4.0**	5.2	L	**32**		Bedrock on both sides of channel and in bed
102	0.0100	1,360	291	30	9.7		L	**5.4**	7.0	L	**155**		Bedrock on both sides of channel and in bed

* = Values are site specific. A shift in location can, in some cases, produce a large change in value.
Note: L = low, L to M = low to medium, M = medium, M to H = medium to high, H = high

Potential for Incision notes:
- L^1 bedrock likely close to surface
- L^2 Upstream of culvert
- M^1 if incision could progress upstream of bridge
- H^1 potential for headcuts to migrate upstream of road to crossing
- H^2 for new channels forming

7.4.2 Vertical Controls

Locating a pipeline crossing upstream of a road or culvert can improve the vertical stability of the crossing. However, if the structure is removed or deteriorates, vertical instability trapped downstream of the structure can migrate through. Old Highway 89 on the Bitter Springs Spur acts as a temporary vertical control at several locations after main culverts have plugged. The old roadbed is being eroded by drainage headcuts migrating uphill. After crumbling bituminous is breached, headcuts will migrate upstream, incising the drainage channel and potentially incising the channel at the proposed pipeline alignment. When a headcut reaches the pipeline crossing, it can remove multiple feet of cover and expose the pipe to further erosion.

Photos from Crossing 24 show the initial stages of erosion attacking the roadbed. The road culvert is fully plugged (figure 7-1), causing a reduction in upstream valley slope (figure 7-2) and gradually plugging the upstream highway culvert (figure 7-3). With no drainage paths, overflow across the road erodes the bed and begins to erode through the roadbed (figure 7-4). A headcut can be blocked by maintaining the old road bed or by constructing another hard point in the drainage between the pipeline crossing and the old roadbed downstream.

Figure 7-1. Aggradation filling downstream culvert at old road.

Figure 7-2. Drainage wide and filled with sediment, upstream of culvert at old road.

Figure 7-3. Upstream culvert at old road also partially filled from drainage deposition.

Figure 7-4. Looking across the downstream culvert at erosion headcuts from water flowing across the top of the old road.

7.4.3 Avoiding Local Scour Conditions

Local scour is often deeper than general or bend scour. The area affected by local scour extends in a horizontal radius upstream of the structure (pier or abutment) for a distance of twice the local scour depth (FHWA, 2012). Wake scour occurs downstream of structures, but it is relatively shallow. At secondary sites, the affected area defined by a radius was estimated to range from 10 feet to 22 feet and was 52 feet at the LCR crossing. A similar distance was assumed for the area affected by contraction scour at bridge and culvert inlets and outlets. Local scour and contraction scour concerns can be avoided by crossing the pipeline a minimum distance upstream or downstream of the structure. Box culverts or culverts with a bed can provide vertical stability for the stream if it is downstream of the pipeline, so it would be preferred to cross the pipeline a minimum distance upstream of structures with fixed beds.

7.4.4 Parallel Road and Stream Drainages

There are several locations where the pipeline alignment has limited space between a stream and the road. Bend migrations or other lateral shifts in the channel position could expose the pipe to channel erosion. Between Crossings 26 and 27, the alignment is in close proximity to an outer bend on the axial wash; however, this section of the alignment appears to be protected from lateral erosion by outcrops of Chinle Formation. Although the material may erode with time, the question is whether the slow rate of deterioration will allow the rock to outlast the 50-year life of the pipeline. There is less protection from lateral erosion in the vicinity of Crossings 25 and 26 near Bodaway Gap and between Crossings 49 and 116 near Cedar Ridge (table 7-1).

7.4.5 Scour Countermeasures

Scour countermeasures may be used at crossings where the pipeline cannot be buried to the maximum scour depth proposed in table 7-1. Alternative materials and methods for scour countermeasures can be used. A good resource for the design of local scour countermeasures is the FHWA HEC-23 manual (FHWA, 2009). Riprap is often effective due to the articulating nature of individual riprap particles. As a scour pattern forms in the bed of the channel, riprap can shift and adjust to cover and slow the removal of sediment on the ever-changing bed or banks. However, countermeasures often require maintenance during the life of the project, and a deep pipeline burial is intended to prevent the need for maintenance.

Concrete blocks in the bed, on the bed, or on the banks of the channel should be avoided. Concrete formed around pipelines increases the surface area of the pipeline and act as an obstruction, causing additional local scour if the blocks are exposed to streamflow.

References

ASCE, 2005. *Predicting Bed Scour for Toe Protection Design for Bank Stabilization Projects.* American Society of Civil Engineers, Continuing Education Seminar Course Workbook.

AGS, 2012. Geologic Hazard Center Web site: http://www.azgs.az.gov/hazards_floods.shtml, accessed September 2013. Arizona Geological Survey.

Bentley Systems, Inc., 2009. Flowmaster V8i SELECT series 1 software.

Doeing, B., and R. Beebee, 2009. Bridge Scour Evaluation of the NRE Tanana River Bridge at Salcha, Alaska. Draft. HDR Memorandum, Job No. 249-26701-28, 13 p. Web site: http://www.akrr.com/pdf/Bridge%20Scour%20Memo_01_14_2010.pdf.

England, J.F., Jr., 1999. Draft User's Manual for EMA (Expected Moment Algorithm) Beta Release. Bureau of Reclamation, Technical Service Center, Flood Hydrology Group, Denver, CO, July.

ESRI, Inc., 2009. ArcInfo Workstation, version 10.1.

ESRI, Inc., 2012. Arc Hydro Tools for 10.1 Beta Version. ArcMap toolbar developed with the Center for Research in Water Resources (CRWR).

FHWA, 2001. *River Engineering for Highway Encroachments - Highways in the River Environment.* FHWA NHI 01-004, Federal Highway Administration, Hydraulic Design Series No. 6, Washington, DC.

FHWA, 2009. *Bridge Scour and Stream Instability Countermeasures: Experience, Selection, and Design Guidance.* Third Edition, Vols. I and II. FHWA-NHI-09-111 HEC-23, Federal Highway Administration, Hydraulic Engineering Circular 23, Washington, DC.

FHWA, 2012. *Evaluating Scour at Bridges.* Fifth Edition. FHWA-HIF-12-003 HEC-18, Federal Highway Administration, Hydraulic Engineering Circular 18, Washington, DC.

Flood Control District of Maricopa County. 2003. Draft Drainage Design Manual, Hydraulics. September.

Froehlich, D.C., 1989. "Local Scour at Bridge Abutments," *Proceedings of the 1989 National Conference on Hydraulic Engineering*. American Society of Civil Engineers, New Orleans, LA, p. 13-18.

Gessler, J., 1971. *Beginning and Ceasing of Sediment Motion*. Editor: H.W. Shen, Water Resources Publications, Fort Collins, CO.

Google Earth, 2013. North Central Arizona Pipeline Stream Study Sites. Web site: http://www.google.com/earth/, accessed February 2013.

Haan, C.T., B.J. Barfield, and J.C. Hayes, 1994. *Design Hydrology and Sedimentology for Small Catchments.* Academic Press, Inc.

Hereford, R., 1984. *Climate and Ephemeral Stream Processes: Twentieth Century Geomorphology and Alluvial Stratigraphy of the LCR, Arizona*. Geological Society of America Bulletin 95, p. 654-668.

Huang, J., and B. Greimann, 2010. *Users Manual for SRH-1D, Sedimentation and River Hydraulics – One Dimension.* Technical Report SRH-2010-25, Bureau of Reclamation, Technical Service Center, Denver, CO.

IACWD, 1982. *Guidelines for Determining Flood Flow Frequency.* Bulletin 17-B, Interagency Committee on Water Data, Hydrology Subcommittee, March 1982 (revised and corrected), 28 p. and appendices.

Lai, Y.G., 2000. "Unstructured Grid Arbitrarily Shaped Element Method for Fluid Flow Simulation," *AIAA Journal,* 38(12), p. 2246-2252.

Laursen, E.M., 1960. "Scour at Bridge Crossings," *ASCE Journal of Hydraulic Engineering,* Vol. 89, No. HY 3.

Laursen, E.M., 1963. "An Analysis of Relief Bridges," *ASCE Journal of Hydraulic Engineering,* Vol. 92, No. HY 3.

Maynord, S.T., 1996. "Toe-Scour Estimation in Stabilized Bendways," *ASCE Journal of Hydraulic Engineering,* Technical Note, p. 460-464.

Miller, M., 2012. *North Central Arizona Water Supply Feasibility Study Test Pit Investigations 2012*. Technical Report, Bureau of Reclamation, Phoenix Area Office, Phoenix, AZ.

NCHRP, 2010. Estimation of Scour Depth at Bridge Abutments. NCHRP Project 24-20, Draft Final Report. National Cooperative Highway Research Program, Transportation Research Board, National Academy of Science, Washington, DC.

NCHRP, 2011. *Evaluation of Bridge Scour Research: Abutment and Contraction Scour Processes and Prediction.* NCHRP Project 24-27(02), National Cooperative Highway Research Program, Transportation Research Board, National Academy of Science, Washington, DC.

Neill, C.R., 1973. *Guide to Bridge Hydraulics.* Published for Road and Transportation Association of Canada.

NOAA, 2013a. Online Positioning User Service (OPUS) Web site: https://www.ngs.noaa.gov/OPUS/, accessed April 2013. National Oceanic and Atmospheric Administration.

NOAA, 2013b. Precipitation Frequency Data Server (PFDS) Web site: http://dipper.nws.noaa.gov/hdsc/pfds/, accessed May 2013. National Oceanic and Atmospheric Administration.

NRCS, 2013. Soil Data Mart Web site: http://soildatamart.nrcs.usda.gov/, accessed May 2013. Natural Resources Conservation Service.

PBS&J, 2008. Scour Spreadsheet, version 1.2, May 28, 2008. Presented by David Williams at Stream Stabilization Short Courses: http://www.dnrc.mt.gov/wrd/water_op/floodplain/streambank_course/.

Pemberton, E.L., and J.M. Lara, 1984. *Computing Degradation and Local Scour.* Technical Guideline for Bureau of Reclamation, Denver, CO.

Reclamation, 2013. Bank Stabilization Guidelines. Draft Technical Report SRH-2014-XX. Bureau of Reclamation, Technical Service Center, Denver, CO.

Richardson, E.V., D.B. Simons, and P. Julien, 1990. *Highways in the River Environment.* FHWA-HI-90-016, U.S. Department of Transportation, Federal Highway Administration, Washington, DC.

Rozovskii, I.L., 1961. *Flow of Water in Bends of Open Channels.* Academy of Sciences of the Ukraine SSR.

Simons Li & Associates, 1985. *Design Manual for Engineering Analysis of Fluvial Systems.* Prepared for Arizona Department of Water Resources.

Thorne, C.R., S.R. Abt, and S.T. Maynord, 1995. "Prediction of Near-Bank Velocity and Scour Depth in Meander Bends for Design of Riprap Revetments," *River, Coastal, and Shoreline Protection: Erosion Control Using Riprap and Armourstone*. Edited by C.R. Thomas, S.R. Abt, F.B.J. Barends, S.T. Maynord, and K.W. Pilarczyk, John Wiley and Sons, New York, NY.

Transportation Research Board, 1989. *Abutment Scour Prediction.* Presentation, Transportation Research Board, Washington, DC (Froehlich, D.C.).

USACE, 2010a. *HEC-RAS, River Analysis System User's Manual.* Version 4.1. U.S. Army Corps of Engineers, Hydrologic Engineering Center, Davis, CA.

USACE, 2010b. *HECRAS River Analysis System, Applications Guide*. Version 4.1. Hydrologic Engineering Center, Davis, CA.

USACE, 1994a. *Hydraulic Design of Flood Control Channels.* EM 1110-2-1601, U.S. Army Corps of Engineers, Waterways Experiment Station, Vicksburg, MS, Platte B41.

USACE. 1994b. *Engineering and Design - Channel Stability Assessment for Flood Control*. EM 1110-2-1418.

USGS, 2013a. The National Map Viewer and Download Platform Web site: http://nationalmap.gov/viewer.html, accessed March 2013. United States Geological Survey.

USGS, 2013b. National Streamflow Statistics (NSS) Program Web site: http://water.usgs.gov/osw/programs/nss/, accessed April 2013. United States Geological Survey.

USGS, 2013c. USGS National Water Information System Web Interface, Peak-Flow Data. Web site: http://nwis.waterdata.usgs.gov/usa/nwis/peak, accessed April 2013. United States Geological Survey.

USGS, 2006. *Analysis of the Magnitude and Frequency of Peak Discharges for the Navajo Nation in Arizona, Utah, Colorado, and New Mexico.* Scientific Investigations Report 2006-5306, United States Geological Survey, Waltemeyer, S.D., 2006, 42 p.

Yalin, S.M. 1964. "Geometric Properties of Sand Waves," *Journal of the Hydraulics Division*, 90(HY5), 105-120.

Appendix A

Study Site Locations

This appendix consists of maps showing the location of all 132 stream crossing sites in the study.

NORTH CENTRAL ARIZONA WATER SUPPLY STUDY MAPSHEET INDEX

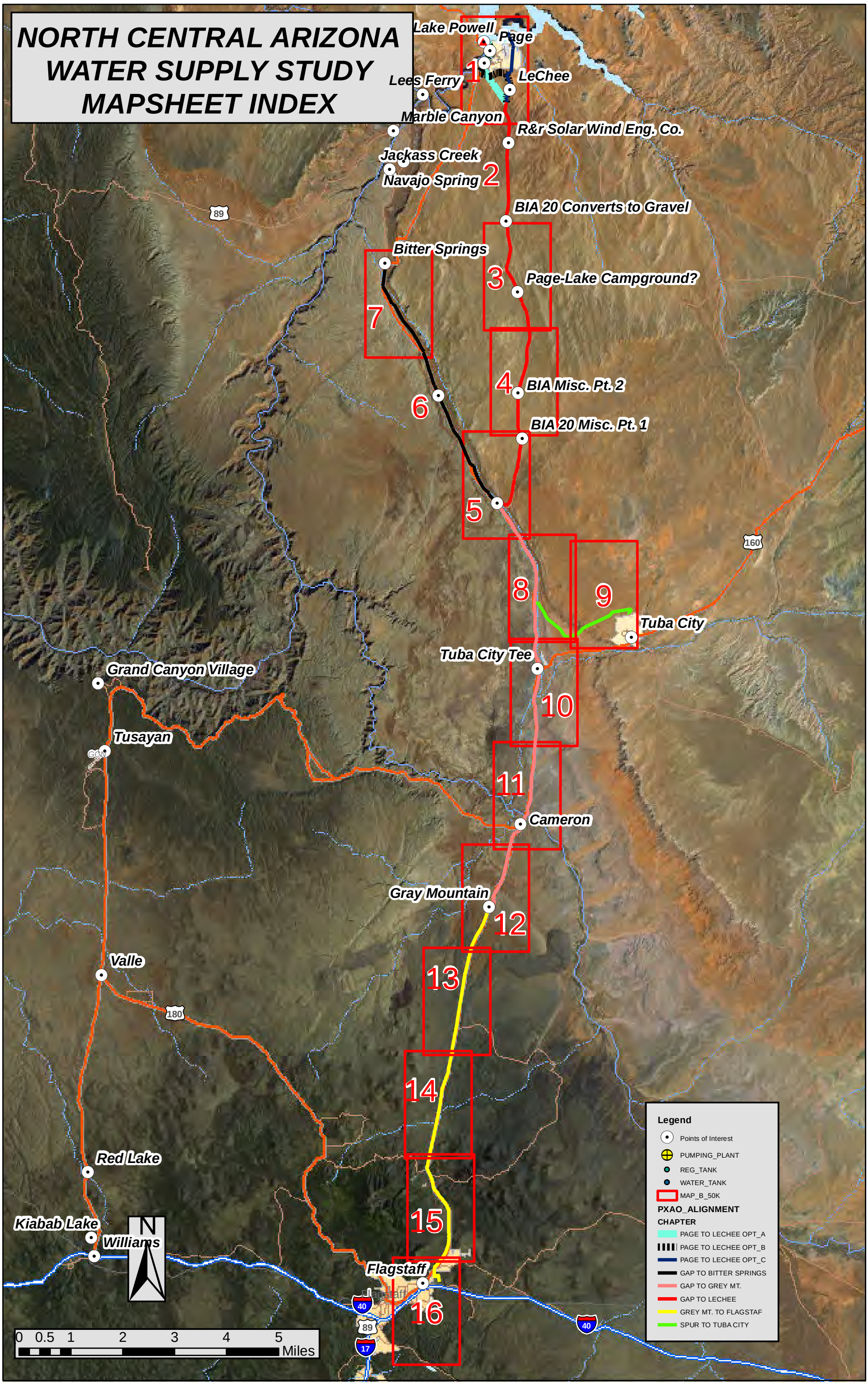

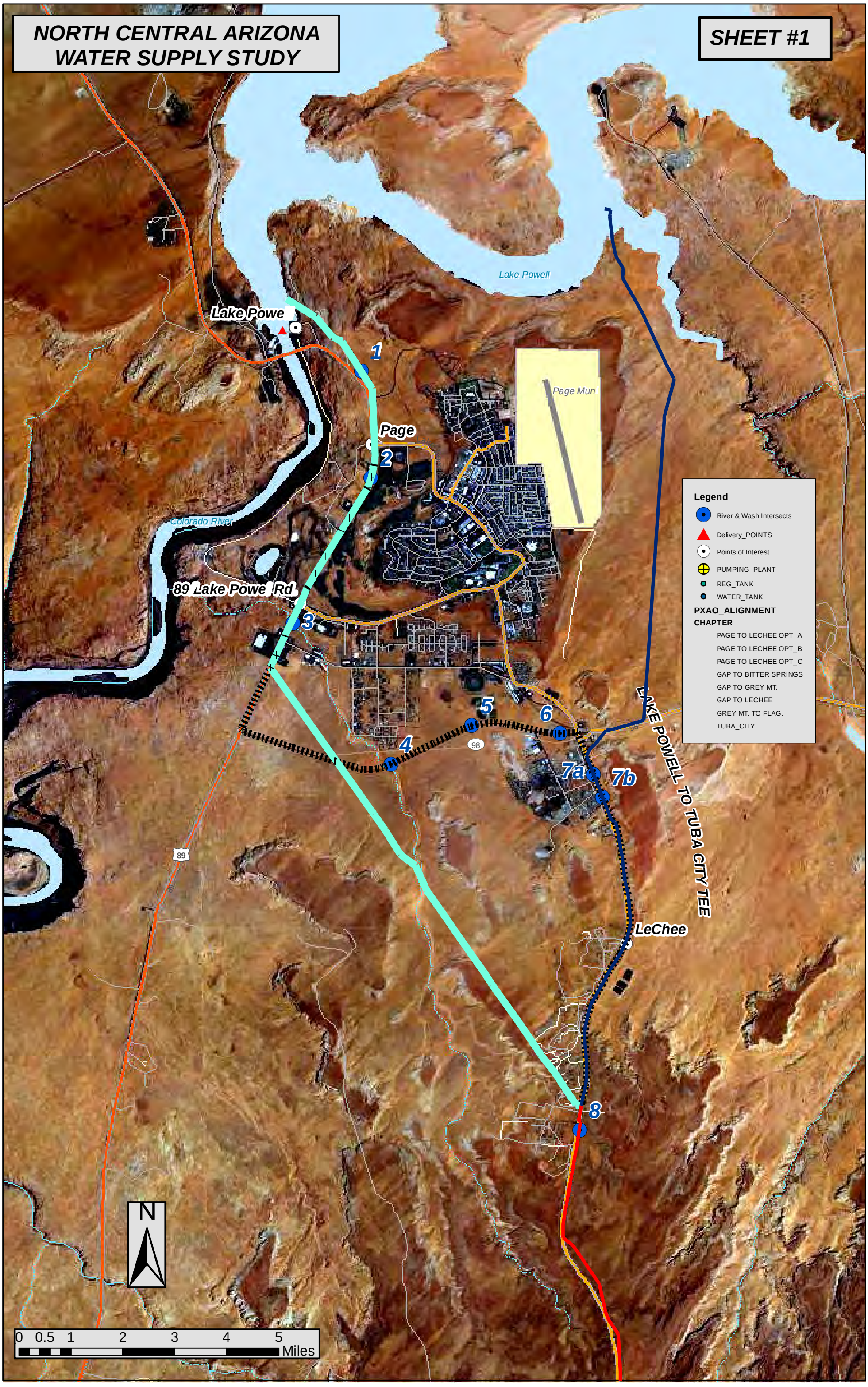
NORTH CENTRAL ARIZONA
WATER SUPPLY STUDY
SHEET #1
Lake Powell
Lake Powe
1
Page Mun
Page
2
Colorado River
89 Lake Powe Rd
3
5
6
4
98
7a
7b
LAKE POWELL TO TUBA CITY TEE
89
LeChee
8
Legend
River & Wash Intersects
Delivery_POINTS
Points of Interest
PUMPING_PLANT
REG_TANK
WATER_TANK
PXAO_ALIGNMENT
CHAPTER
PAGE TO LECHEE OPT_A
PAGE TO LECHEE OPT_B
PAGE TO LECHEE OPT_C
GAP TO BITTER SPRINGS
GAP TO GREY MT.
GAP TO LECHEE
GREY MT. TO FLAG.
TUBA_CITY
N
0 0.5 1 2 3 4 5
Miles

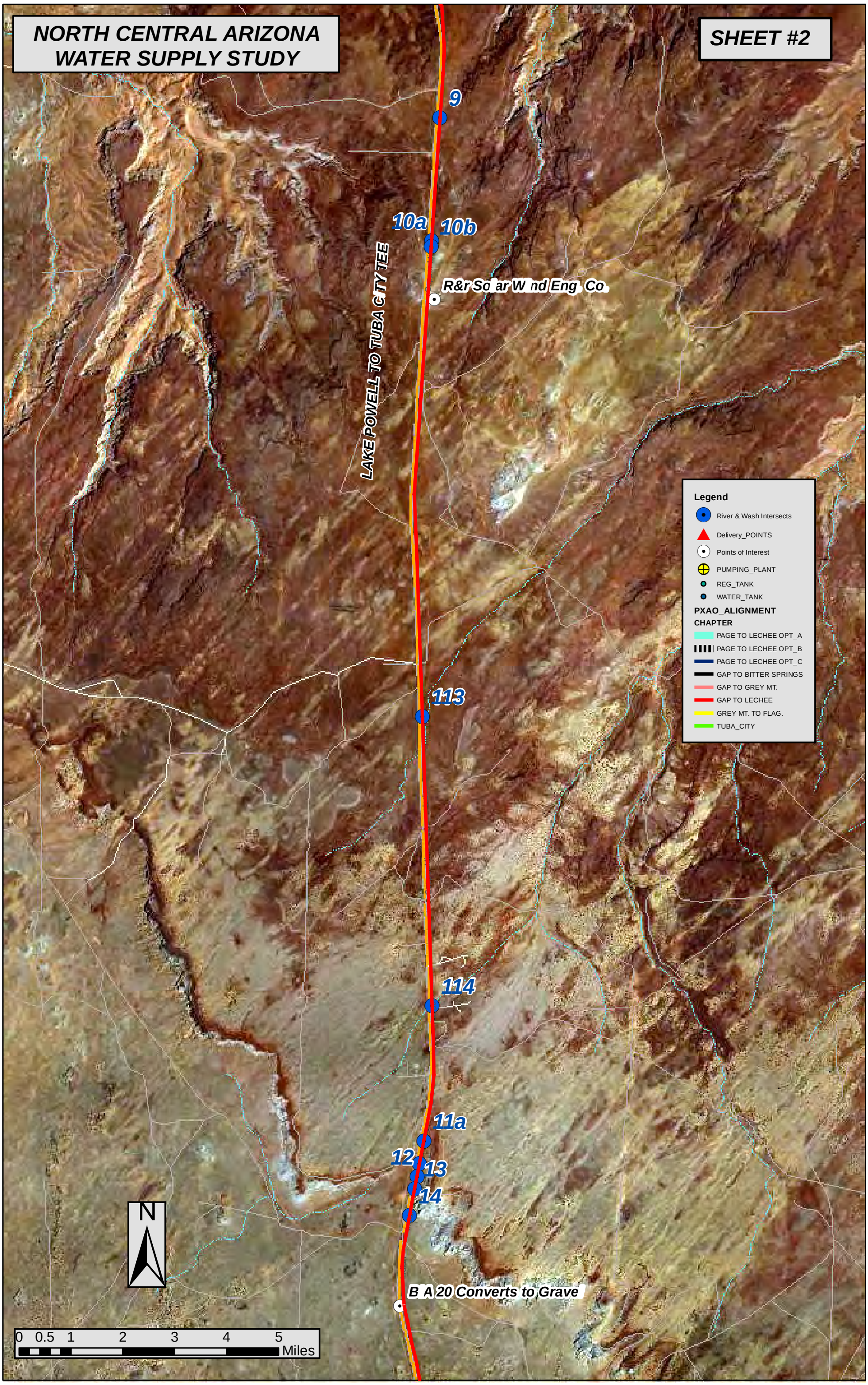
NORTH CENTRAL ARIZONA
WATER SUPPLY STUDY
SHEET #2
9
10a
10b
R&r So ar W nd Eng Co
LAKE POWELL TO TUBA CITY TEE
113
114
11a
12
13
14
B A 20 Converts to Grave
Legend
River & Wash Intersects
Delivery_POINTS
Points of Interest
PUMPING_PLANT
REG_TANK
WATER_TANK
PXAO_ALIGNMENT
CHAPTER
PAGE TO LECHEE OPT_A
PAGE TO LECHEE OPT_B
PAGE TO LECHEE OPT_C
GAP TO BITTER SPRINGS
GAP TO GREY MT.
GAP TO LECHEE
GREY MT. TO FLAG.
TUBA_CITY
N
0 0.5 1 2 3 4 5
Miles

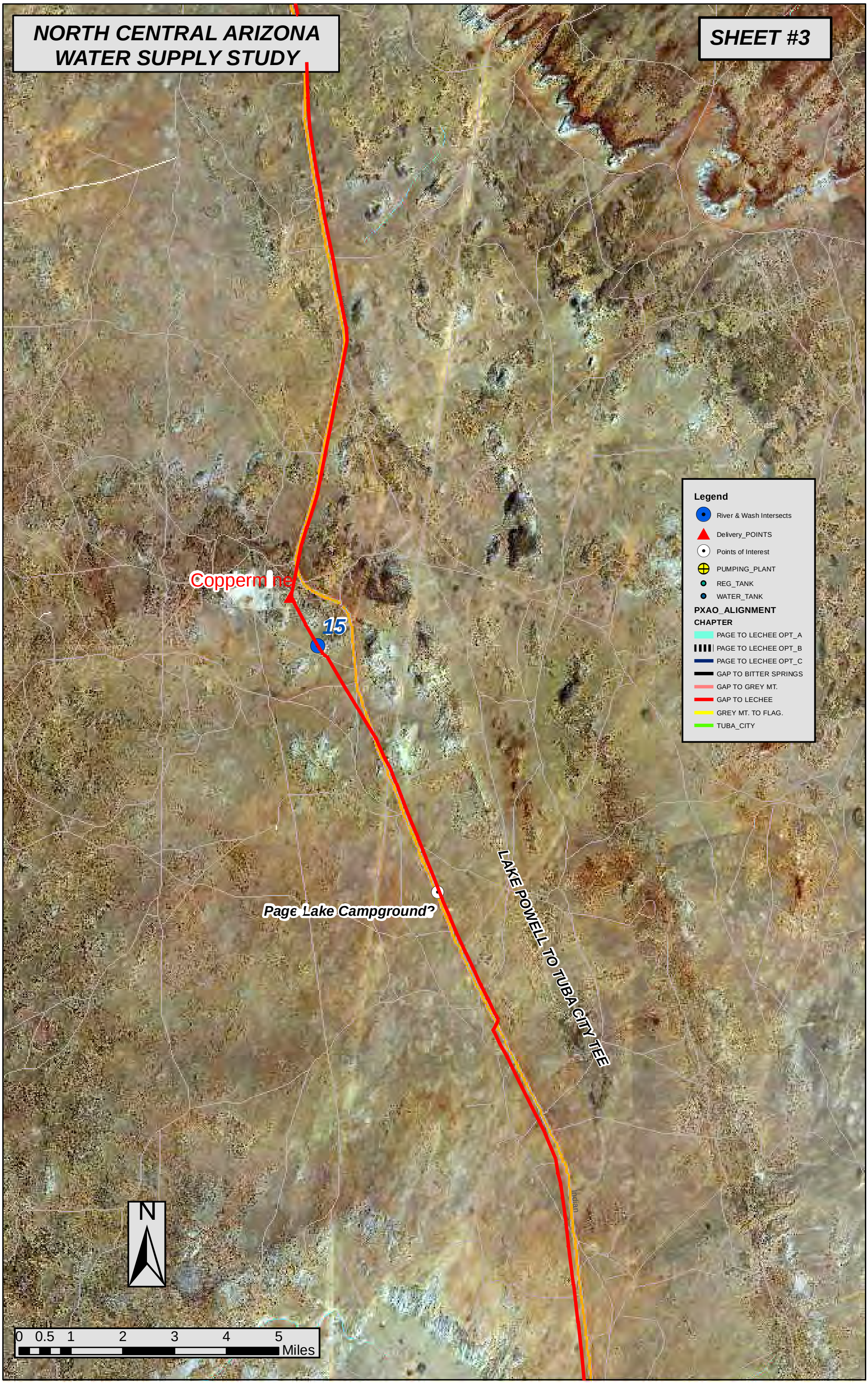
NORTH CENTRAL ARIZONA
WATER SUPPLY STUDY
SHEET #3
Legend
River & Wash Intersects
Delivery_POINTS
Points of Interest
PUMPING_PLANT
REG_TANK
WATER_TANK
PXAO_ALIGNMENT
CHAPTER
PAGE TO LECHEE OPT_A
PAGE TO LECHEE OPT_B
PAGE TO LECHEE OPT_C
GAP TO BITTER SPRINGS
GAP TO GREY MT.
GAP TO LECHEE
GREY MT. TO FLAG.
TUBA_CITY
Copperm ne
15
Page Lake Campground?
LAKE POWELL TO TUBA CITY TEE
N
0 0.5 1 2 3 4 5
Miles

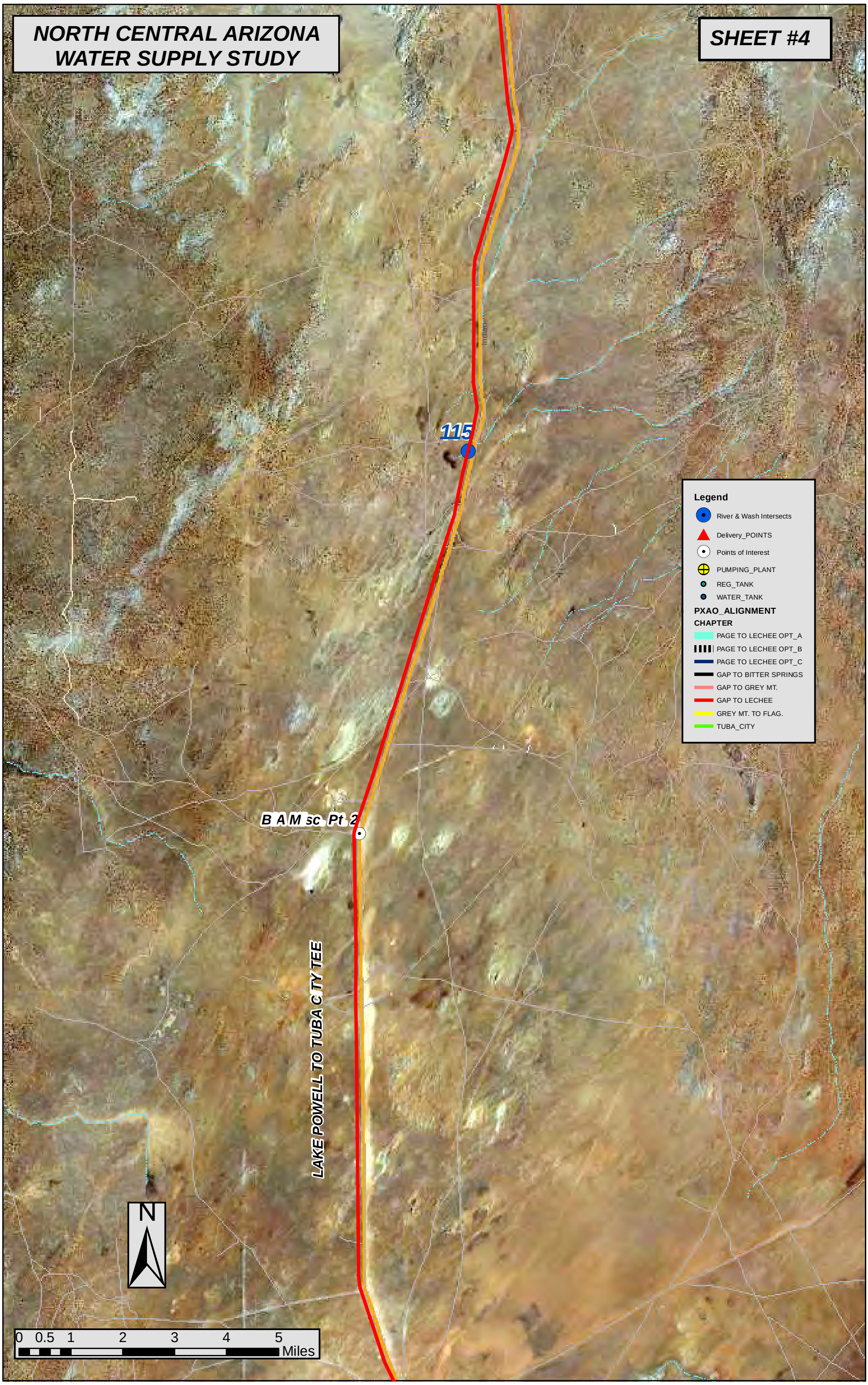
NORTH CENTRAL ARIZONA
WATER SUPPLY STUDY
SHEET #4
115
B A M sc Pt 2
LAKE POWELL TO TUBA C TY TEE
Legend
River & Wash Intersects
Delivery_POINTS
Points of Interest
PUMPING_PLANT
REG_TANK
WATER_TANK
PXAO_ALIGNMENT
CHAPTER
PAGE TO LECHEE OPT_A
PAGE TO LECHEE OPT_B
PAGE TO LECHEE OPT_C
GAP TO BITTER SPRINGS
GAP TO GREY MT.
GAP TO LECHEE
GREY MT. TO FLAG.
TUBA_CITY
N
0 0.5 1 2 3 4 5
Miles

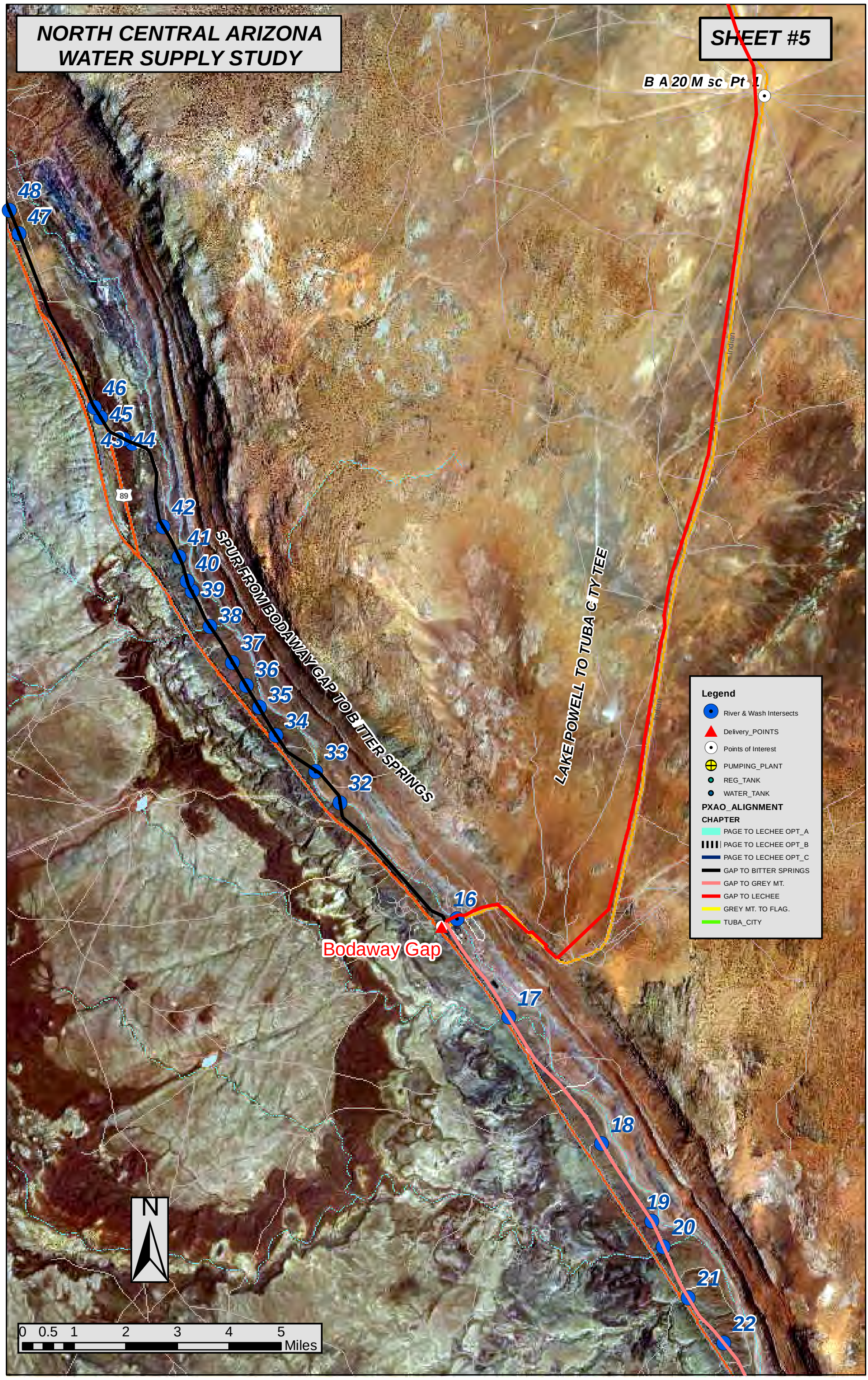
NORTH CENTRAL ARIZONA
WATER SUPPLY STUDY
SHEET #5
B A 20 M sc Pt 1
48
47
46
45
43
44
89
42
41
40
39
38
37
36
35
34
33
32
16
17
18
19
20
21
22
SPUR FROM BODAWAY GAP TO BITTER SPRINGS
LAKE POWELL TO TUBA CITY TEE
Bodaway Gap
Legend
River & Wash Intersects
Delivery_POINTS
Points of Interest
PUMPING_PLANT
REG_TANK
WATER_TANK
PXAO_ALIGNMENT
CHAPTER
PAGE TO LECHEE OPT_A
PAGE TO LECHEE OPT_B
PAGE TO LECHEE OPT_C
GAP TO BITTER SPRINGS
GAP TO GREY MT.
GAP TO LECHEE
GREY MT. TO FLAG.
TUBA_CITY
N
0 0.5 1 2 3 4 5
Miles

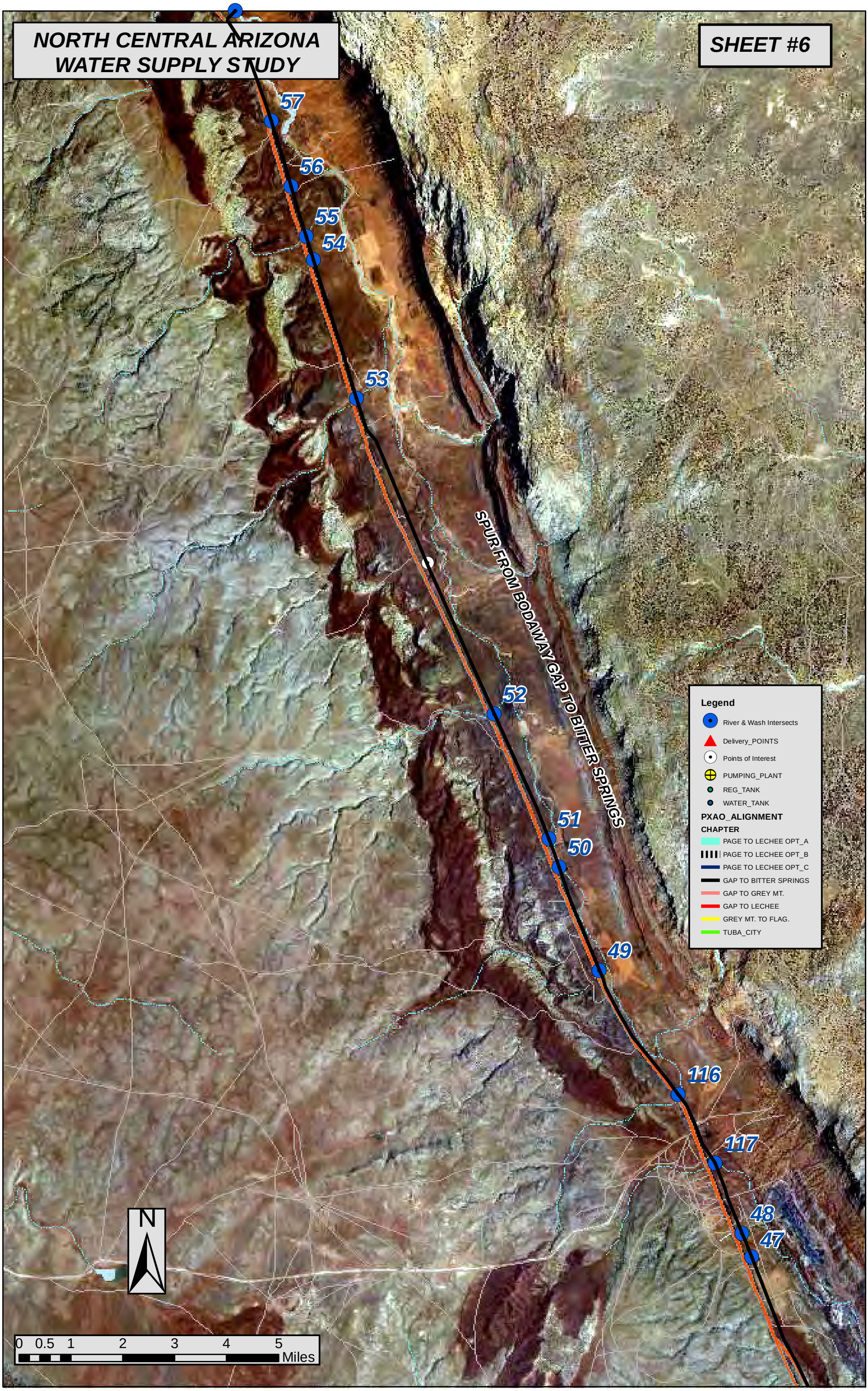
NORTH CENTRAL ARIZONA
WATER SUPPLY STUDY
SHEET #6
57
56
55
54
53
52
51
50
49
116
117
48
47
SPUR FROM BODAWAY GAP TO BITTER SPRINGS
Legend
River & Wash Intersects
Delivery_POINTS
Points of Interest
PUMPING_PLANT
REG_TANK
WATER_TANK
PXAO_ALIGNMENT
CHAPTER
PAGE TO LECHEE OPT_A
PAGE TO LECHEE OPT_B
PAGE TO LECHEE OPT_C
GAP TO BITTER SPRINGS
GAP TO GREY MT.
GAP TO LECHEE
GREY MT. TO FLAG.
TUBA_CITY
N
0 0.5 1 2 3 4 5
Miles

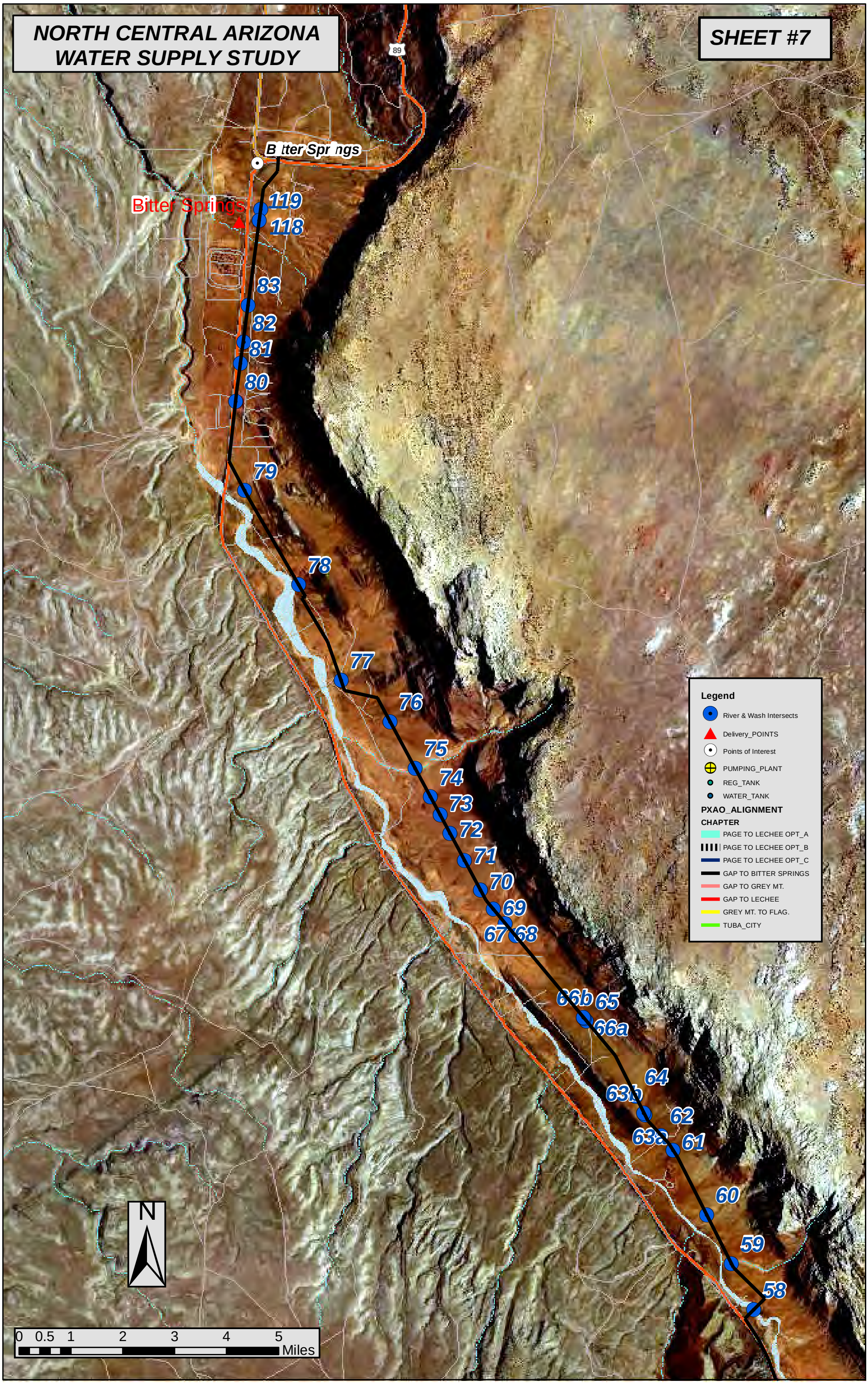
NORTH CENTRAL ARIZONA
WATER SUPPLY STUDY
SHEET #7
89
Bitter Springs
Bitter Springs
119
118
83
82
81
80
79
78
77
76
75
74
73
72
71
70
69
67
68
66b
65
66a
64
63b
62
63a
61
60
59
58
Legend
River & Wash Intersects
Delivery_POINTS
Points of Interest
PUMPING_PLANT
REG_TANK
WATER_TANK
PXAO_ALIGNMENT
CHAPTER
PAGE TO LECHEE OPT_A
PAGE TO LECHEE OPT_B
PAGE TO LECHEE OPT_C
GAP TO BITTER SPRINGS
GAP TO GREY MT.
GAP TO LECHEE
GREY MT. TO FLAG.
TUBA_CITY
N
0 0.5 1 2 3 4 5
Miles

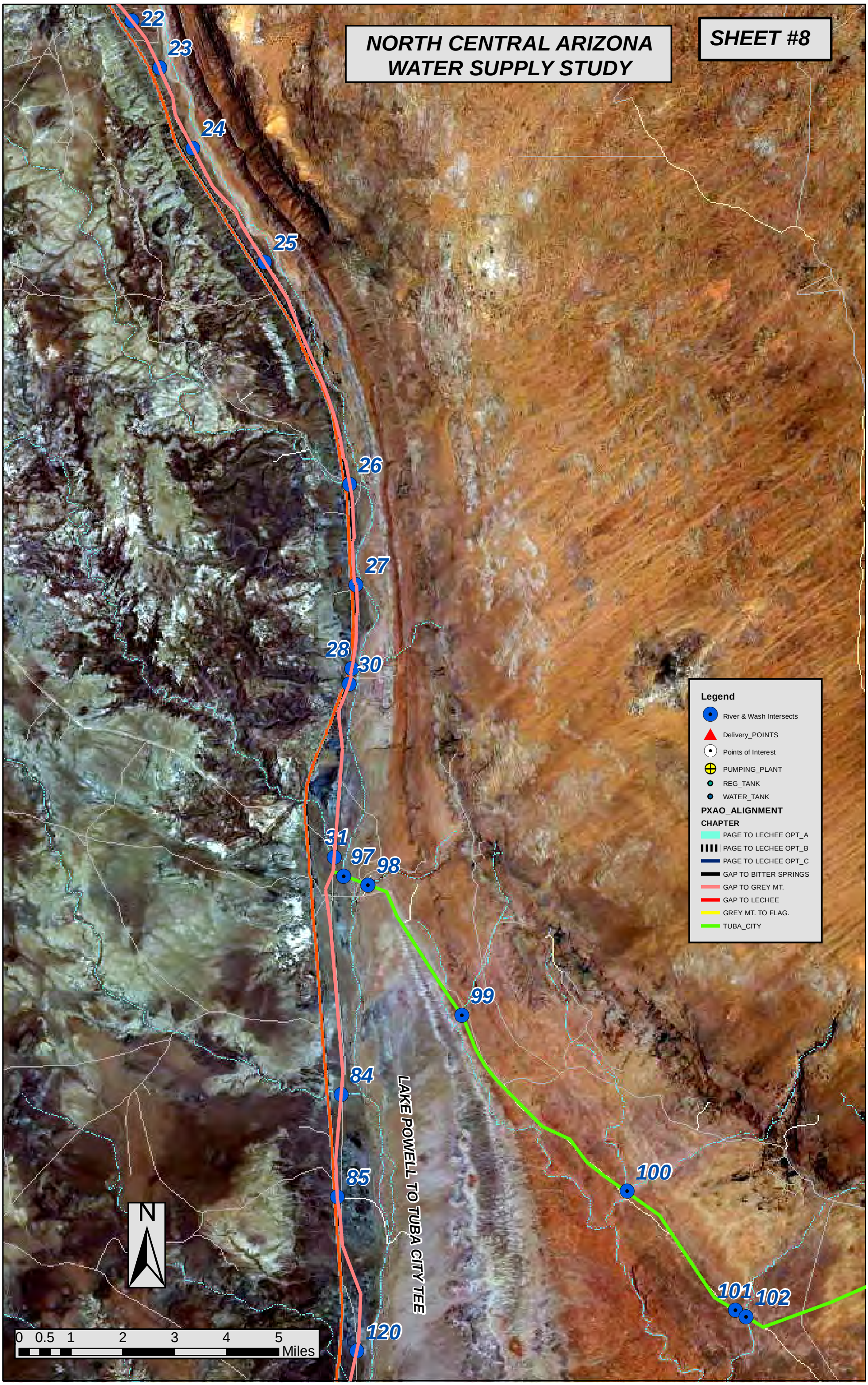
NORTH CENTRAL ARIZONA
WATER SUPPLY STUDY
SHEET #8
22
23
24
25
26
27
28
30
31
97
98
99
84
85
100
101
102
120
LAKE POWELL TO TUBA CITY TEE
Legend
River & Wash Intersects
Delivery_POINTS
Points of Interest
PUMPING_PLANT
REG_TANK
WATER_TANK
PXAO_ALIGNMENT
CHAPTER
PAGE TO LECHEE OPT_A
PAGE TO LECHEE OPT_B
PAGE TO LECHEE OPT_C
GAP TO BITTER SPRINGS
GAP TO GREY MT.
GAP TO LECHEE
GREY MT. TO FLAG.
TUBA_CITY
N
0 0.5 1 2 3 4 5
Miles

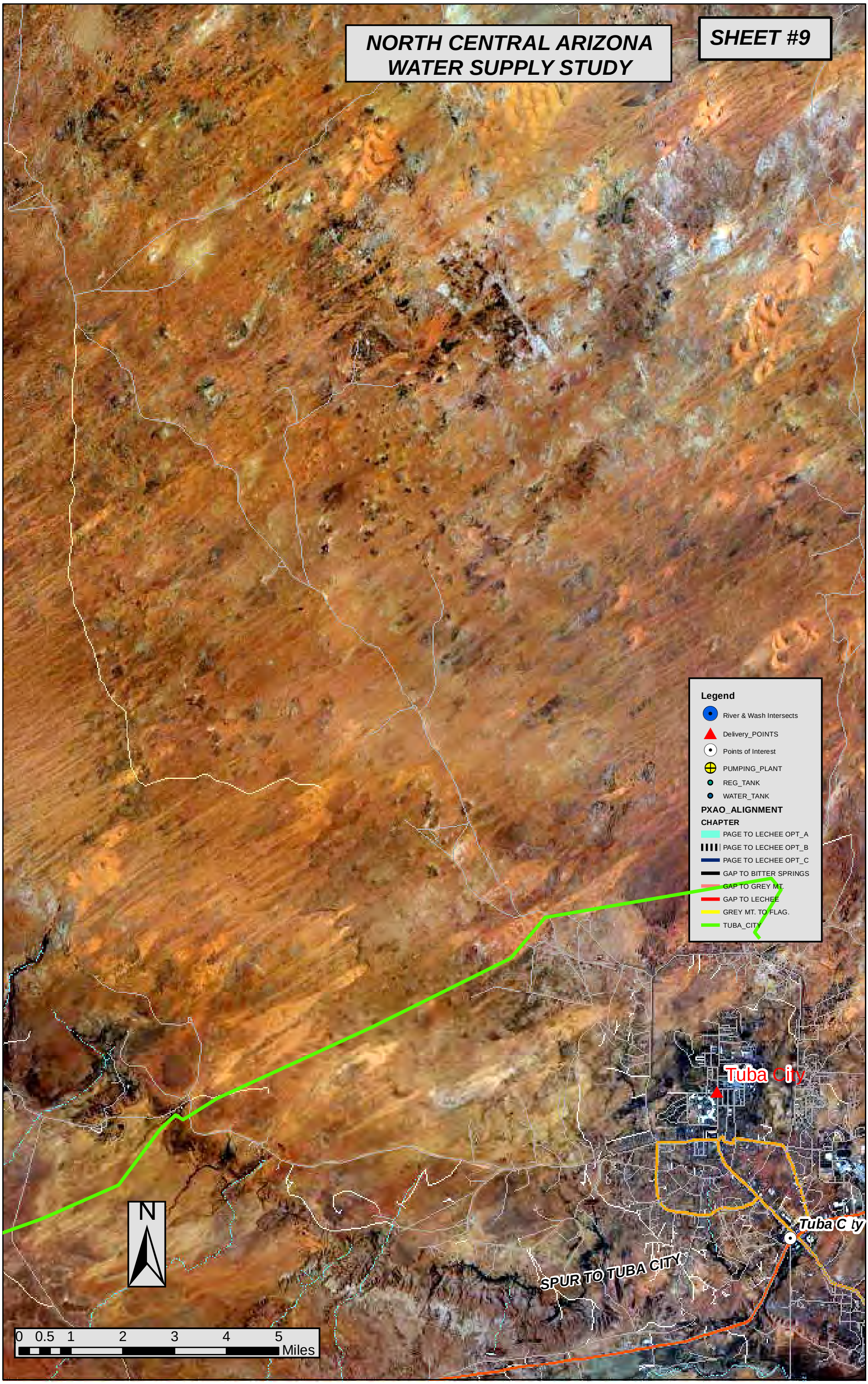
NORTH CENTRAL ARIZONA
WATER SUPPLY STUDY
SHEET #9
Legend
River & Wash Intersects
Delivery_POINTS
Points of Interest
PUMPING_PLANT
REG_TANK
WATER_TANK
PXAO_ALIGNMENT
CHAPTER
PAGE TO LECHEE OPT_A
PAGE TO LECHEE OPT_B
PAGE TO LECHEE OPT_C
GAP TO BITTER SPRINGS
GAP TO GREY MT.
GAP TO LECHEE
GREY MT. TO FLAG.
TUBA_CITY
Tuba City
Tuba City
SPUR TO TUBA CITY
N
0 0.5 1 2 3 4 5
Miles

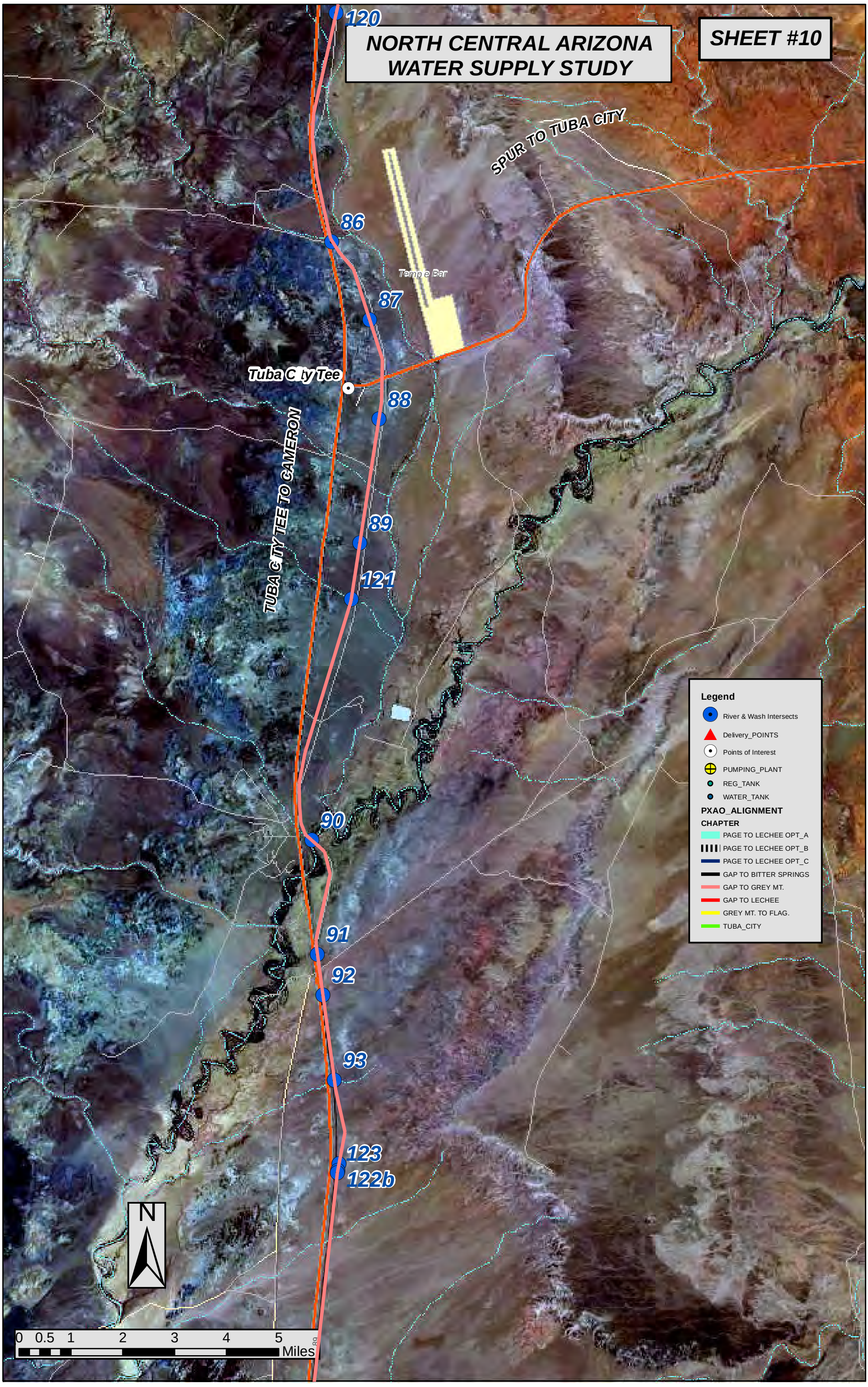
NORTH CENTRAL ARIZONA
WATER SUPPLY STUDY
SHEET #10
SPUR TO TUBA CITY
TUBA CITY TEE TO CAMERON
Tuba City Tee
Temple Bar
120
86
87
88
89
121
90
91
92
93
123
122b
Legend
River & Wash Intersects
Delivery_POINTS
Points of Interest
PUMPING_PLANT
REG_TANK
WATER_TANK
PXAO_ALIGNMENT
CHAPTER
PAGE TO LECHEE OPT_A
PAGE TO LECHEE OPT_B
PAGE TO LECHEE OPT_C
GAP TO BITTER SPRINGS
GAP TO GREY MT.
GAP TO LECHEE
GREY MT. TO FLAG.
TUBA_CITY
N
0 0.5 1 2 3 4 5
Miles

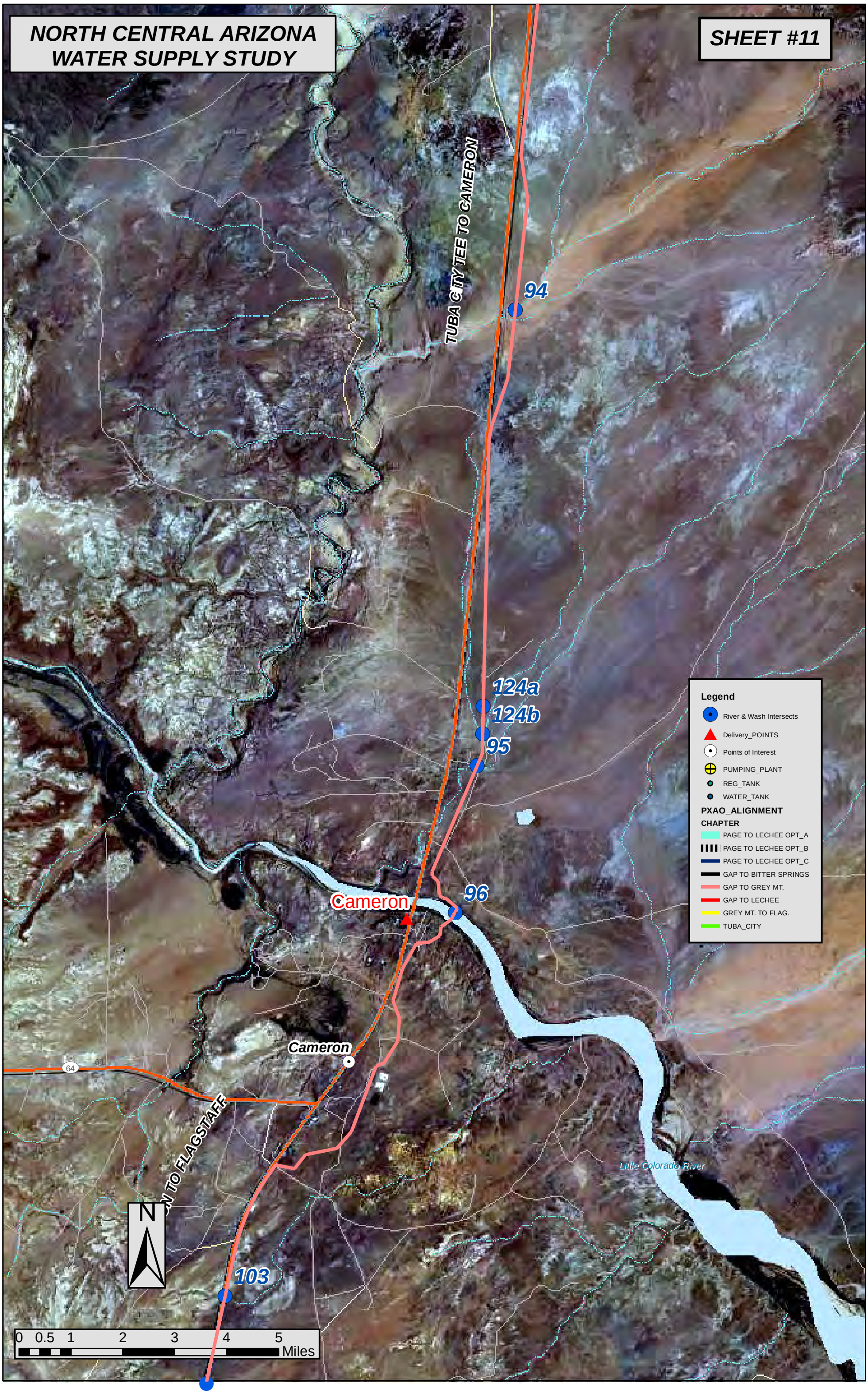
NORTH CENTRAL ARIZONA
WATER SUPPLY STUDY
SHEET #11
TUBA CITY TEE TO CAMERON
94
124a
124b
95
96
Cameron
Cameron
64
N TO FLAGSTAFF
103
Little Colorado River
N
0 0.5 1 2 3 4 5
Miles
Legend
River & Wash Intersects
Delivery_POINTS
Points of Interest
PUMPING_PLANT
REG_TANK
WATER_TANK
PXAO_ALIGNMENT
CHAPTER
PAGE TO LECHEE OPT_A
PAGE TO LECHEE OPT_B
PAGE TO LECHEE OPT_C
GAP TO BITTER SPRINGS
GAP TO GREY MT.
GAP TO LECHEE
GREY MT. TO FLAG.
TUBA_CITY

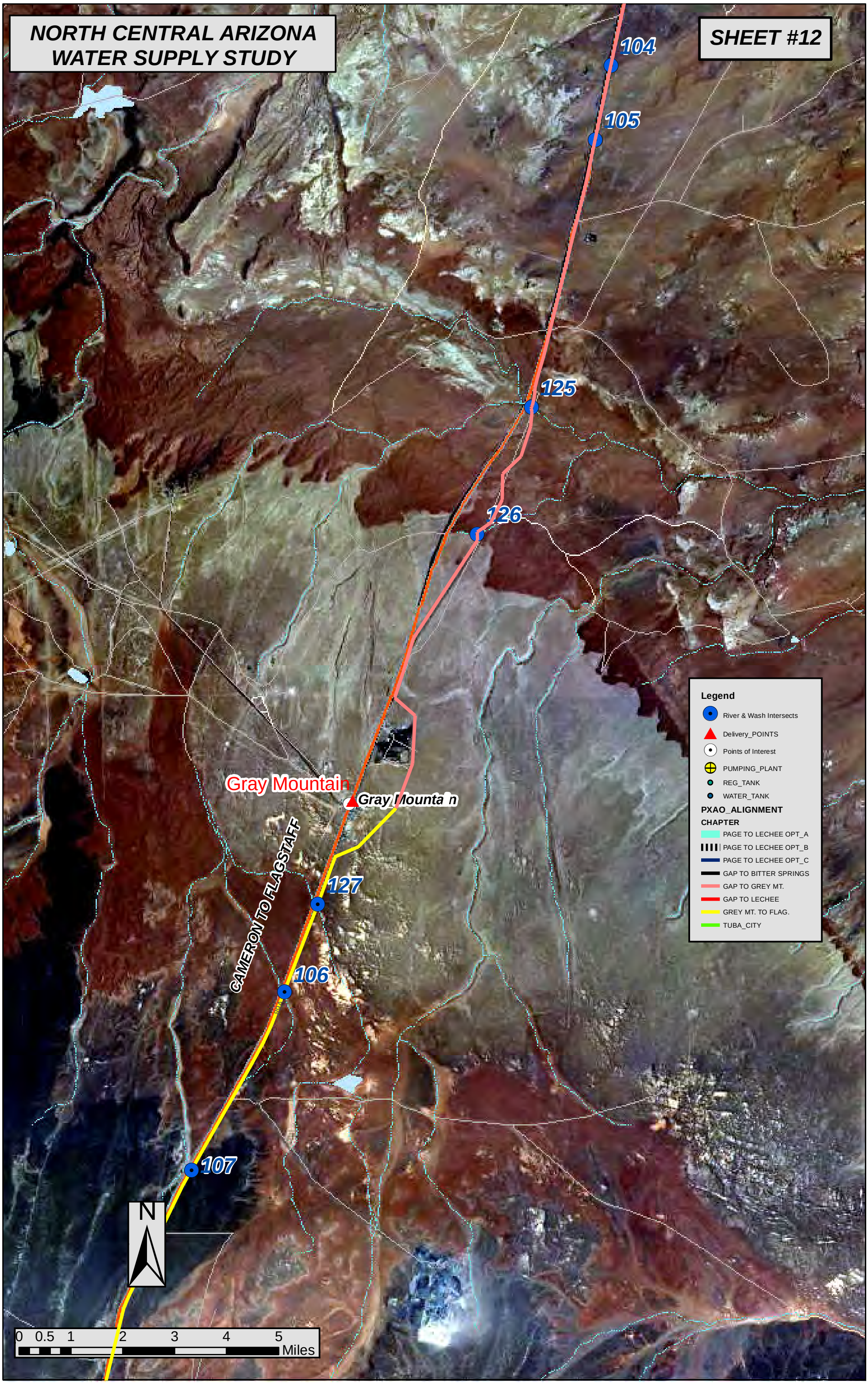
NORTH CENTRAL ARIZONA
WATER SUPPLY STUDY
SHEET #12
104
105
125
126
Gray Mountain
Gray Mounta n
127
CAMERON TO FLAGSTAFF
106
107
N
0 0.5 1 2 3 4 5
Miles
Legend
River & Wash Intersects
Delivery_POINTS
Points of Interest
PUMPING_PLANT
REG_TANK
WATER_TANK
PXAO_ALIGNMENT
CHAPTER
PAGE TO LECHEE OPT_A
PAGE TO LECHEE OPT_B
PAGE TO LECHEE OPT_C
GAP TO BITTER SPRINGS
GAP TO GREY MT.
GAP TO LECHEE
GREY MT. TO FLAG.
TUBA_CITY

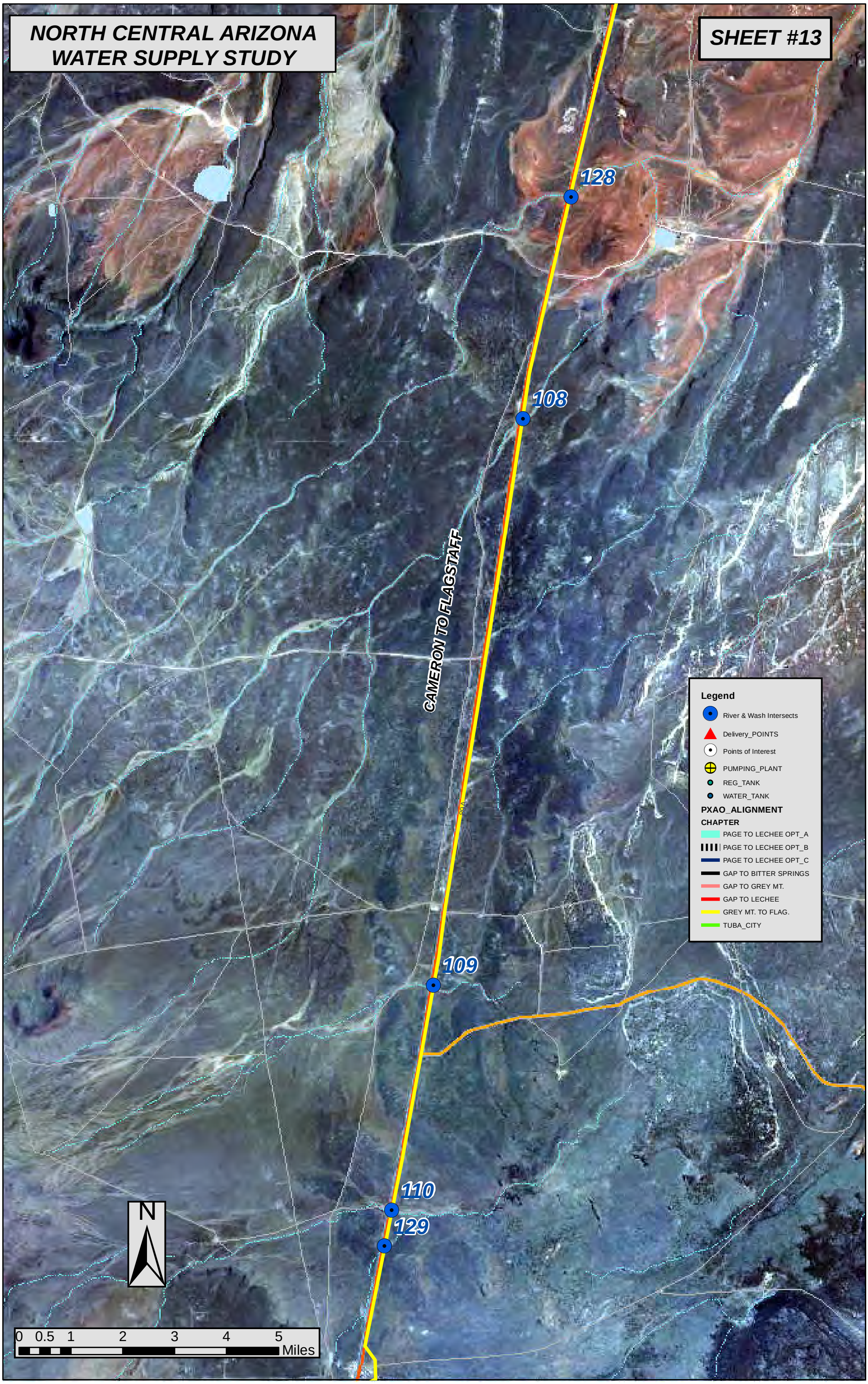
NORTH CENTRAL ARIZONA
WATER SUPPLY STUDY
SHEET #13
128
108
CAMERON TO FLAGSTAFF
109
110
129
Legend
River & Wash Intersects
Delivery_POINTS
Points of Interest
PUMPING_PLANT
REG_TANK
WATER_TANK
PXAO_ALIGNMENT
CHAPTER
PAGE TO LECHEE OPT_A
PAGE TO LECHEE OPT_B
PAGE TO LECHEE OPT_C
GAP TO BITTER SPRINGS
GAP TO GREY MT.
GAP TO LECHEE
GREY MT. TO FLAG.
TUBA_CITY
N
0 0.5 1 2 3 4 5
Miles

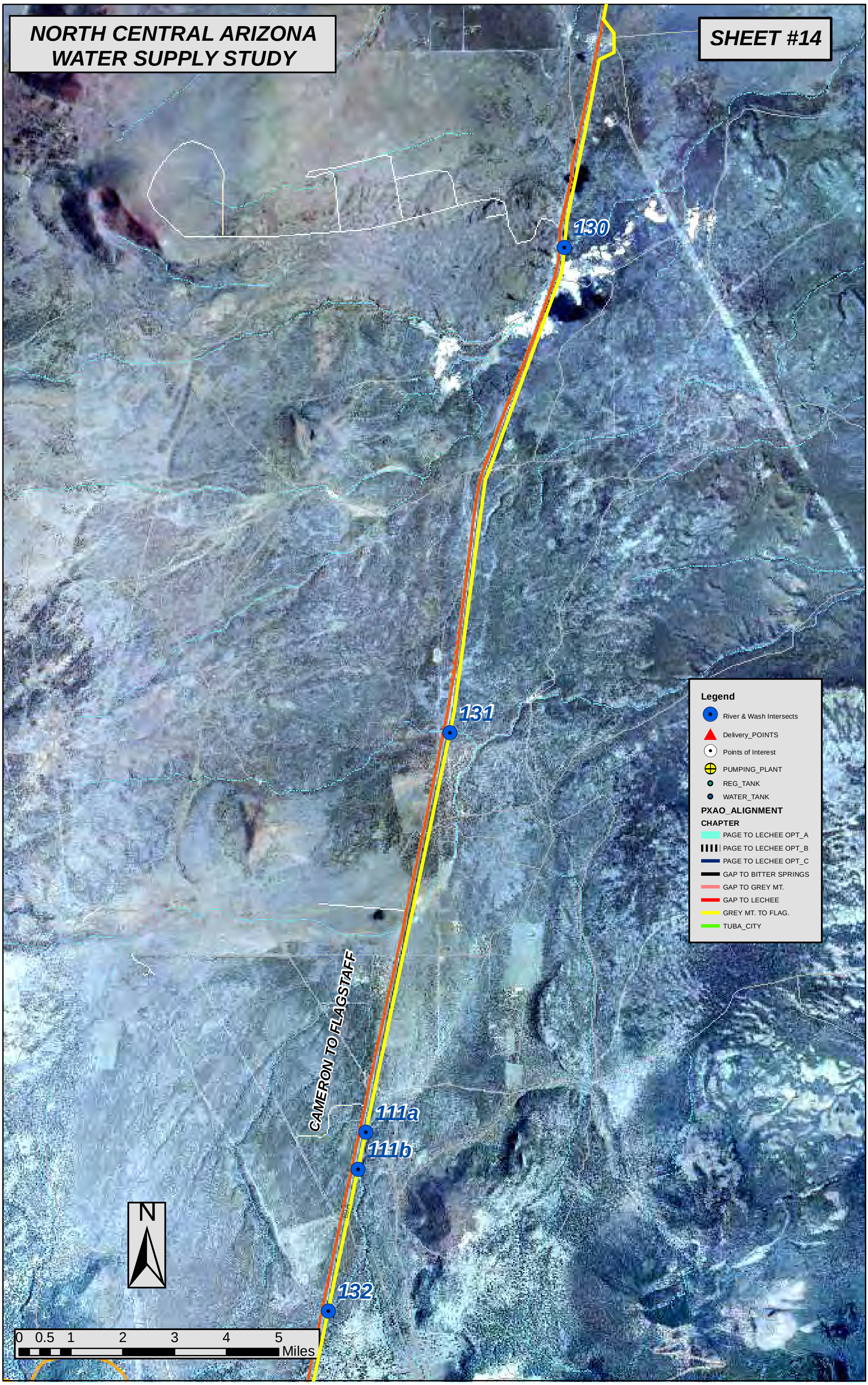
NORTH CENTRAL ARIZONA
WATER SUPPLY STUDY
SHEET #14
130
131
CAMERON TO FLAGSTAFF
111a
111b
132
N
0 0.5 1 2 3 4 5
Miles
Legend
River & Wash Intersects
Delivery_POINTS
Points of Interest
PUMPING_PLANT
REG_TANK
WATER_TANK
PXAO_ALIGNMENT
CHAPTER
PAGE TO LECHEE OPT_A
PAGE TO LECHEE OPT_B
PAGE TO LECHEE OPT_C
GAP TO BITTER SPRINGS
GAP TO GREY MT.
GAP TO LECHEE
GREY MT. TO FLAG.
TUBA_CITY

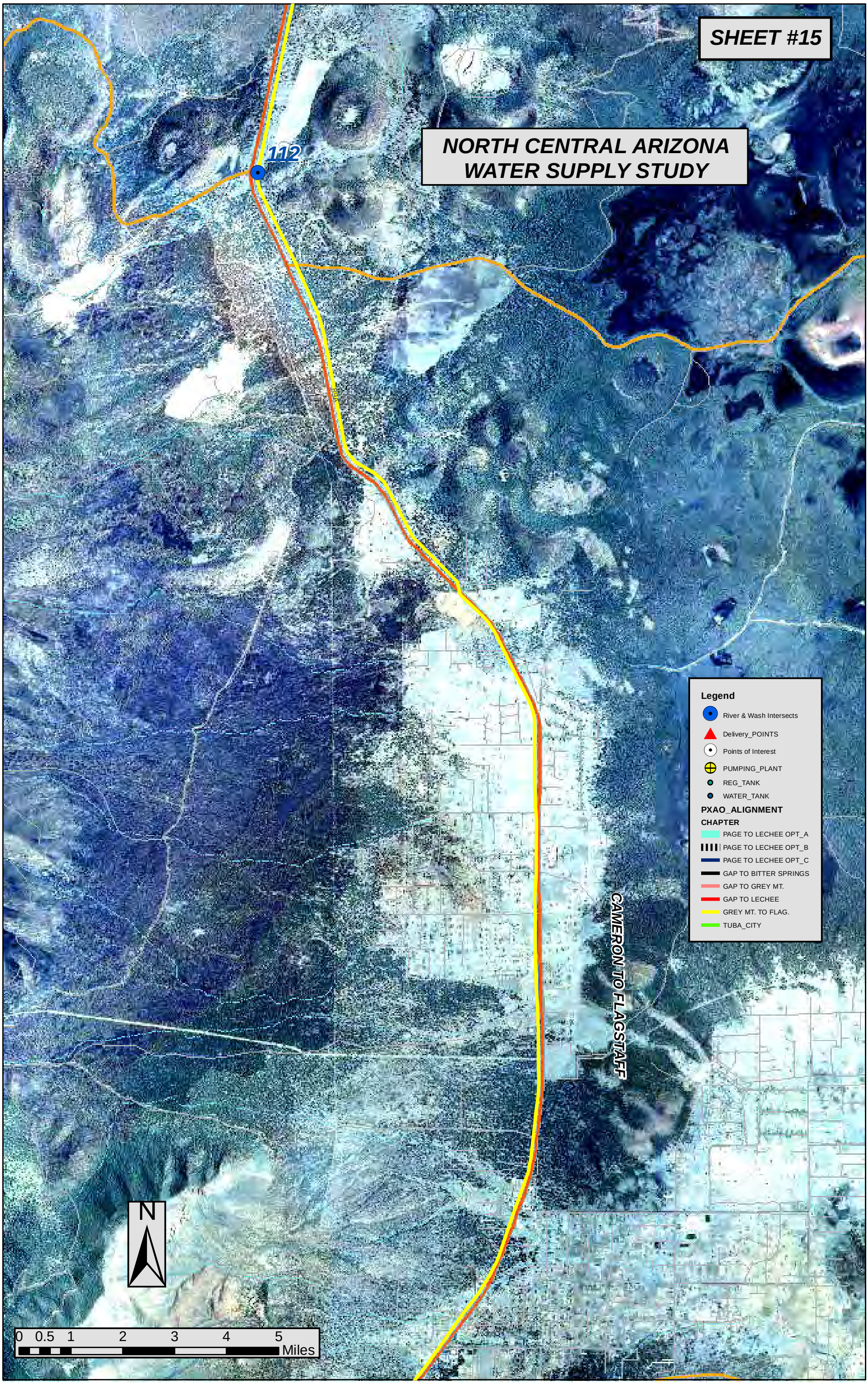
SHEET #15
NORTH CENTRAL ARIZONA
WATER SUPPLY STUDY
112
Legend
River & Wash Intersects
Delivery_POINTS
Points of Interest
PUMPING_PLANT
REG_TANK
WATER_TANK
PXAO_ALIGNMENT
CHAPTER
PAGE TO LECHEE OPT_A
PAGE TO LECHEE OPT_B
PAGE TO LECHEE OPT_C
GAP TO BITTER SPRINGS
GAP TO GREY MT.
GAP TO LECHEE
GREY MT. TO FLAG.
TUBA_CITY
CAMERON TO FLAGSTAFF
N
0 0.5 1 2 3 4 5
Miles

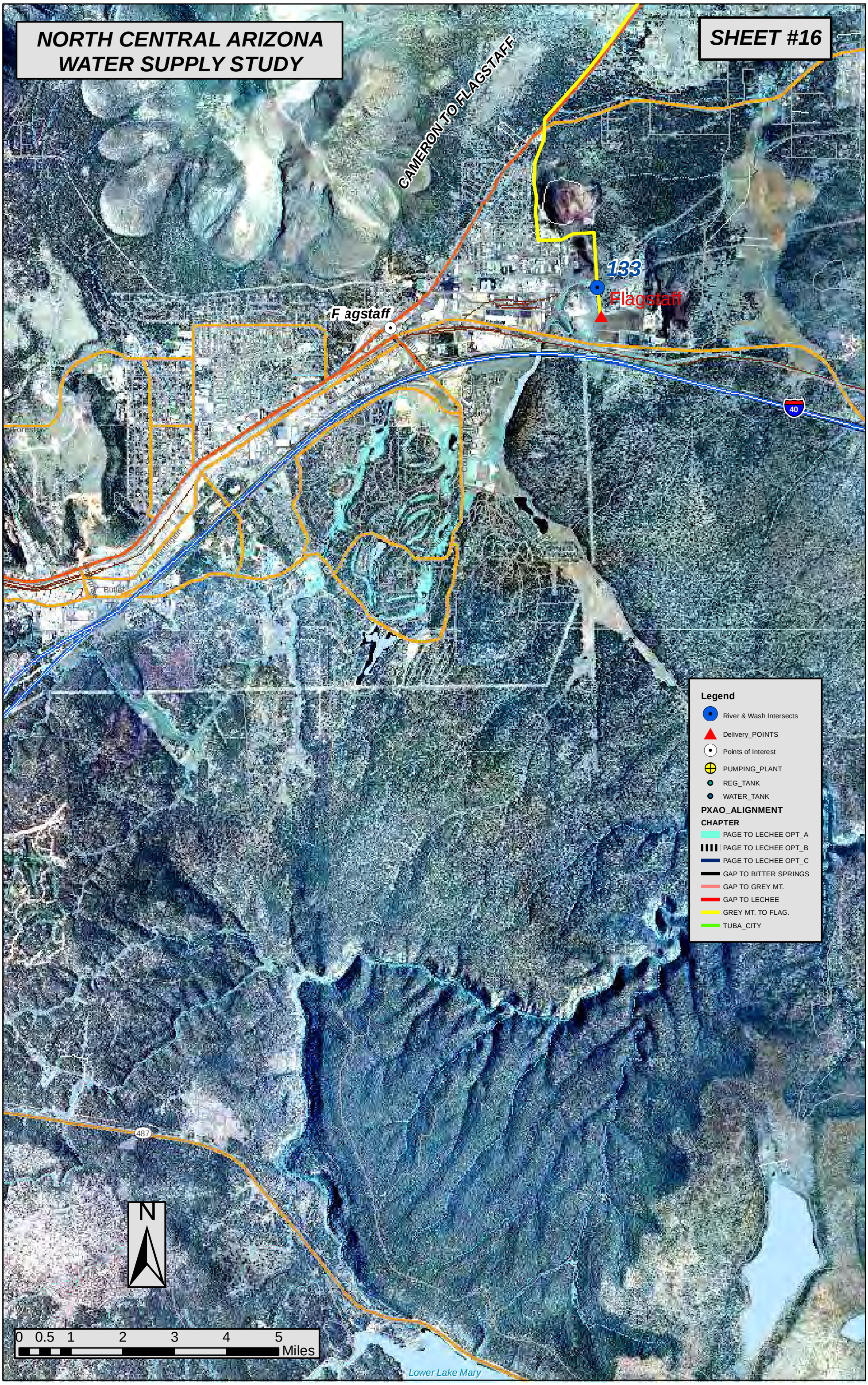
NORTH CENTRAL ARIZONA
WATER SUPPLY STUDY
SHEET #16
CAMERON TO FLAGSTAFF
133
Flagstaff
Flagstaff
Butler
Huntington
Industrial
Forest
40
487
Legend
River & Wash Intersects
Delivery_POINTS
Points of Interest
PUMPING_PLANT
REG_TANK
WATER_TANK
PXAO_ALIGNMENT
CHAPTER
PAGE TO LECHEE OPT_A
PAGE TO LECHEE OPT_B
PAGE TO LECHEE OPT_C
GAP TO BITTER SPRINGS
GAP TO GREY MT.
GAP TO LECHEE
GREY MT. TO FLAG.
TUBA_CITY
N
0 0.5 1 2 3 4 5
Miles
Lower Lake Mary

Appendix B

Hydrology

B.1 Input Parameters

Table B-1. Input Parameters

Crossing	Crossing coordinates		Basin drainage area (mi^2)	Average basin elevation (feet)	Average basin slope (%)	Basin length (feet)	Hydrologic soil type	Runoff curve No.
	Northing	Easting						
1	36.93357	-111.4737	0.03	4,087	0.11	3,200	D	88
2	36.92217	-111.4724	0.42	4,253	0.07	5,800	D	88
3	36.90674	-111.4828	8.93	4,651	0.09	36,200	D	88
4	36.89171	-111.4698	6.64	4,351	0.10	5,000	D	88
5	36.89583	-111.459	0.48	4,503	0.08	12,000	D	88
6	36.89503	-111.4472	1.66	4,771	0.06	29,600	D	88
7a	36.89062	-111.4428	0.01	4,342	0.05	1,150	D	88
7b	36.88819	-111.4416	0.01	4,437	0.13	1,150	D	88
8	36.85272	-111.4446	0.62	4,894	0.07	6,600	D	88
9	36.81915	-111.4397	0.04	5,264	0.03	2,100	D	88
10a	36.80601	-111.4408	0.01	5,363	0.04	930	D	88
10b	36.8054	-111.4409	0.01	5,365	0.06	930	D	88
11a	36.70995	-111.4418	0.01	5,781	0.06	9,800	D	88
11b	36.70751	-111.4425	0.03	5,861	0.10	8,000	D	88
12	36.70615	-111.4428	0.04	5,902	0.14	1,500	D	88
13	36.70487	-111.4431	0.04	5,921	0.29	1,500	D	88
14	36.70198	-111.4438	0.04	5,840	0.28	500	D	88
15	36.62098	-111.4408	0.08	5,909	0.08	800	D	88
16	36.30482	-111.4584	18.73	5,857	0.13	650	D	88
17	36.29416	-111.4515	3.12	5,124	0.08	5,300	B/D	82.5
18	36.28053	-111.4391	1.30	5,142	0.13	4,800	B/D	82.5
19	36.27218	-111.4323	0.40	6,000	0.13	350	D	88
20	36.26946	-111.4308	7.18	5,739	0.08	4,000	B/D	82.5
21	36.26394	-111.4275	2.30	5,433	0.06	2,400	B/D	82.5
22	36.25907	-111.4227	0.34	5,213	0.06	2,600	B/D	82.5
23	36.25404	-111.419	0.02	5,202	0.13	3,600	B/D	82.5
24	36.2454	-111.4146	0.20	5,586	0.12	5,800	B/D	82.5
25	36.23314	-111.4051	0.30	6,019	0.12	4,700	B/D	82.5
26	36.20928	-111.3937	4.09	5,603	0.07	5,200	B/D	82.5
27	36.1985	-111.3929	1.40	5,319	0.12	2,800	B/D	82.5
28	36.1895	-111.3935	0.80	6,472	0.12	31,500	B/D	82.5
30	36.18782	-111.3938	0.80	5,351	0.12	2,200	B/D	82.5
31	36.16923	-111.3958	1.36	5,498	0.05	2,700	B/D	82.5

Table B-1. Input Parameters

Crossing	Crossing coordinates		Basin drainage area (mi^2)	Average basin elevation (feet)	Average basin slope (%)	Basin length (feet)	Hydrologic soil type	Runoff curve No.
	Northing	Easting						
113	36.75553	-111.4421	0.80	5,364	0.05	3,200	B/D	82.5
114	36.72439	-111.4407	0.82	5,814	0.03	3,100	B/D	82.5
115	36.49762	-111.4097	0.10	5,501	0.04	3,000	B/D	82.5
32	36.31731	-111.4741	17.07	5,665	0.12	2,800	B/D	82.5
33	36.32065	-111.4773	14.77	5,383	0.13	3,750	B/D	82.5
34	36.32456	-111.4826	1.02	5,386	0.07	3,300	B/D	82.5
35	36.32759	-111.4848	0.13	5,649	0.13	3,100	B/D	82.5
36	36.32992	-111.4866	0.13	5,542	0.05	3,100	B/D	82.5
37	36.33241	-111.4884	0.06	5,660	0.08	3,100	B/D	82.5
38	36.33629	-111.4914	5.18	5,494	0.10	4,800	B/D	82.5
39	36.34009	-111.4938	0.10	6,044	0.15	5,500	B/D	82.5
40	36.34118	-111.4945	0.12	6,044	0.15	5,500	B/D	82.5
41	36.34377	-111.4956	0.15	5,520	0.15	2,900	B/D	82.5
42	36.34703	-111.4977	0.58	5,483	0.10	3,600	B/D	82.5
43	36.356	-111.5018	1.00	5,479	0.09	5,500	B/D	82.5
44	36.35647	-111.503	1.02	6,194	0.09	5,900	B/D	82.5
45	36.35878	-111.5061	0.20	6,096	0.08	53,800	B/D	82.5
46	36.35988	-111.5069	0.82	6,095	0.08	3,300	B	77
47	36.37859	-111.517	0.80	5,677	0.05	400	D	88
48	36.38114	-111.5183	0.80	5,559	0.06	4,000	B	77
49	36.40934	-111.5373	3.40	5,936	0.09	15,000	B/D	82.5
50	36.42044	-111.5427	8.14	5,936	0.10	9,000	B	77
51	36.42344	-111.544	8.19	6,047	0.10	22,300	B/D	82.5
52	36.43684	-111.5513	11.53	6,097	0.11	24,800	B/D	82.5
53	36.47069	-111.5697	3.30	6,109	0.07	19,600	B	77
54	36.48554	-111.5754	0.40	6,111	0.10	18,500	B	77
55	36.48805	-111.5764	2.27	6,133	0.10	16,000	B/D	82.5
56	36.49343	-111.5784	0.31	6,106	0.02	11,500	B/D	82.5
57	36.50043	-111.581	0.25	6,082	0.11	11,000	B/D	82.5
58	36.51222	-111.5858	34.62	5,933	0.12	5,900	B/D	82.5
59	36.51716	-111.5888	0.42	5,901	0.57	7,600	B/D	82.5
60	36.52239	-111.5921	0.30	5,917	0.03	6,800	B/D	82.5
61	36.52927	-111.5965	0.15	5,916	0.03	4,000	B/D	82.5
62	36.53089	-111.5981	0.06	5,896	0.11	8,900	B/D	82.5
63a	36.53304	-111.6003	0.39	5,892	0.64	8,900	D	88
63b	36.53331	-111.6004	0.39	5,792	0.64	5,500	D	88
64	36.53505	-111.6015	0.38	5,924	0.05	3,500	D	88
65	36.54312	-111.6081	0.15	5,916	0.30	3,700	D	88
66a	36.54341	-111.6083	0.15	5,911	0.36	2,800	D	88
66b	36.54352	-111.6085	0.14	5,959	0.37	20,700	D	88
67	36.55223	-111.6175	0.22	5,542	0.10	3,100	D	88
68	36.55356	-111.6189	0.15	5,452	0.10	3,100	D	88

Table B-1. Input Parameters

Crossing	Crossing coordinates		Basin drainage area (mi^2)	Average basin elevation (feet)	Average basin slope (%)	Basin length (feet)	Hydrologic soil type	Runoff curve No.
	Northing	Easting						
69	36.55511	-111.6205	0.06	5,911	0.45	4,000	D	88
70	36.55718	-111.6222	0.03	5,695	0.24	11,700	D	88
71	36.56031	-111.6243	0.09	5,884	0.57	31,000	D	88
72	36.56321	-111.6262	0.10	5,864	0.10	33,000	D	88
73	36.5652	-111.6276	0.04	5,833	0.34	38,200	D	88
74	36.56711	-111.6289	0.15	5,642	0.10	18,000	D	88
75	36.57018	-111.6309	7.51	5,756	0.13	12,000	D	88
76	36.57518	-111.6342	0.12	5,747	0.10	5,200	D	88
77	36.57958	-111.6408	0.20	5,635	0.33	32,000	D	88
78	36.58981	-111.6464	0.33	5,474	0.13	18,900	D	88
79	36.59987	-111.6536	0.54	5,326	0.45	7,500	D	88
80	36.60941	-111.6548	0.18	5,170	0.10	1,900	D	88
81	36.61346	-111.6541	0.07	5,666	0.10	3,700	D	88
82	36.61573	-111.6537	0.07	5,652	0.46	4,000	D	88
83	36.6197	-111.6531	0.13	5,278	0.54	30,000	B/D	82.5
116	36.39604	-111.5268	1.32	5,580	0.05	13,700	B/D	82.5
117	36.38867	-111.5219	0.86	5,575	0.09	8,200	B	77
118	36.62993	-111.6515	0.36	5,549	0.10	8,200	B	77
119	36.62876	-111.6517	0.36	5,029	0.10	17,300	B/D	82.5
84	36.14371	-111.3949	3.79	5,492	0.05	98,000	B/D	82.5
85	36.13269	-111.3954	0.13	5,037	0.10	9,200	B	77
86	36.09151	-111.3933	22.33	4,950	0.04	7,400	B	77
87	36.08314	-111.3883	0.53	5,061	0.09	31,500	D	88
88	36.07241	-111.3871	0.50	5,094	0.08	25,000	B/D	82.5
89	36.05906	-111.3896	0.39	4,668	0.08	4,000	D	88
90	36.02712	-111.396	0.78	4,651	0.07	7,800	B/D	82.5
91	36.01481	-111.3953	2.34	5,251	0.06	47,800	B/D	82.5
92	36.01042	-111.3946	0.53	4,917	0.09	28,000	D	88
93	36.00126	-111.393	0.40	5,214	0.04	80,500	D	88
94	35.94111	-111.3979	170.97	4,591	0.04	8,600	B/D	82.5
95	35.89202	-111.403	10.13	4,523	0.02	5,900	B/D	82.5
96	35.87613	-111.4059	23,091.90	4,479	0.07	7,100	D	88
120	36.1161	-111.3928	2.75	4,661	0.04	19,400	D	88
121	36.05301	-111.3907	2.25	4,497	0.04	11,200	D	88
122a	35.99223	-111.3924	0.40	4,485	0.10	14,200	B	77
122b	35.9915	-111.3926	0.40	4,487	0.10	10,000	B	77
123	35.99126	-111.3926	0.40	4,390	0.10	6,300	B	77
124a	35.89839	-111.4022	3.48	4,363	0.02	6,400	B	77
124b	35.8954	-111.4023	3.48	4,361	0.02	6,400	B	77
97	36.1672	-111.3946	70.36	5,273	0.11	6,400	B	77
98	36.1662	-111.3913	0.72	4,183	0.15	15,500	B	77
99	36.1522	-111.3788	0.52	4,228	0.13	15,500	B	77

Table B-1. Input Parameters

Crossing	Crossing coordinates		Basin drainage area (mi^2)	Average basin elevation (feet)	Average basin slope (%)	Basin length (feet)	Hydrologic soil type	Runoff curve No.
	Northing	Easting						
100	36.1333	-111.3568	5.85	4,278	0.07	28,000	D	88
101	36.1205	-111.3423	0.47	6,367	0.03	1,250,000	B/D	82.5
102	36.1198	-111.3410	16.50	4,550	0.03	8,100	D	88
103	35.8348	-111.4366	0.46	4,573	0.02	7,500	D	88
104	35.8253	-111.3890	0.62	4,635	0.03	11,000	D	88
105	35.8173	-111.4411	0.84	4,926	0.04	59,000	D	88
106	35.7252	-111.4825	0.41	4,598	0.02	3,700	D	88
107	35.7059	-111.4949	0.40	5,051	0.02	4,200	D	88
108	35.6436	-111.5171	6.18	5,085	0.03	6,300	D	88
109	35.5831	-111.5290	2.97	5,238	0.05	1,800	D	88
110	35.5579	-111.5345	7.06	5,670	0.10	48,400	B	77
111a	35.4225	-111.5698	6.59	5,582	0.17	33,500	B	77
111b	35.4184	-111.5708	6.51	5,822	0.17	24,800	B	77
112	35.3824	-111.5800	0.20	6,137	0.06	36,500	B	77
125	35.7884	-111.4497	14.76	5,833	0.04	20,800	B	77
126	35.7747	-111.4569	0.20	5,921	0.04	20,500	B	77
127	35.7347	-111.4781	0.30	6,400	0.04	10,500	B	77
128	35.6676	-111.5107	5.48	7,251	0.06	26,000	B/C	81
129	35.5540	-111.5355	1.81	7,258	0.05	26,000	B/C	81
130	35.5184	-111.5433	3.40	7,519	0.10	20,100	B	77
131	35.4658	-111.5586	0.66	7,295	0.05	5,500	B	77
132	35.4031	-111.6081	2.13	7,533	0.19	96,000	B	77
133	35.2257	-111.5596	115.77	4,087	0.12	3,200	D	88

Note: mi^2 = square miles

B.2 NSS Regression Equations

Table B-2 Range of Statistically Significant Basin Characteristics Selected for Use in the Regression Analysis

Region	Drainage area (square miles)	Average basin slope (percent)	Average basin elevation (feet)
Region 8	0.06 to 4,350	0.0231 to 0.4447	4,320 to [1]7,750
Region 11	0.11 to 2,150	0.0177 to 0.1545	--
Region high elevation (elevations greater than 7,500 feet)	1.7 to 1,200	--	--
Region 6	0.18 to 7,220	--	--

[1] Two gaging stations used at average basin elevation above 7500 feet.

Note: -- indicates that characteristic is not statistically significant.

Table B-3 Regional Flood-Frequency Equations Using Generalized Least-Squares Regression

Flood-frequency equations	Recurrence interval (years)	Average standard error of estimates: Regression, Log units	Regression, Percent	Prediction, Log units	Prediction, Percent
Region 8					
$Q2 = 1.08 \times 10^{7} A^{0.457} E^{-1.35}$	2	0.386	110	0.397	116
$Q5 = 1.71 \times 10^{10} A^{0.372} S^{0.360} E^{-1.98}$	5	0.282	72	0.294	76
$Q10 = 8.79 \times 10^{10} A^{0.343} S^{0.395} E^{-2.10}$	10	0.238	59	0.250	63
$Q25 = 3.91 \times 10^{11} A^{0.310} S^{0.432} E^{-2.19}$	25	0.206	50	0.220	54
$Q50 = 8.47 \times 10^{11} A^{0.287} S^{0.460} E^{-2.23}$	50	0.199	48	0.214	52
$Q100 = 1.53 \times 10^{12} A^{0.265} S^{0.477} E^{-2.25}$	100	0.203	49	0.219	54
$Q500 = 4.24 \times 10^{12} A^{0.224} S^{0.513} E^{-2.28}$	500	0.237	59	0.256	64
Region 11					
$Q2 = 3.05 \times 10^{2} A^{0.476} S^{0.608}$	2	0.348	95	0.367	102
$Q5 = 8.44 \times 10^{2} A^{0.471} S^{0.653}$	5	0.278	71	0.296	77
$Q10 = 1.49 \times 10^{3} A^{0.466} S^{0.688}$	10	0.262	66	0.280	72
$Q25 = 2.79 \times 10^{3} A^{0.460} S^{0.730}$	25	0.263	67	0.282	72
$Q50 = 4.19 \times 10^{3} A^{0.455} S^{0.759}$	50	0.274	70	0.295	77
$Q100 = 6.03 \times 10^{3} A^{0.450} S^{0.784}$	100	0.290	75	0.313	83
$Q500 = 1.25 \times 10^{4} A^{0.439} S^{0.836}$	500	0.336	91	0.363	101

Note: Q = peak discharge in cubic feet per second for indicated recurrence interval in years; A = drainage area in square miles; S = average basin slope in percent; E = average basin elevation in feet.

B.4 NOAA Atlas 14 Precipitation-Frequency (24-hour duration)

Table B-4. NOAA Atlas 14 Precipitation-Frequency

Crossing	Precipitation-frequency (inches)		
	2-year	10-year	100-year
1	0.966	1.506	2.413
2	0.967	1.509	2.419
3	1.025	1.59	2.538
5	0.987	1.536	2.46
6	1.007	1.565	2.501
4	1.037	1.605	2.56
7a	0.988	1.538	2.462
7b	0.988	1.538	2.462
8	1.051	1.626	2.592
9	1.086	1.677	2.667
10a	1.098	1.696	2.697
10b	1.098	1.696	2.697
113	1.228	1.901	3.029
114	1.228	1.901	3.028
11a	1.216	1.883	2.997
11b	1.216	1.883	2.997
12	1.216	1.883	2.997
13	1.216	1.883	2.997
14	1.214	1.882	2.996
118	1.276	1.948	3.069
119	1.291	1.973	3.109
15	1.227	1.918	3.07
83	1.344	2.055	3.246
82	1.306	1.995	3.143
81	1.306	1.995	3.143
80	1.282	1.953	3.072
79	1.374	2.1	3.316
78	1.382	2.107	3.313
77	1.423	2.177	3.44
76	1.419	2.171	3.428
75	1.459	2.238	3.546
74	1.425	2.181	3.443

Table B-4. NOAA Atlas 14 Precipitation-Frequency

Crossing	Precipitation-frequency (inches)		
	2-year	10-year	100-year
73	1.425	2.181	3.443
72	1.425	2.181	3.443
71	1.423	2.176	3.436
70	1.423	2.176	3.436
69	1.423	2.176	3.436
68	1.406	2.148	3.387
67	1.406	2.148	3.387
66a	1.444	2.209	3.49
65	1.416	2.165	3.416
66b	1.444	2.209	3.49
64	1.434	2.192	3.46
63b	1.444	2.209	3.49
63a	1.444	2.209	3.49
62	1.434	2.192	3.46
61	1.419	2.168	3.418
60	1.444	2.209	3.487
59	1.463	2.24	3.54
58	1.374	2.088	3.274
57	1.367	2.075	3.252
115	1.214	1.852	2.909
56	1.402	2.139	3.367
55	1.346	2.045	3.207
54	1.346	2.045	3.207
53	1.333	2.022	3.164
52	1.344	2.038	3.185
51	1.338	2.026	3.166
50	1.338	2.026	3.166
49	1.338	2.026	3.166
116	1.335	2.016	3.145
117	1.327	2.006	3.13
48	1.322	1.999	3.119
47	1.311	1.981	3.088
46	1.304	1.969	3.068
45	1.304	1.969	3.068
43	1.304	1.969	3.068
44	1.304	1.969	3.068

Table B-4. NOAA Atlas 14 Precipitation-Frequency

Crossing	Precipitation-frequency (inches)		
	2-year	10-year	100-year
42	1.274	1.919	2.983
41	1.311	1.981	3.088
40	1.304	1.969	3.068
39	1.304	1.969	3.068
38	1.286	1.934	3.004
37	1.231	1.849	2.866
36	1.219	1.832	2.839
35	1.295	1.954	3.041
34	1.238	1.858	2.877
33	1.285	1.935	3.009
32	1.285	1.935	3.009
16	1.263	1.9	2.949
17	1.205	1.804	2.788
18	1.243	1.867	2.894
19	1.243	1.867	2.894
20	1.23	1.84	2.843
21	1.176	1.757	2.706
22	1.136	1.696	2.609
23	1.125	1.677	2.579
24	1.206	1.807	2.793
25	1.206	1.807	2.793
26	1.113	1.658	2.545
27	1.188	1.776	2.742
28	1.188	1.776	2.742
30	1.161	1.734	2.672
31	1.069	1.587	2.424
97	1.171	1.749	2.694
98	1.062	1.577	2.411
99	1.051	1.558	2.379
84	1.073	1.591	2.428
100	1.053	1.559	2.378
85	1.039	1.535	2.334
101	1.027	1.518	2.305
102	1.074	1.598	2.446
120	1.061	1.569	2.389
86	1.1	1.63	2.489

Table B-4. NOAA Atlas 14 Precipitation-Frequency

Crossing	Precipitation-frequency (inches)		
	2-year	10-year	100-year
87	1.032	1.516	2.291
88	1.033	1.515	2.286
89	1.034	1.514	2.28
121	1.057	1.547	2.333
90	1.06	1.542	2.312
91	1.027	1.492	2.226
92	1.029	1.494	2.229
93	1.04	1.509	2.252
122a	1.04	1.509	2.251
123	1.04	1.509	2.251
94	1.158	1.693	2.555
124a	1.048	1.513	2.246
124b	1.05	1.518	2.256
95	1.041	1.505	2.237
96	1.296	1.929	2.966
103	1.085	1.563	2.319
104	1.088	1.567	2.324
105	1.1	1.585	2.352
125	1.173	1.69	2.513
106	1.192	1.717	2.553
107	1.211	1.745	2.596
128	1.241	1.782	2.643
108	1.229	1.764	2.616
109	1.267	1.815	2.683
110	1.361	1.95	2.884
129	1.291	1.845	2.721
131	1.515	2.176	3.232
111a	1.847	2.668	3.992
111b	1.847	2.668	3.992
132	1.929	2.79	4.176
112	1.916	2.77	4.146
133	2.159	3.123	4.672
126	1.123	1.617	2.402
127	1.177	1.696	2.521
130	1.312	1.877	2.771

B.4 Gage Data (Little Colorado River near Cameron, Arizona)

Water-Data Report 2012

09402000 LITTLE COLORADO RIVER NEAR CAMERON, AZ

Little Colorado Basin
Lower Little Colorado Subbasin

LOCATION.--Lat 35°55′35″, long 111°34′00″ referenced to North American Datum of 1927, in NW ¼ sec.5, T.29 N., R.8 E., Coconino County, AZ, Hydrologic Unit 15020016, in Navajo Indian Reservation, on left bank 3 mi downstream from Coconino damsite, 9.5 mi downstream from Moenkopi Wash, 9.5 mi northwest of Cameron, and 45 mi upstream from mouth.(unsurveyed).

DRAINAGE AREA.--26,459 mi² of which 368 mi² probably is noncontributing.

SURFACE-WATER RECORDS

PERIOD OF RECORD.--June 1947 to current year.

REVISED RECORDS.--WDR AZ-03-1: 2002(M). WDR AZ-88-1: Drainage area.

GAGE.--Water-stage recorder. Datum of gage is 3,979.2 ft above sea level.

REMARKS.--Records fair except for estimated daily discharges, which are poor. Diversions above station for irrigation of about 32,000 acres. Some regulation by reservoirs above station (combined capacity of principal reservoirs, about 135,000 acre-ft).

EXTREMES FOR PERIOD OF RECORD.--Maximum discharge, 24,900 ft³/s, Jan. 21, 1952, gage height, 20.7 ft; minimum daily, no flow at times in each year.

EXTREMES OUTSIDE PERIOD OF RECORD.--A discharge of about 120,000 ft³/s occurred on Sept. 19 or 20, 1923, based on discharge at Grand Falls.

EXTREMES FOR CURRENT YEAR.-- Maximum discharge, e5,970 ft³/s, Sep 11, gage height, e10.15 ft; minimum daily discharge, 0.00 ft³/s, on many days.

e, estimated.

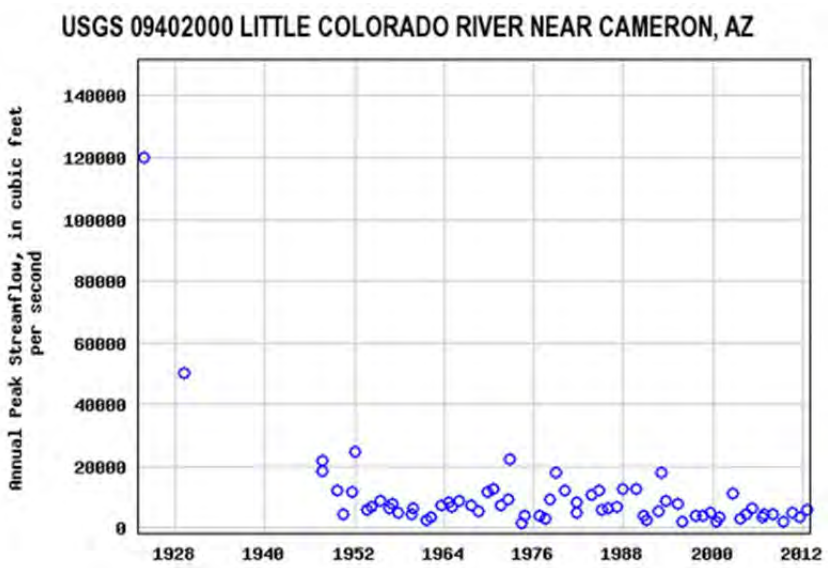

Coconino County, Arizona
Hydrologic Unit Code 15020016
Latitude 35°55'35", Longitude 111°34'00" NAD27
Drainage area 26,459 square miles
Contributing drainage area 26,091 square miles
Gage datum 3,979.20 feet above NGVD29

Output formats

- Table
- Graph
- Tab-separated file
- peakfq (watstore) format
- Reselect output format

Water Year	Date	Gage Height (feet)	Stream-flow (cfs)
1923	Sep. 20, 1923		120,000[2,7]
1929	Apr. 06, 1929		50,000[2,7]
1947	Aug. 09, 1947	19.60	21,900
1948	Oct. 14, 1947	17.90	18,600
1949	Aug. 09, 1949	14.35	12,400
1950	Jul. 18, 1950	8.93	4,340
1951	Aug. 30, 1951	14.00	11,700
1952	Jan. 21, 1952	20.70	24,900
1953	Jul. 30, 1953	10.30	6,230
1954	Mar. 25, 1954	11.00	7,070
1955	Jun. 13, 1955	12.30	8,990
1956	Aug. 17, 1956	10.65	6,650
1957	Jan. 12, 1957	11.42	8,060
1958	Oct. 14, 1957	9.17	4,840
1959	Aug. 07, 1959	9.30	4,600
1960	Nov. 02, 1959	10.67	6,620
1961	Sep. 09, 1961	7.03	2,600
1962	Feb. 17, 1962	7.94	3,470
1963	Sep. 01, 1963	11.43	7,680
1964	Aug. 02, 1964	11.93	8,540
1965	Jan. 11, 1965	10.43	6,770[5]
1966	Jan. 03, 1966	12.10	9,100[5]
1967	Sep. 08, 1967	11.36	7,580[5]
1968	Aug. 12, 1968	9.91	5,600[5]
1969	Sep. 11, 1969	14.00	11,600[5]
1970	Sep. 07, 1970	14.54	12,600[5]
1971	Aug. 27, 1971	11.25	7,290[5]
1972	Jul. 18, 1972	12.50	9,250[5]
1973	Oct. 19, 1972	19.67	22,400[5]
1974	1974	6.00	1,590[5,B]
1975	Nov. 01, 1974	8.65	4,100[5]
1976	Sep. 25, 1976	8.30	3,870[5]
1977	Aug. 20, 1977	7.80	3,300[5]
1978	Mar. 06, 1978	12.50	9,540[5]
1979	Dec. 23, 1978	17.36	17,800[5]
1980	Feb. 20, 1980	14.45	12,400[5]
1981	Sep. 23, 1981	9.30	5,100[5]
1982	Oct. 02, 1981	11.70	8,320[5]
1983	Sep. 30, 1983	13.30	10,600[5]
1984	Aug. 26, 1984	14.62	12,400[5]
1985	Mar. 16, 1985	10.22	6,030[5]
1986	Nov. 30, 1985	10.62	6,530[5]
1987	Jan. 30, 1987	10.77	6,730[5]
1988	Nov. 01, 1987	14.74	12,600[5]
1989	Aug. 19, 1989	14.85	12,800[5]
1990	Sep. 24, 1990	8.58	4,140[5]
1991	Jan. 07, 1991	7.19	2,690[5]
1992	Sep. 19, 1992	9.88	5,620[5]
1993	Jan. 12, 1993	17.83	18,200[5]
1994	Oct. 06, 1993	12.42	8,820[5]
1995	Mar. 10, 1995	11.50	7,700[5]
1996	Nov. 01, 1995	6.64	2,180[5]
1997	Sep. 13, 1997	8.67	4,230[5]
1998	Sep. 11, 1998	8.31	3,850[5]
1999	Sep. 11, 1999	9.29	4,930[5]
2000	Jun. 18, 2000	6.57	2,120[5]
2001	Oct. 22, 2000	7.89	3,420[5]
2002	Sep. 11, 2002	13.99	11,500[5]
2003	Sep. 10, 2003	7.81	3,340[5]
2004	Jul. 15, 2004	9.14	4,760[5]
2005	Feb. 24, 2005	10.60	6,540[5]
2006	Sep. 15, 2006	8.04	3,570[5]
2007	Oct. 06, 2006	8.79	4,370[5]
2008	Feb. 03, 2008	8.85	4,430[5]
2009	May 23, 2009	6.44	2,000[5]
2010	Aug. 07, 2010	9.36	5,010[5]
2011	Sep. 14, 2011	8.20	3,740[5]
2012	Sep. 11, 2012	10.15[5]	5,970[2,5]

B.5 Emfreq Input and Output Text Files

```
'Little Colorado at Cameron'
'USGS Gage Station'
number of thresholds/bounds
0
ns   gage start year
68      1923
alpha  reg skew   reg mse   low outlier threshold parameter
0.4      0.93        0.0            -1.0
number of discharges to estimate annual probabilities
1
list of discharges
1000
year    Qest   tl         tu
1923   120000         114000         126000
1929   50000 47500 52500
1947   21900 21900 21900
1948   18600 18600 18600
1949   12400 12400 12400
1950   4340   4340   4340
1951   11700 11700 11700
1952   24900 24900 24900
1953   6230   6230   6230
1954   7070   7070   7070
1955   8990   8990   8990
1956   6650   6650   6650
1957   8060   8060   8060
1958   4840   4840   4840
1959   4600   4600   4600
1960   6620   6620   6620
1961   2600   2600   2600
1962   3470   3470   3470
1963   7680   7680   7680
1964   8540   8540   8540
1965   6770   6770   6770
1966   9100   9100   9100
1967   7580   7580   7580
1968   5600   5600   5600
1969   11600 11600 11600
1970   12600 12600 12600
1971   7290   7290   7290
1972   9250   9250   9250
1973   22400 22400 22400
1974   1590   1590   1590
1975   4100   4100   4100
1976   3870   3870   3870
1977   3300   3300   3300
1978   9540   9540   9540
1979   17800 17800 17800
1980   12400 12400 12400
1981   5100   5100   5100
1982   8320   8320   8320
1983   10600 10600 10600
1984   12400 12400 12400
1985   6030   6030   6030
1986   6530   6530   6530
1987   6730   6730   6730
1988   12600 12600 12600
1989   12800 12800 12800
1990   4140   4140   4140
1991   2690   2690   2690
1992   5620   5620   5620
1993   18200 18200 18200
1994   8820   8820   8820
1995   7700   7700   7700
1996   2180   2180   2180
1997   4230   4230   4230
```

```
1998   3850   3850   3850
1999   4930   4930   4930
2000   2120   2120   2120
2001   3420   3420   3420
2002   11500 11500 11500
2003   3340   3340   3340
2004   4760   4760   4760
2005   6540   6540   6540
2006   3570   3570   3570
2007   4370   4370   4370
2008   4430   4430   4430
2009   2000   2000   2000
2010   5010   5010   5010
2011   3740   3740   3740
2012   5970   5970   5970


    ***************************************************
    *              PROGRAM EMFREQ                     *
    *      EXPECTED MOMENTS FREQUENCY ANALYSIS        *
    *                                                 *
    *     COMPUTES EXCEEDANCE PROBABILITIES AND       *
    * RETURN PERIOD ESTIMATES VIA PLOTTING POSITIONS, *
    *                                                 *
    * AND COMPUTES MOMENTS, PARAMETERS, AND QUANTILES *
    *        ASSUMING A  LP-III DISTRIBUTION          *
    *         FOR  HISTORICAL, PALEOFLOOD             *
    *      AND SYSTEMATIC (GAGE) PEAK FLOW DATA       *
    *   WITH REGIONAL SKEW AND CONFIDENCE INTERVALS   *
    *                                                 *
    *       BUREAU OF RECLAMATION, DENVER, CO         *
    *            EMFREQ  VERSION  1.20                *
    *           VERSION DATE: 09-NOV-2007             *
    ***************************************************


  EMFREQ Program Input File Name is:          LC.in
  EMFREQ Program Output File Name is:         LC.out
  EMFREQ Program Spreadsheet File Name is:    LC.csv
  EMFREQ Program Error File Name is:          LC.err


  EMFREQ Run Date is:   5/06/2013
  EMFREQ Run Time is:  12:36:17 pm

    'Little Colorado at Cameron'
    'USGS Gage Station'


            INPUT AND CALCULATED CONSTANTS

 Number of User-Input Thresholds/Bounds is:    0

 No Censoring Thresholds/Bounds Entered; Only Systematic (Gage) Record Used

    ns  Gage (systematic) Start Year
    68           1923

    Alpha   reg_skew  reg_mse     gbthresh_in  log10 gbthresh
    0.400      0.930     0.000          -1.0000    -6.00000

  EMFREQ utilizes
  the log-Pearson Type III distribution
  with Base 10 logarithms

  User has selected the Cunnane plotting position
  for estimating exceedance probabilities
  and relative goodness-of-fit
```

Generalized/Regional Skew Coefficient Option
Generalized skew is used with NO skew uncertainty;
NO at-site skew coefficient is used
regional mean square error utilized is: 0.000

Low Outlier Testing/Adjustment Method
An iterative Grubbs-Beck Test will be used
to determine low outlier critical values
and modify any low outliers detected

Input number of floods to estimate
exceedance probabilities is: 1
Input Flood Values
1000.00

INPUT YEAR AND DISCHARGE VALUES FOR PLOTTING

Year	Discharge	Ql	Qu
1923	120000.00	114000.00	126000.00
1929	50000.00	47500.00	52500.00
1947	21900.00	21900.00	21900.00
1948	18600.00	18600.00	18600.00
1949	12400.00	12400.00	12400.00
1950	4340.00	4340.00	4340.00
1951	11700.00	11700.00	11700.00
1952	24900.00	24900.00	24900.00
1953	6230.00	6230.00	6230.00
1954	7070.00	7070.00	7070.00
1955	8990.00	8990.00	8990.00
1956	6650.00	6650.00	6650.00
1957	8060.00	8060.00	8060.00
1958	4840.00	4840.00	4840.00
1959	4600.00	4600.00	4600.00
1960	6620.00	6620.00	6620.00
1961	2600.00	2600.00	2600.00
1962	3470.00	3470.00	3470.00
1963	7680.00	7680.00	7680.00
1964	8540.00	8540.00	8540.00
1965	6770.00	6770.00	6770.00
1966	9100.00	9100.00	9100.00
1967	7580.00	7580.00	7580.00
1968	5600.00	5600.00	5600.00
1969	11600.00	11600.00	11600.00
1970	12600.00	12600.00	12600.00
1971	7290.00	7290.00	7290.00
1972	9250.00	9250.00	9250.00
1973	22400.00	22400.00	22400.00
1974	1590.00	1590.00	1590.00
1975	4100.00	4100.00	4100.00
1976	3870.00	3870.00	3870.00
1977	3300.00	3300.00	3300.00
1978	9540.00	9540.00	9540.00
1979	17800.00	17800.00	17800.00
1980	12400.00	12400.00	12400.00
1981	5100.00	5100.00	5100.00
1982	8320.00	8320.00	8320.00
1983	10600.00	10600.00	10600.00
1984	12400.00	12400.00	12400.00
1985	6030.00	6030.00	6030.00
1986	6530.00	6530.00	6530.00
1987	6730.00	6730.00	6730.00
1988	12600.00	12600.00	12600.00
1989	12800.00	12800.00	12800.00
1990	4140.00	4140.00	4140.00
1991	2690.00	2690.00	2690.00
1992	5620.00	5620.00	5620.00
1993	18200.00	18200.00	18200.00
1994	8820.00	8820.00	8820.00

1995	7700.00	7700.00	7700.00
1996	2180.00	2180.00	2180.00
1997	4230.00	4230.00	4230.00
1998	3850.00	3850.00	3850.00
1999	4930.00	4930.00	4930.00
2000	2120.00	2120.00	2120.00
2001	3420.00	3420.00	3420.00
2002	11500.00	11500.00	11500.00
2003	3340.00	3340.00	3340.00
2004	4760.00	4760.00	4760.00
2005	6540.00	6540.00	6540.00
2006	3570.00	3570.00	3570.00
2007	4370.00	4370.00	4370.00
2008	4430.00	4430.00	4430.00
2009	2000.00	2000.00	2000.00
2010	5010.00	5010.00	5010.00
2011	3740.00	3740.00	3740.00
2012	5970.00	5970.00	5970.00

ns	ne	nqt	nfb_sum	kk_sum	n_qmax
68	0	68	68	0	68

Initial Plotting Positions Before Any Low Outlier Calculations and Adjustments

SORTED DISCHARGE VALUES, CALCULATED EXCEEDANCE PROBABILITIES
AND RETURN PERIOD ESTIMATES

i	Year	Discharge	Exceed. Prob. P (%)	Rt. Per. T	Std. Nor. Var.
1	1923	120000.00	0.8798	113.6667	2.37403
2	1929	50000.00	2.3460	42.6250	1.98701
3	1952	24900.00	3.8123	26.2308	1.77289
4	1973	22400.00	5.2786	18.9444	1.61842
5	1947	21900.00	6.7449	14.8261	1.49507
6	1948	18600.00	8.2111	12.1786	1.39101
7	1993	18200.00	9.6774	10.3333	1.30015
8	1979	17800.00	11.1437	8.9737	1.21892
9	1989	12800.00	12.6100	7.9302	1.14502
10	1988	12600.00	14.0762	7.1042	1.07690
11	1970	12600.00	15.5425	6.4340	1.01344
12	1984	12400.00	17.0088	5.8793	0.95382
13	1980	12400.00	18.4751	5.4127	0.89741
14	1949	12400.00	19.9413	5.0147	0.84372
15	1951	11700.00	21.4076	4.6712	0.79236
16	1969	11600.00	22.8739	4.3718	0.74301
17	2002	11500.00	24.3402	4.1084	0.69540
18	1983	10600.00	25.8065	3.8750	0.64932
19	1978	9540.00	27.2727	3.6667	0.60459
20	1972	9250.00	28.7390	3.4796	0.56103
21	1966	9100.00	30.2053	3.3107	0.51851
22	1955	8990.00	31.6716	3.1574	0.47690
23	1994	8820.00	33.1378	3.0177	0.43611
24	1964	8540.00	34.6041	2.8898	0.39603
25	1982	8320.00	36.0704	2.7724	0.35658
26	1957	8060.00	37.5367	2.6641	0.31767
27	1995	7700.00	39.0029	2.5639	0.27924
28	1963	7680.00	40.4692	2.4710	0.24122
29	1967	7580.00	41.9355	2.3846	0.20354
30	1971	7290.00	43.4018	2.3041	0.16615
31	1954	7070.00	44.8680	2.2288	0.12900
32	1965	6770.00	46.3343	2.1582	0.09201
33	1987	6730.00	47.8006	2.0920	0.05516
34	1956	6650.00	49.2669	2.0298	0.01838
35	1960	6620.00	50.7331	1.9711	-0.01838
36	2005	6540.00	52.1994	1.9157	-0.05516
37	1986	6530.00	53.6657	1.8634	-0.09201
38	1953	6230.00	55.1320	1.8138	-0.12900
39	1985	6030.00	56.5982	1.7668	-0.16615
40	2012	5970.00	58.0645	1.7222	-0.20354
41	1992	5620.00	59.5308	1.6798	-0.24122

42	1968	5600.00	60.9971	1.6394	-0.27924
43	1981	5100.00	62.4633	1.6009	-0.31767
44	2010	5010.00	63.9296	1.5642	-0.35658
45	1999	4930.00	65.3959	1.5291	-0.39603
46	1958	4840.00	66.8622	1.4956	-0.43611
47	2004	4760.00	68.3284	1.4635	-0.47690
48	1959	4600.00	69.7947	1.4328	-0.51851
49	2008	4430.00	71.2610	1.4033	-0.56103
50	2007	4370.00	72.7273	1.3750	-0.60459
51	1950	4340.00	74.1935	1.3478	-0.64932
52	1997	4230.00	75.6598	1.3217	-0.69540
53	1990	4140.00	77.1261	1.2966	-0.74301
54	1975	4100.00	78.5924	1.2724	-0.79236
55	1976	3870.00	80.0587	1.2491	-0.84372
56	1998	3850.00	81.5249	1.2266	-0.89741
57	2011	3740.00	82.9912	1.2049	-0.95382
58	2006	3570.00	84.4575	1.1840	-1.01344
59	1962	3470.00	85.9238	1.1638	-1.07690
60	2001	3420.00	87.3900	1.1443	-1.14502
61	2003	3340.00	88.8563	1.1254	-1.21892
62	1977	3300.00	90.3226	1.1071	-1.30015
63	1991	2690.00	91.7889	1.0895	-1.39101
64	1961	2600.00	93.2551	1.0723	-1.49507
65	1996	2180.00	94.7214	1.0557	-1.61842
66	2000	2120.00	96.1877	1.0396	-1.77289
67	2009	2000.00	97.6540	1.0240	-1.98701
68	1974	1590.00	99.1202	1.0089	-2.37403

Flood Frequency Computation Results
Based on EMA Estimation

Grubbs-Beck Low Outlier Test Results
Iterative Grubbs-Beck Test used

Iteration No.	No. Low Outliers	Critical Value	Threshold Value
1	0	835.0	1590.0

Final number of low outliers censored = 0
Final critical value = 835.0
Final threshold value = 1590.0

Final EMA Estimated LP-III Moments
(Log-10 Moments)

At-Site only with no regional skew weighting

Mean	Variance	Std. Dev	Skew	At-Site MSE
3.845436	0.103485	0.321691	0.929989	0.223330

Final Weighted Moments (at-site with regional skew)

Mean	Variance	Std. Dev	Skew
3.845436	0.103485	0.321691	0.930000

The user chose regional skew = 0.9300 and regional mse = 0.000
The Final EMA Moments listed above INCLUDE this regional skew weighting

Final EMA LP-III Parameters

Location (Tau)	Shape (Alpha)	Scale (Beta)
3.153628	4.624812	0.149586

Final EMA LP-III Frequency Curve and 90% Confidence Interval

CDF	Return Period T	Standard Normal	Model Q	Lower 5% Conf. Limit	Upper 95% Conf. Limit
0.005000	1.005	-2.575829	1954.55	1460.59	2404.07

0.010000	1.010	-2.326348	2081.52	1577.43	2540.15
0.050000	1.053	-1.644854	2592.16	2056.18	3087.60
0.100000	1.111	-1.281552	3007.96	2451.50	3538.34
0.200000	1.250	-0.841621	3722.68	3128.66	4336.59
0.333333	1.500	-0.430727	4705.68	4030.29	5505.09
0.500000	2.000	0.000000	6255.53	5355.21	7530.34
0.570800	2.330	0.178411	7125.32	6054.16	8753.32
0.800000	5.000	0.841621	12351.96	9875.83	17016.42
0.900000	10.000	1.281552	18893.89	14192.29	28877.87
0.960000	25.000	1.750686	31415.12	21753.51	54735.21
0.980000	50.000	2.053749	45012.72	29360.88	86231.14
0.990000	100.000	2.326348	63550.41	39104.93	133471.68
0.995000	200.000	2.575829	88721.65	51567.61	203804.55
0.998000	500.000	2.878162	136085.87	73475.63	350876.90
0.999000	1000.000	3.090232	186579.63	95375.69	524017.97
0.999500	2000.000	3.290527	254364.95	123201.20	777139.84
0.999800	5000.000	3.540084	380382.33	171741.91	1296677.55
0.999900	10000.000	3.719016	513323.80	219923.64	1898856.24
0.999950	20000.000	3.890592	690320.53	280790.40	2768642.47
0.999980	50000.000	4.107480	1016506.25	386313.89	4531504.38
0.999990	100000.000	4.264891	1357984.08	490473.77	6552732.36
0.999995	200000.000	4.417173	1809874.79	621471.35	9447362.34
0.999998	500000.000	4.611382	2637223.79	847477.45	15260578.81
0.999999	1000000.000	4.753424	3498329.94	1069585.86	21872476.62

RELATIVE GOODNESS-OF-FIT

i	Exceed. Prob	Q Observed	Q Estimated	Relative Difference
1	0.0087977	120000.00	67644.18	-0.4363
2	0.0234604	50000.00	41496.70	-0.1701
3	0.0381232	24900.00	32226.96	0.2943
4	0.0527859	22400.00	27060.06	0.2080
5	0.0674487	21900.00	23642.91	0.0796
6	0.0821114	18600.00	21163.97	0.1378
7	0.0967742	18200.00	19257.52	0.0581
8	0.1114370	17800.00	17730.99	-0.0039
9	0.1260997	12800.00	16471.94	0.2869
10	0.1407625	12600.00	15409.71	0.2230
11	0.1554252	12600.00	14497.30	0.1506
12	0.1700880	12400.00	13702.10	0.1050
13	0.1847507	12400.00	13000.65	0.0484
14	0.1994135	12400.00	12375.57	-0.0020
15	0.2140762	11700.00	11813.71	0.0097
16	0.2287390	11600.00	11304.85	-0.0254
17	0.2434018	11500.00	10840.96	-0.0573
18	0.2580645	10600.00	10415.62	-0.0174
19	0.2727273	9540.00	10023.60	0.0507
20	0.2873900	9250.00	9660.63	0.0444
21	0.3020528	9100.00	9323.14	0.0245
22	0.3167155	8990.00	9008.16	0.0020
23	0.3313783	8820.00	8713.17	-0.0121
24	0.3460411	8540.00	8436.03	-0.0122
25	0.3607038	8320.00	8174.89	-0.0174
26	0.3753666	8060.00	7928.17	-0.0164
27	0.3900293	7700.00	7694.48	-0.0007
28	0.4046921	7680.00	7472.61	-0.0270
29	0.4193548	7580.00	7261.50	-0.0420
30	0.4340176	7290.00	7060.21	-0.0315
31	0.4486804	7070.00	6867.90	-0.0286
32	0.4633431	6770.00	6683.84	-0.0127
33	0.4780059	6730.00	6507.35	-0.0331
34	0.4926686	6650.00	6337.84	-0.0469
35	0.5073314	6620.00	6174.76	-0.0673
36	0.5219941	6540.00	6017.62	-0.0799
37	0.5366569	6530.00	5865.98	-0.1017
38	0.5513196	6230.00	5719.42	-0.0820
39	0.5659824	6030.00	5577.58	-0.0750
40	0.5806452	5970.00	5440.09	-0.0888
41	0.5953079	5620.00	5306.65	-0.0558

42	0.6099707	5600.00	5176.95	-0.0755
43	0.6246334	5100.00	5050.71	-0.0097
44	0.6392962	5010.00	4927.67	-0.0164
45	0.6539589	4930.00	4807.57	-0.0248
46	0.6686217	4840.00	4690.18	-0.0310
47	0.6832845	4760.00	4575.26	-0.0388
48	0.6979472	4600.00	4462.61	-0.0299
49	0.7126100	4430.00	4351.98	-0.0176
50	0.7272727	4370.00	4243.18	-0.0290
51	0.7419355	4340.00	4135.97	-0.0470
52	0.7565982	4230.00	4030.15	-0.0472
53	0.7712610	4140.00	3925.47	-0.0518
54	0.7859238	4100.00	3821.69	-0.0679
55	0.8005865	3870.00	3718.56	-0.0391
56	0.8152493	3850.00	3615.79	-0.0608
57	0.8299120	3740.00	3513.04	-0.0607
58	0.8445748	3570.00	3409.95	-0.0448
59	0.8592375	3470.00	3306.08	-0.0472
60	0.8739003	3420.00	3200.86	-0.0641
61	0.8885630	3340.00	3093.61	-0.0738
62	0.9032258	3300.00	2983.40	-0.0959
63	0.9178886	2690.00	2868.92	0.0665
64	0.9325513	2600.00	2748.26	0.0570
65	0.9472141	2180.00	2618.30	0.2011
66	0.9618768	2120.00	2473.33	0.1667
67	0.9765396	2000.00	2300.59	0.1503
68	0.9912023	1590.00	2055.25	0.2926

GOODNESS-OF-FIT
Via Average Relative Deviations (ARD) and Mean Squared Deviations (MSD)

Number of observations: 68
Number of observations that exceed any threshold/bound: 0

All Observations

ARD	MSD
0.0761	0.0125

Maximum Observed

ARD_Q1	MSD_Q1
0.4363	0.1904

ESTIMATED EXCEEDANCE PROBABILITIES FROM FITTED DISTRIBUTION

i	Input Q	Exceed Prob P (%)	T
1	1000.00	100.00000000	1.000

EMFREQ Program Run time: 0.172 seconds

B.6 Alternative Little Colorado Peak Annual Streamflow Analysis

These results are shown for comparison purposes only. The more conservative results, which includes all peak annual streamflow gage data currently available, are recommended for use as peak discharge estimates at the Little Colorado River crossing.

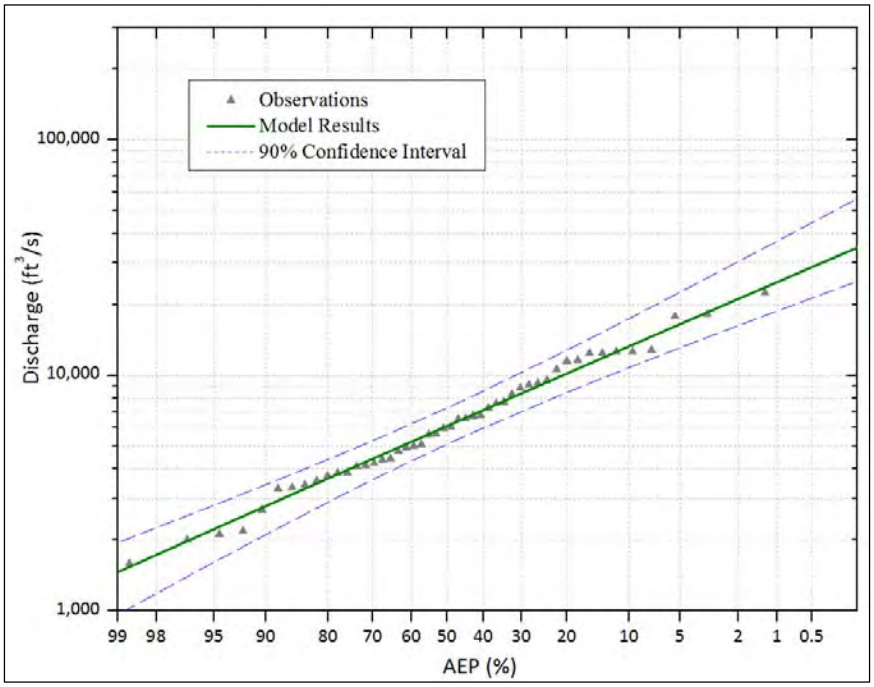

Figure B-1. Alternative (1965-present gage data only). Peak annual streamflow analysis, Little Colorado River near Cameron, Arizona.

Table B-5. Alternative (1965 - present gage data only) Peak Discharge Estimates for Peak Annual Streamflow Analysis (Little Colorado River near Cameron, Arizona)

AEP	Return period	[1]Peak discharge (ft^3/s)		
		Best estimate	5% confidence limit	95% confidence limit
0.5	2	6,100	5,100	7,300
0.2	5	10,200	8,500	12,800
0.1	10	13,300	10,800	17,400
0.04	25	17,600	13,900	24,400
0.02	50	21,100	16,300	30,400
0.01	100	24,900	18,700	37,100
0.005	200	28,800	21,300	44,500
0.002	500	34,500	24,900	55,600

[1] Peak discharge values rounded to the nearest 100 ft^3/s.
Note: ft3/s – cubic feet per second.

Appendix C

Geomorphology

C.1 Aerial Photo Review for Lateral Stability (1950-1980)

Point no.	1951 index	1953 index	1975 index	1977 index	1980 index
1					
2					
3					
4					
5					
6					
7					
8					
9					
10					
11					
12					
13	AR1QZ0000150156				
14					
15					
16		AR1VAX000010128			
17					
18		AR1VAX000010128			
19					
20		AR1VAX000010128			
21		AR1VAX000010128	AR1VDWG00010056 (blurry)		NB1NHAP800048018 (blurry)
22					
23					
24					
25					
26		AR1VAX000010138			
27					
28					
29					
30					
31		AR1VAX000010140			
32		AR1VAX000010128			
33		AR1VAX000010128			
34					
35					

Point no.	1951 index	1953 index	1975 index	1977 index	1980 index
36					
37					
38	AR1QZ0000150145-blurry				
39					
40					
41					
42					
43					
44					
45					
46					
47					
48					
49					
50		AR1VAX000010083			
51		AR1VAX000010083			
52		ARVAX000010083			
53					
54					
55	AR1QZ0000150117--hard to see				
56	AR1QZ0000150117--hard to see				
57	AR1QZ0000150148				
58	AR1QZ0000150118				
59	AR1QZ0000150117--hard to see				
60					
unmarked	AR1QZ0000150117--hard to see				
61	AR1QZ0000150117--hard to see				
62					
63	AR1QZ0000150117--hard to see				
64	AR1QZ0000150117--hard to see				
65					
66					
unmarked	AR1QZ0000150117--hard to see				
67					
68					
69					
70	AR1QZ0000150047				
71					
72					
73					
74					
75	AR1QZ0000150116				
76					

Point no.	1951 index	1953 index	1975 index	1977 index	1980 index
77	AR1QZ0000150114 (blurry)			AR1VELE00020113 (washed out)	
78	AR1QZ0000150116 (blurry)				
79	AR1QZ0000150114 (blurry)				
80					
81					
82					
83					
84		AR1VAX000010140			
85					
86		AR1VAX000010142			
87					
88					
89					
90		AR1VAX000010144			
91					
92		AR1VAX000010144			
93					
94		AR1VAX000010146			
95		AR1VAX000010148			
96		AR1VAX000010150	none		NC1NHAP800061037; NC1NHAP800059243
97		AR1VAX000010140			
98		AR1VAX000010140			
99					
100					
101					
102					
103		AR1VAX000010152?			
104		AR1VAX000010152?			
105					
106					
107					
108					
109					
110					
111					
112					
113					
114					
115					
116					
117					
118					

Point no.	1951 index	1953 index	1975 index	1977 index	1980 index
119					
120					
121					
122					
123					
124					
125		AR1VAX000010152			
126					
127					
128					
129					
130					
131					
132					
133					

COLOR CODE: certainty of data evaluation

High	visited crossing and detailed site description
Moderate	visited crossing in field with no detailed site description
Low	did not visit crossing in field

Appendix D

Scour

D.1 Bend Scour Equations

Note: The information in appendix D is preliminary only and based on an early draft from the Bank Stabilization Guidelines (Reclamation, 2013).[1]

A bend in a channel will induce transverse or "secondary" currents that scour sediment from the outside of a bend and cause it to be deposited along the inside of the bend. The following four methods to predict the depth of scour in a river bend were developed after methods presented in Neil (1973) and Pemberton and Lara (1984).

D.1.1 Zeller Bend Scour Equation

[Reference: Simons, Li & Associates, 1985]

(Equation D-1) $y_{bs} = 0.0685 y_{max} V^{0.8} / (y_h^{0.4} S_e^{0.3}) * [(2.1(\sin^2 (\alpha/2) / \cos \alpha)^{0.2} - 1)]$

Where:

- y_{bs} = Zeller depth of bend scour (ft^2),[2] measured below minimum channel elevation
- y_{max} = Maximum depth of upstream flow (ft)
- y_h = Hydraulic depth of upstream flow (ft)
- V = Mean velocity of upstream flow (ft/s)
- S_e = Upstream energy slope (ft/ft)
- = Angle formed by projection of channel centerline from point of curvature (P.C.) to a point which meets a line tangent to the outer bank of channel (degrees)
- r_c = Radius of curvature to centerline of channel (ft)
- W = Channel top width of upstream flow (ft)
- α = Angle formed by projection of channel centerline from P.C. to a point which meets a line tangent to the outer bank of channel (degrees)

Note the term with the α coefficients. Rather than determine the angle α, the entire $\sin^2(\alpha/2)/\cos \alpha$ term can be determined using the following formula:

(Equation D.2) $\sin^2(\alpha/2)/\cos \alpha = W / (4 r_c)$

---

[1] Complete information for references can be found in the "References" section of the main report.
[2] Measurements used in this appendix are as follows: ft = feet, ft/s = feet per second, ft/ft = feet per foot, ft^2/s = square feet per second, ft^3/s = cubic feet per second, $ft^3/s/ft$ = cubic feet per second per foot, lb/ft^2 = pounds per square foot, lb/ft^3 = pounds per cubic foot

The longitudinal extent of the bend scour component is difficult to quantify. The Rozovskii (1961) equation can be used for predicting the distance from the end of a bend to where the secondary currents will be a minimum.

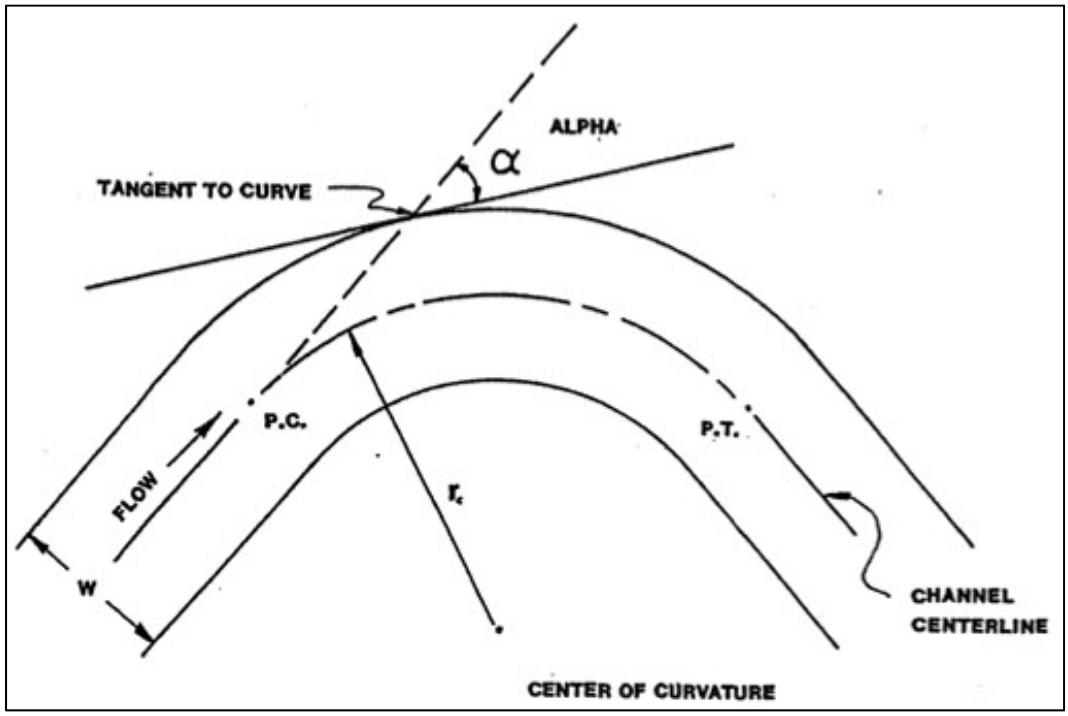

Figure D-1. Illustration of terminology for bend scour (Simons, Li & Associates, 1985, figure 5.25).

As a conservative estimate of the longitudinal extent of bend scour, both upstream and downstream of the curve, assume it extends a distance X upstream of the P.C. and a minimum of X downstream of the P.T. The following is a modified version of the Rozovskii (1961) equation to estimate distance X:

(Equation D.3) $X = 2.3\,(C/g^{1/2})\,y$
$= (0.6\,y^{1.17}) / n$

Where:

- α = Distance from the end of channel curvature (point of tangency [P.T.]) to the downstream point at which secondary currents have dissipated (ft)
- C = Chezy coefficient = $(1.486/n)\,R^{1/6}$
- g = Gravitational acceleration (32.17 ft^2/s)
- y = Depth of flow: use the maximum flow depth, exclusive of scour within the bend (ft)
- n = Manning's roughness coefficient

Notes:

Zeller's equation estimates the maximum scour in sand bed channels.
The equation is based on the assumption of constant stream power through the channel bend.

D.1.2 Maynord Bend Scour Equation

[Reference: Maynord, 1996]

(Equation D-4) $y_{mxb} = y_u * (1.8 - 0.051 (r_c / W_u) + 0.0084 (W_u / y_u))$

(Equation D-5) $y_{bs} = y_{mxb} - y_u$

Where:

y_{mxb}	=	Maximum water depth in the bend (ft)
y_u	=	Average water depth in the crossing upstream of bend (ft)
y_{bs}	=	Depth of bend scour below thalweg (ft)
r_c	=	Centerline radius of bend (ft)
W_u	=	Water surface width at upstream end of bend (ft)

Notes:

No safety factor incorporated into this equation. A safety factor of 1.08 is recommended.

The equation is limited to: $r_c / W_u < 10$ and $W_u / y_u < 125$
If $r_c / W_u < 10$, then $r_c / W_u = 1.5$ recommended
If $W_u / y_u < 125$, then $r_c / W_u = 20$ recommended

Not recommended where there is significant overbank flow. Limited to overbank depths of less than 20 percent of main channel depth.

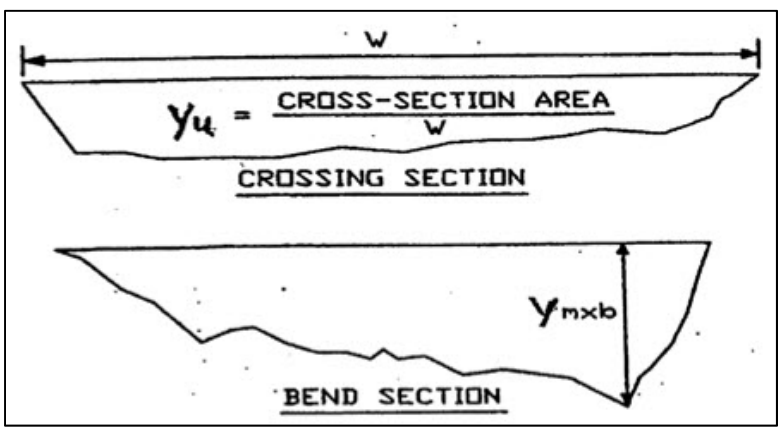

Figure D-2. Definition sketch for bend scour (Maynord, 1996).

D.1.3 Thorne Bend Scour Equation

[Reference: Thorne, et al., 1995]

(Equation D-6) $y_{max} / y_u = 2.07 - 0.19 * \log_{10}(r_c / W_u - 2)$
(Equation D-7) $y_{bs} = y_{max} - y_u$

Where:

y_{max} = Maximum water depth in the bend (ft)
y_u = Average depth in the crossing upstream of bend (ft)
y_{bs} = Depth of bend scour below thalweg (ft)
r_c = Centerline radius of bend (ft)
W_u = Water surface width at upstream end of bend (ft)

Notes:

The equation is limited to $rc / W_u > 2$.

D.1.4 Corps of Engineers Bend Scour

[Reference: USACE, 1994b]

Scour in bends is determined from design curves found in Plate B-42 of the USACE manual. These are designated as safe design curves because they fall on the conservative side of the data. They are based on the ratio of maximum water depth in the bend to the mean water depth in the approach channel. Note that the maximum depth in the bend ranges from about 1.5 to 3.5 times the mean depth in the approach channel. Figure D-3 represents the upper limit for channels with irregular alignment – use 10-percent reduction from the bend scour design curve for relatively smooth alignment.

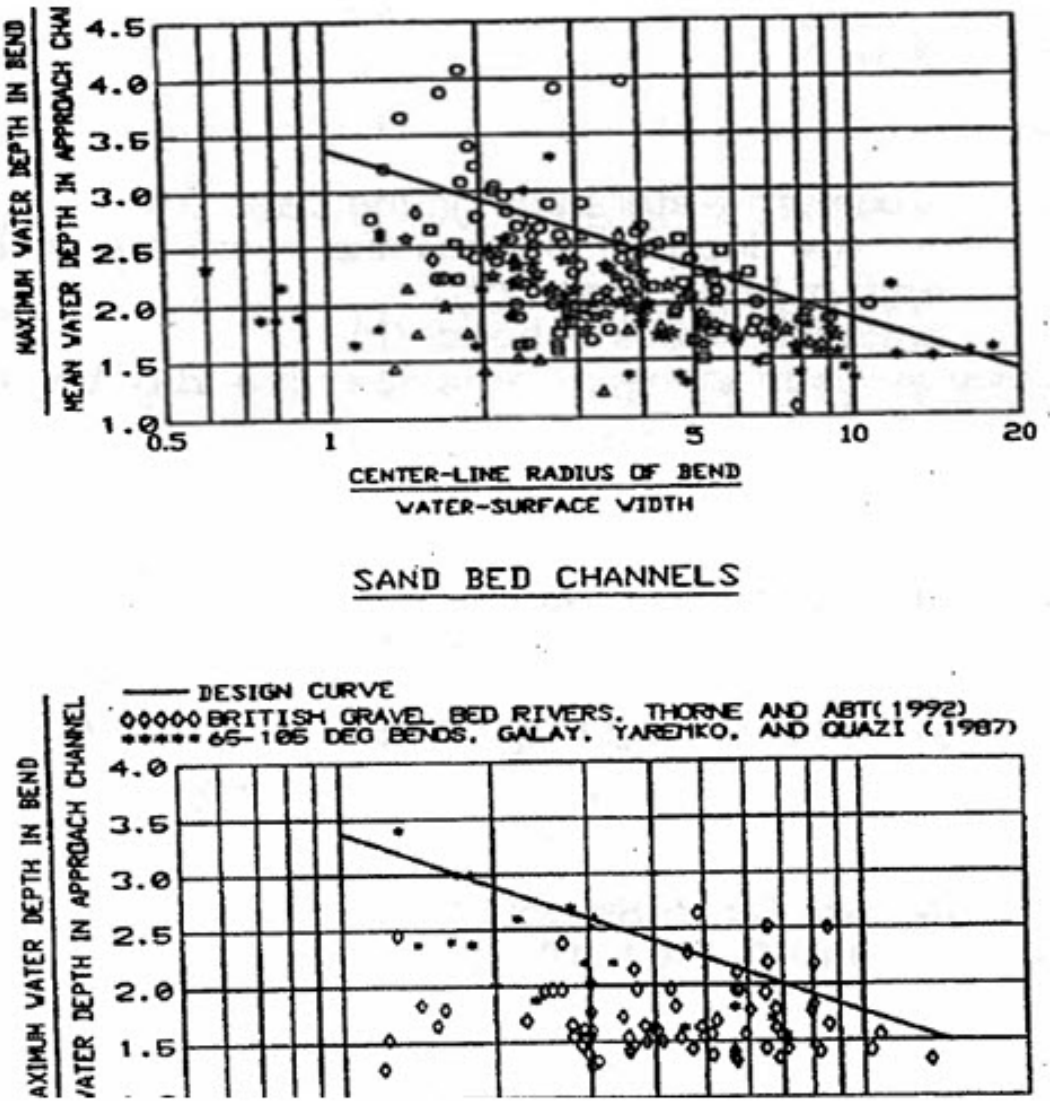

Figure D-3. Scour depth in bends (USACE, 1994b; plate B-42).

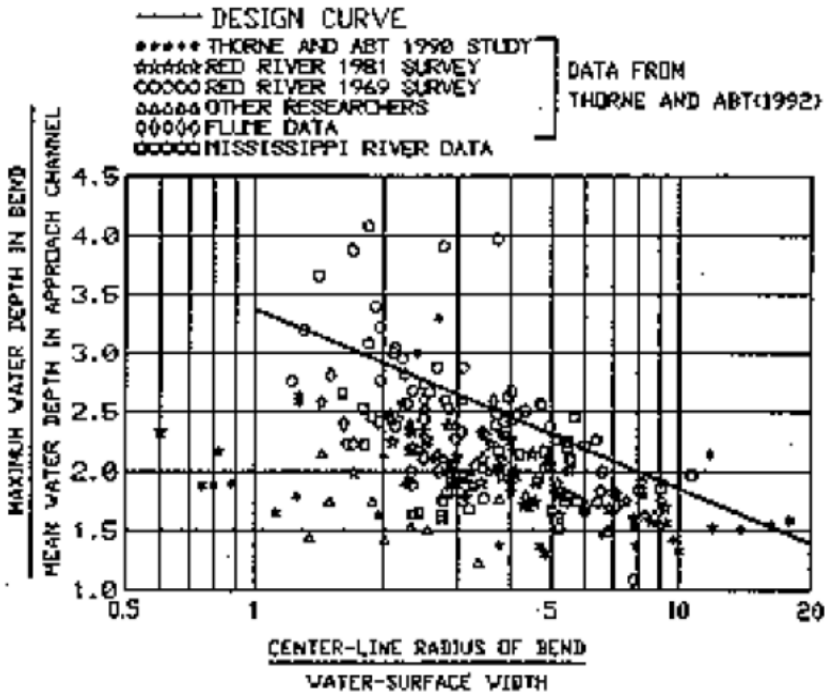

SAND BED CHANNELS

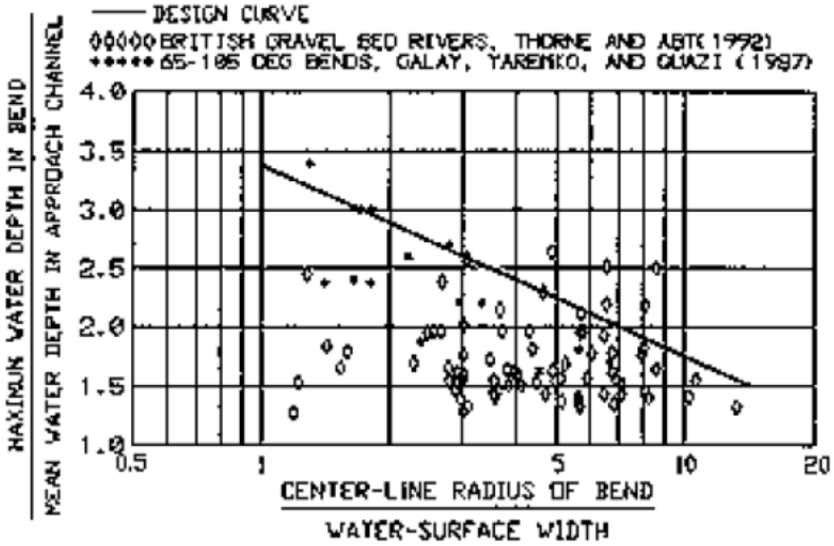

GRAVEL BED CHANNELS

Figure D-4. South depth in bends.

D.2 Scour Equations for Locations Adjacent to Structures

D.2.1 Contraction Scour – Modified Laursen's Live-Bed Equation

Shown below is the modified version of Laursen's live-bed equation (Laursen,1960), as presented in HEC-18 (FHWA, 2012):

(Equation D-8) $$\frac{y_2}{y_1} = \left(\frac{Q_2}{Q_1}\right)^{6/7} \left(\frac{W_1}{W_2}\right)^{k_1}$$

Where:

y_s = $y_2 - y_0$
y_1 = Average depth in the upstream main channel (ft)
y_2 = Average depth in the contracted section (ft)
y_0 = Existing depth in the contracted section before scour (ft) (see note 7 on the following page)
Q_1 = Flow in the upstream channel transporting sediment (ft^3/s)
Q_2 = Flow in the contracted channel (ft^3/s)
W_1 = Bottom width of the upstream main channel that is transporting bed material (ft)
W_2 = Bottom width of main channel in contracted section less pier width(s) (ft)
k_1 = Correction factor for the mode of bed material transport from table D-1.

Table D-1. Correction Factor, k_1, for Mode of Bed Material Transport

V_* / T	k_1	Mode of bed material transport
< 0.50	0.59	Mostly contact bed material discharge
0.50 to 2.0	0.64	Some suspended bed material discharge
>2.0	0.69	Mostly suspended bed material discharge

Where:

V_* = $t_0 / r = (gy_1 S_1)^{1/2}$, shear velocity in the upstream section (ft/s)
T = Fall velocity of bed material based on the D_{50} (figure D-5)
G = Acceleration of gravity (32.2 ft^2/s)
S1 = Slope of energy grade line of main channel (ft/ft)
t_0 = Shear stress on the bed (lb/ft^2)
r = Density of water (1.94 $slugs/ft^3$)

Notes:

1. Case 1 involves overbank flow on a flood plain being forced back to the main channel by the approaches to the bridge. Case 1 conditions include:

a. The river channel width becomes narrower, either due to the bridge abutments projecting into the channel or the bridge being located at a narrowing reach of the river;

b. No contraction of the main channel, but the overbank flow area is completely obstructed by an embankment; or

c. Abutments are set back from the stream channel. See HEC-18 (FHWA, 2012) for more information on Case 1 and Cases 2-4.

2. Q2 may be the total flow going through the bridge opening, as in Cases 1a and 1b. It is not the total flow for Case 1c. For Case 1c, contraction scour must be computed separately for the main channel and the left and/or right overbank areas.

3. Q1 is the flow in the main channel upstream of the bridge, not including overbank flows.

4. The Manning n ratio can be eliminated in Laursen live-bed equation as explained here. The ratio can be significant for a condition of dune bed in the upstream channel and a corresponding plane bed, washed out dunes, or antidunes in the contracted channel. However, Laursen's equation does not correctly account for the increase in transport that will occur as the result of the bed planning out (which decreases resistance to flow, increases the velocity, and increases the transport of bed material at the bridge). That is, Laursen's equation indicates a decrease in scour for this case; whereas in reality, there would be an increase in scour depth. In addition, at floodflows, a plane bedform will usually exist upstream and through the bridge waterway, and the values of Manning n will be equal. Consequently, the n value ratio is not recommended or presented in the equation.

5. W1 and W2 are not always easily defined. In some cases, it is acceptable to use the top width of the main channel to define these widths. Whether top width or bottom width is used, it is important to be consistent, so that W1 and W2 refer to either bottom widths or top widths.

6. The average width of the bridge opening (W2) is normally taken as the bottom width, with the width of the piers subtracted.

7. Laursen's equation will overestimate the depth of scour at the bridge if the bridge is located at the upstream end of a natural contraction, or if the contraction is the result of the bridge abutments and piers. At this time, however, it is the best equation available.

8. In sand channel streams where the contraction scour hole is filled in on the falling stage, the y_0 depth may be approximated by y_1. Sketches or surveys through the bridge can help in determining the existing bed elevation.

9. Scour depths with live-bed contraction scour may be limited by coarse sediments in the bed material armoring the bed. Where coarse sediments are present, it is recommended that scour depths be calculated for live-bed scour conditions using the clear-water scour equation (given in HEC-18 [FHWA, 2012]), in addition to the live-bed equation, and that the smaller calculated scour depth be used.

10. See FHWA, 2012 for example problems and for information on adjusted approaches for cohesive soils, erodible rock, open bottom culverts, and pressure flow at bridges.

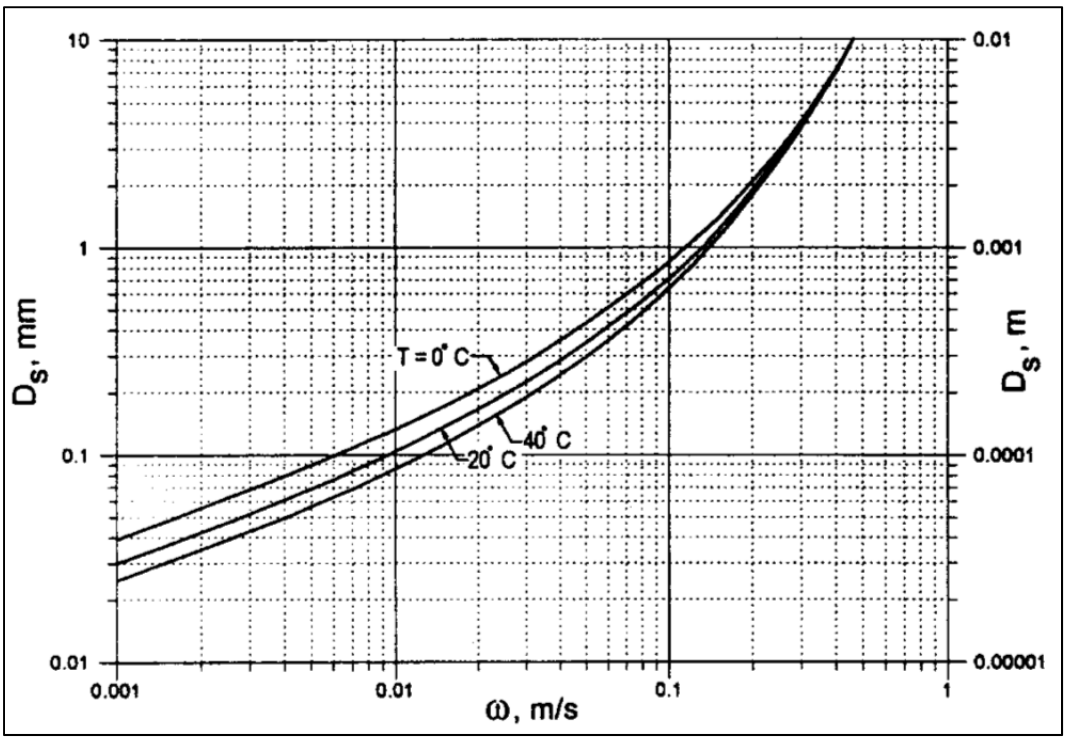

Figure D-5. Fall velocity of sand-sized particles with specific gravity of 2.65 in metric units.

D.2.2 Local Scour at a Pier – CSU Equation

[Reference: FHWA, 2012; Richardson et al., 1990]

The HEC-18 approach, based on the Colorado State University (CSU) equation, predicts a maximum scour depth for alluvial sand bed streams and is used for both live-bed and clear water conditions.

The HEC-18 equation is:

(Equation D-9) $$\frac{y_s}{y_1} = 2\ K_1\ K_2\ K_3\ \left(\frac{a}{y_1}\right)^{0.65} Fr_1{}^{0.43}$$

As a rule of thumb, the maximum scour depth for round nose piers aligned with the flow is:

(Equation D-10) $y_s \leq 2.4$ times the pier width (a) for $Fr_1 \leq 0.8$
$y_s \leq 3.0$ times the pier width (a) for $Fr_1 > 0.8$

In terms of y_s/a, Equation D-2 is:

(Equation D-11) $$\frac{y_s}{a} = 2\ K_1\ K_2\ K_3\ \left(\frac{y_1}{a}\right)^{0.35} Fr_1{}^{0.43}$$

Where:

- y_s = Scour depth (ft)
- y_1 = flow depth directly upstream of the pier (approach flow depth) (ft)
- K_1 = Correction factor for pier nose shape from table D-2.
- K_2 = Correction factor for angle of attack of flow from table D-3 or equation D-5.
- K_3 = Correction factor for bed condition from table D-4.
- A = Pier width (ft)
- L = Length of pier (ft)
- Fr_1 = Froude number directly upstream of the pier = $V_1/(gy)^{1/2}$
- V_1 = Mean velocity of flow directly upstream of the pier (ft/s)
- g = Acceleration of gravity (32.2 ft/s^2)

Table D-2. Correction Factor, K_1, for Pier Nose Shape

Shape of pier nose	K_1
Square nose	1.1
Round nose	1.0
Circular cylinder	1.0
Group of cylinders	1.0
Sharp nose	0.9

The correction factor, K_2, for angle of attack of the flow, a, is calculated using the following equation:

(Equation D-12) $$K_2 = (Cos\ \alpha + \frac{L}{a}\ Sin\ \alpha)^{0.65}$$

Where:

a = Skew angle of flow with respect to the pier

If L/a is larger than 12, use L/a = 12 as a maximum in equation D-5 and table D-3. Table D-3 illustrates the magnitude of the effect of the angle of attack, a, on local pier scour.

Table D-3. Correction Factor, K_2, for Angle of Attack, a, of the Flow

Angle, α	L/a = 4	L/a =8	L/a = 12
0	1	1	1
15	1.5	2	2.5
30	2	2.75	3.5
45	2.3	3.3	4.3
90	2.5	3.9	5

The correction factor, K_3, accounts for the effects of bedforms and bedform troughs.

H = Height of bedforms

Table D-4. Correction Factor, K_3, for Bed Condition

Bed condition (bedforms)	Dune height, H, ft	K_3
Clear water scour	NA	1.1
Plane bed and anti-dune flow	NA	1.1
Small dunes	10 > H > 2	1.1
Medium dunes	30 > H >or= 10	1.2 to 1.1
Large dunes	H > or = 30	1.3

Notes from HEC-18 (FHWA, 2012):

1. The correction factor K_1 for pier nose shape should be determined using table D-2 for angles of attack up to 5 degrees. For greater angles, K_2 dominates and K_1 should be considered as 1.0. If L/a is larger than 12, use the values for L/a = 12 as a maximum in table D-3 and equation D-5.

2. The values of the correction factor K_2 should be applied only when the field conditions are such that the entire length of the pier is subjected to the angle of attack of the flow. Using this factor will significantly overpredict scour if: (1) a portion of the pier is shielded from the direct impingement of the flow by an abutment or another pier; or (2) an abutment or another pier redirects the flow in a direction parallel to the pier. For such cases, judgment must be exercised to reduce the value of

the K_2 factor by selecting the effective length of the pier actually subjected to the angle of attack of the flow. Equation B7.4 should be used for evaluation and design. Table D-3 is intended to illustrate the importance of angle of attack in pier scour computations and to establish a cutoff point for K_2 (i.e., a maximum value of 5.0).

3. The correction factor K_3 results from the fact that for plane-bed conditions, which are typical of most bridge sites for the flood frequencies employed in scour design, the maximum scour may be 10 percent greater than computed with equation D-2. In the unusual situation where a dune bed configuration with large dunes exists at a site during floodflow, the maximum pier scour may be 30 percent greater than the predicted equation value. This may occur on very large rivers, such as the Mississippi. For smaller streams that have a dune bed configuration at floodflow, the dunes will be smaller, and the maximum scour may be only 10 to 20 percent larger than equilibrium scour. For anti-dune bed configuration, the maximum scour depth may be 10 percent greater than the computed equilibrium pier scour depth.

4. Piers set close to abutments (for example, at the toe of a spill through abutment) must be carefully evaluated for the angle of attack and velocity of the flow coming around the abutment.

5. See HEC-18 (FHWA, 2012) for information on the treatment of pier groups, wide piers, complex pier foundations, multiple skewed columns, scour debris, hole top widths, coarse bed materials, cohesive bed materials, and erodible rock.

D.2.3 Abutment Scour

D.2.3.1 Froehlich Equation

[References: FHWA, 2012; Froehlich, 1989)

Froehlich (Transportation Research Board, 1989) analyzed 170 live-bed scour measurements in laboratory flumes by regression analysis to obtain the following equation:

(Equation D-13) $$\frac{y_s}{y_a} = 2.27\, K_{a1}\, K_{a2} \left(\frac{L'}{y_a}\right)^{0.43} {Fr_1}^{0.61} + 1$$

Where:

y_s = Scour depth (ft)
y_a = Average depth of flow on the flood plain (A_e/L) (ft)
A_e = Flow area of the approach cross section obstructed by the embankment (ft^2)
L_a = Length of embankment projected normal to the flow (ft)

K_{a1} = Coefficient for abutment shape (figure D-6 and table D-5)
K_{a2} = Coefficient for angle of embankment to flow, θ
L' = Length of active flow obstructed by the embankment (ft). Length of blockage of ineffective flow is subtracted from total length of embankment. If the flow in a significant portion of the cross section has low velocity and/or is shallow, then the length of embankment blocking this flow should not be used.
One-dimensional flow models including SRH-1D (Huang, J., and B. Greimann, 2010) and HEC-RAS (USACE, 2010b) can easily compute conveyance versus distance across a cross section. See HEC-18 (FHWA, 2012) for additional guidance on estimating L′.
Fr_1 = Froude number of approach flow upstream of the abutment = $V_e/(gy_a)^{1/2}$
V_e = Q_e/A_e (ft/s)
Q_e = Flow obstructed by the abutment and approach embankment (ft^3/s)
g = Acceleration of gravity (32.2 ft/s^2)

(Equation D-14) $$K_{a2} = \left(\frac{\theta}{90}\right)^{0.13}$$

Where:
Θ < 90 degrees if the embankment points downstream (figure D-6),
Θ > 90 degrees if the embankment points upstream

It should be noted that equation D-6 is not consistent with the fact that as L′ tends to 0, y_S also tends to 0. The 1 was added to the equation to envelope 98 percent of the data.

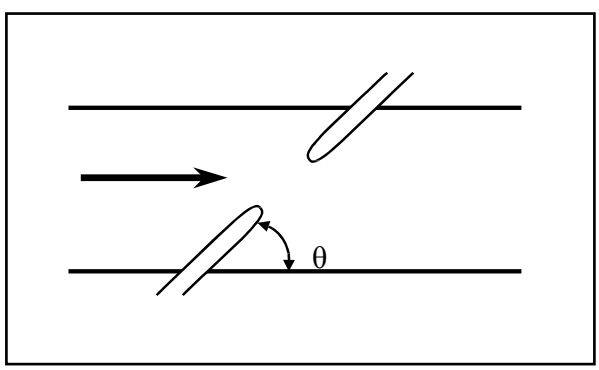

Figure D-6. Orientation of abutment embankment angle to the flow (FHWA, 2012).

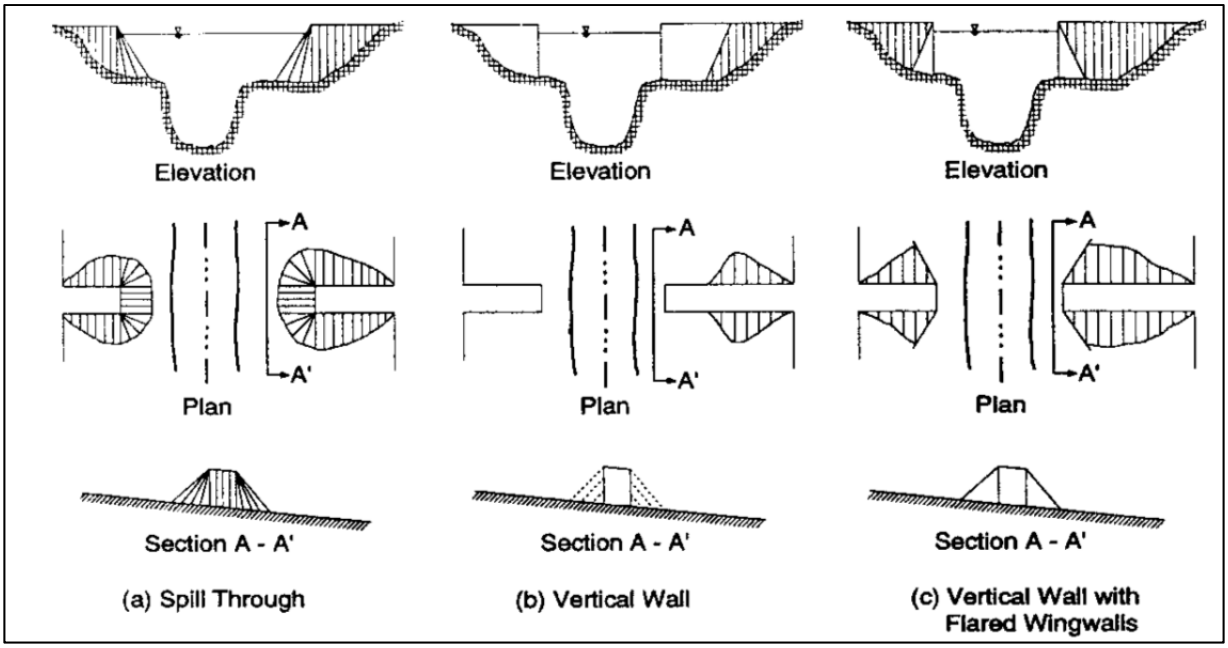

Figure D-7. Categories of abutment shape (FHWA, 2012).

Table D-5. Abutment Correction Factor K_1 for Shape of Opening

Description	K_{a1}
Vertical wall abutment	1.00
Vertical wall with wing walls	0.82
Spill-through abutment	0.55

D.2.3.2 HIRE Abutment Scour Equation

[References: FHWA, 2012; FHWA 2001)

Based on USACE field data from spurs in the Mississippi River, this equation is applicable when:

(Equation D-15) $L/y_1 > 25$

Where:

L_a = Abutment length (ft)
y_1 = Flow depth upstream of the abutment (ft)

(Equation D-16) $$\frac{y_s}{y_1} = 4\, Fr_1^{\,0.33}\ \frac{K_{a1}\, K_{a2}}{55}$$

Where:

y_s = Scour depth (ft)
y_1 = Flow depth directly upstream of the abutment (approach flow depth) on the overbank or in the main channel (ft)

K_{a1} = Correction factor for abutment shape from table D-5
K_{a2} = Correction factor for skew angle of abutment to flow calculated as shown in figure D-6.
Fr_1 = Froude number directly upstream of the abutment = $V_1/(gy)^{1/2}$
V_1 = Mean velocity of flow directly upstream of the abutment (ft/s)
g = Acceleration of gravity (32.2 ft^2/s)

D.2.3.3 NCHRP 24-20 Abutment Scour Approach

[References: FHWA, 2012; NCHRP, 2010b)

This equation is based on a contraction scour estimate. Contraction scour is multiplied by a factor to account for large-scale turbulence adjacent to the abutment. Flow is more concentrated in the vicinity of the abutment, and the contraction scour component is larger than average conditions in the constricted opening (FHWA, 2012). The three scour conditions (figure D-6) are:

1. Scour occurring when the abutment is in (or close to) the main channel

2. Scour occurring when the abutment is set back from the main channel

3. Scour occurring when the embankment breaches and the abutment foundation acts as a pier.

The NCHRP 20-24 approach assumes that there is a limiting depth of abutment scour when the geotechnical stability of the embankment or channel bank is reached. The equation gives a total scour depth that includes contraction scour effects. Contraction scour should not be added separately when using this equation. Three advantages to using this equation are noted in HEC-18:

1. Effective embankment length, L', which can be difficult to determine, is not used in these computations.

2. Equations are more physically representative of the abutment scour process.

3. Contraction scour is included and does not need to be computed separately.

Scour equations for conditions a and b are:

(Equation D-17) $y_{max} = \alpha_a \, y_c$

or $y_{max} = \alpha_b y_c$

(Equation D-18) $y_s = y_{max} - y_o$

Where:

y_{max} = Maximum flow depth resulting from abutment scour (ft)
y_c = Flow depth including live-bed or clear-water contraction scour (ft)
α_a = Amplification factor for live-bed conditions
α_b = Amplification factor for clear water conditions
y_s = Abutment scour depth (ft)
y_o = Flow depth prior to scour (ft)

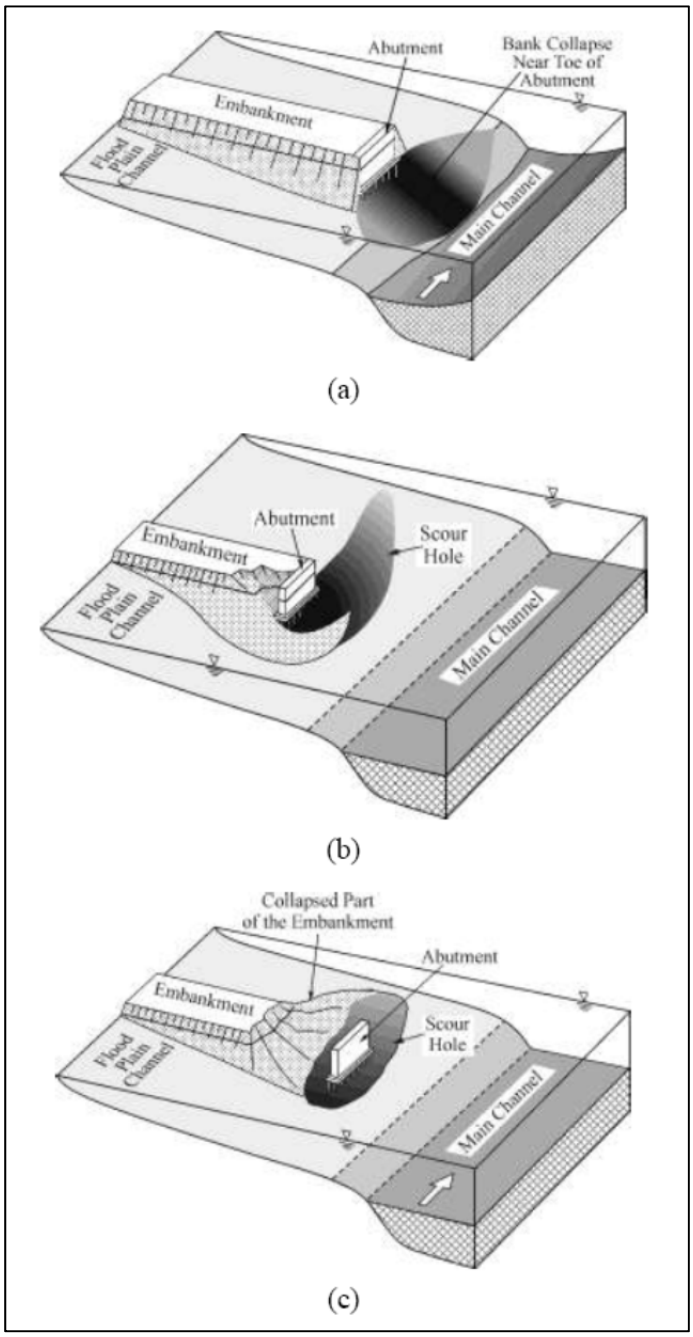

Figure D-8. Abutment scour condtions (NCHRP, 2010).

Condition A

If L_a > or = $0.75B_1$, then Condition A and the contraction scour calculation are performed using a live-bed scour calculation.

Where:
L_a = Abutment length (ft)
B_1 = Width of the flood plain (ft)

The contraction scour equation is:

(Equation D-19) $$y_c = y_1 \left(\frac{q_{2c}}{q_1}\right)^{6/7}$$

Where:
y_c = Flow depth including live-bed contraction scour (ft)
y_1 = Upstream flow depth (ft)
q_1 = Upstream unit discharge (ft^2/s)
q_{2c} = Unit discharge in the constricted opening accounting for nonuniform flow distribution (ft^2/s)

Unit discharge can be estimated either by discharge, Q, divided by width, w, or by the product of velocity and depth, v*y.

Condition B

If L_a < $0.75B_1$, then Condition B and the contraction scour calculation are performed using a clear water scour calculation. Two clear water contraction scour equations can be used. The first equation is the standard equation based on grain size:

(Equation D-20) $$y_c = \left(\frac{q_{2f}}{K_u {D_{50}}^{1/3}}\right)^{6/7}$$

Where:
y_c = Flow depth including clear water contraction scour (ft)
q_{2f} = Unit discharge in the constricted opening accounting for nonuniform flow distribution (ft^2/s)
K_u = 11.17, English units
K_u = 6.19, International System of Units (SI units)
D_{50} = Particle size with 50 percent finer (ft)

A lower limit of particle size of 0.2 mm is reasonable because cohesive properties limit the critical velocity and shear stress for cohesive soils. If the critical shear stress is known for a flood plain soil, then an alternative clear water scour equation can be used:

(Equation D-21) $$y_c = \left(\frac{\gamma}{\tau_c}\right)^{3/7} \left(\frac{nq_{2f}}{K_u}\right)^{6/7}$$

Where:

- n = Manning n of the flood plain material under the bridge (ft)
- $\boldsymbol{t_c}$ = Critical shear stress for the flood plain material (lb/ft^2)
- g = Unit weight of water (lb/ft^3)
- K_u = 1.486, English units
- K_u = 1.0, SI units

Notes:

The recommended procedure for selecting the velocity and unit discharge for abutment scour calculation is to use two-dimensional modeling. If one-dimensional modeling is used, velocity and unit discharge are estimated as presented in FHWA (2012).

The value of αB is selected from figure D-8 for spill through abutments and figure D-9 for wingwall abutments. The solid curves should be used for design.

The dashed curves represent theoretical conditions that have yet to be proven experimentally.

For scour estimates determined for either condition (a) or (b), the geotechnical stability of the channel bank or embankment should be considered. If the channel bank or embankment is likely to fail, then the limiting scour depth is the geotechnically stable depth, and erosion will progress laterally. This may cause the embankment to breach, and another scour estimate can be performed treating the abutment foundation as pier.

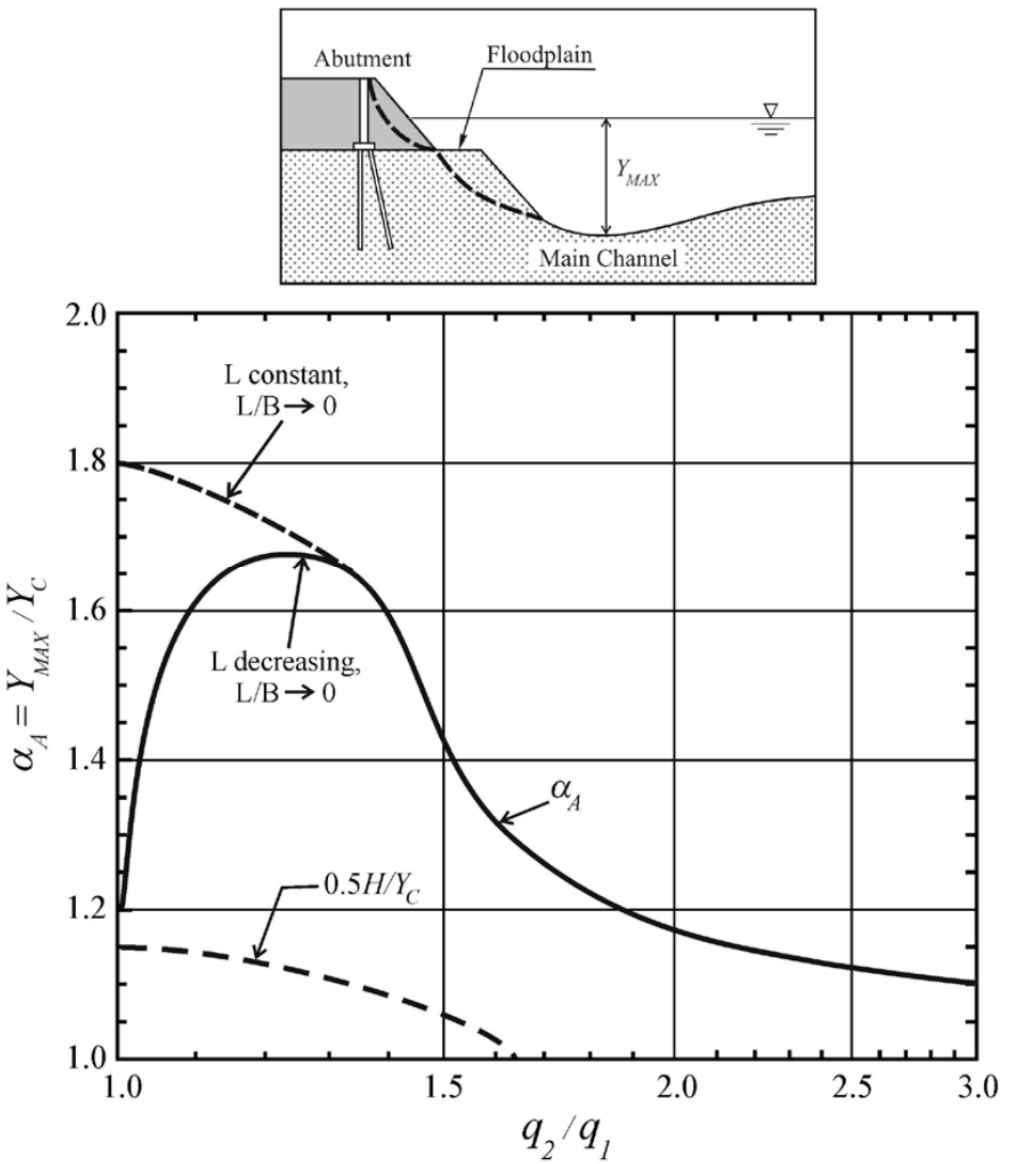

Figure D-9. Scour amplification factor for spill-through abutments and live-bed conditions (NCHRP, 2010).

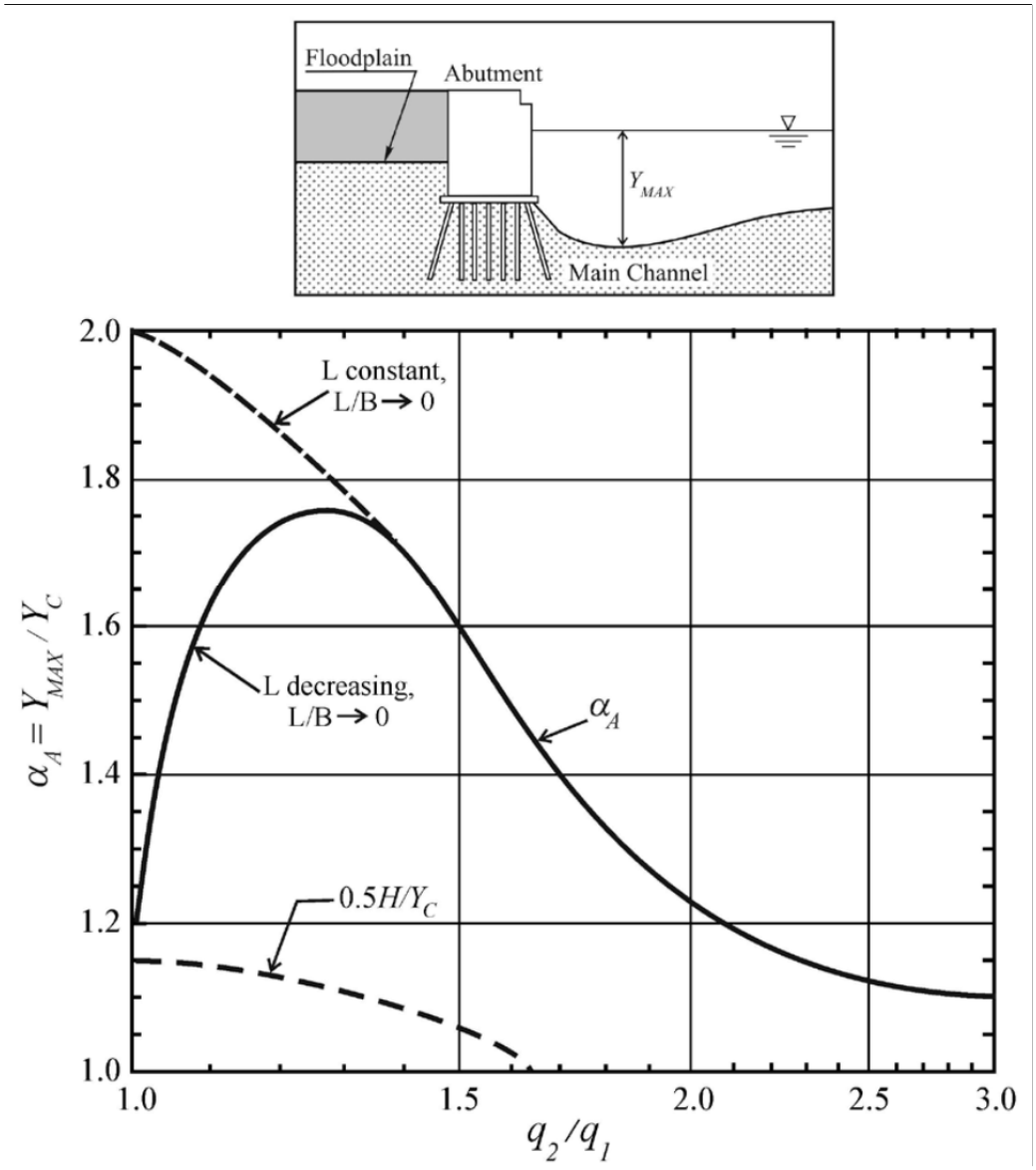

Figure D-10. Scour amplification factor for wingwall abutments and live-bed conditions (NCHRP, 2010).

D.3 Methods and Equations for Determining Equilibrium Slope

D.3.1 Schoklitsch Method

[Reference: Pemberton and Lara, 1984〕

`(Equation D-22) $$S_L = K\left(\frac{DB}{Q}\right)^{\frac{3}{4}}$$

Where:

S_L = Stable slope (ft/ft)
K = 0.00174 inch-pound units
B = Bankfull width (ft)
D = Mean bed particle size
Q = Dominant discharge (ft^3/s)

Note: Assumes zero or negligible sediment transport

D.3.2 Meyer-Peter, Muller Method

[Reference: Pemberton and Lara, 1984]

(Equation D-23) $$S_L = K \left(\frac{Q}{Q_B}\right) \left(\frac{n_s}{D_{90}{}^{1/6}}\right)^{3/2} \frac{D}{d}$$

Where:

S_L = Stable slope (ft/ft)
K = 0.19
$\frac{Q}{Q_B}$ = Ratio of total flow to flow over the channel
Q = Dominant discharge (ft^3/s)
n_s = Manning's n for the streambed
D_{90} = Bed sediment diameter for 90% finer
D = Mean bed sediment diameter
d = Mean depth (ft)

Note: Assumes zero or negligible sediment transport

D.3.3 Shields Diagram Method

[Reference: Pemberton and Lara, 1984〕

The use of Shields diagram for computing a stable slope involves the relationship of the boundary Reynolds number varying with the dimensionless shear stress shown on figure D-11 (Simons, Li & Associates, 1985; figure 5.12).

(Equation D-24) $$R_* = \frac{U_* D}{\upsilon}$$

Where:

R_* = Boundary Reynolds number
U_* = Shear velocity = $\sqrt{S_L R g}$
S_L = Slope (ft/ft)
R = Hydraulic radius or mean depth for wide channels (ft)
g = Acceleration of gravity (32.2 ft/s^2)
D = Mean particle diameter (ft)
υ = Kinematic viscosity of water varying with temperature (ft^2/s) and:

$$T_* = \frac{T_c}{(\gamma_s - \gamma_w)\, D}$$

Where:

T_* = Dimensionless shear stress
T_c = Critical shear stress
γ_s = Specific weight of particles (165.4 lb/ft^2) equal to γ_w d S_L
γ_w = Specific weight of water (62.4 lb/ft^3)
D = Mean depth (ft)

Note: Assumes zero or negligible sediment transport

Figure D-11. Shields' relation from beginning of motion (adapted from Gessler, 1971).

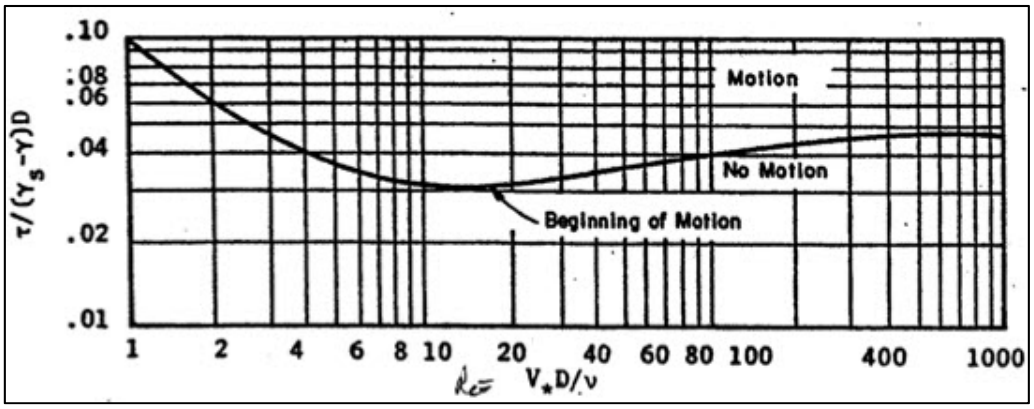

D.3.4 Lane's Tractive Force Method

[Reference: Pemberton and Lara, 1984]

(Equation 2-25) $S_L = \frac{T_c}{(\gamma_w d)}$

Where:

S_L = Stable slope (ft/ft)
d = Mean flow depth (ft)
T_c = Critical tractive force (lb/ft^2) [may be read from figure B-5., use value from the curves for canals with clear water]
g_w = Specific weight of water

Notes:

Method is based on results of the study by Lane, where he summarized the results of many studies in the relationship of critical tractive force versus mean particle size.

Assumes zero or negligible sediment transport.

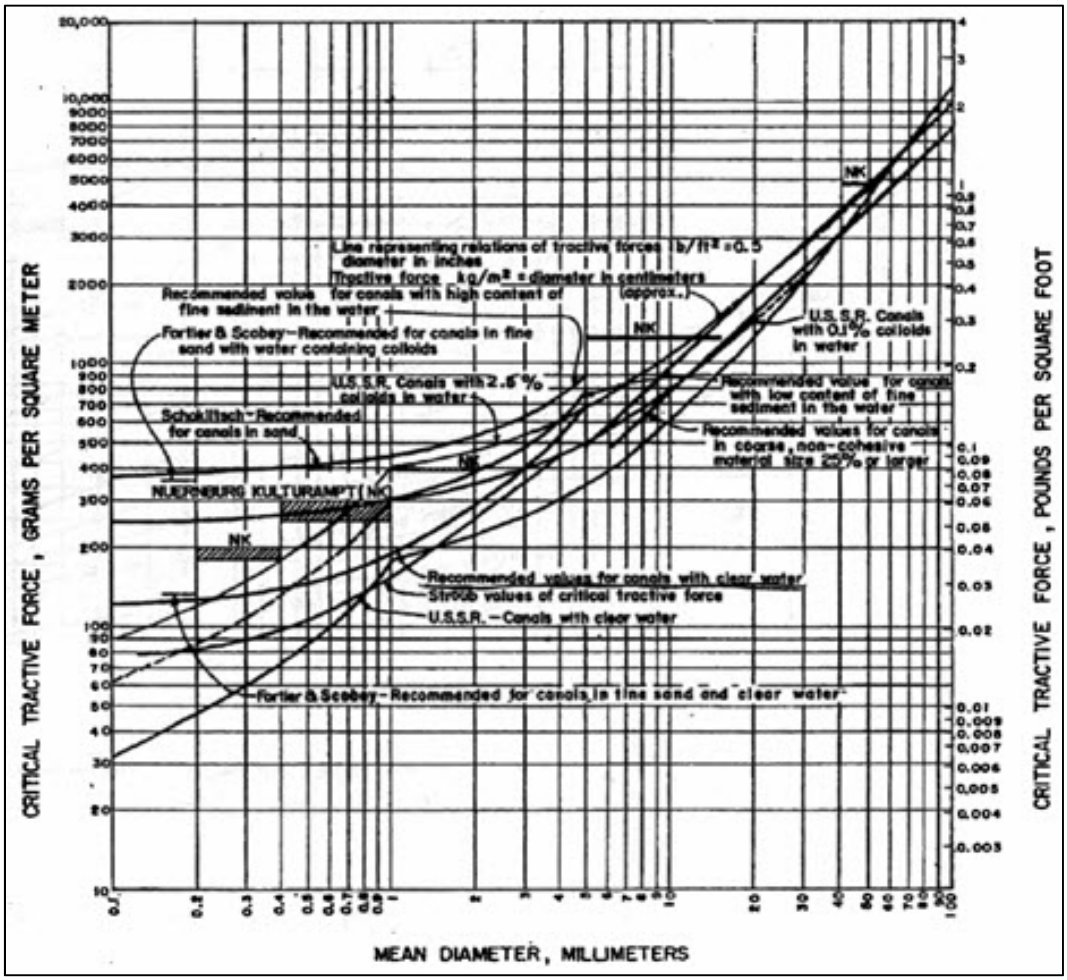

Figure D-12. Tractive force versus transportable sediment size – after Lane (Pemberton and Lara, 1984; figure 4).

D.3.5 USACE Nomograph Method

[Reference: USACE, 1994b]

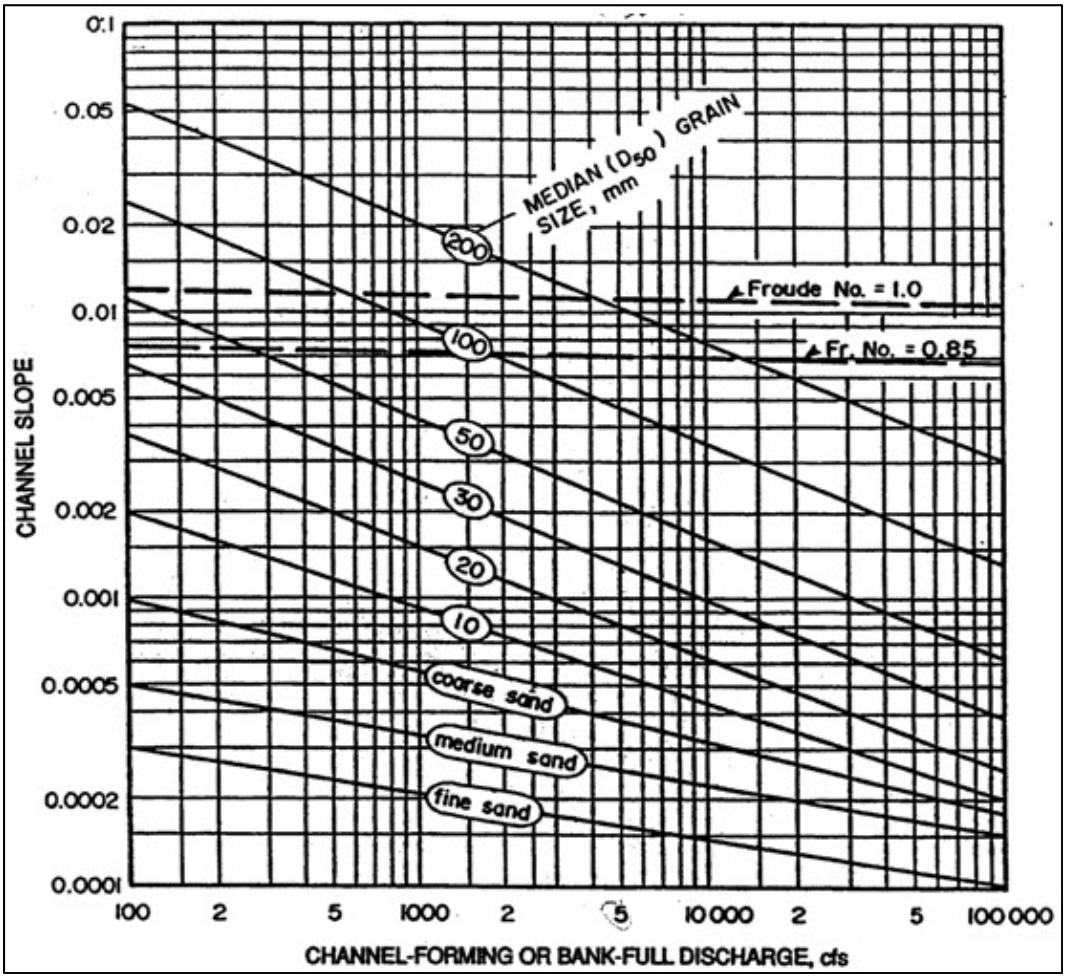

Figure D-13. Tentative guide to slope-discharge relationships for erodible channels (USACE, 1994b; figure 5-11).

Notes:

The nomograph was developed assuming a low bed-material transport rate. The slopes may be much higher with high sediment transport, especially sand beds in ephemeral channels where much of the flow occurs as flash floods with very high sediment transport.

This approach offers a tentative design guideline and helps bracket the stable slope.

D.4 Input Parameters to PBS&J Spreadsheet at 22 Main Sites

(Reference: PMS&J, 2008)

NCAP Main Site No.	16	20	21	26	31	32	33	50	51	52	57	58	84	86	90	92	94	95	96	97	98	125	
Design discharge, Q	4555	2020	980	1335	685	4180	4190	2590	2575	3190	580	5490	980	2105	640	695	695	890	63600	7195	1180	1560	ft^3/s
Design top width, T (top width at design Q)	237	228	100	99	123	202	269	249	142	139	91	524	109	342	56	229	229	273	450	413	181	117	ft
Design average/ hydraulic/ mean depth	3.02	1.61	1.17	1.87	1.17	2.51	2.67	2.22	3.23	2.89	1.54	2.31	1.5	1.26	3.95	0.94	0.94	1.47	19.88	2.63	1.28	2.01	ft
Design hydraulic radius	2.96	1.6	1.16	1.85	1.17	2.51	2.66	2.21	3.13	2.77	1.5	2.3	1.48	1.26	3.79	0.94	0.94	1.45	18.44	2.62	1.25	2	ft. Usually same or similar to mean depth)
Design maximum depth	5.35	3.96	1.83	2.86	1.76	3.53	5.06	6.24	7.04	6.07	3.83	6.05	2.19	2.73	5.58	2.48	2.48	3.66	24.08	3.81	2.67	3.18	ft
Design average velocity	6.36	5.5	8.4	7.22	4.74	8.23	5.84	4.67	5.61	7.94	4.13	4.54	6.03	4.89	2.9	3.24	3.24	2.23	7.11	6.62	5.1	6.65	ft/s
Bankfull depth at channel-forming discharge	2.36	0.81	0.88	2.74	0.56	1.17	2.32	2.75	2.84	3.55	2.57	1.76	0.93	1.08	5.63	1.82	1.82	1.84	4.38	2.68	1.55	0.8	ft
Bankfull or channel-forming discharge	565	102	101	1240	36	284	797	381	371	1069	195	499	144	136	652	272	272	158	1171	3482	356	264	ft^3/s

NCAP Main Site No.	16	20	21	26	31	32	33	50	51	52	57	58	84	86	90	92	94	95	96	97	98	125	
Bankfull width at channel-forming discharge	91	64	77	96	64	149	98	41	36	37	25	74	84	157	56	144	144	74	124	351	89	89	ft
Energy slope	0.009	0.014	0.026	0.019	0.015	0.01	0.008	0.008	0.007	0.016	0.01	0.007	0.02	0.013	0.001	0.009	0.009	0.003	0.001	0.009	0.02	0.008	Dimensionless
Manning n-value	0.03	0.03	0.03	0.03	0.03	0.03	0.03	0.03	0.03	0.03	0.03	0.03	0.03	0.03	0.03	0.03	0.03	0.03	0.03	0.03	0.03	0.03	
Inputs for Bend Scour only:																							
Design top width, T	237	228	100	99	123	202	269	249	142	139	91	524	109	109	56	229	229	273	450	413	181	117	ft. At upstream/ approach section (for bend scour)
Average/ hydraulic/ mean depth	4.5	1.61	1.17	1.87	1.17	2.51	2.67	2.22	3.23	2.89	1.54	2.31	1.5	1.5	3.95	0.94	0.94	1.47	19.88	2.63	1.28	2.01	ft. At upstream/ approach section (for bend scour)
Maximum depth	5.35	3.96	1.83	2.86	1.76	3.53	5.06	6.24	7.04	6.07	3.83	6.05	2.19	2.19	5.58	2.48	2.48	3.66	24.08	3.81	2.67	3.18	ft. At upstream/ approach section (for bend scour)
Bankfull width	237	64	100	96	64	149	98	41	36	37	25	74	84	84	56	144	144	74	124	351	89	89	ft. At upstream end of bend (for Maynord bend scour)
Average velocity	6.36	5.5	8.4	7.22	4.74	8.23	5.84	4.67	5.61	7.94	4.13	4.54	6.03	6.03	2.9	3.24	3.24	2.23	7.11	6.62	5.1	6.65	ft. At upstream/ approach section (for bend scour)
Energy slope	0.009	0.014	0.026	0.019	0.015	0.01	0.008	0.008	0.007	0.016	0.01	0.007	0.02	0.02	0.001	0.009	0.009	0.003	0.001	0.009	0.02	0.008	At upstream end (for Zeller bend scour)

NCAP Main Site No.	16	20	21	26	31	32	33	50	51	52	57	58	84	86	90	92	94	95	96	97	98	125	
Other																							
Water temperature	70	70	70	70	70	70	70	70	70	70	70	70	70	70	70	70	70	70	70	70	70	70	Degrees F. To determine kinematic viscosity for Shield's diagram
Bed form regime	dune	dune	dune	dune	dune	dune	dune	dune	dune	dune	dune	dune	dune	dune	dune	dune	dune	dune	dune	dune	dune	dune	Enter dune, antidune, or plane
Dune scour fraction	0.167	0.167	0.167	0.167	0.167	0.167	0.167	0.167	0.167	0.167	0.167	0.167	0.167	0.167	0.167	0.167	0.167	0.167	0.167	0.167	0.167	0.167	Dune scour as fraction of flow depth (recommended 0.1 to 0.5, or 0.167 per Yalin [1964]).
Use Laceys regime equation For mean water depth?	no	no	no	no	no	no	no	no	no	no	no	no	no	no	no	no	no	no	no	no	no	no	
D_{50}	2.4	2.9	1.6	0.64	0.8	1.1	2.38	0.43	0.45	0.4	1.3	0.53	1.3	0.4	0.28	0.32	0.32	0.59	0.08	0.59	0.11	1	mm. Median grain size
D_{90}	16	13	7.9	3.4	6.35	12	33	9.53	4.1	130	15.24	18	4	5.72	22	2.7	2.7	2.6	0.19	5.8	0.27	9.53	mm. 90% finer than grain size.
Neill incised exponent	0.7	0.7	0.7	0.7	0.7	0.7	0.7	0.7	0.7	0.7	0.7	0.7	0.7	0.7	0.7	0.7	0.7	0.7	0.7	0.7	0.7	0.7	Exponent varying from 0.67 for sand to 0.85 for coarse gravel
Bend radius R, in feet, at design Q	1100	1100	500	400	400	950	1300	1200	700	650	450	2500	500	1700	250	1100	1100	1300	2200	2000	850	550	ft. Enter zero if no bend.

NCAP Main Site No.	16	20	21	26	31	32	33	50	51	52	57	58	84	86	90	92	94	95	96	97	98	125	
Severe bend	X	X	X	X	X	X	X	X	X	X	X	X	X	X X		X	X	X	X	X	X	X	
Additional scour components																							
Low-flow incisement/ thalweg scour	0	0	0	0	0	0	0	0	0	0	0	0	0	0	0	0	0	0	0	0	0	0	ft
Calculated:																							
R/T	4.641	4.825	5	4.04	3.252	4.703	4.833	4.819	4.93	4.676	4.945	4.771	4.587	4.971	4.464	4.803	4.803	4.762	4.889	4.843	4.696	4.701	Degree of curvature
Recommended degree of bend based on R/T	severe	severe	severe	severe	severe	severe	severe	severe	severe	severe	severe	severe	severe	severe	severe	severe	severe	severe	severe	severe	severe	severe	Less than 5 is severe, 5 to 10 is moderate, greater than 10 is straight
Design flood discharge per unit width, q	19.22	8.86	9.8	13.48	5.569	20.69	15.58	10.4	18.13	22.95	6.374	10.48	8.991	6.155	11.43	3.035	3.035	3.26	141.3	17.42	6.519	13.33	$ft^3/s/ft.$ = Q/T

Appendix E

Sediment and Slope

Depth of scour is affected by the type of sediment. Several general scour equations and bend scour equations require representative grain size values (D_{50} and D_{90}) to calculate scour depth. Sediment size information was available from field observations, 23 sediment samples collected in the field, and sediment samples from test pit study. Bulk soil samples were collected from the bed of the channel at main sites. Most of the streams were dry, so the sample could be collected with a shovel. An approximate 1-foot-diameter hole was dug from the channel thalweg to a maximum depth of 1 foot. Samples were 20 to 40 pounds. Samples were sent to a lab for a sieve analysis. The gradations are included in section E.1 below.

E.1 Bulk Channel Bed Sediment Samples

Table E-1 shows the D_{50} and D_{90} grain size for sediment samples for the main sites. These values were computed from the sediment sample gradations provided by the lab (table E-2).

Table E-1. D_{50} and D_{90} Grain Size for Main Sites

Sediment diameter parameters from sediment samples		
Site	D_{50}	D_{90}
4	0.25	0.55
13	0.25	3.60
16	2.40	17.00
20	2.90	13.00
21	1.60	7.90
26	0.64	3.40
31	0.80	6.35
32	1.10	12.00
33	2.38	33.00
50	0.43	9.53
51	0.45	4.10
58	0.53	18.00
78	0.40	6.35
84	1.30	4.00
90	0.28	22.00
92	0.32	2.70
94	0.59	3.90
95	0.59	2.60
96 downstream	0.10	0.22
96 upstream	0.06	0.15
97	0.59	5.80
98	0.11	0.27
125	1.00	9.53

Table E-2. Sediment Sample Gradations

Sieve size			Site No. — Accumulative percent passing by weight																						
Inch or No.	Inch	Milli-meter	4	13	16	20	21	26	31	32	33	50	51	58	78	84	90	92	94	95	96d*	96u**	97	98	125
3	3	76.2	100	100	100	100	100	100	100	100	100	100	100	100	100	100	100	100	100	100	100	100	100	100	100
2	2	50.8	100	100	100	100	100	100	100	100	97	94	100	100	100	100	100	100	100	100	100	100	100	100	100
1-1/2	1.5	38.1	100	100	100	99	100	100	100	99	93	94	100	97	100	100	95	100	100	100	100	100	100	100	100
1	1	25.4	100	100	95	98	98	100	100	98	84	94	100	94	98	100	91	100	100	100	100	100	100	100	99
3/4	0.75	19.1	100	100	92	96	98	100	99	96	81	93	100	91	96	99	88	100	98	100	100	100	100	100	98
1/2	0.5	12.7	100	98	86	91	95	98	97	91	77	91	98	85	94	99	84	98	97	98	100	100	97	100	95
3/8	0.375	9.53	99	98	80	84	93	96	94	87	74	90	96	81	93	99	80	98	97	98	100	100	94	100	90
1/4	0.25	6.35	98	96	70	72	86	94	90	78	67	88	93	74	90	96	77	96	94	97	100	100	91	100	81
No. 4	0.187	4.75	98	94	64	63	79	93	87	73	63	86	91	70	88	94	75	94	92	96	100	100	88	100	75
No. 8	0.094	2.38	96	85	49	45	63	87	77	62	50	80	84	62	81	76	72	89	85	89	100	100	79	100	64
No. 10	0.079	2.00	95	81	46	41	58	84	73	59	47	78	82	60	79	69	72	88	84	87	100	100	77	100	62
No. 16	0.047	1.19	94	72	39	32	42	75	62	52	38	73	76	57	76	46	70	85	79	75	100	100	68	100	53
No. 20	0.033	0.841	93	69	34	25	29	64	52	46	33	69	72	55	73	34	68	81	74	63	100	100	60	100	45
No. 30	0.023	0.594	93	68	28	21	22	46	41	42	26	66	68	54	70	24	65	77	67	50	100	100	50	99	36
No. 40	0.017	0.419	80	65	20	15	13	27	25	32	19	48	46	40	52	14	60	64	51	31	100	100	36	98	27
No. 50	0.012	0.297	59	60	15	11	8	14	15	22	12	30	25	23	37	7	52	47	35	18	100	100	23	94	19
No. 100	0.006	0.150	27	21	8	8	4	5	6	9	6	13	9	9	19	2	31	21	15	8	76	94	8	70	12
No. 200	0.003	.0737	4.4	3.6	4.8	5.1	2.3	2.8	3.3	5.8	3.7	4.9	3.7	4.1	9 .1	1.1	10	10	6 .8	4.7	29	61	3.2	23	8.9

*57' downstream from old bridge in damp, left bank
**60' upstream from old bridge in damp, left bank

E.2 Comparison of Sediment Grain Sizes

A D_{50} and D_{90} grain size was also estimated onsite; the D_{50} from the channel thalweg, and the D_{90}, was measured from four to six coarse materials lying on low adjacent bars. Table E-3 compares the field estimate of grain size to the D_{50} and D_{90} values (table E-1) computed from the sediment gradations provided by the lab (table E-2).

Table E-3. Comparison of Sediment D_{50} and D_{90} Values

Site	Field estimate D_{50} (average mm)	Sediment sample D_{50} (mm)	Field estimate D_{90} (average mm)	Sediment sample D_{90} (mm)
4		0.25		0.55
13	0.13	0.25	4.00	3.60
16	0.40	2.40	4.00	16.00
18	0.40		15.24	
20	0.40	2.90	6.35	13.00
21	0.40	1.60	8.89	7.90
26	0.40	0.64	3.81	3.40
31	0.40	0.80	5.72	6.35
32	0.40	1.10	10.16	12.00
33	0.40	2.38	7.62	33.00
38	13.00			
43	130.00		415.00	
44			415.00	
45	130.00		415.00	
46	0.40			
50	0.40	0.43		9.53
51	0.40	0.45	4.00	4.10
52	0.40		130.00	
57	1.30		15.24	
58		0.53		18.00
75	0.40		7.62	
78	0.40	0.40	13.00	6.35
84	0.40	1.30	5.08	4.00
86	0.40		5.72	
90	0.13	0.28	0.40	22.00
92	0.40	0.32	5.08	2.70
94	0.40	0.59	6.35	3.90
95		0.59		2.60
96 upstream	0.13	0.06?	0.40	0.15
96 downstream	0.13	0.10	0.40	0.22
97	0.40	0.59	3.18	5.80
98	0.13	0.11	0.40	0.27
103	0.40		1.30	
104	0.40		4.00	
125	1.30	1.00	8.89	9.53

E.3 Slope Comparison

Values for the parameter, channel slope, were measured in the office at the pipeline stream crossing from Geographic Information System (GIS), Interferometric Synthetic Aperture Radar (IfSAR), 5-foot contours. The distance upstream and downstream of the crossing was defined by the 5-foot contours bordering a consistent slope. The vertical differential between upstream and downstream 'border' contours ranged from 5 feet to 90 feet, and the average value was 18 feet. The horizontal distance between the selected contours ranged from 105 feet to 2,585 feet but averaged 842 feet. The vertical differential was divided by the horizontal differential (distance between border contours) to calculate the channel slope at each pipeline stream crossing. See table E-4 below.

Table E-4. Comparison of Slope Computations

Crossing	Slope (ft/ft) from:	
	5-ft contour map	All survey points
16	0.0076	0.0091
20	0.0157	0.0138
21	0.0339	0.0258
26	0.0184	0.0189
31	0.0162	0.0150
81/84	0.0195	0.0201
86	0.0129	0.0126
90	0.0020	0.0010
92	0.0110	0.0091
94	0.0062	0.0046
95	0.0044	0.0028
96	0.0021	0.0011
125	0.0068	0.0082
58	0.0074	0.0069
57	0.0176	0.0102
52	0.0149	0.0160
51	0.0067	0.0070
50	0.0099	0.0080
33	0.0100	0.0080
32	0.0102	0.0100
97	0.0108	0.0092
98	0.0135	0.0198
	Difference within + or - 0.002	
	Greater than 0.002 difference	

Slope was also measured at 22 main sites, from points surveyed in the channel bed upstream and downstream of the pipeline crossing. Surveyed values for slope were compared against values measured from IfSAR mapping. Initially, 9 of the 22 values differed by more than 0.002 ft/ft. After reviewing the map measures and reducing the number of contours included in the computation of slope, the number of crossings that differed in the comparison of values decreased to 3 crossings (table E-4). This change gives some indication of uncertainty associated with the values for slope. Surveyed slopes are used for 22 crossings, and contour mapping slopes are used for the remaining 110 pipeline stream crossings. Uncertainty can be assigned based on a mapped (9 out of 22 > 0.002 difference) or surveyed (3 out of 22 > 0.002 difference) value. All values for slope used in scour computations are listed in table E-5.

Table E-5. Slope Values Used in Scour Computations

	Slope		Slope		Slope
Lake Powell Intake		Tuba City Spur		Bitter Springs Spur	
1	0.0472	Tuba City Spur Road		118	0.0235
Page		81	0.0201	119	0.0238
2	0.0425	85	0.0144	83	0.0254
89 Lake Powell Road		120	0.0198	82	0.0326
3	0.0184	86	0.0126	81	0.0355
4	0.0121	87	0.0109	80	0.0239
5	0.0333	RD160 Tuba City Tee		79	0.0130
6	0.0000	88	0.0091	78	0.0138
7a	0.0245	89	0.0102	77	0.0173
7b	0.0538	121	0.0114	76	0.0307
8	0.0159	90	0.0010	75	0.0192
LeChee		91	0.0069	74	0.0206
9	0.0243	92	0.0091	73	0.0313
10a	0.0441	93	0.0943	72	0.0409
10b	0.0000	122a	0.0103	71	0.0314
R&R Solar Wind Engineering Company		122b	0.0103	70	0.0358
113	0.0122	123	0.0193	69	0.0230
114	0.0092	94	0.0046	68	0.0253
11a	0.0522	124a	0.0056	67	0.0206
11b	0.0490	124b	0.0056	66b	
12	0.0460	95	0.0028	66a	0.0197
13	0.0472	96	0.0011	65	0.0285
14	0.0178	103	0.0174	64	0.0195
BIA 20 converts to gravel		104	0.0158	63b	
15	0.0601	105	0.0152	63a	0.0198

Table E-5. Slope Values Used in Scour Computations

	Slope		Slope		Slope
Page Lake Campground		Cameron		62	0.0492
115	0.0514	125	0.0082	61	0.0384
Bitter Springs Spur		126	0.0368	60	0.0306
16	0.0091	Gray Mountain (Black Mesa pump station)		59	0.0247
Bodeaway Gap		127	0.0033	58	0.0069
17	0.0173	106	0.0062	57	0.0102
M	0.0391	107	0.0577	56	0.0228
M	0.0289	128	0.0000	55	0.0187
18	0.0247	108	0.0107	54	0.0235
M	0.0398	109	0.0000	53	0.0169
19	0.0307	110	0.0157	Cedar Ridge	
20	0.0138	129	0.0269	52	0.0160
21	0.0258	130	0.0820	51	0.0070
22	0.0355	131	0.0093	50	0.0080
23	0.0957	111a	0.0352	49	0.0175
24	0.0771	111b		116	0.0156
25	0.0225	132	0.0505	117	0.0154
26	0.0189	112	0.0568	48	0.0268
27	0.0000	133	0.0023	47	0.0247
28	0.0000	Flagstaff		46	#DIV/0!
30	0.0000			45	0.1368
31	0.0150			44	0.0266
Tuba City Spur				43	0.0328
Tuba City Spur Road				42	0.0206
				41	0.0365
		Tuba City Spur		40	0.0764
		97	0.0092	39	0.0751
		98	0.0198	38	0.0185
		99	0.0085	37	0.0442
		100	0.0100	36	0.0551
		101	0.0065	35	0.0641
		102	0.0100	34	0.0274
				33	0.008
				32	0.010